TECHNICAL REPORT N-75-2

COLLAPSE STRENGTH OF A TWO-WAY-REINFORCED CONCRETE SLAB CONTAINED WITHIN A STEEL FRAME STRUCTURE

by

William L. Huff

Weapons Effects Laboratory
U. S. Army Engineer Waterways Experiment Station
P. O. Box 631, Vicksburg, Miss. 39180

June 1975
Final Report

Prepared for Defense Civil Preparedness Agency
Washington, D. C. 20301

Under Contract DAHC 20-68-W-0192
Work Unit 1127E

Unclassified

SECURITY CLASSIFICATION OF THIS PAGE (When Data Entered)

REPORT DOCUMENTATION PAGE		READ INSTRUCTIONS BEFORE COMPLETING FORM
1. REPORT NUMBER Technical Report N-75-2	2. GOVT ACCESSION NO.	3. RECIPIENT'S CATALOG NUMBER
4. TITLE (and Subtitle) COLLAPSE STRENGTH OF A TWO-WAY-REINFORCED CONCRETE SLAB CONTAINED WITHIN A STEEL FRAME STRUCTURE		5. TYPE OF REPORT & PERIOD COVERED Final report 6. PERFORMING ORG. REPORT NUMBER
7. AUTHOR(s) William L. Huff		8. CONTRACT OR GRANT NUMBER(s) Contract DAHC 20-68-W-0192
9. PERFORMING ORGANIZATION NAME AND ADDRESS U. S. Army Engineer Waterways Experiment Station Weapons Effects Laboratory P. O. Box 631, Vicksburg, Miss. 39180		10. PROGRAM ELEMENT, PROJECT, TASK AREA & WORK UNIT NUMBERS Work Unit 1127E
11. CONTROLLING OFFICE NAME AND ADDRESS Defense Civil Preparedness Agency Washington, D. C. 20301		12. REPORT DATE June 1975 13. NUMBER OF PAGES 204
14. MONITORING AGENCY NAME & ADDRESS(if different from Controlling Office)		15. SECURITY CLASS. (of this report) Unclassified 15a. DECLASSIFICATION/DOWNGRADING SCHEDULE

16. DISTRIBUTION STATEMENT (of this Report)

Approved for public release; distribution unlimited.

17. DISTRIBUTION STATEMENT (of the abstract entered in Block 20, if different from Report)

18. SUPPLEMENTARY NOTES

19. KEY WORDS (Continue on reverse side if necessary and identify by block number)

Basements	Reinforced concrete
Collapse	Shelters
Concrete slabs	Static tests
Dynamic tests	Steel frame structures
Fallout shelters	Subsurface structures

20. ABSTRACT (Continue on reverse side if necessary and identify by block number)

The objective of the study reported herein was to determine the response, up to collapse, of a conventional floor and framing system typical of the systems which would be located over a basement fallout shelter in a steel frame building. Static and dynamic tests were conducted on two 1/4.5-scale models of the basement shelter area from a multistory steel frame prototype structure designed for this study. The prototype structure consisted of a five-story

(Continued)

DD FORM 1 JAN 73 1473 EDITION OF 1 NOV 65 IS OBSOLETE

Unclassified

SECURITY CLASSIFICATION OF THIS PAGE (When Data Entered)

20. ABSTRACT (Continued).

rigid frame building having a column spacing of 20 feet in each direction. In plan the prototype contained three bays in each direction, providing the three possible types of floor panels (edge, corner, and interior). The design of the prototype structure followed the requirements of the American Institute of Steel Construction (AISC) specifications for the steel frame and the requirements of the 1963 American Concrete Institute (ACI) Building Code for the floor slabs and basement walls. The model tests were conducted in the 22-foot-10-inch-diameter test chamber of the Large Blast Load Generator located at the U. S. Army Engineer Waterways Experiment Station. Approximately 80 channels of data consisting of strains, pressures, deflections, and accelerations were recorded during each test. In the static test, one of the corner panels of the three-bay by three-bay model collapsed at an applied pressure of 8.8 psi. The remaining floor panels of the model had permanent deflections of approximately 0.12 times the clear span of the slab panels. All panels, as evidenced by their deflection and recorded strain, were acting as tensile membranes when the test was terminated due to the collapse of the corner panel. The steel frame of the static model showed no signs of failure at the end of the test. The dynamic model was subjected to a peak blast pressure of 10.2 psi. The negative moment reinforcing steel ruptured along 70 to 100 percent of the outside edges on all four of the corner panels. Two edge panels also suffered a rupture on the majority of the negative moment reinforcing along their outside edges. Recorded strains on the steel framing beams indicated that the beams were near their yield stress when the floor slabs collapsed. A tensile membrane theory developed for two-way slabs having fixed edges was used to predict the response of the three panel types in the model. Good correlation was obtained using this theory, even though the edges of the slab panels in the models were restrained only by the adjacent slab panels. However, the tensile membrane theory predicted the interior panel to be the weakest panel of the floor system, whereas the test results proved the corner panel to be the weakest. It is pointed out that the tensile membrane theory did not consider any load-carrying capacity for negative moment reinforcing steel extending into a slab panel from adjacent slab panels. Insufficient data were available from these tests to define the full benefit of this reinforcing steel. In both static and dynamic tests, the steel frame of the rigid frame models had recorded strains of near yield strain along the framing beams. There were no visible signs of damage to the beam-column connections in either model. Predictions were made for the response of a simple frame prototype structure designed to carry the same service loads as the rigid frame prototype used in this test program. The framing beams and connections of the simple frame prototype structure were found to have collapse loads essentially equal to those of the reinforced concrete floor slabs.

THE CONTENTS OF THIS REPORT ARE NOT TO BE USED FOR ADVERTISING, PUBLICATION, OR PROMOTIONAL PURPOSES. CITATION OF TRADE NAMES DOES NOT CONSTITUTE AN OFFICIAL ENDORSEMENT OR APPROVAL OF THE USE OF SUCH COMMERCIAL PRODUCTS.

PREFACE

This study, sponsored by the Defense Civil Preparedness Agency (DCPA) under Contract No. DAHC 20-68-W-0192, Work Unit 1127E, was conducted at the U. S. Army Engineer Waterways Experiment Station (WES) during the period August 1971 through December 1973.

The study was under the general supervision of Mr. W. J. Flathau, Chief of the Weapons Effects Laboratory, and Mr. J. T. Ballard, Chief of the Structures Division, and under the direct supervision of Mr. T. E. Kennedy, Structures Division. This report was prepared by Mr. W. L. Huff of the Research Projects Group, Structures Division.

BG E. D. Peixotto, CE, and COL G. H. Hilt, CE, were Directors of WES during the conduct of the study and the preparation and publication of this report. Mr. F. R. Brown was Technical Director.

CONTENTS

FIGURES

CONVERSION FACTORS, U. S. CUSTOMARY TO METRIC (SI) UNITS OF MEASUREMENT

U. S. customary units of measurement used in this report can be converted to metric (SI) units as follows:

Multiply	By	To Obtain
mils	0.0254	millimeters
inches	2.54	centimeters
feet	0.3048	meters
square inches	6.4516	square centimeters
cubic inches	16.38706	cubic centimeters
cubic yards	0.764555	cubic meters
pounds (mass)	0.45359237	kilograms
gallons (U. S. liquid)	3.785412	cubic decimeters
pounds per foot	14.59390	newtons per meter
pounds per square inch	0.6894757	newtons per square centimeter
pounds per cubic inch	27,679.90	kilograms per cubic centimeter
pounds per square foot	47.88026	newtons per square meter
pounds per cubic foot	16.0185	kilograms per cubic meter
inches per second	2.54	centimeters per second
inch-pounds	0.1129848	meter-newtons
inch-kips	0.0001129848	meter-kilonewtons
Fahrenheit degrees	5/9	Celsius degrees or Kelvins[a]

[a] To obtain Celsius (C) temperature readings from Fahrenheit (F) readings, use the following formula: $C = (5/9)(F - 32)$. To obtain Kelvin (K) readings, use: $K = (5/9)(F - 32) + 273.15$.

COLLAPSE STRENGTH OF A TWO-WAY-REINFORCED CONCRETE SLAB CONTAINED WITHIN A STEEL FRAME STRUCTURE

CHAPTER 1

INTRODUCTION

1.1 BACKGROUND

The Defense Civil Preparedness Agency (DCPA) is developing analytical procedures for the prediction of the collapse strength of existing structures subjected to nuclear blast. Programs conducted at the U. S. Army Engineer Waterways Experiment Station (WES) have provided useful data for determining the resistance of reinforced concrete structures to blast overpressures. However, little experimental data exist on the effects of blast overpressures on steel frame structures.

In 1967 the Research Triangle Institute (RTI) conducted a statistical sampling of structures containing fallout shelters with regard to such items as the year of construction, type of structural frame, number of stories, floor area, and general construction characteristics (Reference 1). Portions of these data have been retabulated to determine the structural characteristics of the steel frame buildings contained in the RTI survey (Reference 2). It was found that 33 percent of the shelter spaces contained in the surveyed buildings were located in steel frame buildings. However, the steel frame buildings comprised only 15 percent of the total number of buildings surveyed.

A survey (Reference 2) of building failures caused by earthquakes showed that buildings having structural steel frames with curtainwalls generally withstood the earthquake without structural damage. Therefore, these structures should also resist a nuclear blast equally as well.

In 1972, DCPA conducted a preliminary all-effects shelter survey of 221 structures containing fallout shelters. The purpose was to develop a survey system that would provide sufficient data to permit analysis of the structures in the National Fallout Shelter Survey (NFSS)

with regard to the blast and radiation effects caused by the detonation of a nuclear device. Preliminary results indicated that a much larger percentage of the structures had steel frames than was found in the 1967 survey.

1.2 OBJECTIVES

The general objective of this study was to determine, through model testing, the dynamic response, up to collapse, of a conventional floor and framing system typical of the systems which would be located over a basement shelter in a steel frame building.

Specific objectives were to determine the static and dynamic load-deflection relationships for individual floor panels which were a part of the floor systems, to determine strength variations between the various parts of the floor system (i.e., floor slab, connections, beams), and to determine strength variations between the different types of floor panels that make up the entire system (i.e., corner, edge, and interior panels).

1.3 SCOPE

Reviewing the 1967 and 1972 RTI surveys of the NFSS buildings provided the basic characteristics for the prototype floor and framing system which was to be modeled and tested in this program. The prototype structure selected consisted of the basement area from a five-story steel frame building having three 20-foot[1] bays in each direction. The 60-foot-square prototype was large enough to be realistic and small enough to be modeled at a reasonable scale.

The entire steel frame for the five-story prototype structure was designed to determine the size of the columns in the basement area. For the model test, it was assumed that the portion of the structure above the basement roof would not affect the response of the steel frame in the basement area nor the response of the roof over the basement.

---

[1] A table of factors for converting U. S. customary units of measurement to metric (SI) units is presented on page 9.

The models constructed for the laboratory investigation were 1/4.5-scale representations of the basement area of the prototype structure. The responses of the basement roof and the steel framework in the basement area were of primary concern; however, basement walls were included in the model to simulate as accurately as possible the conditions that would exist around the perimeter of the prototype structure and to seal the underside of the shelter roof during the static and dynamic tests.

Two 1/4.5-scale (13-1/3-foot-square) multipanel models were constructed. One was slowly loaded to failure using water pressure; the other was subjected to blast loadings which simulated the blast pressure from the detonation of a nuclear device. Both models were tested in the Large Blast Load Generator (LBLG) at WES.

CHAPTER 2

SELECTION OF PROTOTYPE STRUCTURE

To better satisfy the objectives of this study, it was necessary to choose a prototype structure which would be typical of the structures in the NFSS. Initial efforts sought an NFSS structure whose plans and specifications could be obtained, allowing part of the basement shelter or the entire basement shelter to be modeled. In the 1967 survey (Reference 1), 32 of the 309 structures surveyed had steel frames, none of which were suitable for modeling. In the 1972 all-effects survey, 93 structures had been surveyed at the time of the selection of the prototype for this study; of these, 37 were steel frame structures, most of which were high-rise buildings located in the northeast United States. Due to the extreme height and size of these buildings, they were not considered good candidates for modeling. Hence, it was decided that a structure meeting the requirements of this study would be designed rather than trying to scale an existing design.

The following is a discussion of the various parameters which influenced the final selection of the prototype structure.

2.1 STRUCTURE SIZE

Since it was decided that a prototype structure would be designed for the model study rather than use an existing building, the prototype could be designed to minimize problems associated with modeling. The largest model which can be placed in the 22-foot-10-inch-diameter LBLG test chamber is approximately 14 feet square. The smallest prototype structure having one floor panel of each of the three different types--i.e. corner, edge, and interior panels--is a three- by three-bay structure. Assuming that the model scale was to be 1:4, the prototype structure would be 56 feet square with approximately 18-foot bays.

The Building Design Data Manual published by the United States Steel Corporation (Reference 3) discusses the effects of bay size on the weight of structural steel used in a building. The 19 buildings discussed were designed as rigid frames with bent spacings of 20 and

28 feet and aisle widths of 20, 25, 30, and 60 feet. From the data presented, an aisle width of 20 feet with bent spacings of 20 feet was one of the more economical spacings. Based on this information, the dimensions of the prototype structure for this study were chosen to be 60 feet by 60 feet with a column spacing of 20 feet in each direction.

The story height was chosen somewhat arbitrarily to be 10 feet 6 inches. Reference 3 gives the structural characteristics for six office and apartment buildings. The floor to floor heights for these structures ranged from 9 feet 6 inches to 13 feet 8 inches. The 10-foot-6-inch story height was chosen assuming that the girders would be 12 inches deep, the floor slab 6 inches thick, and the ceiling height 8 feet. With these dimensions there would be 12 inches between the bottom of the beam and the ceiling. This was assumed adequate for any piping or wiring that had to be run above the ceiling.

Selection of a five-story prototype structure satisfied the requirement that the shelter come from a multistory building and reduced the calculations necessary to determine the beam and column sizes in the shelter area.

2.2 FRAME TYPE

The specification section of the AISC Manual of Steel Construction (Reference 4) permits three basic types of construction for structural steel frames. These are: Type I, designated as rigid frame and unconditionally permitted under the specification; Type II, designated as simple framing and permitted with stipulations on how the wind-loads are carried; and Type III, designated as semirigid and allowed if evidence can be furnished that the connections are capable of providing a predictable proportion of full end restraint.

Information contained in the RTI surveys was insufficient to determine which type of steel frames the surveyed buildings have. Most structural steel frame buildings are designed as Type II structures (Reference 5). However, it was felt that, by testing a rigid frame structure, sufficient information on the frame loading would be obtained to determine the response of a simple frame structure, whereas the

testing of a simple frame structure would not provide sufficient information to determine the response of a rigid frame structure.

2.3 FLOOR SYSTEM

Eight of the most common concrete floor systems found in steel frame buildings are shown in Figure 2.1. Composite action may be utilized with the open-web steel joist system (Figure 2.1a) and the steel decking floor system as it is shown with the steel beams (Figures 2.1b and c).

The following were the floor types listed for the first floor in the steel frame buildings surveyed by RTI in 1967:

Floor Type	Percentage of Buildings
1. Concrete--ordinary slab (cast-in-place)	75
2. Concrete--one-way ribbed joist	18
3. Cellular steel and concrete	3-1/2
4. Wood plank	3-1/2

The ordinary concrete slab is described as a flat slab with conventional reinforcement. This includes the floor slabs shown in Figures 2.1b, c, and g. In the preliminary results of the 1972 survey, there were 37 steel frame structures. The following is a listing of the frequency of occurrence of the floor types noted in the 1972 survey:

Floor Type	Percentage of Buildings
1. Steel beam and concrete slab	73
2. Cellular steel and concrete	6
3. Steel beam with tile or brick arch	6
4. Steel beam--one-way ribbed	6
5. Open-web steel joist	6
6. Flat plate	3

The category designated "steel beam and concrete slab" includes the floor slabs shown in Figures 2.1b, c, and h.

It was difficult to determine from the information in the surveys

whether the floor slabs were conventional one-way or two-way slabs. A one-way slab is essentially a wide beam whose response can be predicted readily by conventional two-dimensional analysis. Therefore, it was decided that the floor slabs in the prototype structures of this study would be conventional two-way slabs.

2.4 CONFIGURATION OF THE PROTOTYPE STRUCTURE

The prototype structure chosen (Figure 2.2) was five stories high with a 10-foot-6-inch floor-to-floor height for the aboveground stories and a 12-foot floor-to-floor height in the basement area. In plan, the structure had an aisle width and bent spacing of 20 feet. In order to simplify the model, the prototype structure contained only four bents. It contained all the column and floor panel types found in a structure (i.e. corner, edge, and interior panels).

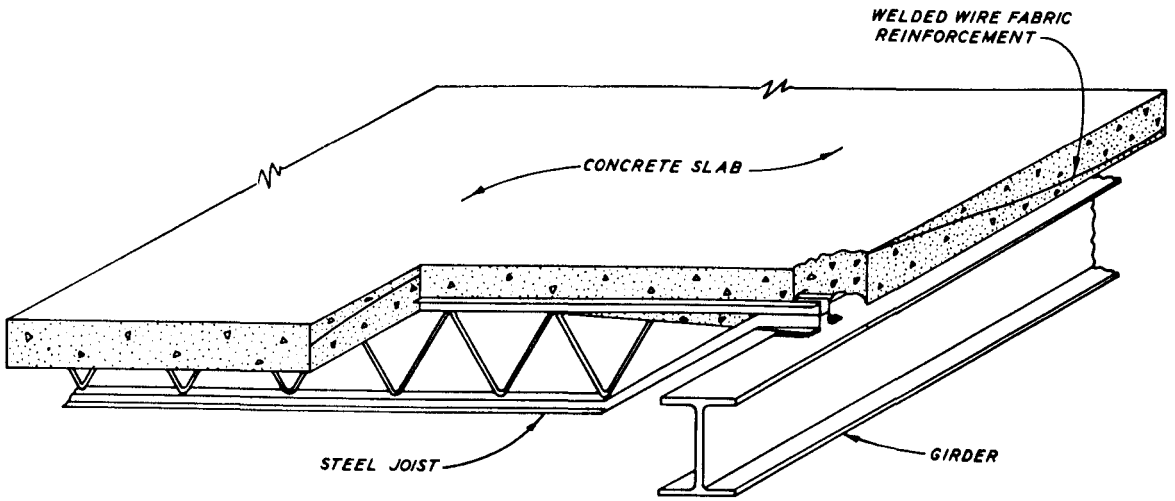

a. Concrete slab supported on open-web steel joist.

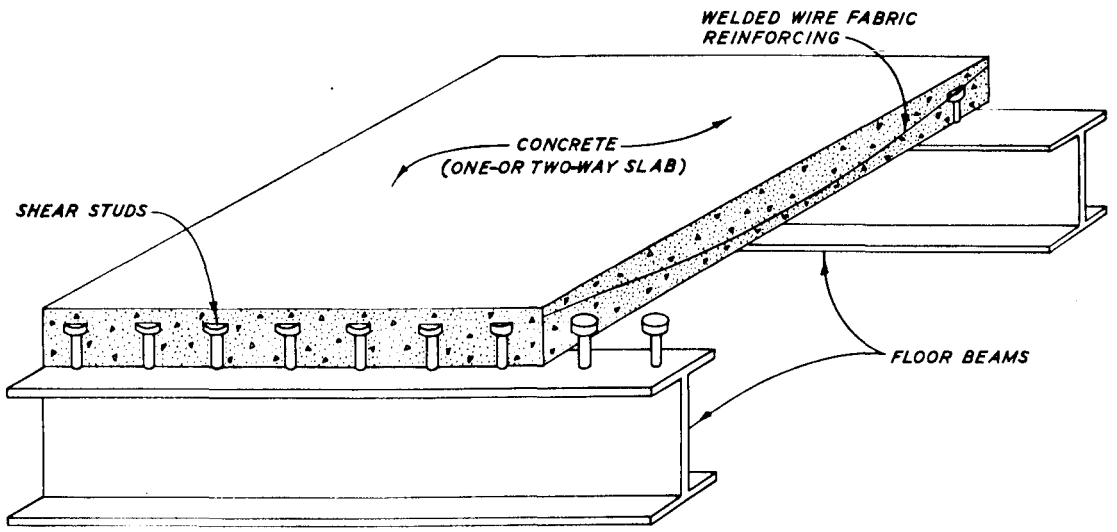

b. One- or two-way-reinforced concrete slab supported on steel beams.

Figure 2.1 Typical floor systems found in steel frame structures (sheet 1 of 4).

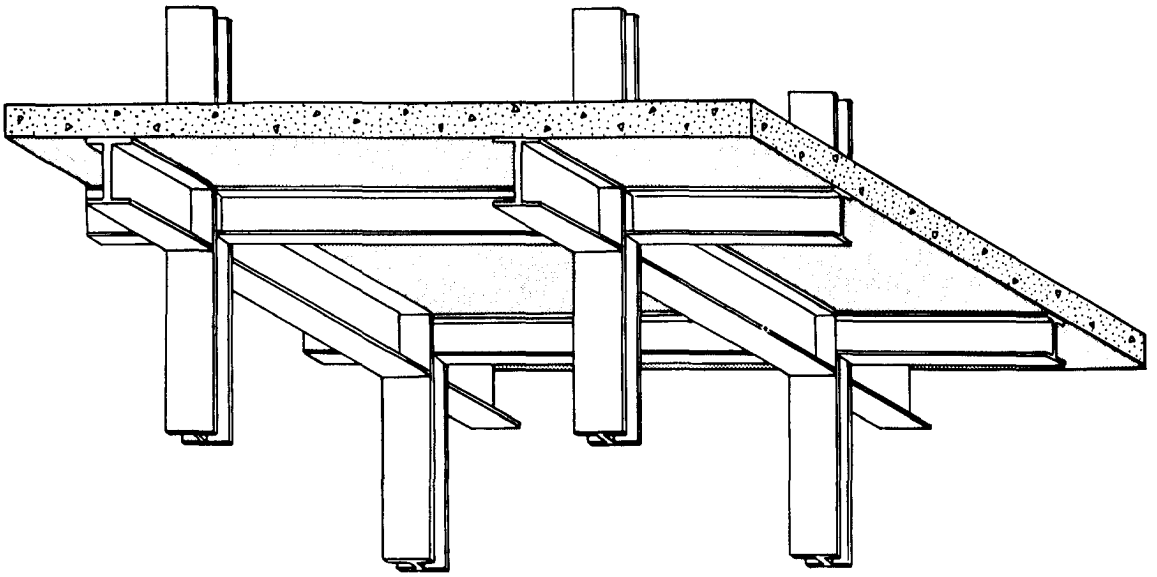

c. Concrete slab and steel beam composite floor.

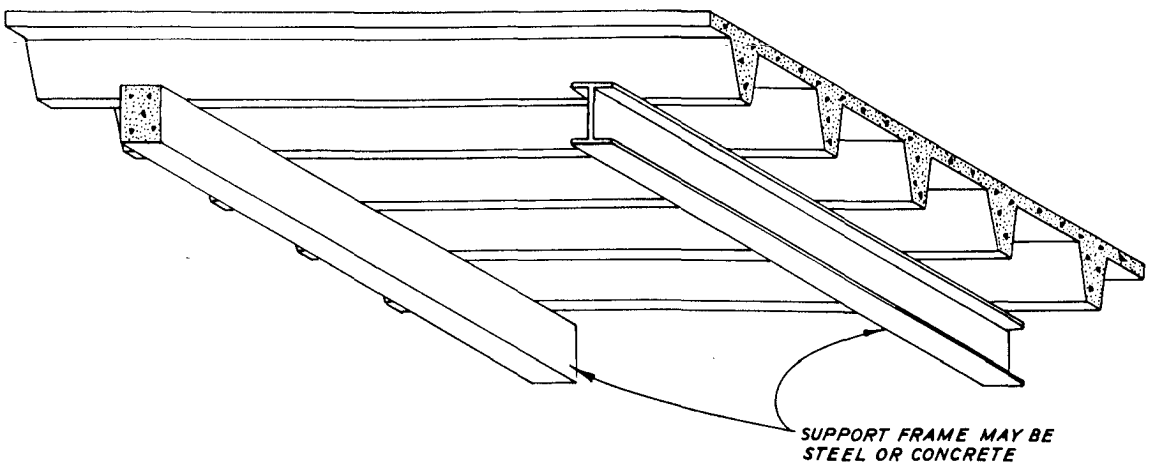

d. Concrete pan floors.

Figure 2.1 (sheet 2 of 4).

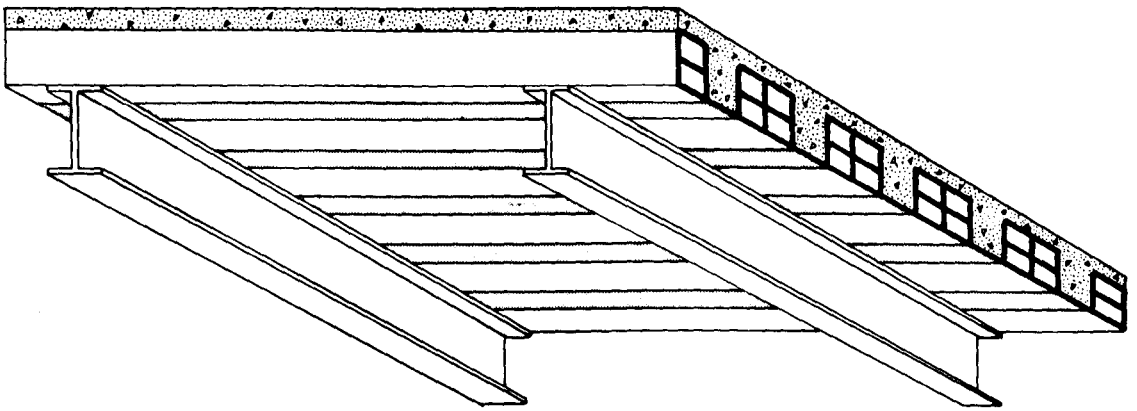

e. Structural clay tile, gypsum tile, or concrete block floor.

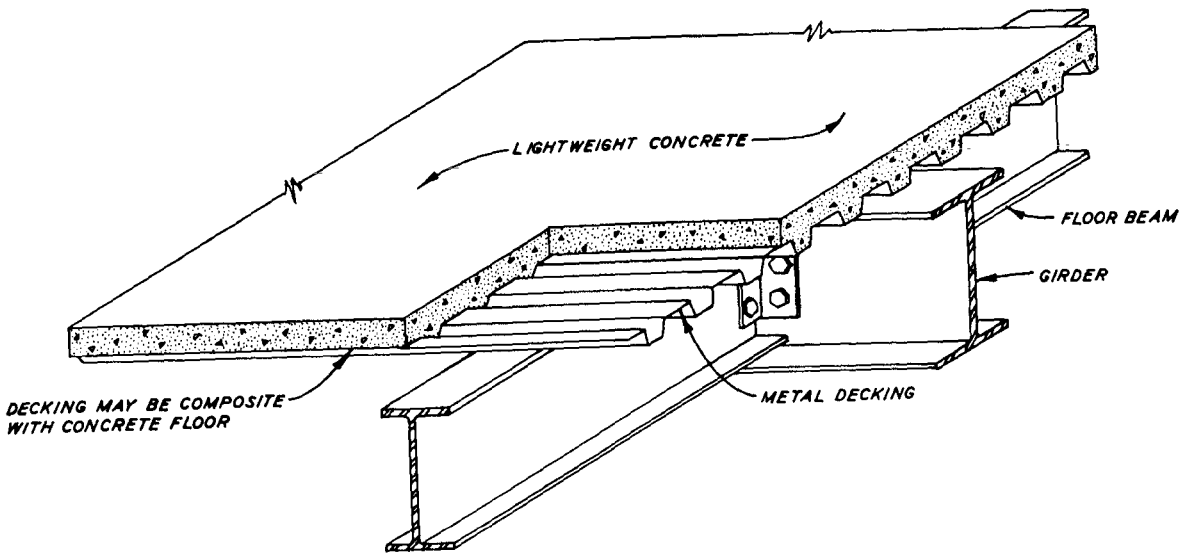

f. Steel decking floors.

Figure 2.1 (sheet 3 of 4).

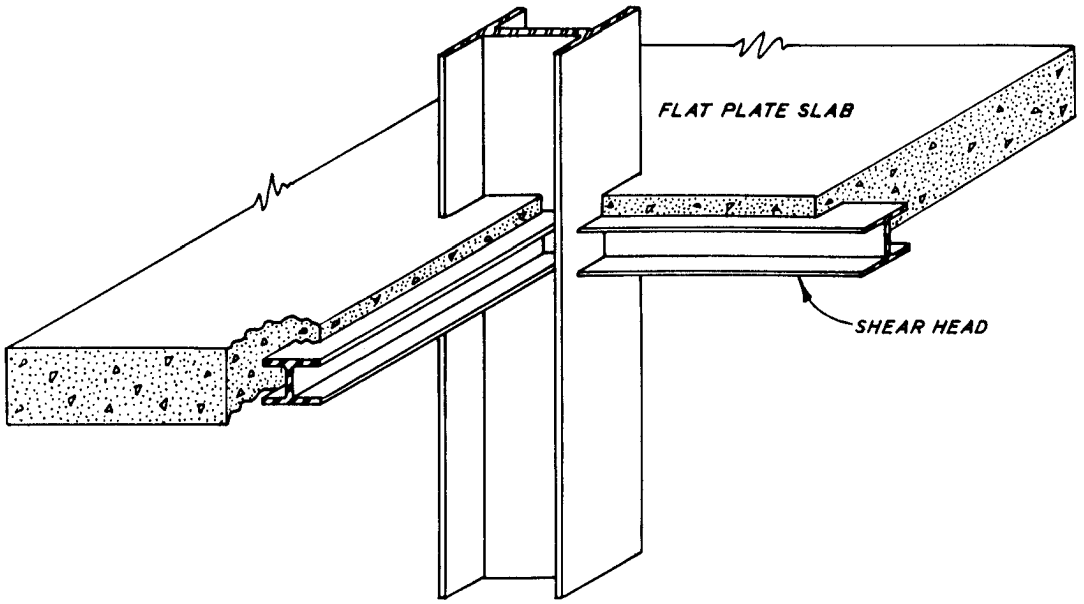

g. Flat plate floor system.

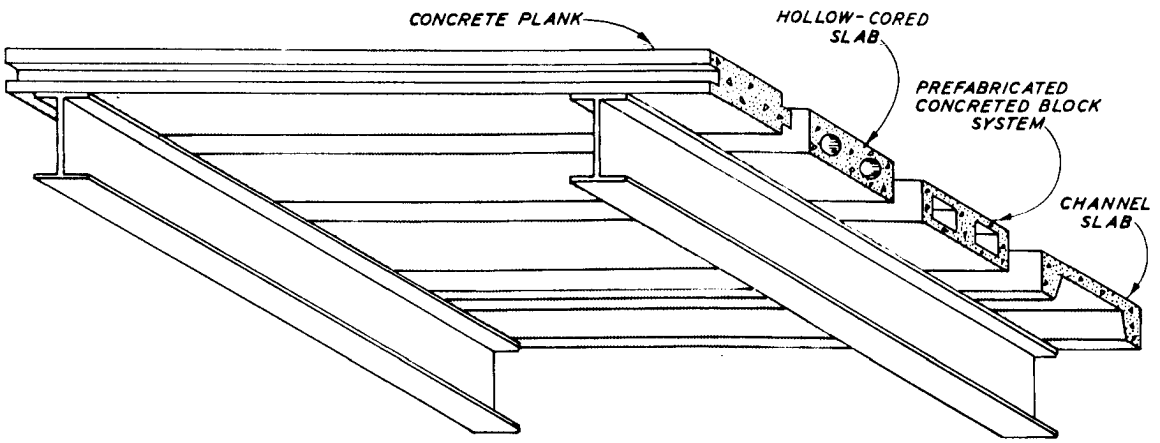

h. Precast concrete slab floor.

Figure 2.1 (sheet 4 of 4).

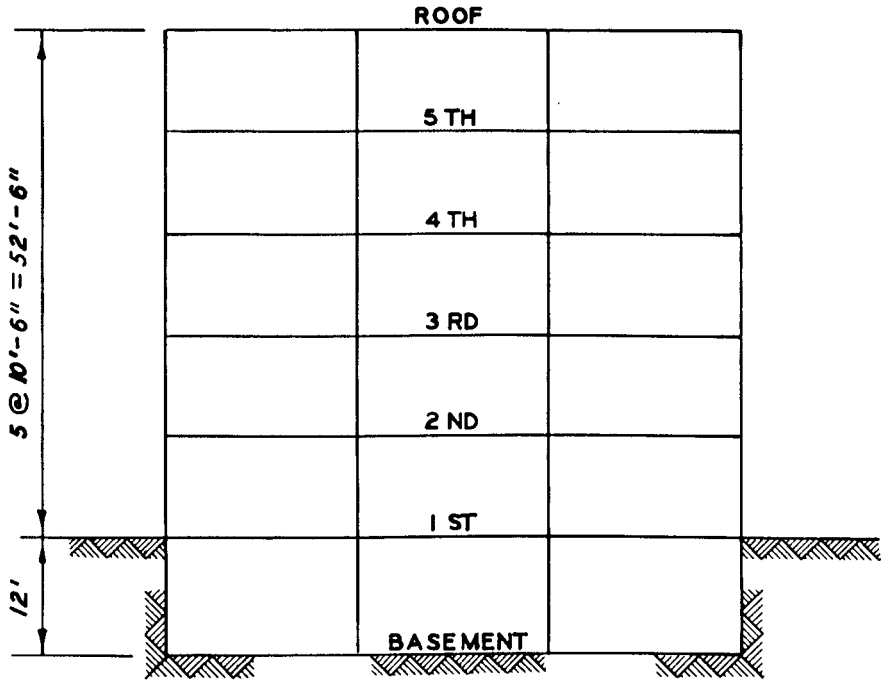

a. Elevation.

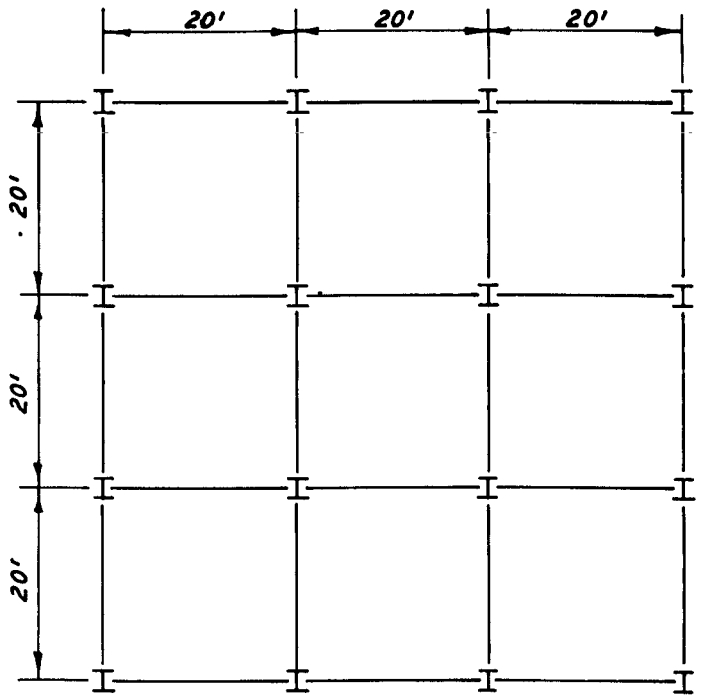

b. Plan.

Figure 2.2 Prototype geometry.

CHAPTER 3

DESIGN OF THE PROTOTYPE AND MODEL

The plan and elevation chosen for the prototype structure were discussed in Chapter 2. For purposes of this study, the building plan was to be square. However, the final results will also be applicable to a larger rectangular structure. The prototype can be considered to be a rectangular structure in which all but one of the inside bays have been removed and the end bays have been pushed toward the center, forming a three-bay by three-bay structure (Figure 3.1).

3.1 PROTOTYPE DESIGN SPECIFICATIONS

The prototype structure was assumed to be a commercial office building located in the Mississippi-Louisiana area and to have been constructed prior to 1955, since in the mid 1950's most structural steel buildings contained steel decking floor systems (see Figure 2.1f).

Windloads and floorloads used in the design of the prototype were obtained from the 1970 edition of the Uniform Building Code (Reference 6).

3.1.1 Windloads. According to References 5 and 7, it can be assumed that the wind forces acting on a structure which is three to five stories high and has a height to width ratio of unity or less can be resisted by composite action between the structural frame and the floor and exterior walls. The prototype structure for this study had a height to width ratio of approximately one in both directions and was five stories high. Since the square structure design was marginal with regard to windloads, wind forces were applied to the structure only in the direction perpendicular to the strong axes of the columns. The weak axes of the columns are normally placed perpendicular to the long dimension of a building. Therefore, if the prototype structure were rectangular, the height to width ratio in the direction of the weak axes of the columns would become much less than unity, eliminating the need for designing for windloads in that direction.

The design wind loading and its distribution to the steel frame of the prototype structure are shown in Figure 3.2.

3.1.2 Floorloads. Floors two through five were considered to be commercial office space and were designed only to the point of determining the loads which would be transmitted to the supporting beams. In Reference 6, design live loads are given as 80 psf for commercial office areas with an additional 20 psf for movable partitions. Dead loads are listed as 75 psf for floor slabs, 5 psf for the floor finish, and 5 psf for suspended ceilings of the rooms on the floor below. The total design loads for the upper floor slabs in this study were 100-psf live load and 85-psf dead load.

The roof was designed to carry 40-psf live load and 50-psf dead load consisting of a 4-inch concrete slab, 6-psf insulating concrete, and 5 psf for built-up roofing.

A complete design was done for the first floor slab since it was the slab of concern in the model test program. The design live load was 140 psf, consisting of 120 psf for live load (due to a large lobby area) and 20 psf for movable partitions. The design dead load was 100 psf, consisting of 75 psf for the 6-inch-thick concrete floor slab, 15 psf for the floor finish, and 10 psf for the equipment hanging from the underside of the floor slab.

3.1.3. Steel Frame. Loads on the steel frame were obtained from the windloads and floorloads previously discussed with the exception of the outside edge beams which also carried the weight of the exterior walls.

The exterior walls were assumed to be 50 percent brick and 50 percent glass. Based on Reference 4, the brick wall weight was assumed to be 80 psf and the weight of the glass portion (including the frame and sash) was taken to be 8 psf. The loading per foot from the weight of the wall was 462 lb/ft.

The floors were assumed to transfer their loads to the supporting beams in a uniform manner along the length of the beams.

The steel frame was designed as a rigid frame using steel with a yield strength of 36,000 psi following specifications in the sixth

edition of the AISC Steel Construction Manual (Reference 4).

The connections were designed as rigid bolted connections using A-307 bolts. Bolted connections were chosen over riveted and welded connections because they were becoming more prevalent in modern construction.

3.2 PROTOTYPE DESIGN

3.2.1 Steel Frame. As mentioned previously, the structural steel frame of the prototype structure was designed as a rigid frame. The beam-column connections on the flange of the columns were designed to carry windload and floorload moments. The beam-column connections to the web of the columns were designed to resist floorload moments only.

The structure was divided into four frames and loaded with the windloads and floorloads as shown in Figures 3.2 and 3.3a. Trial column and beam sizes were obtained by using the Portal method (Reference 7) to obtain moments due to the windloads and by adding the moments obtained by calculating the fixed-end moments for the beams due to the uniform loading from the floors. The SAP Code (Reference 8), a three-dimensional structural analysis code, was used in two dimensions to calculate moments, shears, and axial loads for the trial frames which were loaded with the design windloads and floorloads. After each computer run, the columns and beams were changed as necessary to keep the maximum stress levels within the allowable range given in the AISC specifications. The allowable stresses were increased by 1/3, since the structure was being designed for windloads.

After obtaining column and beam sizes which had stress levels below, but near, the allowable stress, the floor loading was changed from a uniform loading on all spans to a pattern loading (Figure 3.3b). Since this loading, consisting of placing the design dead load on all spans and the live load on alternating spans, was found to be the most severe, it was used to obtain the final design. The final beam and column sizes are shown in Figure 3.4.

The output of the SAP code included horizontal deflections for the frames at each story level. These deflections were compared with the allowable deflection of 0.002 times building height given in Reference 9.

For the columns, the output of the code gave the moments at both ends of the column and the axial loads on the column. The moment on the column was converted to an axial load by the procedure given in Part 3 of the AISC manual. The required column size was then obtained from the tables in the manual. The combined axial and bending stresses were checked for both axes of the column.

During the selection of the beams and columns, consideration was given to the thickness of the webs and flanges since the structural members were ultimately to be modeled. In doing this, the minimum weight section having the required moment of inertia was not necessarily chosen. The minimum weight section usually was slightly deeper with a thinner web and flange.

To provide fire protection for the beams and columns of the prototype structure they were considered to have been embedded in concrete. Composite action between the concrete cover and the embedded steel sections was not considered in the design since the structure was designed to represent older steel frame construction and composite design was approved by the AISC specifications in 1952 (Reference 5). Composite design was initially used only for bridges but, since its acceptance by AISC, has gained popularity for steel frame structures.

The bolted connections were designed to carry the end moments calculated by the SAP code for the framing beams. The split-beam type connection, classified as a semirigid connection, was used for all connections (Figure 3.5). However, they are often considered fully rigid connections (Reference 9) as was the case in this design.

3.2.2 Floor Slabs. The first floor slab was designed using working stress design and Method 1 for two-way-reinforced slabs in the 1963 ACI Building Code (Reference 10). Since this structure was to represent the older steel frame structures in the NFSS, the oldest design method for two-way slabs accepted by the ACI was chosen for the design. Method 1 was originally developed for the 1939 New York City building code and was adopted by the ACI building code in 1941.

Reference 7 states that for slab panels that are square or almost square and supported on beams on all four sides, the slab depth and

reinforcing are often designed for half the load and the resulting steel is then placed in both directions, the top layer of steel being placed at the design depth below the top of the slab. This method results in a more conservative design than the method given in the ACI building code. Since there is no way of determining which method was used most frequently by designers, the ACI code method was used.

Figure 3.6 shows the design moments obtained by using Method 1 and the required steel percentages to resist these moments. Cutoff points and bend locations for the reinforcing steel were obtained from Figure E.13 of Reference 11. This figure was based on the 1956 edition of the ACI code. However, the portion of the 1956 ACI code on which Figure E.13 was based was not changed substantially in the 1963 edition. The concrete strength used for the design was 3000 psi, and the reinforcing steel was Grade 40.

As mentioned previously, only the first floor slab was designed completely. The design loads were 140-psf live load and 100-psf dead load. Number 4 rebars were used at all locations in the prototype slab to avoid having different size bars in the model which would complicate its fabrication.

3.3 MODELING OF THE PROTOTYPE

3.3.1 Model Scale. A model scale of 1/4.5 was chosen for the experimental study. It was desirable for the model to be as large as possible to reduce the problems associated with fabricating the structural steel members for the model and to ease the fabrication of formwork for the model. The 1/4.5 scale gave the largest model that could be accommodated in the 22-foot-10-inch-diameter LBLG test chamber and still have enough soil around the walls of the model to allow development of soil-structure interaction. However, this scale was not large enough to allow the use of small-aggregate concrete for the floor slabs in the model and thus mortar had to be used for these slabs.

3.3.2 Relationships of Quantities in the Models and in the Prototype. Since gravity cannot be scaled, the model carried slightly more load than the prototype. The deadweight of the model floor slabs

was approximately 80 percent less than that of the prototype slabs, giving the model an approximately 0.4-psi increase in load-carrying capacity over the prototype.

From the laws of similitude, stresses and strains scale directly between model and prototype. The deflections and time scales (model to prototype) were 1 to 4.5. Velocities in the model and the prototype scaled one to one. Accelerations in the model were 4.5 times those in the prototype.

3.4 DESIGN AND DESCRIPTION OF THE MODELS

3.4.1 Description of the Models. The features of the prototype structure which were of primary interest for the model test program were the floor slabs above the basement area and the steel frame which supported these slabs. This portion of the multistory prototype was modeled as an open box-type unit consisting of the first floor slab, supporting beams for the slabs, the basement columns, and the basement walls.

To simulate fixity of the base of the basement columns and basement walls, the model was bolted on a heavily reinforced concrete base slab.

Dimensions of the model were obtained by dividing prototype dimensions by 4.5. Figures 3.7 and 3.8 show a plan view and cross section for one of the models.

3.4.2 Model Steel Framing Members. Dimensions of the prototype beams and columns were divided by 4.5 to obtain the required dimensions for the model members. Since the model structural steel members did not match the size of any of the small wide flange beams, junior beams, or miscellaneous beams commercially available, it was necessary to fabricate these members. This was accomplished by welding strips of steel sheet together to form the model structural members.

The web and flange thicknesses required for the model members were in between the standard thicknesses of steel sheet and plate. By using the steel sheet with a thickness closest to that required for the model webs and flanges, the mechanical properties of the model structural members were off by as much as 10 percent. The scaled heights and widths of the model members were adjusted slightly to obtain areas and moments

of inertia as close as possible to the scaled values. Final moments of inertia were within 0.6 percent of the scaled values and the cross-sectional areas were within 6 percent of the scaled values. Figure 3.9 shows the final dimensions and mechanical properties of the model beams and columns.

3.4.3 Connections. The web and flange thickness of the model structural tee's for the connections presented the same problems as the webs and flanges of the model beams. By using steel sheet with a thickness closest to that required, model moments of inertia and areas varied a maximum of 7 percent from scaled areas and moments of inertia. Since the structural tee's had many holes in them for the bolt connections, it was not possible to adjust the flange width and web height to obtain moments of inertia and areas closer to the scaled values. The dimensions of the model structural tee's and their properties are given in Figure 3.10. A typical beam-column connection is shown in Figure 3.11.

The bolts in the prototype connections were 1- and 1-1/8-inch-diameter, coarse-threaded A307 bolts. The root area of the threads of both bolt sizes was divided by 20.25 ($4.5 \times 4.5 = 20.25$) to obtain the root area of the threads for the model bolts. The two prototype bolt sizes could be modeled with 1/4-inch-diameter bolts having fine and coarse threads. The 1/4-inch fine-threaded bolt modeled the 1-1/8-inch prototype bolts; the 1/4-inch coarse-threaded bolt modeled the 1-inch prototype bolt. These bolts were available in the same material as the prototype bolts.

3.4.4 Floor Slabs. The model slab thickness, reinforcement spacing, reinforcing cutoff points, and bend locations for the truss bars were derived by dividing the corresponding quantities in the prototype slabs by 4.5. The model dimensions for the No. 4 rebars reinforcing the slab were derived by dividing the cross-sectional area of the prototype bars by 20.25 to obtain the required cross-sectional area for the model bars. The area of the model reinforcing bars was 0.00987 $in.^2$, requiring a bar with a diameter of 0.112 inch (between 11 and 12 gage). Eleven gage wire remnants from a previous test program were used for the model. To adjust for the slight increase in area due to the 11 gage

wire being larger than required, the reinforcement spacing was multiplied by the ratio of the diameter of the 11 gage wire to the required diameter (0.1205/0.112).

The reinforcing bar schedule for the models is given in Table 3.1, and the bar layout is shown in Figure 3.12. Details of the slab reinforcing are shown in Figure 3.13.

3.4.5 Beam and Column Fireproofing. The beams and columns of the prototype structure were assumed to be encased in concrete for fireproofing. The dimensions of the encasement and reinforcing mesh required to hold the concrete in place for the prototype structure were obtained from Section 4303 of the Uniform Building Code (Reference 6).

To receive a 4-hour fire rating, the columns had to be covered with a minimum of 1-1/2 inches of concrete and the beams covered with a minimum of 2 inches of concrete. The scaled thicknesses for the fireproofing were 7/16 and 1/3 inch for the beams and columns, respectively. Since these were minimum thicknesses, the cover for the prototype columns was increased to 2-1/2 inches, giving a model fireproofing thickness of 9/16 inch for the columns. Hence, the placement of the fireproofing concrete around the columns was more easily achieved.

The reinforcing steel in the fireproofing concrete, as specified by Reference 6, was 0.025 $in.^2/ft$ in both directions for beams and a minimum of 0.18-inch-diameter wire wrapped spirally around the columns on a pitch not exceeding 8 inches providing 0.038 $in.^2$ of steel per foot of column height. The scaled areas of steel were 0.0055 $in.^2/ft$ for the beams and 0.00845 $in.^2/ft$ for the columns.

Standard size wire mesh had steel areas per foot much larger than required. Attempts were made to pull and cut wires out of a close woven wire mesh to obtain the desired steel area per foot; however, both methods proved impractical.

The lightest gage hexagonal netting (chicken wire) available was made from wires 0.348 inch in diameter with a steel area of 0.0114 $in.^2/ft$, approximately twice the required steel area for beams and 1.35 times the required steel area for columns. The design of the hexagonal netting prevented cutting of wires to reduce the steel area.

Since the steel mesh reinforcing in the fireproofing was not used for structural reinforcing, the hexagonal netting was used for fireproofing the beams and columns in the model (Figure 3.14).

3.4.6 Wall Design. The basement walls were included in the model primarily to close off the underside of the floor slabs during the tests. The walls also transmitted in-plane forces due to the soil loading on the walls to the floor slabs. In a previous test (Reference 12), this in-plane loading increased the slab's strength by approximately 30 percent.

The measured horizontal soil forces (Reference 12) varied from 0.2 times the overpressure near the base of the wall to 1.35 times the overpressure near the top of the wall. With an expected slab failure in the 10-psi range, the loading on the basement wall of the model would vary from 2 psi near the base of the wall to 13.5 psi near the top of the wall. Steel frame structures normally have either concrete block or reinforced concrete basement walls. From the results of tests conducted on concrete block wall panels (Reference 13), the expected loading would fail this type of wall. Therefore, the prototype structure was assumed to have reinforced concrete basement walls.

The basement walls were designed using conservative assumptions to prevent a wall failure prior to failure of the floor slabs or steel frame. The design load was taken as the loading from the soil backfill only and then as a uniform loading of 10 psi. The top of the wall was assumed pinned for both loading cases, and the base was assumed fixed for one condition and pinned for the other. The fixed-pinned condition with the 10-psi uniform loading was the most severe condition and therefore was used for the design. The base of the model wall was to be bolted to a base slab on which the model would be tested.

Reinforcing for the model basement walls (Figure 3.15) consisted of an inside and outside mat of welded wire fabric having a 4- by 4-inch mesh of No. 4 wires.

To provide access to the inside of the model after it had been placed in the test chamber, an opening of approximately 24 by 27 inches was provided in one wall of each model. The opening was framed by an

8-inch-wide by 5-2/3-inch-deep beam, which was reinforced with No. 4 rebars (Figure 3.16).

TABLE 3.1 BENDING SCHEDULE FOR FLOOR SLAB REINFORCING

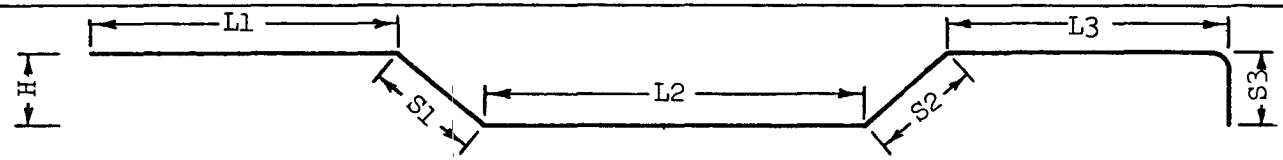

Mark	H	L1	S1	L2	S2	L3	S3
S01	7/8 in.	2 ft 4-7/16 in.	1-1/2 in.	2 ft 9-15/32 in.	1-1/2 in.	9-29/32 in.	3 in.
S02	7/8 in.	1 ft 9 in.	1-1/2 in.	2 ft 9-15/32 in.	1-1/2 in.	9-29/32 in.	3 in.
S03	7/8 in.	0	0	3 ft 8-25/32 in.	1-1/2 in.	9-29/32 in.	3 in.
S04	7/8 in.	2 ft 4-7/16 in.	1-1/2 in.	2 ft 6-9/16 in.	1-1/2 in.	2 ft 4-7/16 in.	0
S05	7/8 in.	1 ft 9 in.	1-1/2 in.	2 ft 6-9/16 in.	1-1/2 in.	1 ft 9 in.	0
S06	5/8 in.	2 ft 4-7/16 in.	7/8 in.	2 ft 9-15/32 in.	7/8 in.	9-29/32 in.	3 in.
S07	5/8 in.	1 ft 9 in.	7/8 in.	2 ft 9-15/32 in.	7/8 in.	9-29/32 in.	3 in.
S08	5/8 in.	0	0	3 ft 8-25/32 in.	7/8 in.	9-29/32 in.	3 in.
S09	5/8 in.	2 ft 4-7/16 in.	7/8 in.	2 ft 6-9/16 in.	7/8 in.	2 ft 4-7/16 in.	0
S10	5/8 in.	1 ft 9 in.	7/8 in.	2 ft 6-9/16 in.	7/8 in.	1 ft 9 in.	0
Straight bars	0	0	0	4 ft 5-1/8 in.	0	0	0

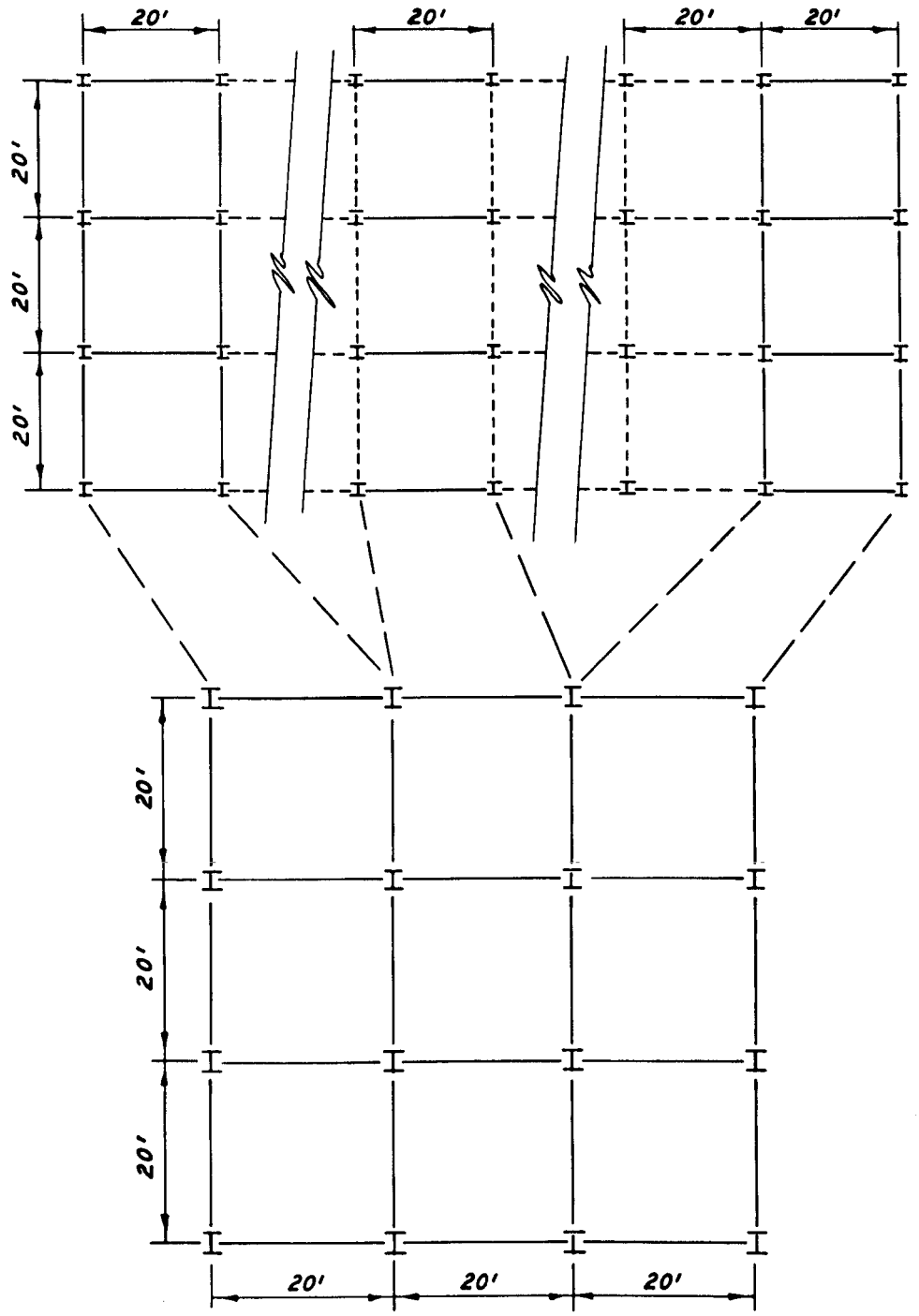

Figure 3.1 Reduction of rectangular prototype structure to square configuration.

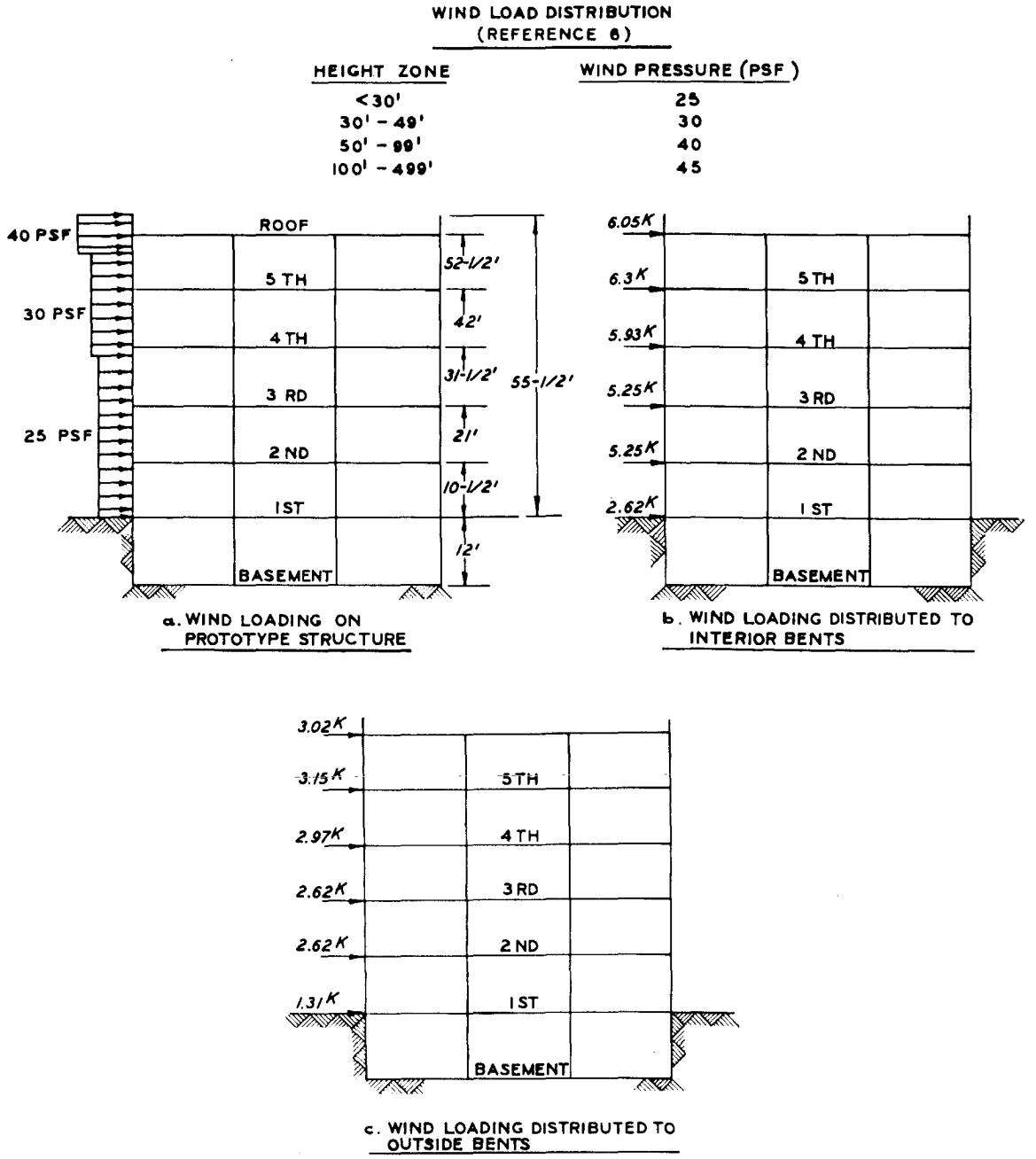

Figure 3.2 Distribution of windloads on prototype structure.

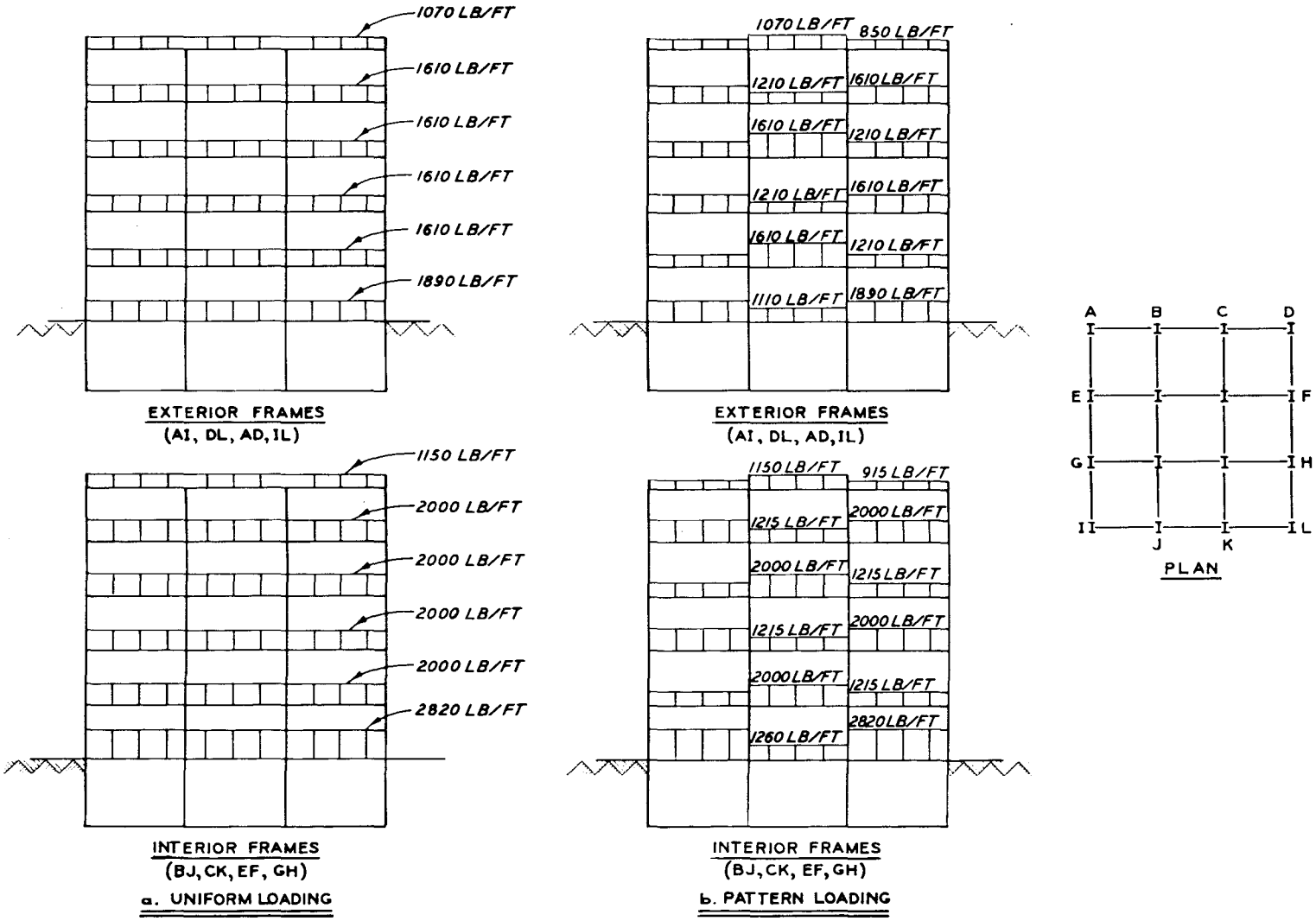

Figure 3.3 Roofloads and floorloads used for prototype frame design.

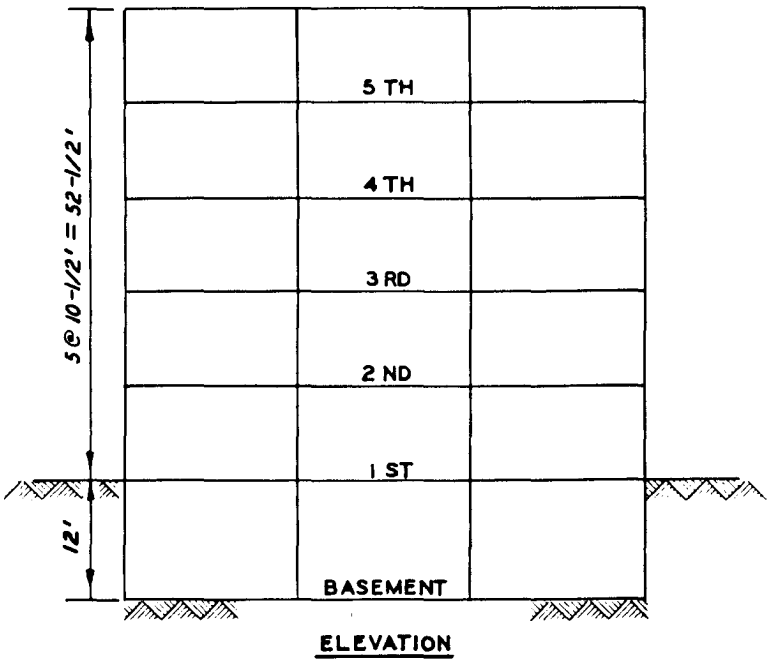

GIRDER SCHEDULE

LEVEL	SIZE
ROOF	W12 X 22
5TH	W14 X 26
4TH	W14 X 26
3RD	W14 X 30
2ND	W14 X 30
1ST	W16 X 36

COLUMN SCHEDULE

LEVEL	SIZE
ROOF - 5 TH	W12 X 45
5TH - 4TH	W12 X 58
4TH - 3RD	W12 X 58
3RD - 2 ND	W12 X 79
2 ND - 1 ST	W12 X 79
1 ST - BASEMENT	W12 X 106

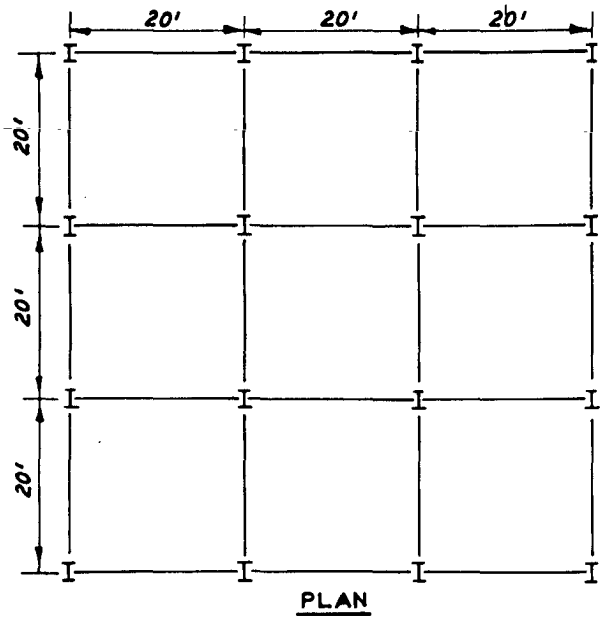

Figure 3.4 Beam and column schedule for prototype structure.

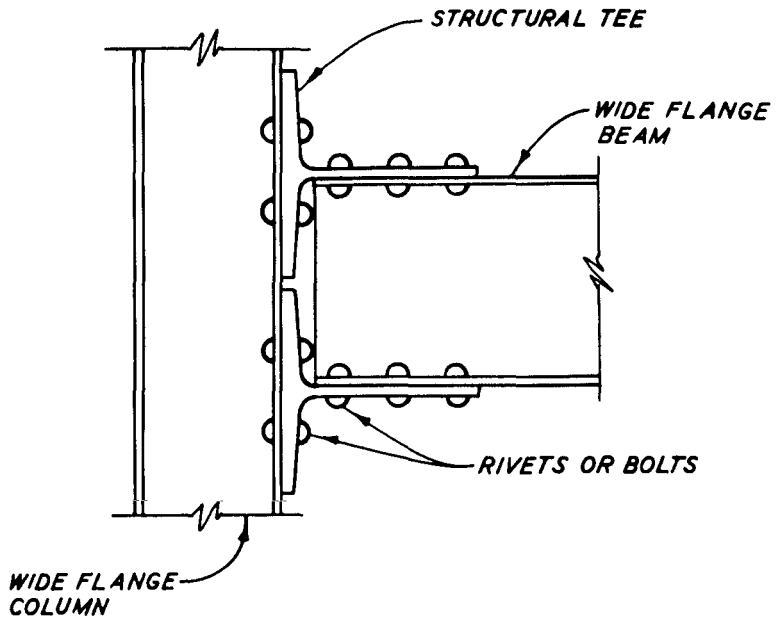

Figure 3.5 Split-beam rigid connection.

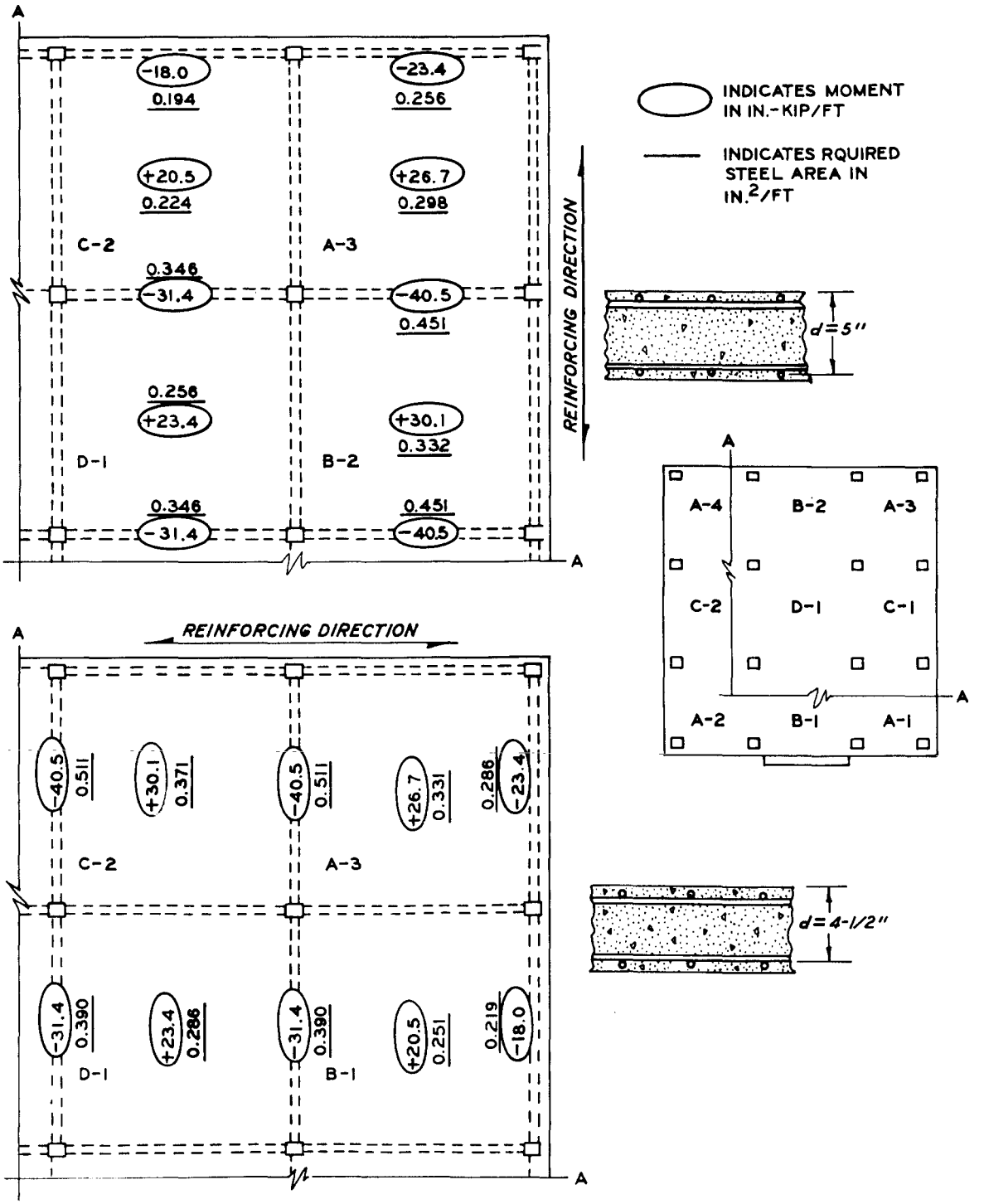

Figure 3.6 Design moments and reinforcing steel areas for prototype floor slabs.

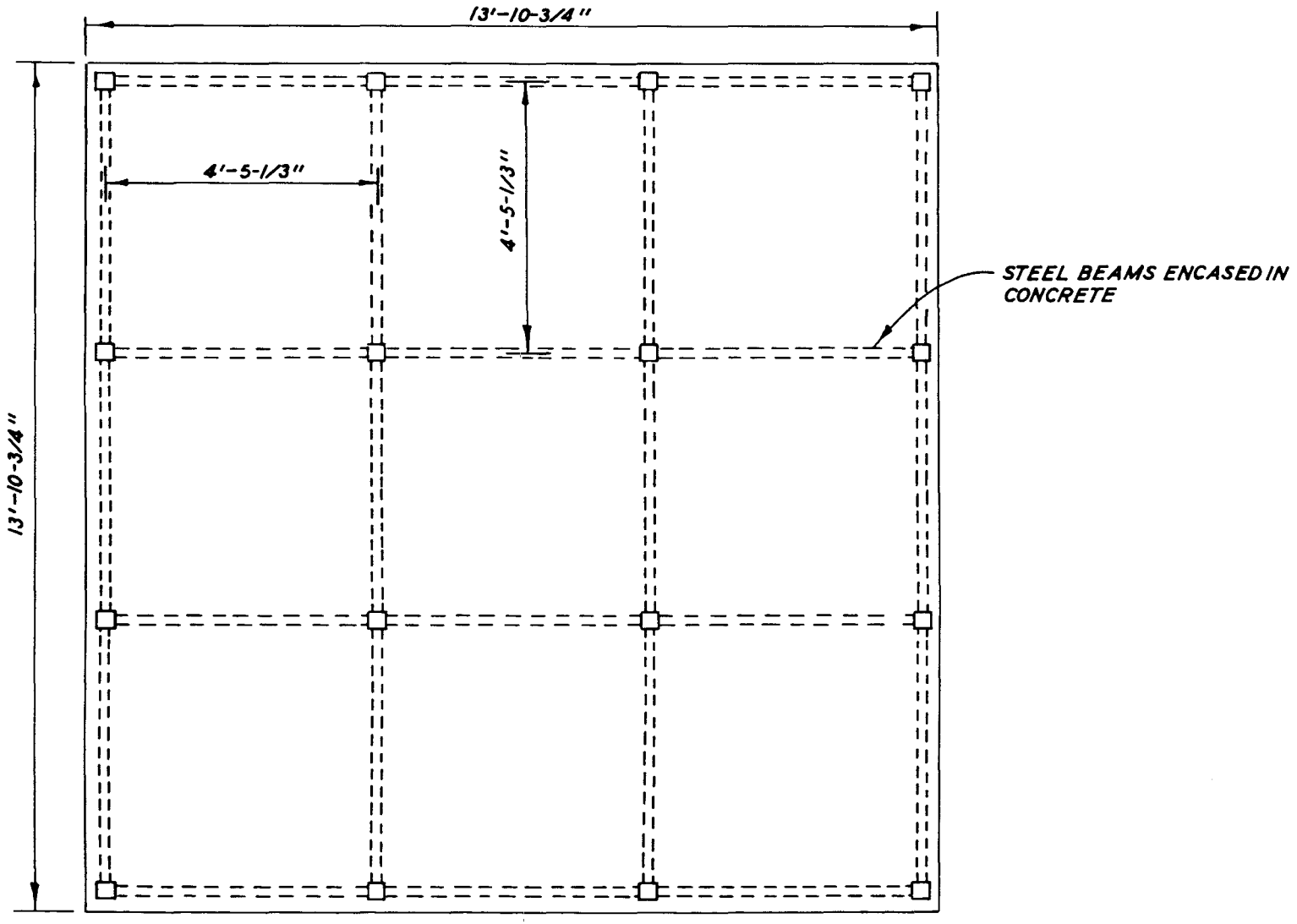

Figure 3.7 Plan view of model.

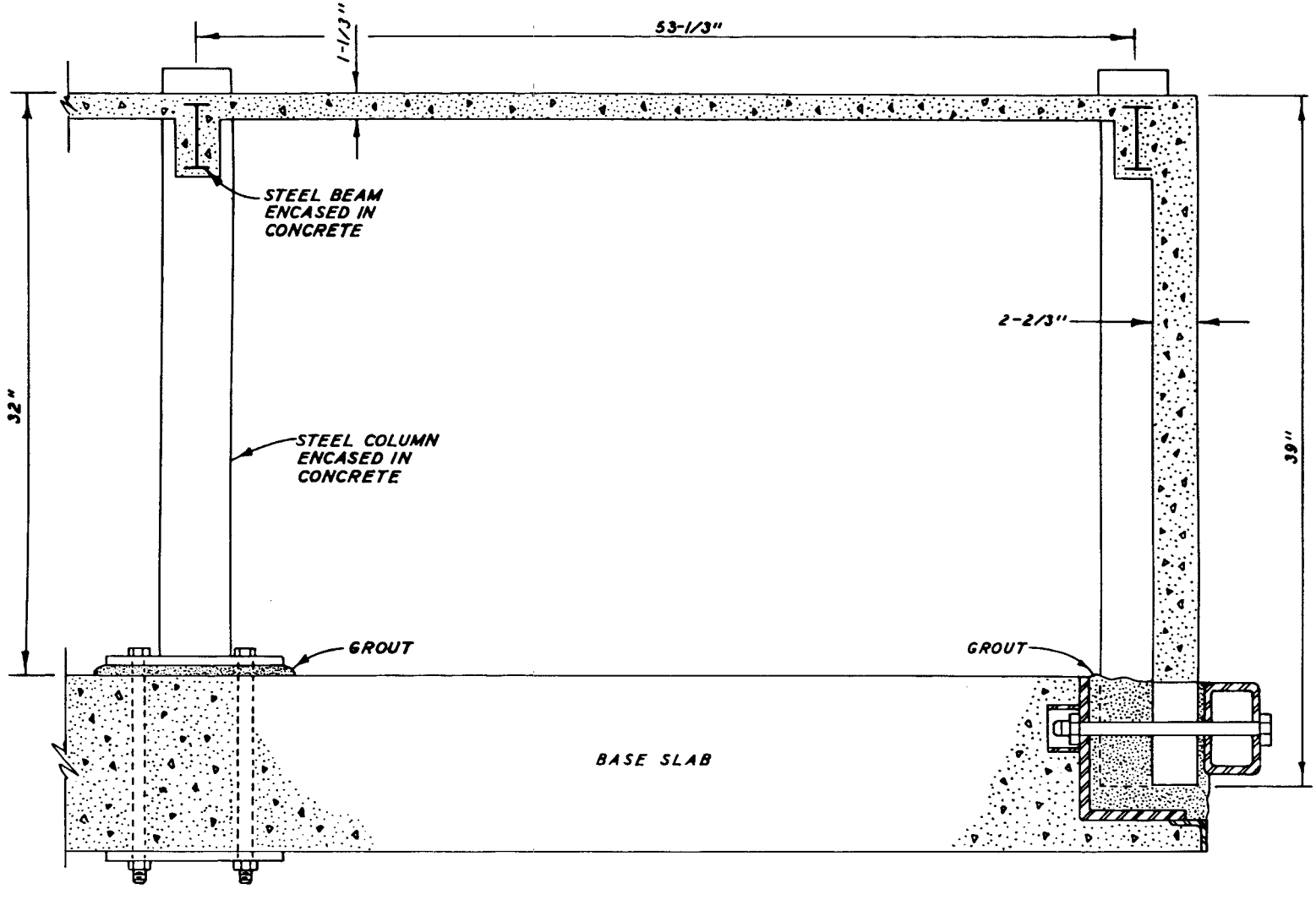

Figure 3.8 Partial cross section of model on the base slab.

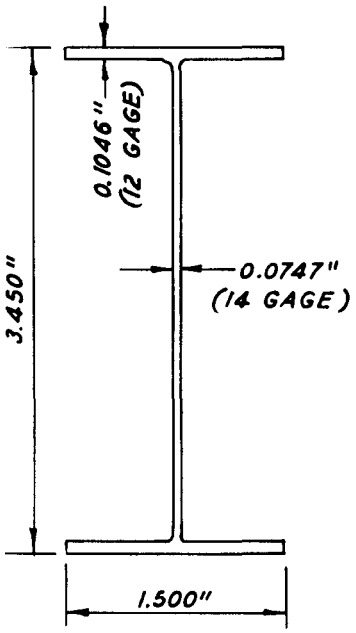

MODEL BEAM
W16 X36

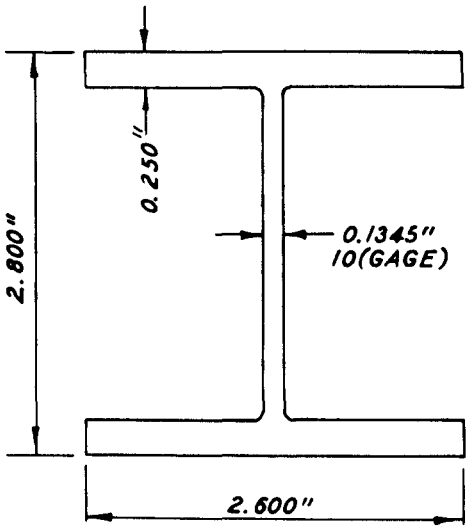

MODEL COLUMN
W12 X106

MECHANICAL PROPERTIES

		PROTOTYPE	SCALED	MODEL	$\frac{\text{SCALED}}{\text{MODEL}} \times 100\%$
W16 X 36	I_{XX}	447 IN.^{4}	1.090 IN.^{4}	1.090 IN.^{4}	100%
	I_{YY}	24.4 IN.^{4}	0.059 IN.^{4}	0.059 IN.^{4}	100%
	AREA	10.6 IN.^{2}	0.524 IN.^{2}	0.556 IN.^{2}	94.6%
W12 X 106	I_{XX}	931 IN.^{4}	2.270 IN.^{4}	2.256 IN.^{4}	100.6%
	I_{YY}	301 IN.^{4}	0.734 IN.^{4}	0.733 IN.^{4}	100.1%
	AREA	31.2 IN.^{2}	1.541 IN.^{2}	1.609 IN.^{2}	95.7%

Figure 3.9 Dimensions and mechanical properties of model beams and columns.

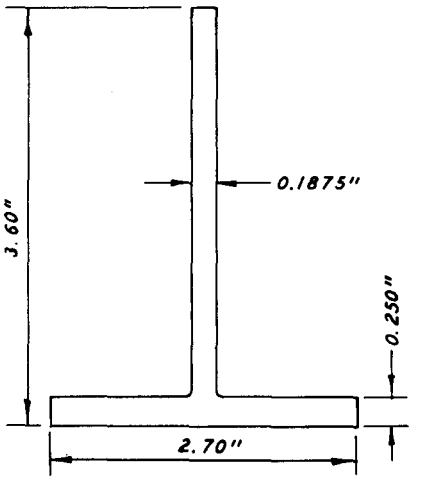

MODEL ST 18 X 97

	SCALED	MODEL	MODEL/SCALED
I_x	1.571	1.645	1.05
I_y	0.433	0.412	0.95
A	1.332	1.303	0.98

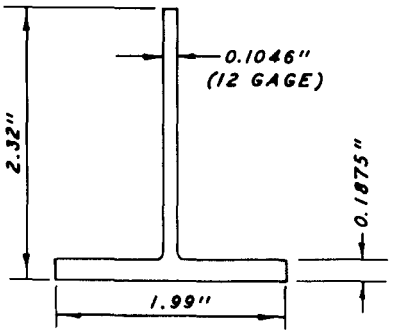

MODEL ST 10 X 41

	SCALED	MODEL	MODEL/SCALED
I_x	0.282	0.273	0.97
I_y	0.117	0.123	1.05
A	0.589	0.596	1.01

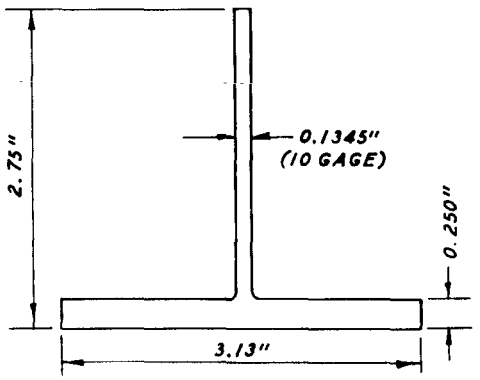

MODEL ST 12 X 80

	SCALED	MODEL	MODEL/SCALED
I_x	0.662	0.623	0.94
I_y	0.655	0.639	0.98
A	1.153	1.119	0.97

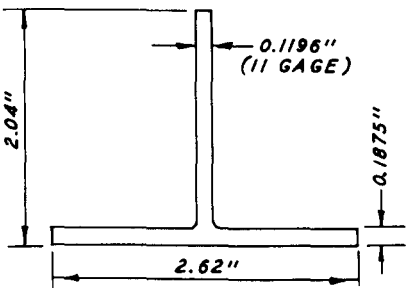

MODEL ST 9 X 52.5

	SCALED	MODEL	MODEL/SCALED
I_x	0.229	0.224	0.97
I_y	0.303	0.281	0.93
A	0.756	0.713	0.94

Figure 3.10 Dimensions and mechanical properties of model structural tee's.

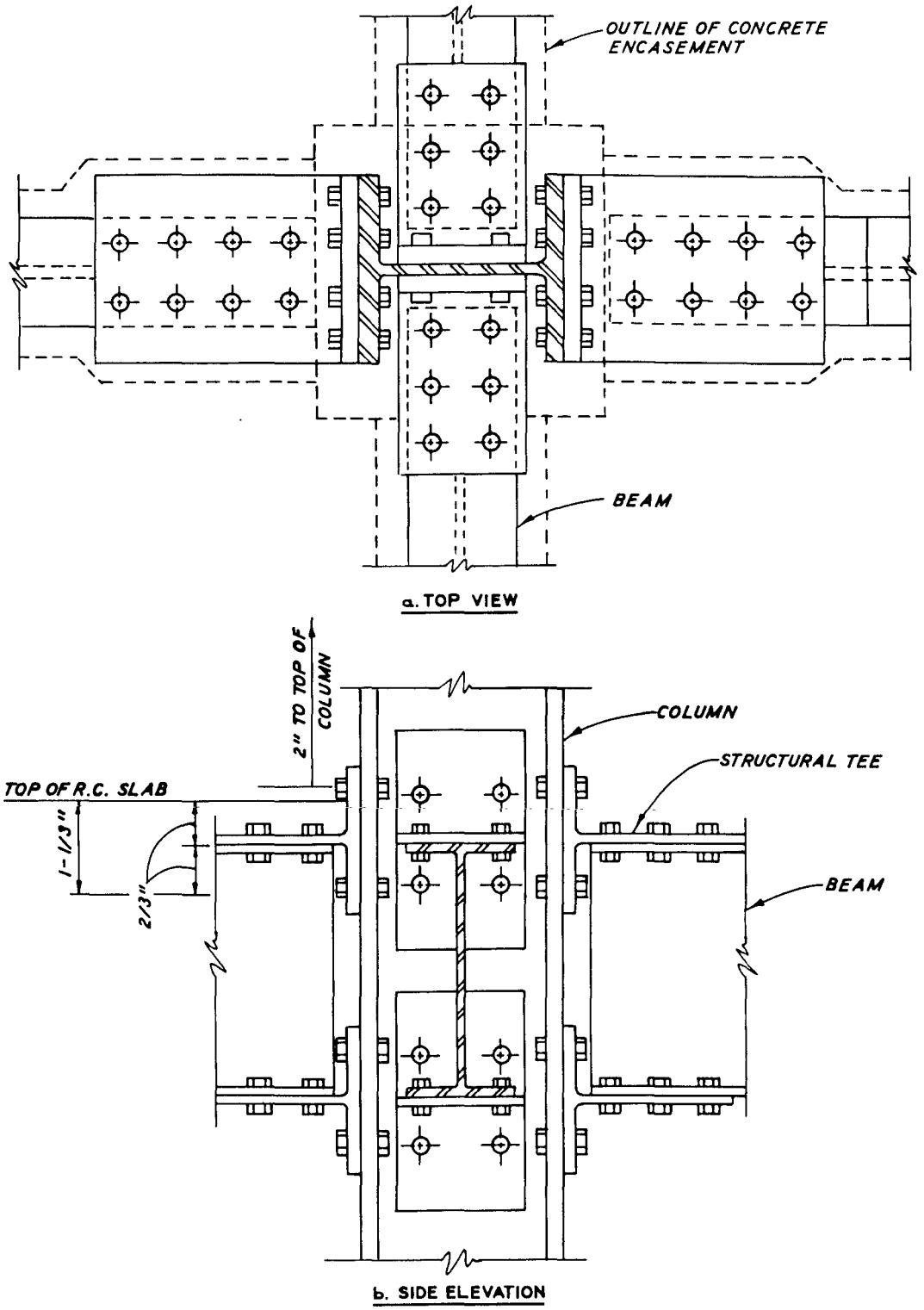

Figure 3.11 Typical interior beam-column connection detail.

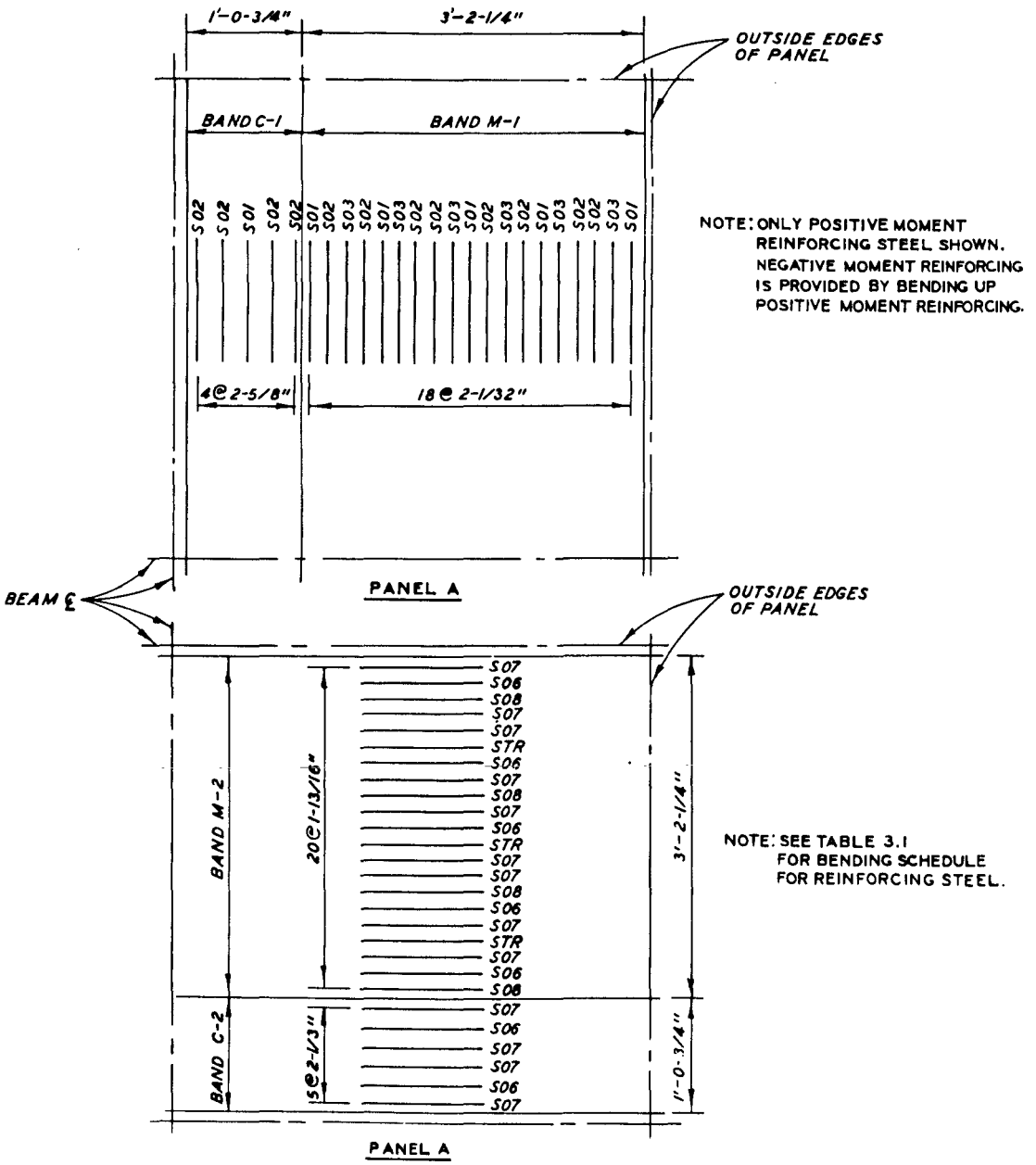

Figure 3.12a Reinforcing steel layout (sheet 1 of 5).

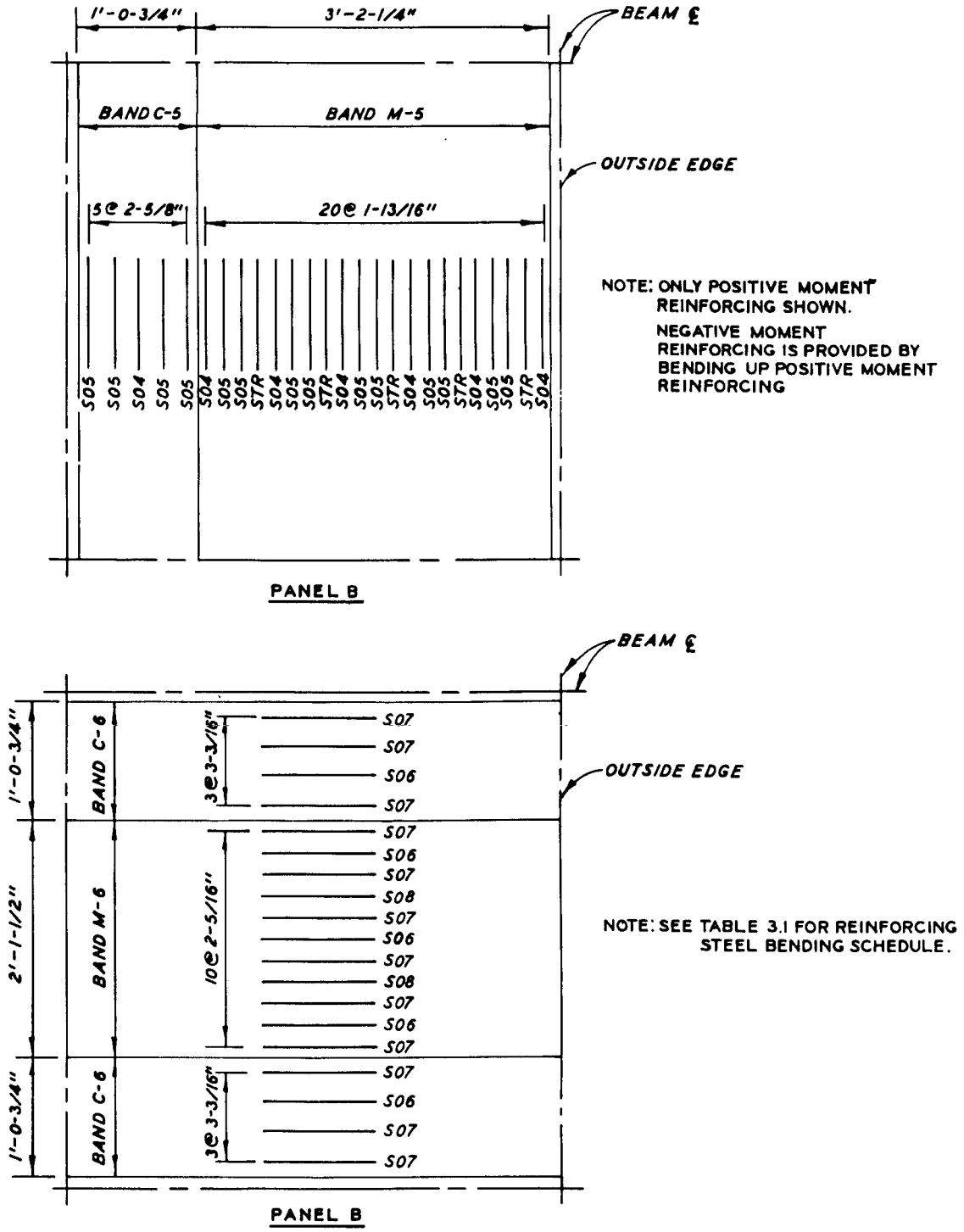

Figure 3.12b (sheet 2 of 5).

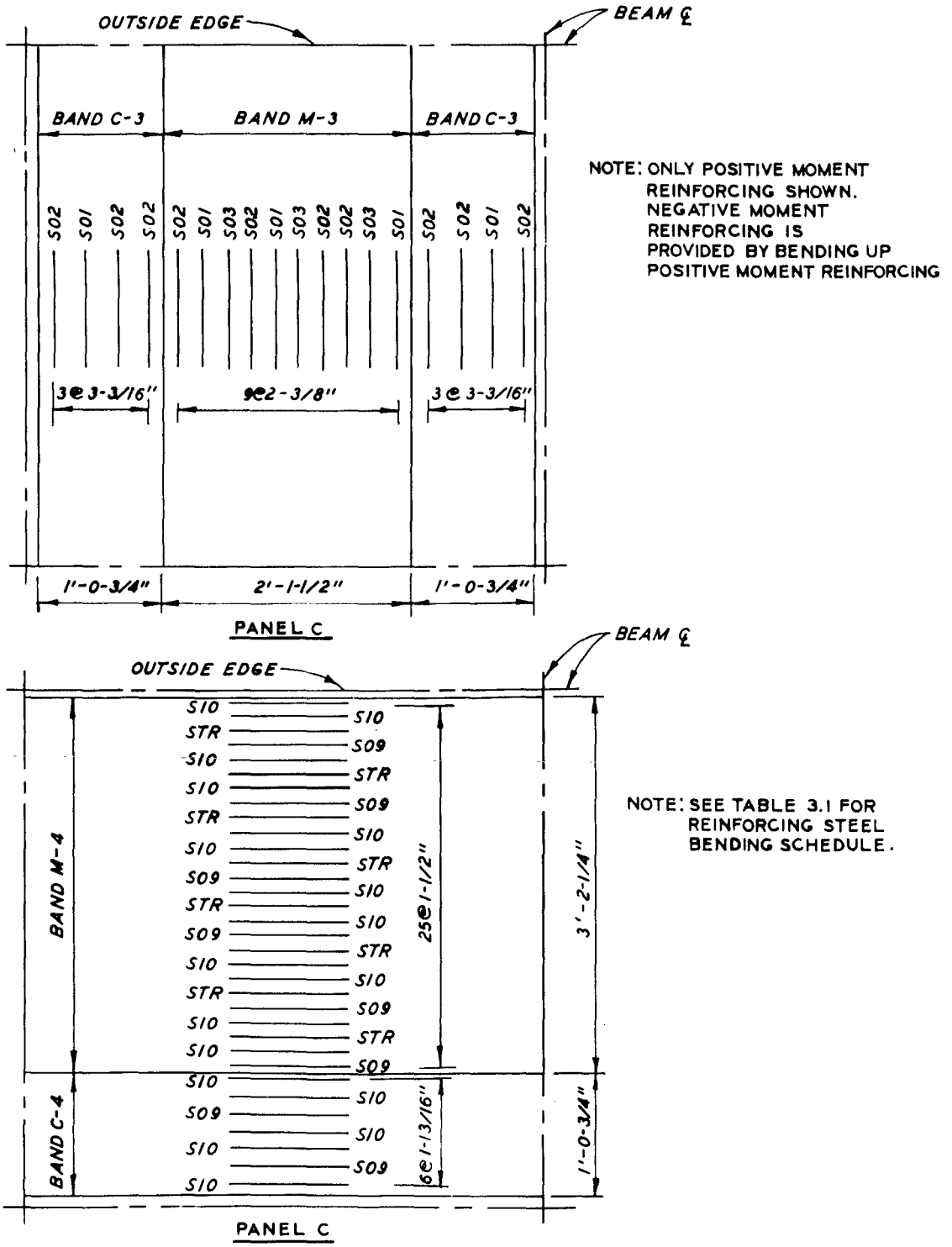

Figure 3.12c (sheet 3 of 5).

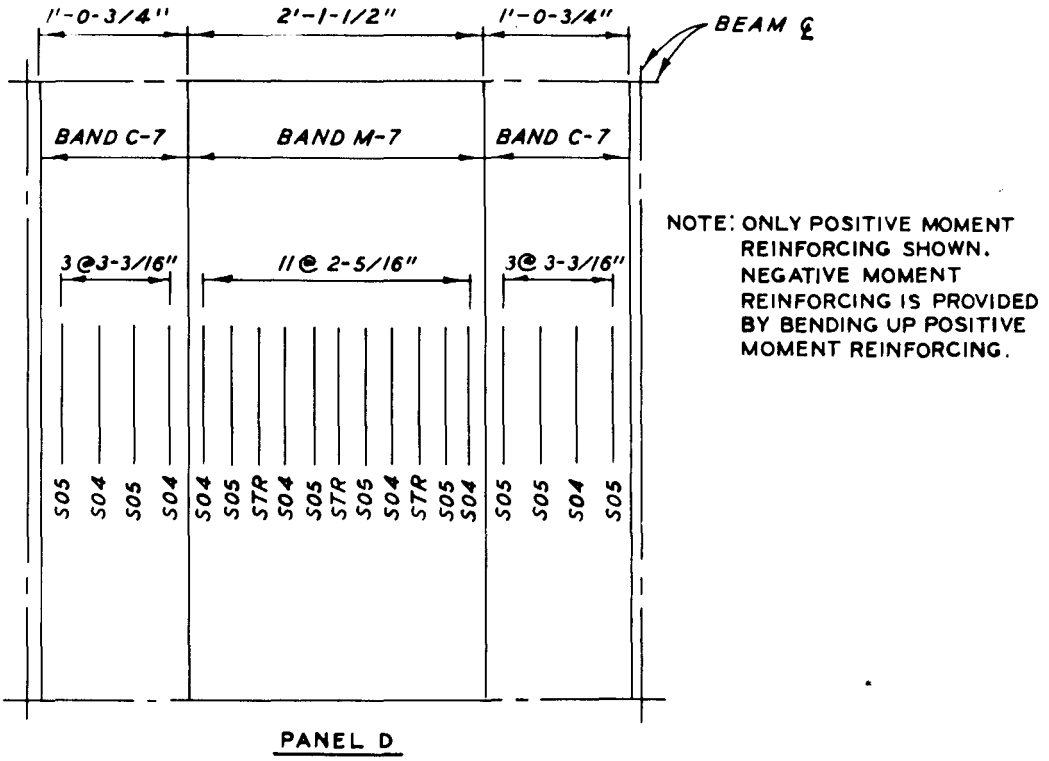

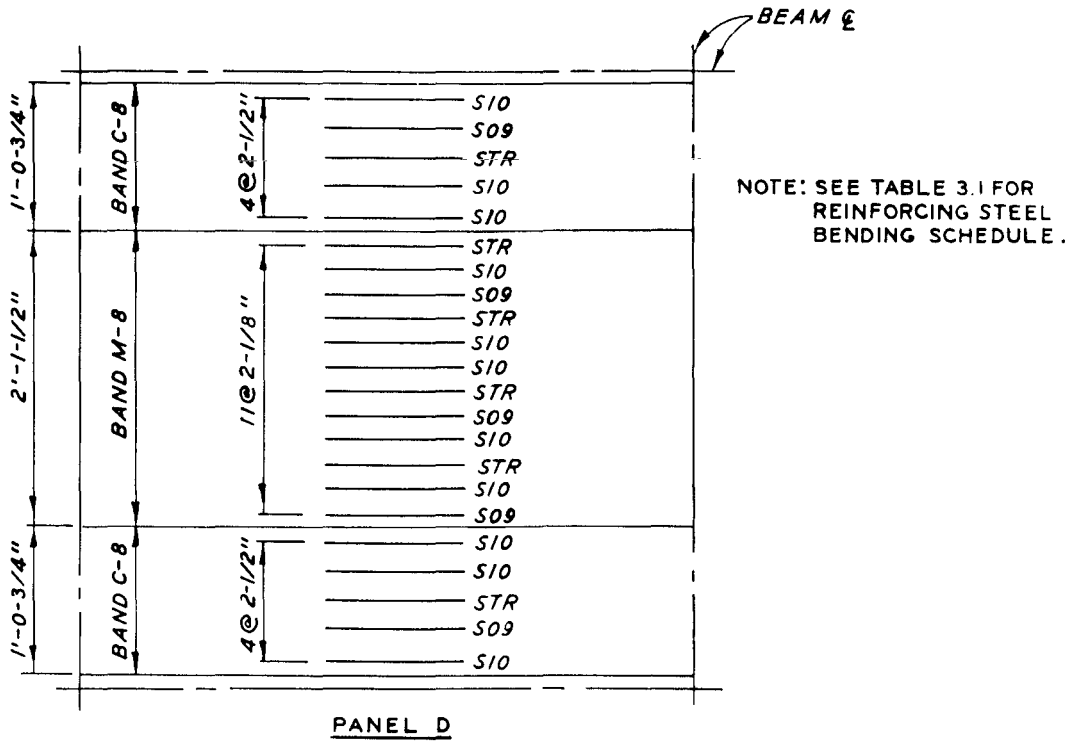

Figure 3.12d (sheet 4 of 5).

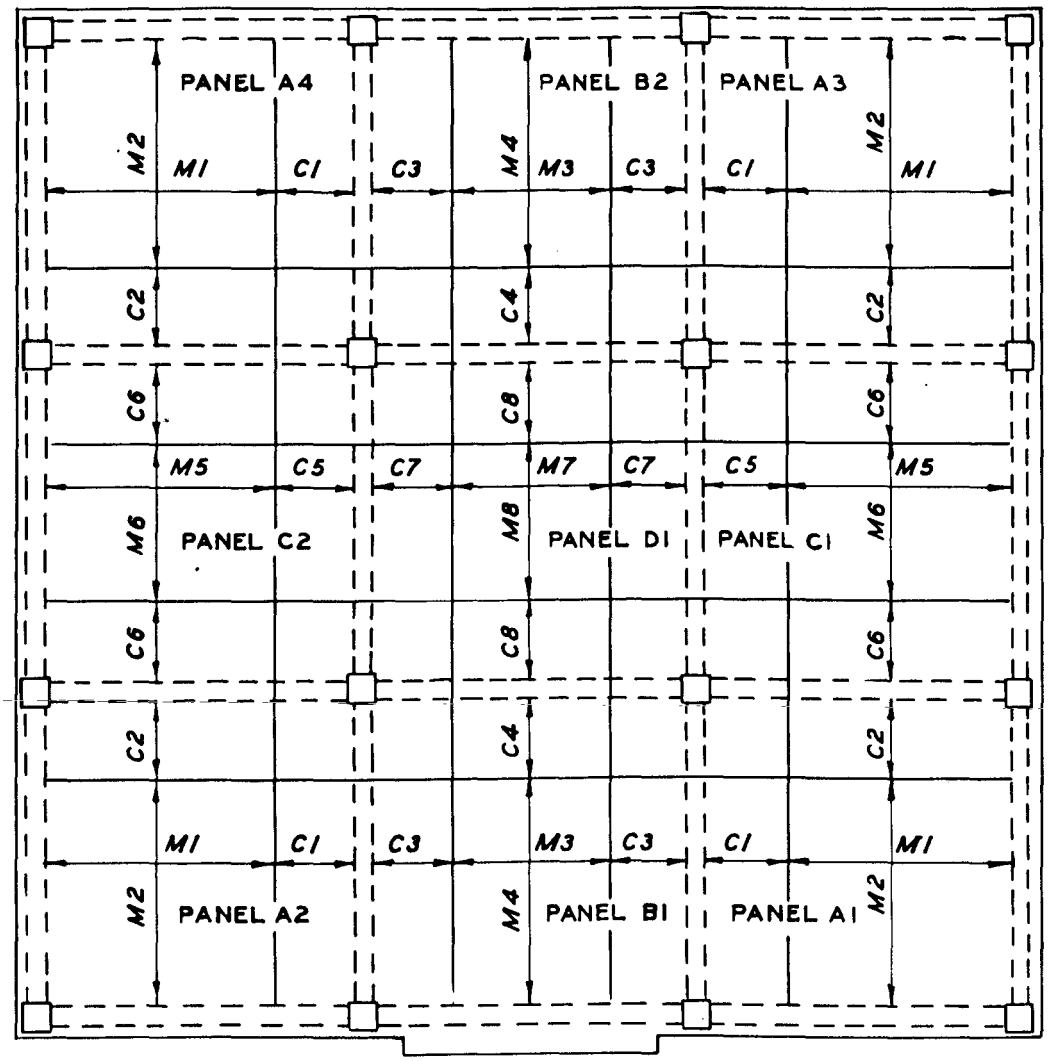

Figure 3.12e (sheet 5 of 5).

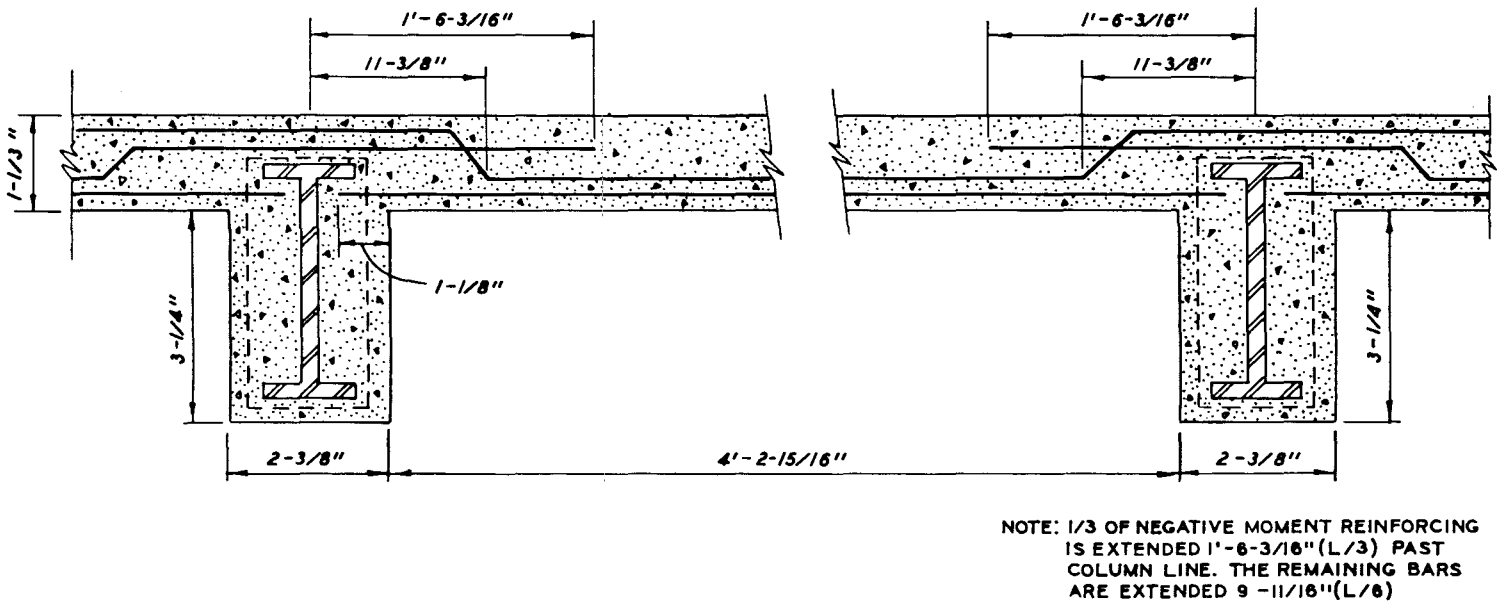

Figure 3.13a Typical placement of reinforcing steel in floor slabs (sheet 1 of 2).

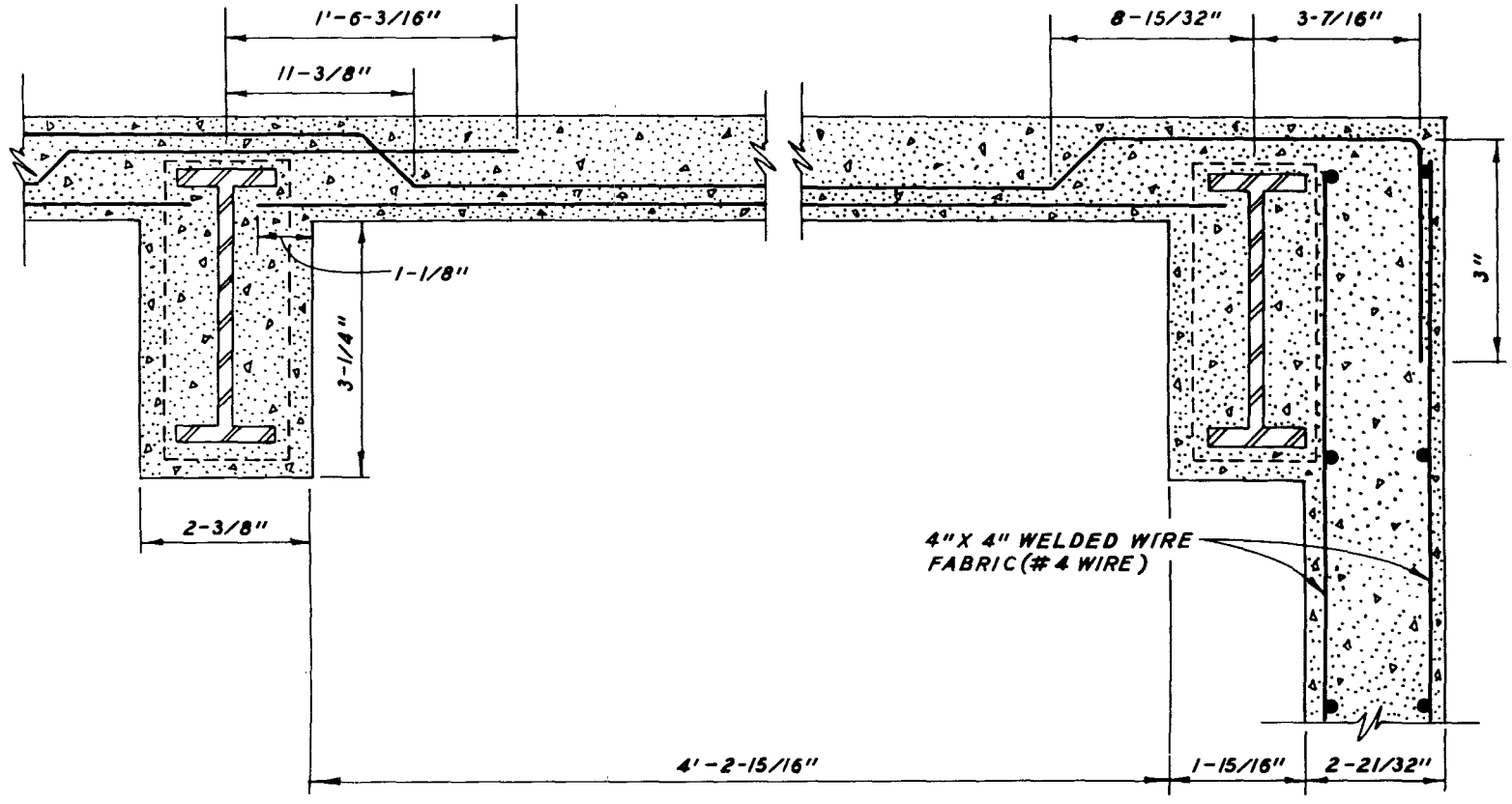

Figure 3.13b (sheet 2 of 2)

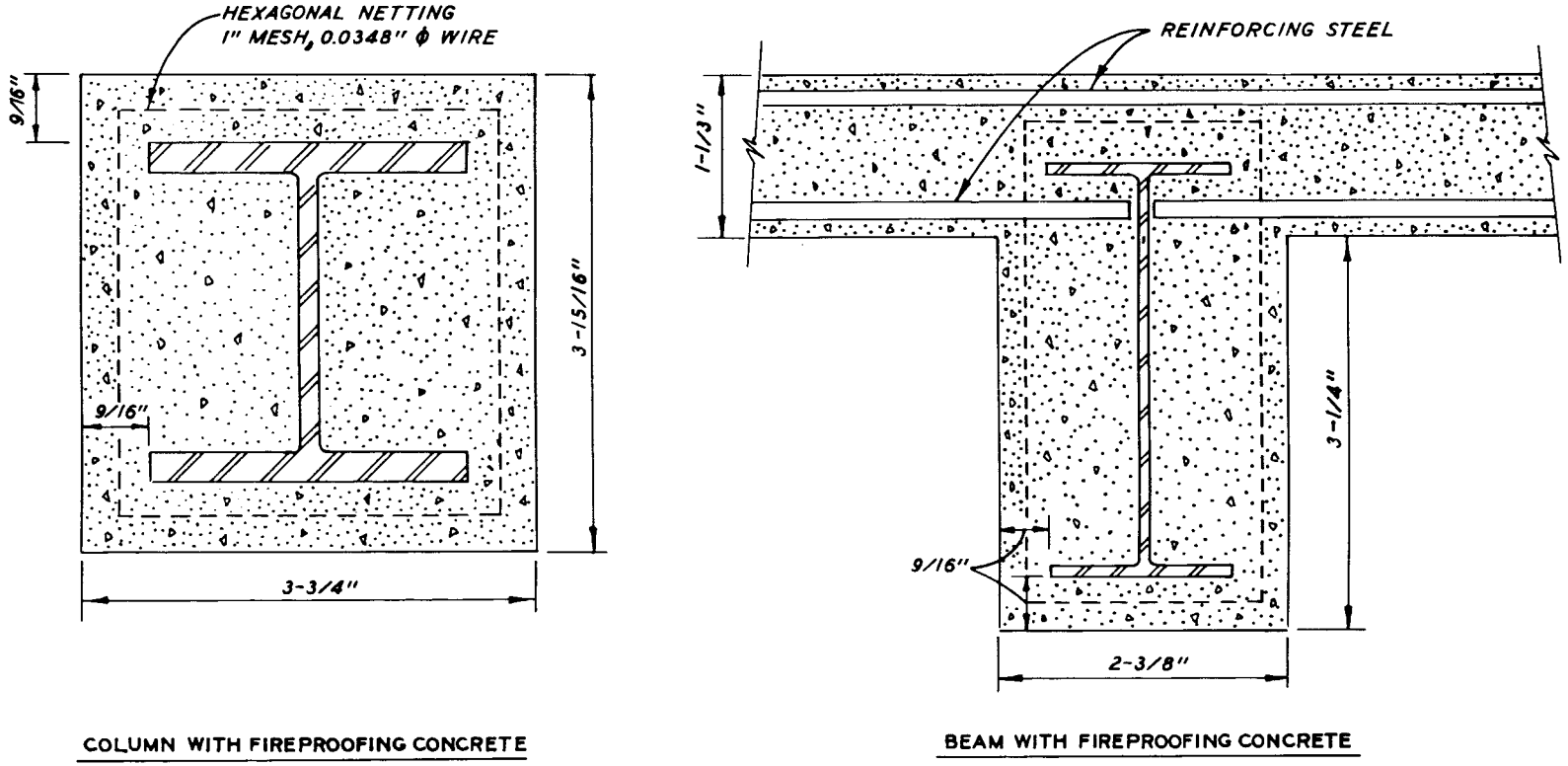

Figure 3.14 Beam and column fireproofing.

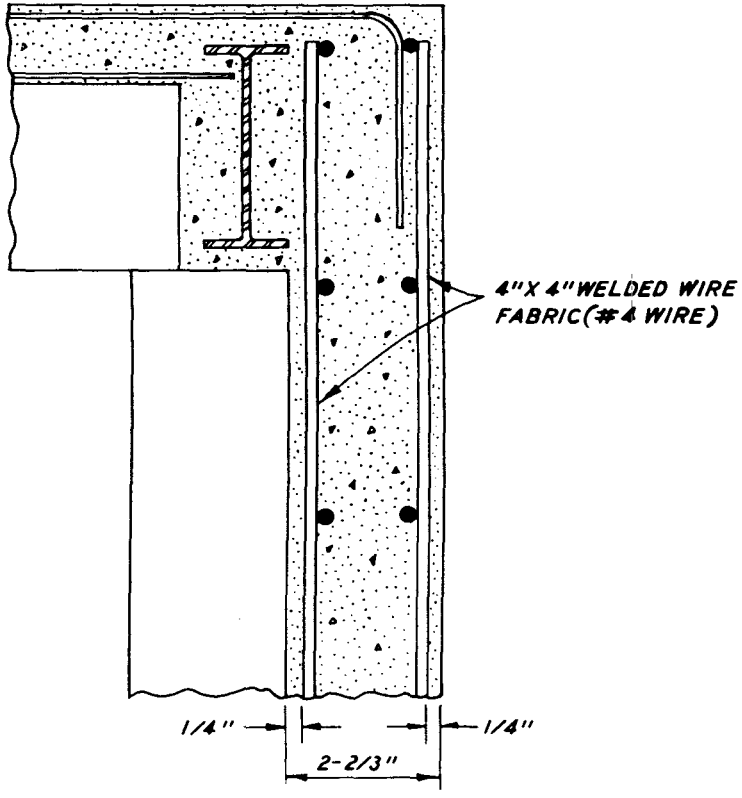

Figure 3.15 Basement wall reinforcing.

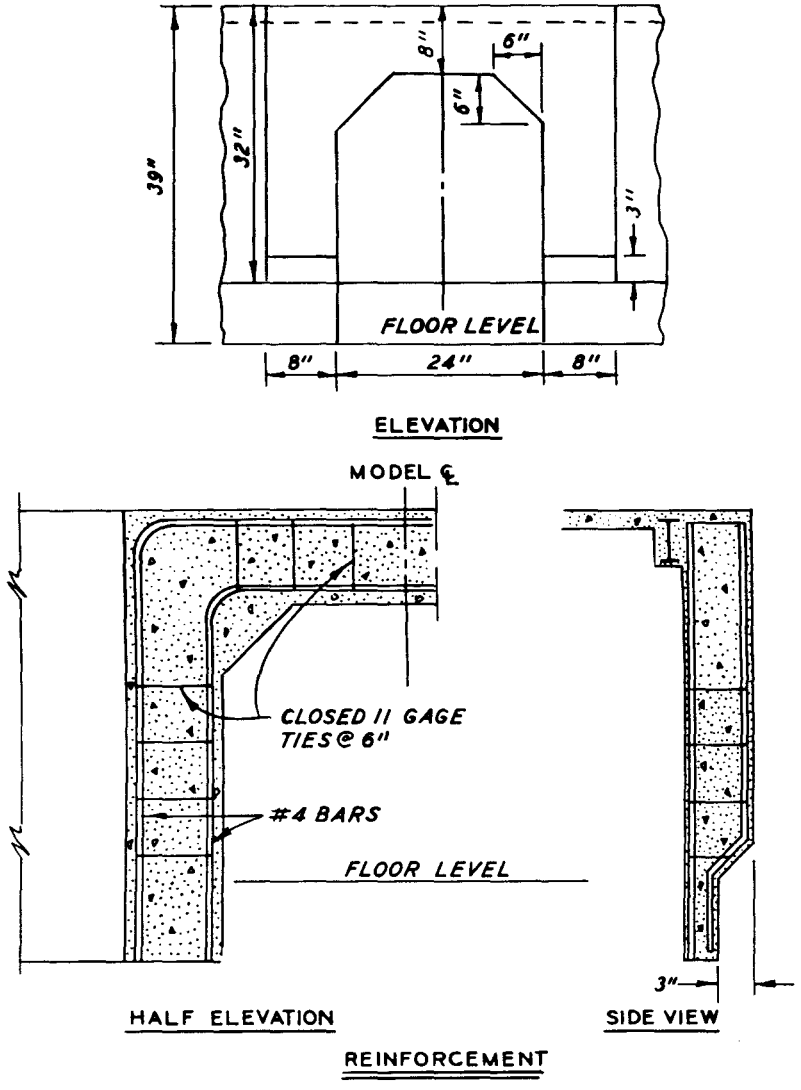

Figure 3.16 Reinforcing around opening in basement wall.

CHAPTER 4

EXPERIMENTAL PROCEDURES

4.1 MATERIALS

4.1.1 Concrete. The two models were cast using two different concrete mixtures for model floor slabs and walls, each proportioned for a 28-day strength of 3000 psi.

Mixture 1 was used in both models for the floor slabs and for the beam and column fireproofing. The proportion by weight for Mixture 1 was 1:5.82 (cement:fine aggregate); the water-cement ratio by weight was 0.82.

Mixture 2 was used for the walls of both models. The mixture proportion by weight was 1:3.38:3.43 (cement:fine aggregate:coarse aggregate); the water-cement ratio by weight was 0.80.

Type I cement was used for both mixtures. The fine aggregate (No. 4 sieve maximum) for Mixtures 1 and 2 and the coarse aggregate (3/8-inch maximum) for Mixture 2 were crushed limestone. The two mixtures were proportioned to produce a concrete with an average slump of 2 inches.

4.1.2 Structural Steel and Concrete Reinforcing. The steel beams and columns in the models were fabricated from A-36 steel sheets and plates.

The concrete reinforcing steel used in the floor slabs of the models was 11-gage (0.120-inch-diameter) steel wire cut into 7-foot lengths and annealed in a large oven by a local manufacturing firm. It was heated to approximately 1200°F for two hours and allowed to cool slowly.

In order to improve the bond characteristics, the wire was soaked in a muriatic acid solution to remove the scale which formed on the outside of the wires during the annealing process and to slightly etch the surface of the wires. After removal from the acid bath, the wires were washed to remove the acid and allowed to rust. Prior to placing the wires in the model, the loose rust was removed from the wires by rubbing them with steel wool.

The 4- by 4-inch, 4-gage welded wire fabric used in the model walls met the requirements of ASTM Specification A82.

4.1.3 Material Test. Twelve standard 6- by 12-inch concrete control cylinders were cast for each structure, six from each of the two mixtures used to cast the structures. Three control cylinders from each mixture were tested in compression and three were tested in tension (split cylinder) on the test date of the corresponding model structure. Results of the control cylinder tests are given in Table 4.1. Average concrete compressive strengths were 3880 and 4090 psi for the floor slab and walls, respectively, in the static test structure and 4600 and 4340 psi for the floor slab and walls, respectively, in the dynamic test structure. Typical stress-strain curves obtained from cylinders instrumented with 6-inch-long strain gages are shown in Figure 4.1.

The properties of the 11-gage annealed wire used for the slab reinforcement were determined from 20 tensile tests conducted on lengths of wire selected at random. The average yield stress and ultimate strength were 40,200 and 59,100 psi, respectively (Table 4.2). As can be seen in Figure 4.2, the stress-strain curves displayed a sharp yield point followed by a flat plateau extending to a strain of 0.04 in./in. The elongation at rupture over a 4-inch gage length was 25 percent.

Standard tensile coupons were cut from each of the six plate thicknesses used to fabricate the beams and columns for the two models. Results of the static tensile tests on these coupons are shown in Table 4.3. Figure 4.3 is a typical stress-strain curve for the tensile coupons.

4.2 MODEL FABRICATION

The first steps in the construction of the models were to fabricate the structural steel members used for framing and to cast a base slab on which the models could be assembled and tested. Initially, it was thought that some of the miscellaneous or junior beam sizes could be used as models of the wide flange beams in the prototype structure. However, when the design of the prototype structure was initiated, it was determined that the only means of providing accurate models of the

prototype structural members would be to fabricate them.

4.2.1 Base Slab. The base slab served two purposes, to provide a rigid base to which the models could be fastened for testing and to provide a flat level platform on which the formwork for the models could be fabricated and the models cast.

The base slab consisted of a 14-foot-square 10-inch-thick reinforced concrete slab with an approximately 4-foot-square opening in the center. During assembly of the model, the base slab was inverted and placed on 6- by 12-inch timbers with one side resting on the edge of a 2-foot-deep by 30-foot-wide pit located on the LBLG floor and the other side resting on a platform spanning the pit. This left a 30-inch-high crawl space beneath the base slab which allowed access to the center hole in the slab for entry into the model during construction.

A 6- by 8- by 1/2-inch steel angle formed the outside edge of the slab. The angle was placed with the 6-inch leg outstanding to provide a ledge for the walls of the model to rest on (Figure 4.4).

The slab was reinforced with No. 6 Grade 40 bars placed in both faces (Figure 4.5) and around the access hole. At the lifting points, the 6- by 8-inch angles were reinforced with a 3/4-inch-thick plate. Blockouts were placed in the slab where the interior columns were to be bolted down. Figure 4.6 shows the inverted base slab prior to casting.

The 28-day strength of the ready-mix concrete placed in the base slab, as determined by the breaking of three control cylinders, was 3910 psi.

4.2.2 Fabrication of Model Structural Steel Sections. The wide-flange and tee sections for the models were fabricated from strips of steel sheet machined to the required widths for the web and flange pieces and then welded together to form the model structural steel sections. The web and flange pieces were machined to tolerances of $\pm$0.002 inch. The experience of the welder was relied upon to produce sections that were not warped or twisted. The procedure developed by the welder for fabricating the sections consisted of clamping a web piece to a flange piece resting on a flat steel welding table and placing tack welding on alternate sides of the web at approximately 1-inch intervals.

The resulting tee-shaped sections were then inverted, clamped in place on another flange piece, and tack welded as before. The final 1/8-inch continuous welds on each side of the web were placed in a continuous operation in which each weld was completed for the total length of the section before beginning the next weld. This procedure produced straighter sections than other methods in which short continuous welds were alternately placed along the sides of the webs. However, it was necessary to complete all four continuous welds before stopping, otherwise the section would begin to cool, causing the section to warp or twist.

Structural tee's for the connections were fabricated in 4-foot-long sections in the same manner as the wide-flange sections and then cut to the lengths required for the connections. The completed structural tee's and wide-flange sections are shown in Figure 4.7.

Holes for bolt connections were drilled in the wide-flange and tee sections using an alignment jig to insure accurate and uniform placement of holes in all sections.

4.2.3 Formwork. The formwork for the models was constructed atop the inverted base slab using dimensioned lumber and 3/4-inch exterior A-C grade plywood. The forms were constructed to allow the entire model, including walls, floor slab, and concrete cover around the structural steel frame, to be cast in one pour.

The inside wall forms shown in place in Figure 4.8 were fabricated in sections that covered the area from the base of the wall to the underside of the floor slab and from inside to inside edge of the columns. The wall form sections were joined at the column locations by fastening them to a 2- by 6-inch spacer that had been planed to the 4-inch width of the finished columns. The spacers were set back from the wall side of the forms to produce a recess for the steel columns. An inset was provided along the top edge of the forms for the floor slab outside framing beams.

Blockouts were placed along the base of the wall to allow the bolts fixing the wall base and the lifting projection at each corner to pass through the walls (Figure 4.8). An opening was provided in the front

wall (Figure 4.8) to allow access into the model after the model had been placed in the test chamber.

The forms for the floors consisted of plywood sheeting nailed to 2- by 10-inch joists which were supported by the wall forms on the ends and by 2- by 4-inch posts near the column lines. The joists were spaced to leave a channel at the locations of the steel floor support beams. Notches were cut in the joists to leave channels for the steel framing beams orthogonal to the wood joists. Two- by four-inch spacers were nailed between the joists at the locations of the notches. The diagonal bracing supporting the wall forms and the floor joists can be seen in Figure 4.9.

The completed inside forms are shown in Figure 4.10. Light gage sheet metal forms were placed in the channels left for the steel framing beams, and plywood sheeting was nailed to the joists to complete the floor forms.

To insure smooth surfaces in the model, all joints in the forms were filled with wood putty and sanded smooth. The levelness of the floor slab forms was examined at approximately 50 scattered locations. The forms were shimmed at various locations to bring them within the tolerances desired. The extreme variations measured in the forms were 1/16 and 3/64 inch for the static and dynamic test models, respectively.

The outside wall forms were fabricated in four sections, one for each side of the model. The plywood sheeting was nailed to the 2- by 4-inch frame, leaving the plywood approximately 1 inch higher than the top 2-by-4. When the outside wall forms were placed, elevations were shot around the edges and the plywood was sanded to bring it down to the desired height.

4.2.4 Steel Frame Assembly. The steel frame was assembled above the forms to provide adequate room for tightening the bolted connections. To accomplish this, the columns were placed on 7-inch-high wooden blocks, which raised the beams approximately 4 inches above the floor slab forms. Prior to bolting the frame together, the beams and columns were wrapped with a light gage hexagonal wire mesh (chicken wire) which was used to model the welded wire fabric placed around the structural frame of the

prototype structure to hold the concrete fireproofing in place.

Figure 4.11 shows the elevated steel frame being assembled. The assembly sequence for the steel frame was the same as it would have been for the prototype structure: the columns, the lower split tee for the connections, the beams, and finally the upper split tee for the connections. All of the bolts in the connections were finger-tightened and the frame was leveled prior to tightening the bolts to the desired torque. Connection details can be seen in Figure 4.12 which shows a mock-up of the beam-column connection for the four interior columns.

In bolted construction, the bolts are torqued quite often by the turn-of-the-nut method. Using this method, the nut is wrenched from the snug tight position 1/2 or 2/3 turn, depending on the length of the bolt. This is sufficient to load the bolt to 100 percent of its proof load, or beyond, into the plastic range. In the model connections some of the flanges on the beams, columns, and split tees were bowed slightly by welding. During the torquing of the bolts, the flanges flattened out, making it difficult to determine the snug-tight position from which to begin the turn-of-the-nut torquing procedure. While one bolt of the connection was being tightened, another bolt previously tightened would become loose. Therefore, it was decided that it would be better to tighten the bolts with a torque wrench. To determine the point to which the bolts were to be torqued, a test connection was made up and the bolts were torqued to failure. The fine- and coarse-thread bolts broke at torques of 145 and 125 in.-lb, respectively. Using an empirical formula relating bolt tension to torque, it was determined that a 100-in.-lb torque was sufficient to induce the proof load in a 1/4-inch bolt; therefore, this torque level was chosen for the bolts in the model connections.

After torquing the bolts, a strongback was attached to the four center columns and the entire steel frame assembly was lifted to allow removal of the wooden blocks supporting the frame. The frame was then lowered into the plywood forms. Shims were placed under the columns to raise the top of the steel beams to the desired level above the forms for the floor slab. This completed the assembly of the steel frame for the model.

4.2.5 Fabrication and Placement of Reinforcing Steel. To avoid interference between the hooked bars from the floor slab and the wall steel, the inside mat of wall steel was placed first, then the floor steel, and finally the outside mat of wall steel. The inside mat of welded wire fabric (WWF) reinforcing the walls was cut into sections that fit between the columns and was nailed to the inside wall forms using small wire staples. This reinforcing mat was supported by short pieces of No. 4 wire to maintain the required cover spacing.

The outside mats of wall steel were placed in sections that were the full length of the walls and were tied to the inside mats of WWF to hold them in place. The spacing between the inside and outside wall steel mats was maintained by slotted sheet metal spacers that rested against the inside and outside of the wall forms. Figure 4.13 shows the south and west sides of the static test model with the inside wall reinforcing mat in place.

After the loose rust had been removed from the floor slab reinforcing bars, the bars were cut to length and bent according to the schedule shown in Table 3.1. Figure 4.14 shows each of the ten types of bars used in the floor slabs of the models.

To insure accuracy of placement of the reinforcement, the reinforcing pattern was laid out on the plywood forms. Lines were drawn on the forms at the rebar locations, and each location was labeled to identify the type of rebar to be used.

Placement of the reinforcing steel was begun at one of the corner panels and continued around the outside panels of the models, leaving the center panel until last. The bar placement sequence for each panel consisted of placing all straight bars in the bottom layer of reinforcing in the east-west direction, placing the north-south bars outside the bend points for the east-west bars, placing all bent bars in the east-west direction, and placing the remaining bent and straight bars in the north-south direction. After all bars had been placed in a panel, they were tied at every other rebar intersection using 20-gage stove pipe wire. Figure 4.15 shows the placement of the floor slab reinforcing for the static model.

When the reinforcing steel in all the panels had been placed and tied, spacers consisting of short pieces of 8-gage wire were placed at approximately 150 locations under the bottom layer of bars to provide the required cover. At each spacer location, the rebar mat was stapled to the forms to prevent the rebar mat from shifting during concrete placement.

Figure 4.16 shows a closeup of one of the corner panels and an overall view of the static test model with all the reinforcing steel in place.

4.2.6 Casting and Curing of the Models. The bolted connections between the steel floor slab support beams and the four interior columns made it almost impossible to place the fireproofing concrete around the interior columns from the top side of the forms. To get the fireproofing concrete around these columns with a minimum of honeycombing, they were cast prior to casting the remainder of the model. Before the steel frame was assembled, the four interior columns were formed to within 1 inch of the connection and the fireproofing concrete was placed around them. The columns were allowed to moist cure for 3 days. The forms were then stripped and the columns used in the steel frame assembly. The two models were cast 7 to 10 days after the interior columns.

The remainder of the model was cast in one continuous operation. Concrete was placed in the walls first, then around the beams supporting the floor slab, and then in the floor slab itself. As the concrete was placed in the model, it was vibrated using an internal vibrator with a 1-1/4-inch-square head. Figure 4.17 shows the concrete placement under way on the static model.

The top surface was screeded using a 6- by 2-inch aluminum structural tube. Since the columns protruded above the slab approximately 2 inches, it was necessary to screed the slab several times in both directions to insure that the slab surface was level along the column lines. After screeding of the slab, forms 2 inches high with an inside dimension of 4 by 4 inches were placed around the protruding ends of the columns and filled with concrete to cover the ends of the columns. This was done to cover the sharp edges of the steel columns so they would not

cut the diaphragm to be used during the static test or the EMP shield used during the dynamic test. Once the concrete reached the required degree of set, the slab surface was finished with a steel trowel.

Concrete for the walls and the floor slab was mixed in a 1/2-yd^3 cyclo-turbine-mixer using the mixture proportions given in Section 4.1.1. Three batches were required for the walls and two for the floor slab.

Twelve concrete control cylinders were cast at random from the batches prepared from each mixture design. Three cylinders from each mixture design were broken to obtain the 7-day, 28-day, and test date compressive strengths. The remaining three cylinders from each mixture were broken in split tension on the test date. Results from the cylinders broken on the test date are shown in Table 4.1. The control cylinders were cast in standard 6- by 12-inch steel molds and vibrated for 15 seconds using an internal vibrator with a 1-1/4-inch-diameter round head. The models and control cylinders were cured for 7 days under wet burlap and then allowed to air cure until the test date.

At the end of 21 days the forms were stripped, and at 28 days the models were removed from the base slab. Prior to removing the interior column supports, a strongback was secured to the walls and to the four interior columns of the model to support the interior columns when the blocks under the columns were removed.

After removal of the formwork, the models were removed from the base slab and stored indoors until test time. Upon removal of the forms, several honeycombs were found in both models on the inside of the perimeter columns near the column-beam connections. These honeycombs were in the fireproofing concrete and were not considered to affect the structural integrity of the models.

Several hairline cracks were found in the floor slab of the static model after it had been removed from the base slab. At first, these cracks were thought to have occurred when the model was lifted from the base slab or when the forms were removed from under the slab. However, when the dynamic model was cast, hairline cracks were found in the floor slab before the forms had been removed. These cracks did not follow the reinforcing or any other noticeable pattern; therefore, it was assumed

that they were shrinkage cracks that developed during curing. Figures 4.18 and 4.19 are photographs that were taken with and without the cracks being marked.

Figure 4.20 shows two views of the underside of the dynamic test model immediately after removal of the forms.

4.3 TESTING PROCEDURE

4.3.1 Preparation of Test Specimen. With the base slab in its upright position, the 6- by 8- by 3/8-inch perimeter angle formed a support ledge for the walls of the model. The model was placed over the base slab and set on 2-inch-high wooden blocks on the perimeter angle, leaving approximately 1-inch clearance between the steel base plate on the columns and the base slab.

A nonshrink concrete grout was poured in the void beneath the column base plates and between the model walls and the base slab (see Figure 4.4). The mixture design for the nonshrink grout was:

Type III cement	94 pounds
Fine sand (Cook's Bayou sand, D_{50} = 0.33 mm)	100 pounds
Water	6 gallons
Powdered aluminum	2 grams
7-day strength	3000 psi

The exposed areas of the grout were covered with wet burlap and cured for 7 days, at which time the high-strength bolts through the 5- by 3- by 3/8-inch structural steel tubing and the 1/2-inch bolts through the base slab and column base plates were tightened.

With the model secured to the base slab, the strongback used to lift the model and to support the interior columns was removed. Moving of the model could now be accomplished by lifting it from the lugs provided on the base slab. Pressure gages, concrete strain gages, and a wooden frame to support the deflecting gages were installed in the models with the model in the position shown in Figure 4.21.

4.3.2 Loading Device. The LBLG at WES was used to test both the statically and dynamically loaded models. This device, shown in Figure 4.22, consists of two basic components, the Central Firing Station (CFS) and the test chamber. The test chamber consists of three 22-foot-10-inch-ID high-strength steel rings stacked on a movable platen to form a cylindrical chamber 10 feet deep. After the model to be tested and backfill material are placed in this chamber, a ring containing baffled firing tubes and a lid are placed on the three rings of the tank below and moved into the CFS, a massive posttensioned concrete reaction structure.

To obtain dynamic loadings, Primacord explosive is placed in the firing tubes and detonated, resulting in a downward-traveling plane wave. The LBLG can simulate the pressures produced by kiloton and megaton nuclear devices. Surface airblast overpressures from less than 10 to as much as 500 psi can be produced with rise times of 1 to 10 msec and durations ranging from 0.5 to 2 seconds.

Slowly applied or static loading of up to 1000 psi can be obtained by sealing the exhaust ports of the top ring of the tank and using the tank as a pressure vessel.

More complete descriptions of the LBLG, its performance, and calibration are given in References 14 and 15.

4.3.3 Placement of Model and Backfill. Before the model structure was placed in the test chamber, the chamber was filled to the elevation of the base slab with a fine, fairly uniform sand and leveled to provide a uniform support for the model base slab foundation. The base slab elevation was selected so that the top of the structure would be slightly below the top of the three rings of the test chamber.

A steel entranceway box approximately 3 feet square, 4 feet deep, and with one side and top open was placed adjacent to the access hole at the center of the one wall of the model. The test chamber was then backfilled to the level of the slab surface (see Figure 4.23), care being taken to uniformly compact the backfill material.

The sand used for backfill material, known locally as Cook's Bayou sand, was used for several previous studies conducted in the LBLG.

The sand has a specific gravity of 2.65, minimum and maximum laboratory dry unit weights of 93.3 and 110.3 pcf, and a D_{50} value of 0.33 mm; 87 percent of the material is between a number 30 and a number 100 U. S. standard sieve size and consists of predominantly subround to round shapes. Other properties of the sand are presented in References 16 and 17. The density of the backfill as placed was approximately 103 pcf.

The electrical leads for the transducers were connected to cables running from the instrumentation room adjacent to the LBLG, through the base of the test chamber, and through the hole in the base slab serving as a foundation for the model structure. After the instrumentation had been checked, the lid of the entranceway box was closed, and the model and soil surface were sealed as required.

4.3.4 Static Test. For the static test, water pressure was used to apply a uniform load. Thus, it was necessary to seal the backfill material and the structure from the water. A 6-mil-thick layer of polyethylene was placed over the model and sand surface and taped to the sides of the chamber. The top layer of the water seal was a 0.035-inch-thick polyurethane diaphragm covering the test area surface and glued to the sides of the chamber.

To prevent the column stubs from cutting the diaphragm, they were encircled with 2- by 2-inch wooden strips cut on a 45-degree angle. The column stubs and the wooden strip were covered with 1/16-inch-thick unreinforced neoprene, producing a smooth transition between the column stub and the roof slab of the model.

Water pressure rather than air pressure was chosen as a method of loading to prevent the sudden failure that air expansion would cause when the resistance of the structure began to decrease. Water loading allowed a better determination of the entire deflection-resistance curve.

After the water seal had been completed, the top ring and lid of the test chamber were installed and the chamber was moved into the CFS. The air void above the model was then filled with water; an approximately 3-inch-thick layer of air remained at the top of the tank and above the exhaust ports.

Water pressure for loading was obtained by passing tap water through

a pressure regulator. The water pressure in the water main at the time of testing was approximately 80 psi. The first step in the static test was to record calibration steps for the 75 transducers. Water pressure was then applied to the slab surface at a rate of approximately 1 psi per minute until a load peak was obtained nearly 8 minutes into the test. One water pressure transducer, two slab panel center deflection channels, and one Bourdon-type mechanical pressure gage connected to the water chamber above the model were monitored throughout the test.

The test chamber was then rolled out of the CFS, the top rings, lid, and sealing membranes were removed, and the damaged model structure was examined and photographed. The backfill was excavated to the base slab, and the model was removed from the test chamber to allow inspection of the walls and further inspection and photographing of the slab portion of the model.

4.3.5 Dynamic Test. One of the differences between the procedures for the static and dynamic tests was in the sealing. A 6-mil-thick layer of polyethylene was taped to the edge of the model and the test chamber walls to serve as a barrier to prevent the airblast pressure from entering into the sand. Approximately 1 inch of sand was placed over the polyethylene to protect it from heat. The roof of the model was not covered with the polyethylene. A fine mesh copper screen was placed over the surface to shield the model instrumentation from electrical disturbances resulting from the explosion.

Before the top ring and lid were placed on the test chamber, the amount of Primacord explosive necessary to produce the desired pressure was placed in the firing tubes atop the model location in the test chamber. The explosive loading was determined from calibration tests conducted prior to placing the model in the test chamber. The test chamber was then closed and placed in the CFS.

After the calibration of the transducers had been completed and the magnetic-tape recorders had reached operating speed, the Primacord was detonated.

After the test, the test chamber was removed from the CFS, the lid removed, and the model inspected for damage.

4.4 TEST MEASUREMENTS AND INSTRUMENTATION

4.4.1 Pressure Measurements. The magnitude of the applied load during the static test was measured by three 0- to 100-psia-range Consolidated Electrodynamics Corporation (CEC) pressure transducers placed 120 degrees apart around the lid of the test chamber. A Bourdon-type mechanical pressure gage was connected to the test chamber at the water pressure inlet and physically monitored during the test.

Ten Tyco-Bytrex AB-200 pressure transducers of 0- to 200-psia range were employed to measure airblast pressure in the dynamic test. Five were placed at various locations on the surface of the floor slab, three were placed in the sand backfill on the east and south sides of the model, and two were placed inside the model on the base slab to determine the pressure rise as the floor slab failed (see Figure 4.24). Mounts for the transducers consisted of a tapered hole in a steel plug cast in the floor slab. Gage mounts identical with those cast in the concrete slab were used to cast a Bywax 601 filler compound around the gages. The Bywax 601 served to reduce the acceleration and ringing experienced by the transducer. The coated transducer was then placed in the mounts which held the gage flush with the slab surface. The mounting apparatus and pressure transducers used to measure overpressures, interface pressures, and vertical soil pressures are shown in Figure 4.25.

The interface pressure acting on the model wall was monitored at eight locations on the north half of the west wall. The mounted transducers can be seen in the west wall of the static model in Figure 4.21. Modeling clay was used to fill in around the gage mounts to maintain a smooth surface in the area of the gages. The locations shown in Figure 4.26 were used for both structures. The CEC pressure transducers (0- to 100-psia range) were held flush with the wall surface by hollow Teflon mounting bolts placed in formed holes in the walls. The Teflon mounting bolts reduced the acceleration and ringing in the transducer.

Four low-pressure wafer-type-diaphragm soil pressure transducers were placed as shown in Figure 4.26 to measure vertical free-field stress in the region of the upper two interface pressure transducers in the center of the west wall.

4.4.2 Strain Measurements. The locations of the strain gages placed on the structural steel frame, the reinforcing steel, and the slab surface are shown in Figures 4.27 and 4.28.

Steel strains were measured on the structural steel members using Micro-Measurements EA-06-250BG-120 epoxy-backed foil gages having a nominal grid size of 1/4-inch length by 1/8-inch width and on the reinforcing steel with Micro-Measurements EA-06-125B-120 epoxy-backed foil gages having a nominal grid size of 1/8-inch length by 1/16-inch width. The gage resistance for all gages was 120 $\pm$ 0.2 ohms.

The reinforcing steel was prepared for gaging by cleaning and lightly sanding with emery cloth at the gage location. Gage locations on the structural steel members were ground smooth with a disk grinder and cleaned. The gages were then bonded to the bar with a heat-curing epoxy. After the installed gages had been inspected, lead wires were attached to the gage tabs and the gages were waterproofed with several layers of Gagekote synthetic rubber compound.

Gages were placed on the bent bars at 90-degree angles to the bend. Straight bars were tied in the reinforcement layers with the gages on the side of the bar. This placement procedure was used to reduce the influence of any bending of the bar without using two strain gages per gage location.

Budd CG-1161-B, epoxy-backed foil gages having a nominal grid size of 1-inch length by 3/32-inch width and a gage resistance of 120 $\pm$ 0.2 ohms were used to determine the concrete strains at the locations shown in Figure 4.27. After the concrete voids at the gage locations had been filled with a thin layer of Epocast epoxy, the location was sanded until the concrete surface was exposed. The gage was bonded to the concrete with Eastman 910 cement and waterproofed with Gagekote synthetic rubber.

4.4.3 Deflection and Acceleration Measurements. Deflection of the reinforced concrete slab and its supporting frame was measured at the locations shown in Figure 4.29.

Two types of transducers were used to obtain the deflection measurements. At locations D3, D4, D6, and D7 a linear variable differential

transformer (LVDT) was used, and at locations D1, D2, and D5 a potentiometer-type transducer was used. These transducers were clamped in mounting brackets bolted to a wooden framework inside the model. For the statically tested model, the probes of the deflection transducers were attached with Shrinktubing flexible plastic tubing to short studs on a 1-1/2-inch-square pull pad which had been epoxied to the underside of the slab. For the dynamic test, the transducer probes were connected with Shrinktubing to the exposed threads of 3/16-inch-diameter bolts which had been embedded in the slab when it was cast.

Accelerations were recorded during the dynamic test at five locations (Figure 4.29). Vertical accelerations were recorded at the locations of four of the deflection gages, three of which were measuring center panel deflection and the remaining one was measuring the deflection of the floor slab support beam. The fifth accelerometer was placed on the base plate of one of the columns to measure movement of the base slab. The accelerometers (Endevco, Model 2260-250) used had a range of ±250 g's and were rigidly fastened to a mounting bracket embedded in the slab.

The deflection and acceleration transducers used are shown in Figure 4.30.

4.4.4 Data Recording and Processing. All data for the static and dynamic tests were recorded on three 14-channel and two 32-channel magnetic-tape recorders (Sangamo Model 4700 and Sangamo Sabre III) with a recording speed of 7-1/2 in./sec during the static test and 60 in./sec during the dynamic test. A 1000-Hz timing signal was placed on one channel for the dynamic test. Timing and correlation for the static test were obtained by recording the output of a time-code generator on the last channel of each tape machine.

The signals from all transducers except the Collins LVDT were amplified by WES differential analog module (DAM 103) amplifiers, which also provided excitation for the gages and contained the calibrating and balancing circuitry.

Calibration for the data was provided by electrically inserting a known equivalent gage output into the circuitry of each data channel and

recording the resulting output for a brief interval prior to each test. The effects of cable resistance were included in the calibration.

The data were later reproduced on photographic paper using the tape output as the input to a CEC Data-Graph S-133 recorder. An analog-to-digital converter was used to digitize the records. The data were then processed and plotted with the aid of a computer. The accelerations were doubly integrated (numerically) to obtain deflections.

TABLE 4.1 RESULTS OF TESTS ON CONCRETE CONTROL SPECIMENS

Specimen No.	Location in Model	Test Age days	Cylinders: Compressive Strength f'_c psi	Cylinders: Strain at Maximum Load μin./in.	Cylinders: Tensile Splitting Strength psi
		Static Test Model			
1	Floor slab	123	3780	2500	--
2	Floor slab	123	3960	2600	--
3	Floor slab	123	3890	2550	--
4	Floor slab	123	--	--	535
5	Floor slab	123	--	--	465
6	Floor slab	123	--	--	530
		Average	3880	2550	510
7	Walls	123	4140	2700	--
8	Walls	123	4100	2750	--
9	Walls	123	4020	2550	--
10	Walls	123	--	--	440
11	Walls	123	--	--	390
12	Walls	123	--	--	390
		Average	4090	2670	405
		Dynamic Test Model			
1	Floor slab	101	4550	3000	--
2	Floor slab	101	4650	2850	--
3	Floor slab	101	4590	2900	--
4	Floor slab	101	--	--	560
5	Floor slab	101	--	--	550
6	Floor slab	101	--	--	550
		Average	4600	2920	555
7	Walls	101	4400	2700	--
8	Walls	101	4350	2600	--
9	Walls	101	4270	3000	--
10	Walls	101	--	--	500
11	Walls	101	--	--	440
12	Walls	101	--	--	500
		Average	4340	2770	480

TABLE 4.2 RESULTS OF STATIC TENSILE TESTS OF REINFORCING STEEL

Specimen No.	Diameter in.	Load at Yield lb	Yield Stress psi	Ultimate Load lb	Ultimate Stress psi
1	0.125	446	36,300	689	57,100
2	0.128	485	37,700	796	61,900
3	0.128	503	39,100	810	63,000
4	0.121	426	37,000	714	62,000
5	0.122	515	44,000	725	62,000
6	0.127	495	39,100	792	62,500
7	0.126	636	51,000	835	66,900
8	0.121	439	38,200	690	60,000
9	0.126	512	41,000	740	59,400
10	0.126	544	43,500	755	60,500
11	0.120	461	40,700	515	57,100
12	0.128	440	34,200	715	55,600
13	0.121	445	38,700	612	53,200
14	0.120	544	48,200	685	60,500
15	0.123	408	34,400	651	54,800
16	0.122	412	35,200	656	56,100
17	0.120	450	39,800	640	56,500
18	0.120	484	42,700	640	56,500
19	0.120	520	46,000	656	58,000
20	0.126	514	41,200	740	59,300
Average	0.123	484	40,200	703	59,100

TABLE 4.3 RESULTS OF STATIC TENSILE TESTS ON COUPONS FROM STEEL FRAME

Specimen No.	Gage	Loading Rate in./min	Yield Stress psi	Ultimate Stress psi	Rupture Stress psi
1a	14 (0.0747 in.)	0.05	40,450	48,750	34,800
1b	14 (0.0747 in.)	0.05	42,050	47,500	36,150
1c	14 (0.0747 in.)	0.05	41,250	48,450	37,900
		Average	41,250	48,250	36,300
2a	12 (0.1046 in.)	0.05	39,950	57,350	47,400
2b	12 (0.1046 in.)	0.05	40,150	56,200	44,150
2c	12 (0.1046 in.)	0.05	43,200	59,650	46,650
		Average	41,100	57,750	46,050
3a	11 (0.1196 in.)	0.05	44,300	63,550	51,850
3b	11 (0.1196 in.)	0.05	50,150	70,550	60,550
3c	11 (0.1196 in.)	0.05	49,000	69,250	55,700
		Average	47,800	67,800	56,050
4a	10 (0.1345 in.)	0.05	52,950	61,250	50,550
4b	10 (0.1345 in.)	0.05	53,550	62,450	51,450
4c	10 (0.1345 in.)	0.05	49,350	57,850	45,350
		Average	51,950	60,500	49,100
5a	0.1875 in.	0.05	47,750	67,200	50,650
5b	0.1875 in.	0.05	48,650	68,000	51,150
5c	0.1875 in.	0.05	49,500	69,100	50,250
		Average	48,650	68,100	50,700
6a	0.250 in.	0.05	39,850	61,000	46,000
6b	0.250 in.	0.05	41,050	61,600	46,400
6c	0.250 in.	0.05	41,100	62,000	46,000
		Average	40,650	61,550	46,150

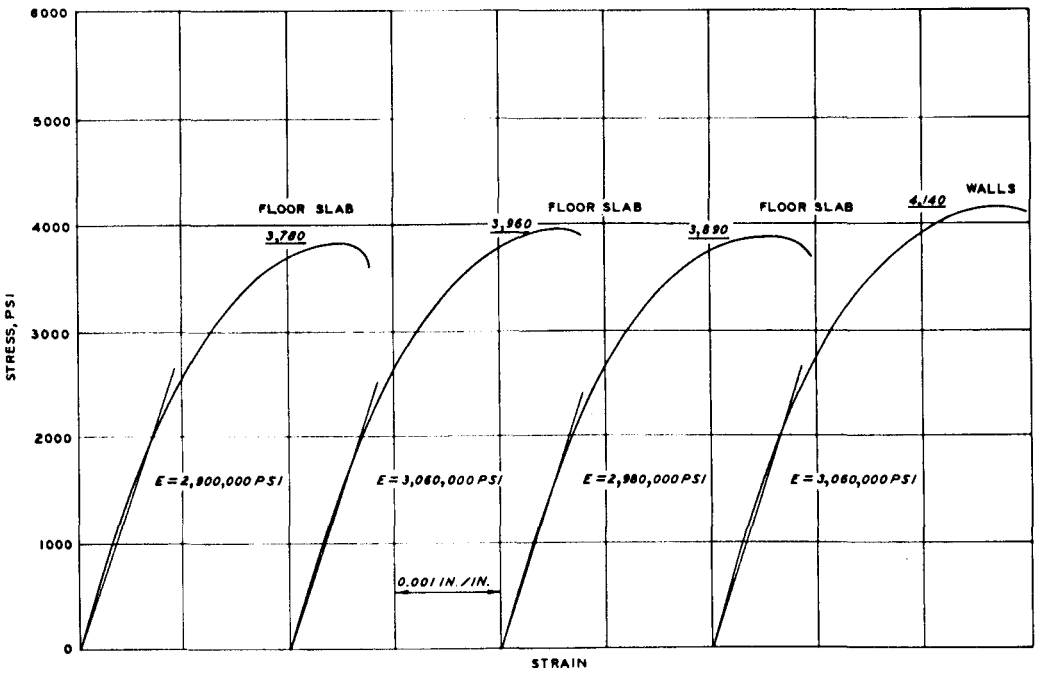

a. Cylinders corresponding to structure for static testing.

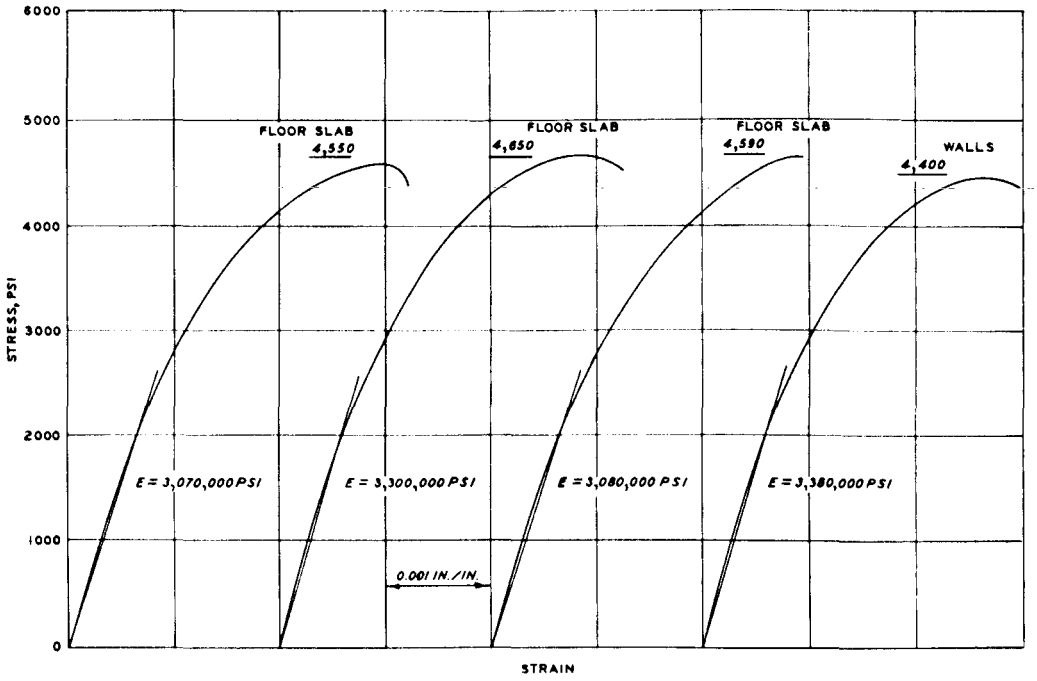

b. Cylinders corresponding to structure for dynamic testing.

Figure 4.1 Typical static stress-strain curves for concrete control cylinders.

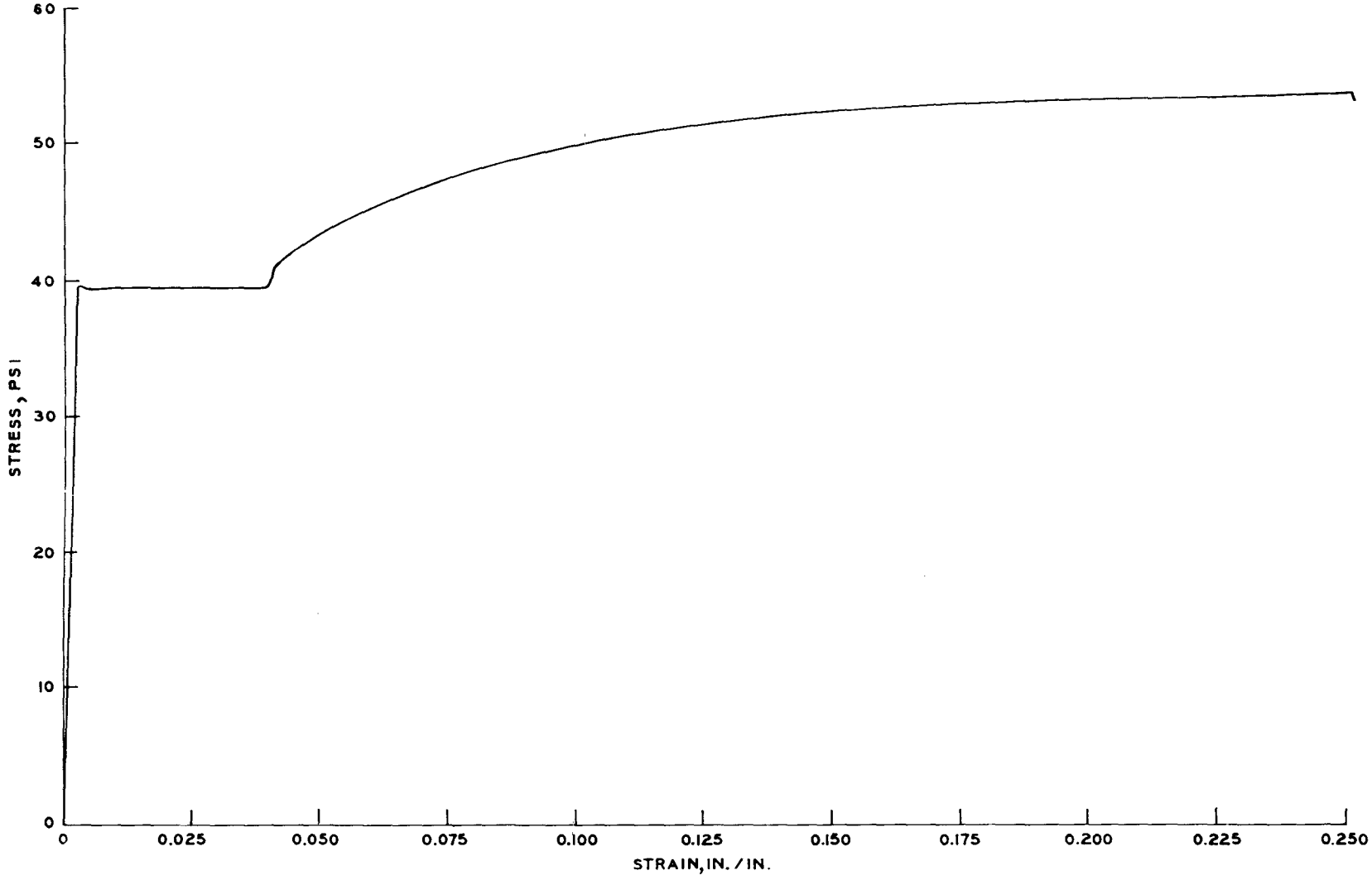

Figure 4.2 Typical stress-strain curve for reinforcing steel.

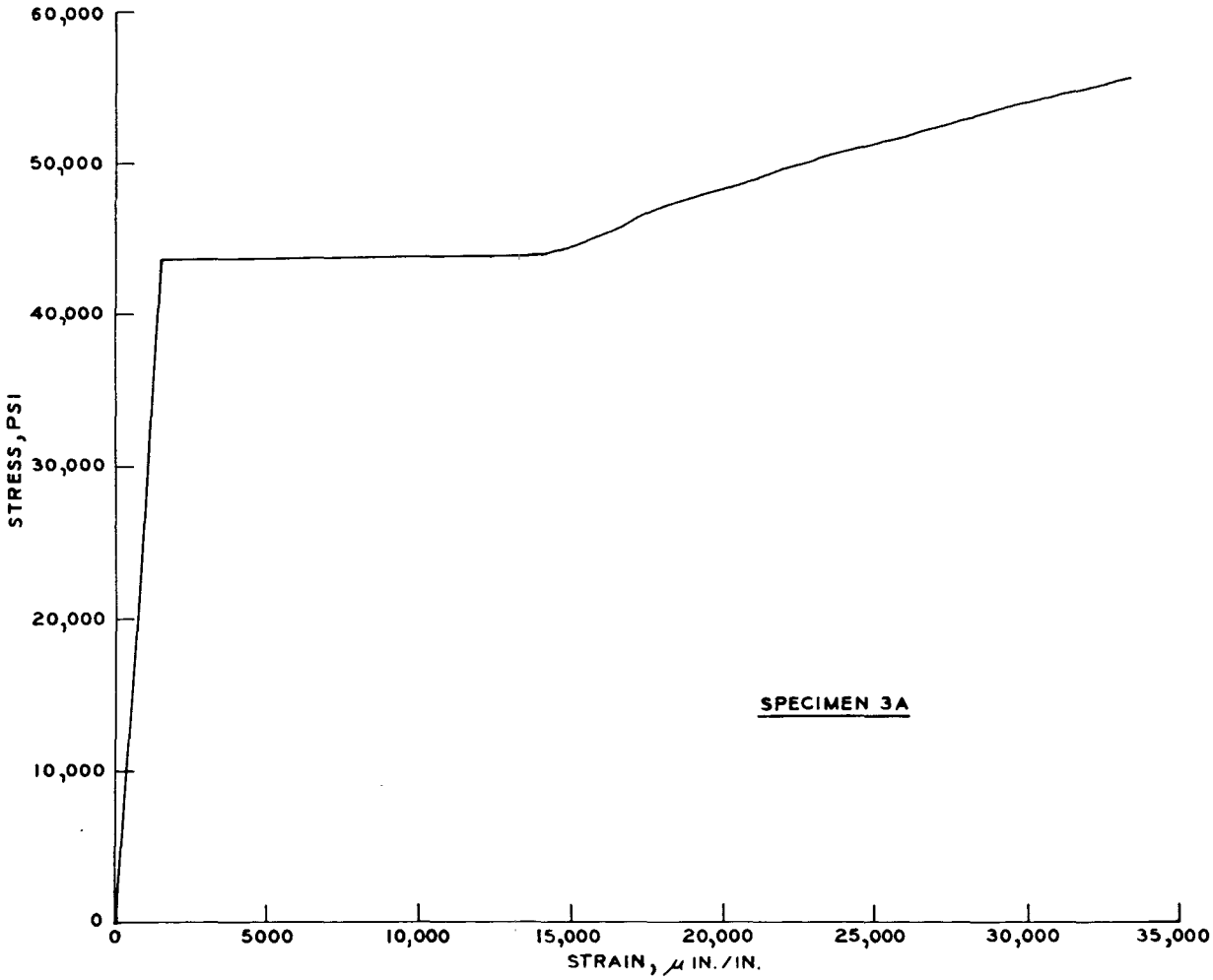

Figure 4.3 Typical stress-strain curve for tensile coupon from steel frame.

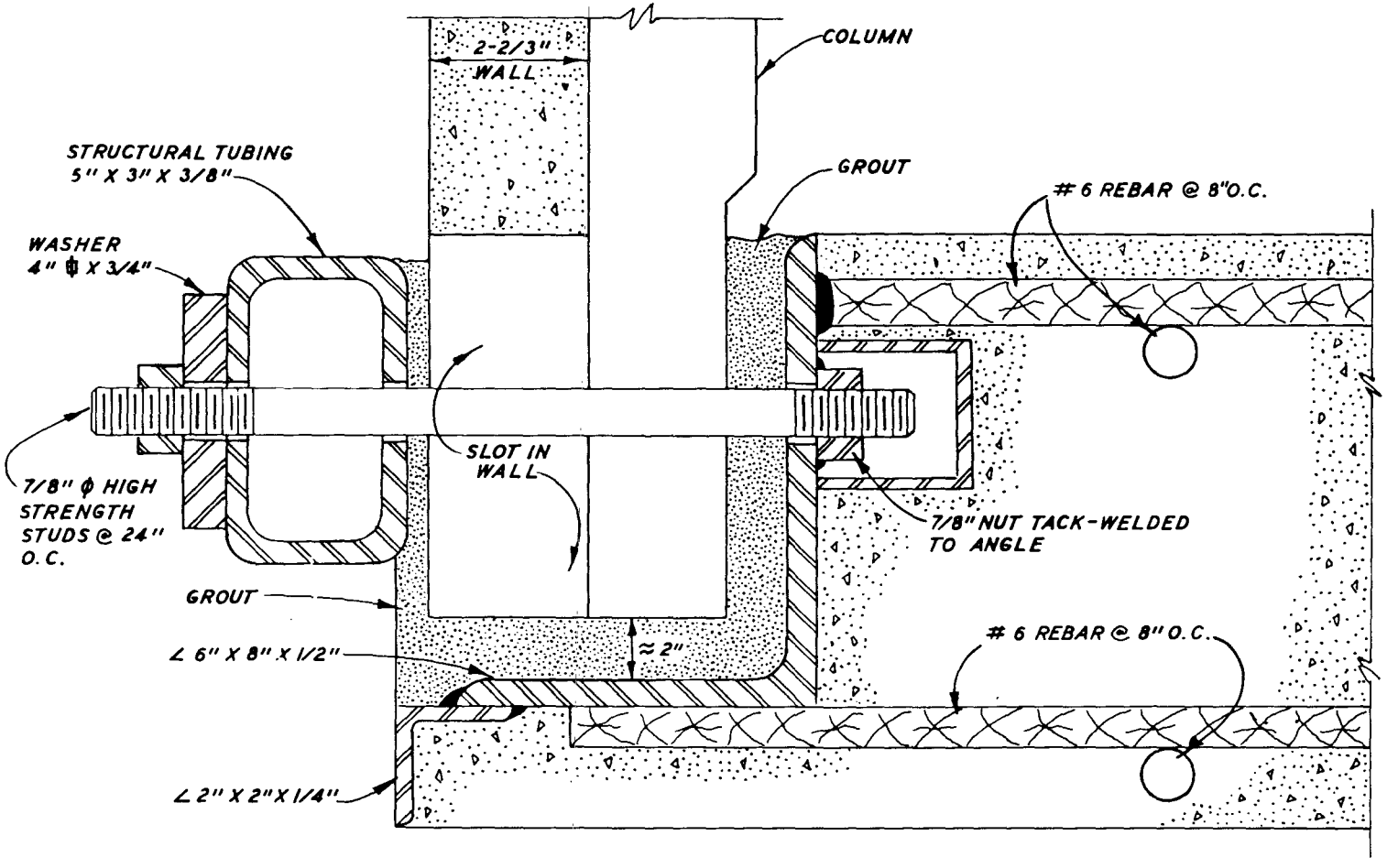

Figure 4.4 Detail of base slab edge and attachment to model wall.

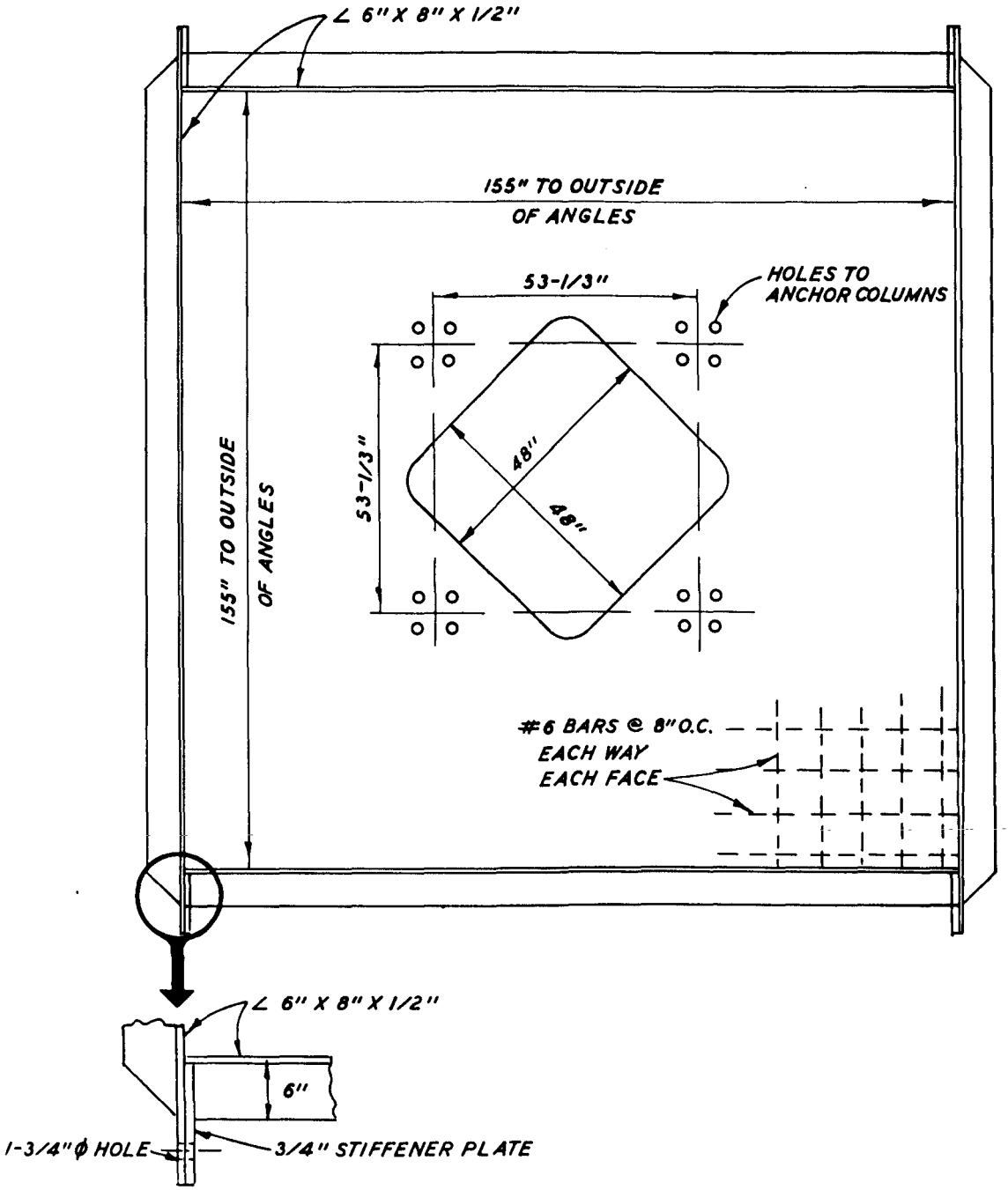

Figure 4.5 Plan view of base slab.

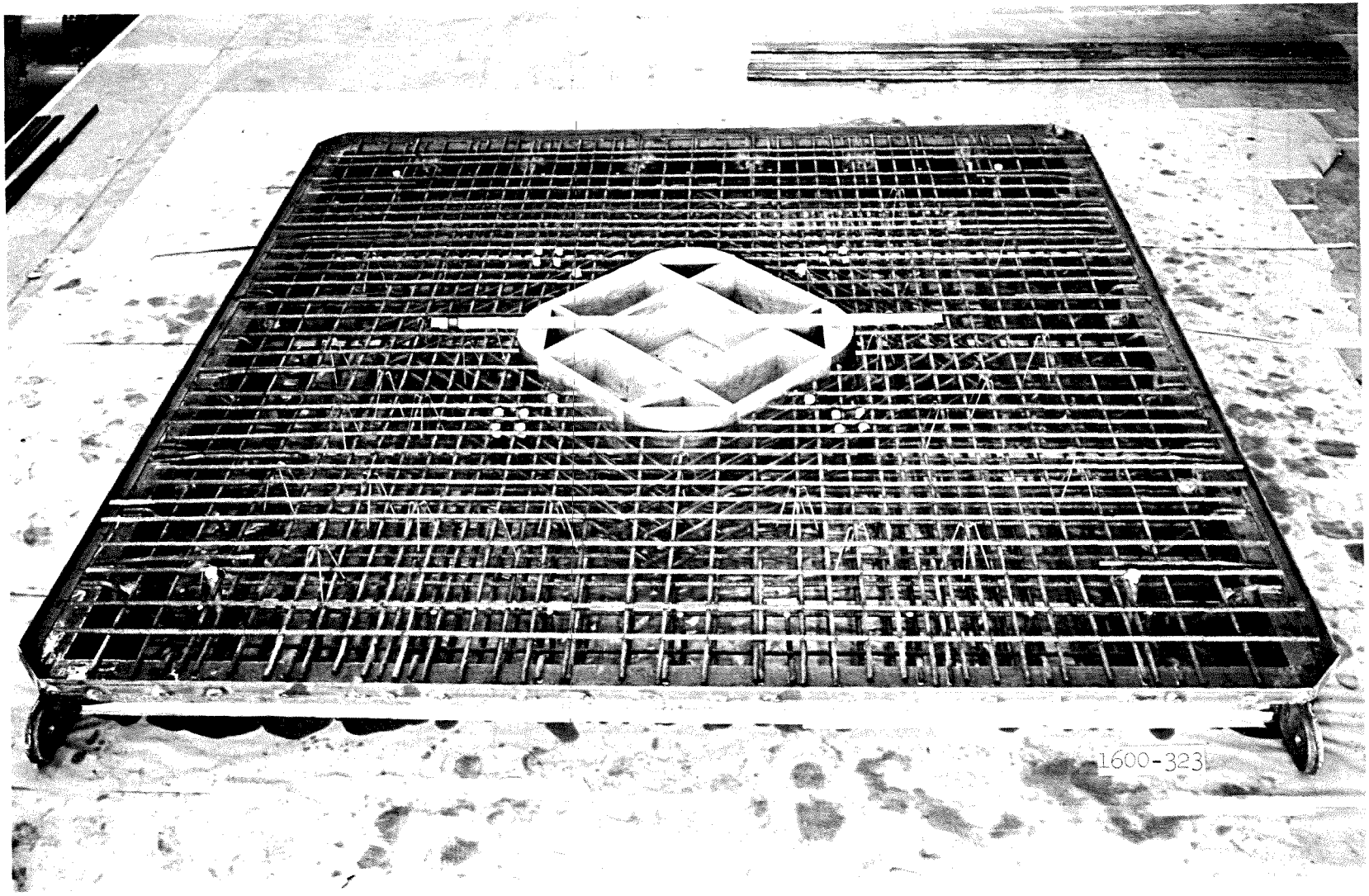

Figure 4.6 Base slab (inverted) before casting of concrete.

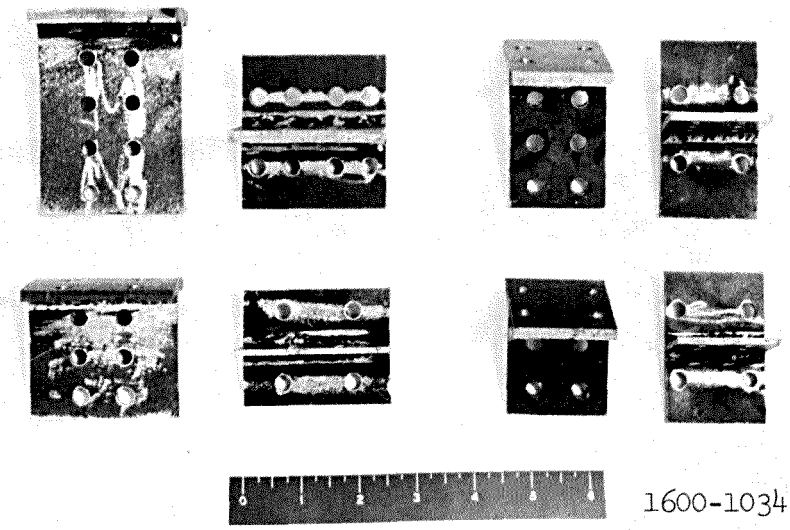

a. Structural tee's.

b. Wide-flange sections.

Figure 4.7 Model structural steel sections.

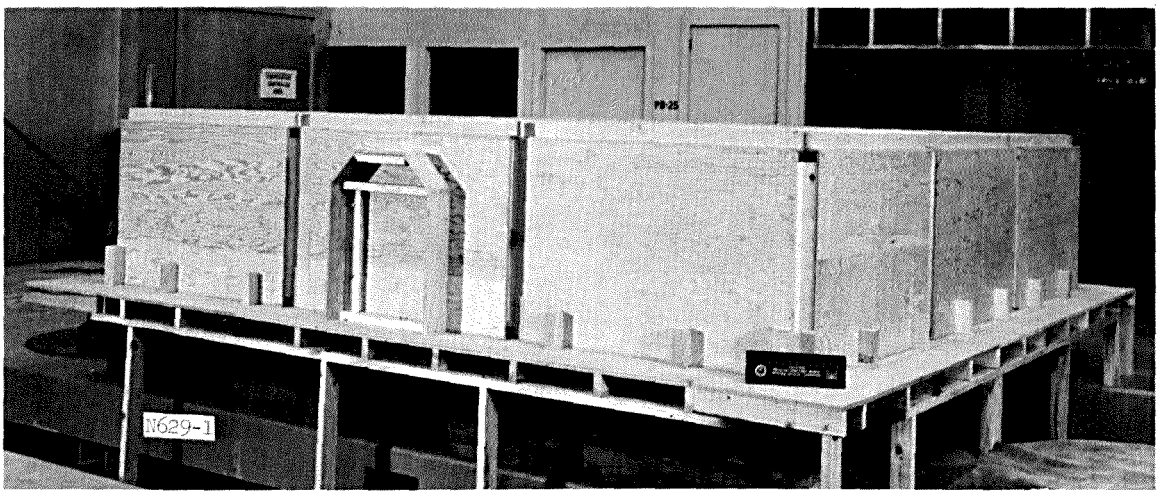

Figure 4.8 Inside wall forms in place.

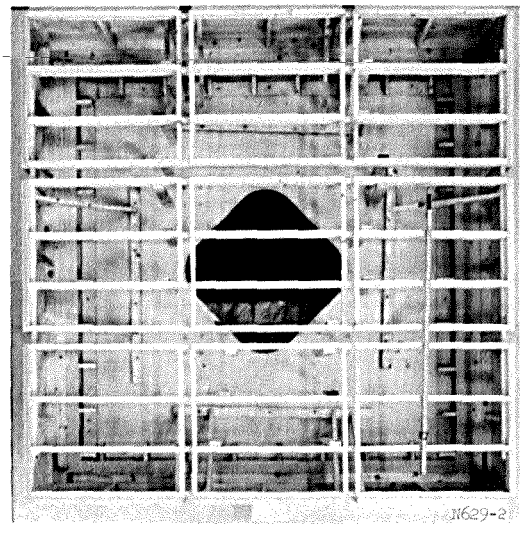

Figure 4.9 Floor framing.

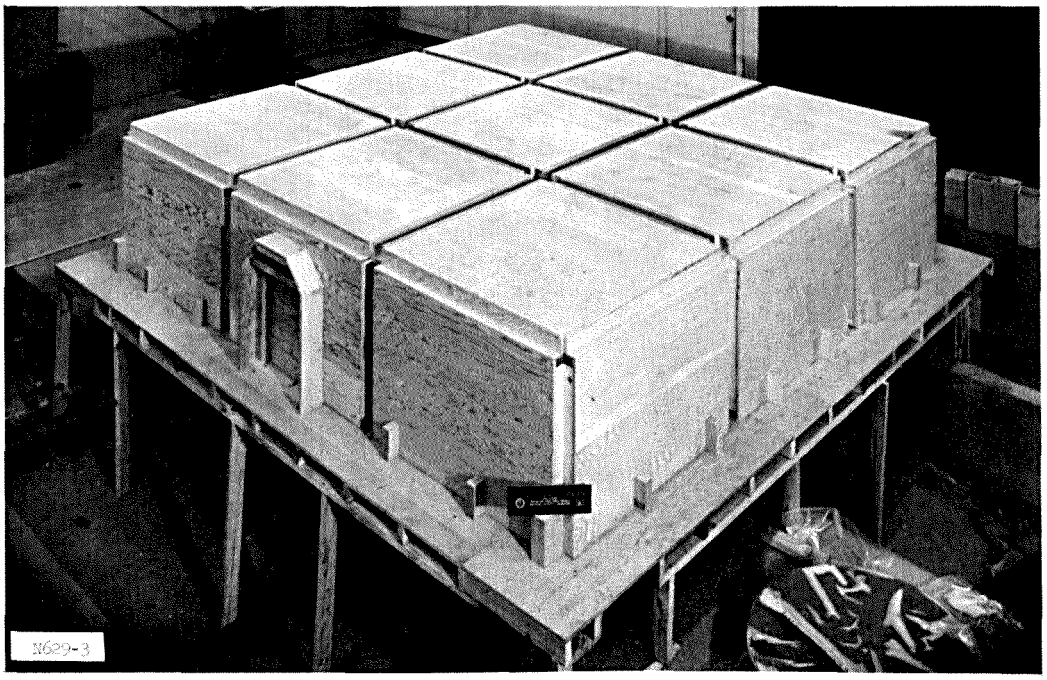

Figure 4.10 Complete inner formwork.

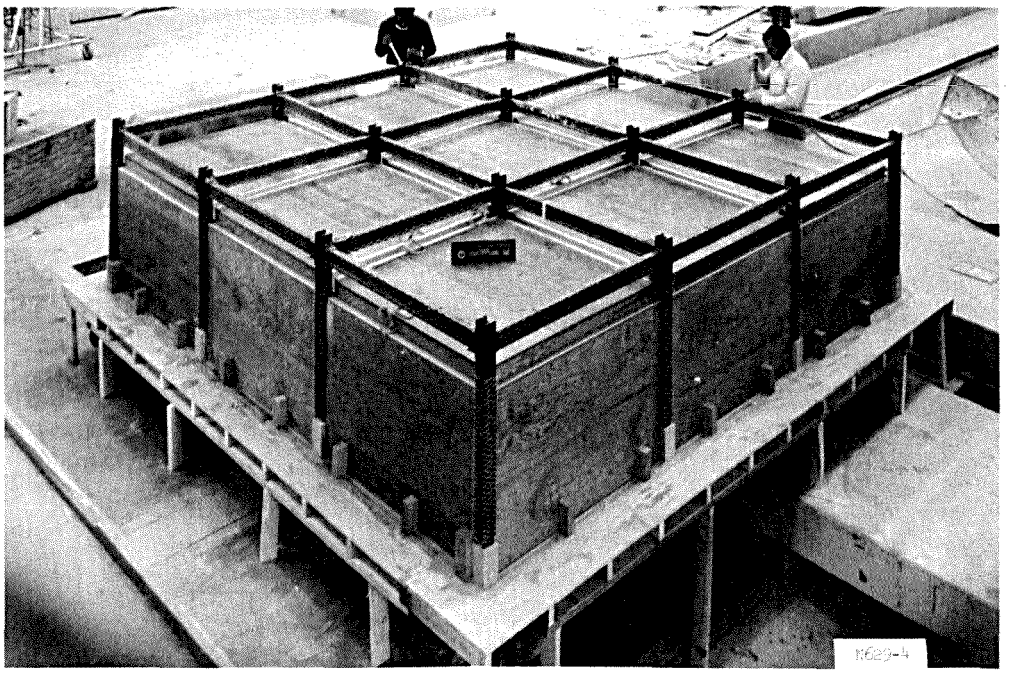

Figure 4.11 Steel frame partially assembled.

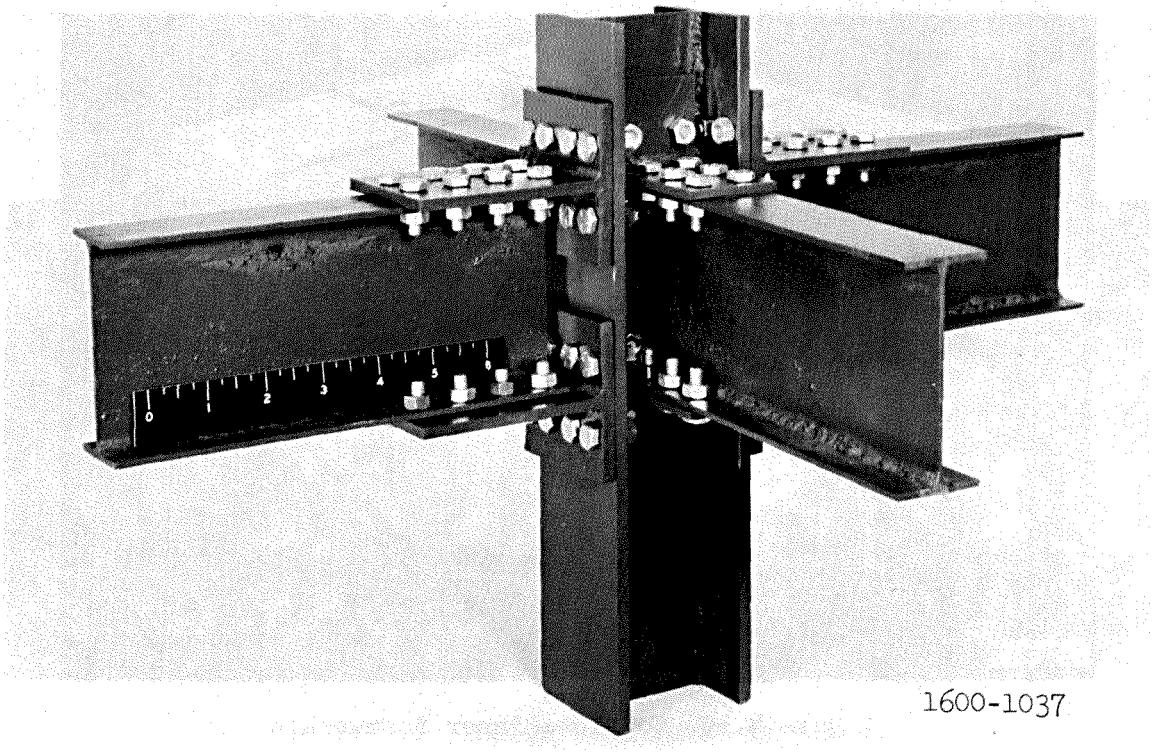

Figure 4.12 Detail of interior beam-column connection.

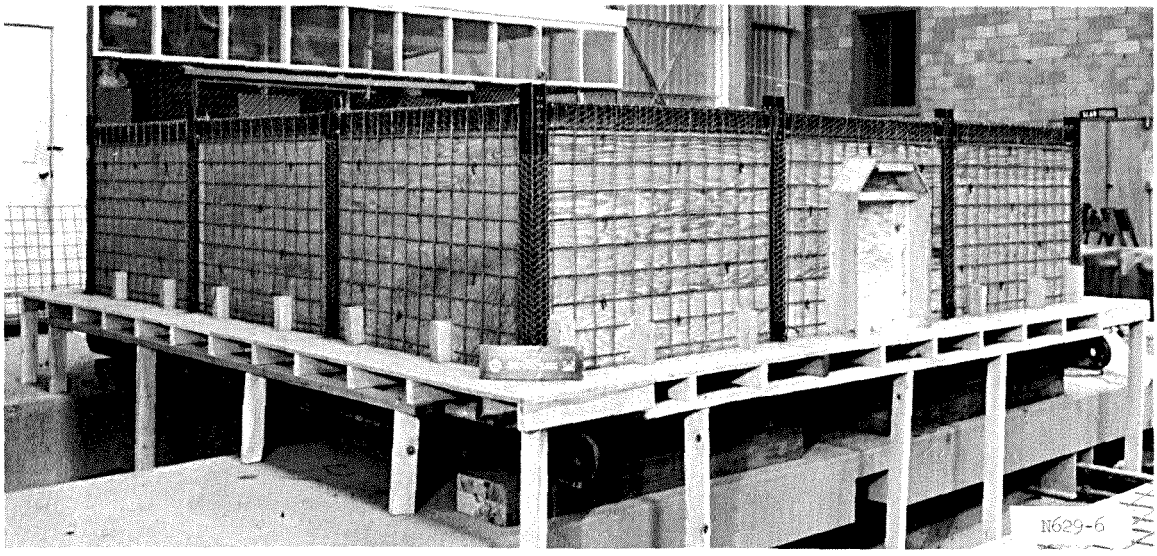

Figure 4.13 Inside wall reinforcing mat (static model).

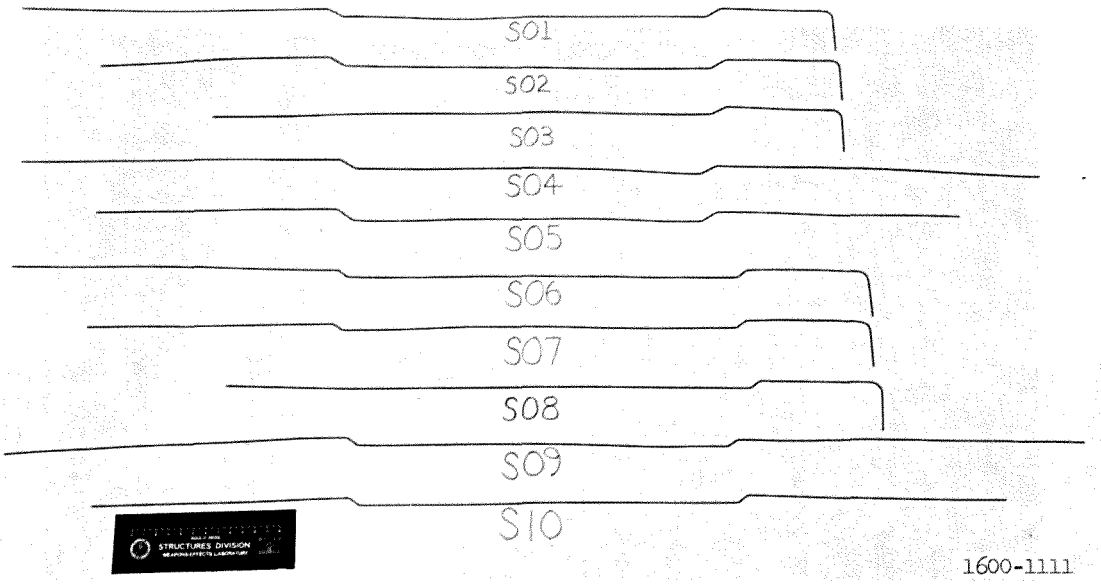

Figure 4.14 Detail of bent reinforcing bars.

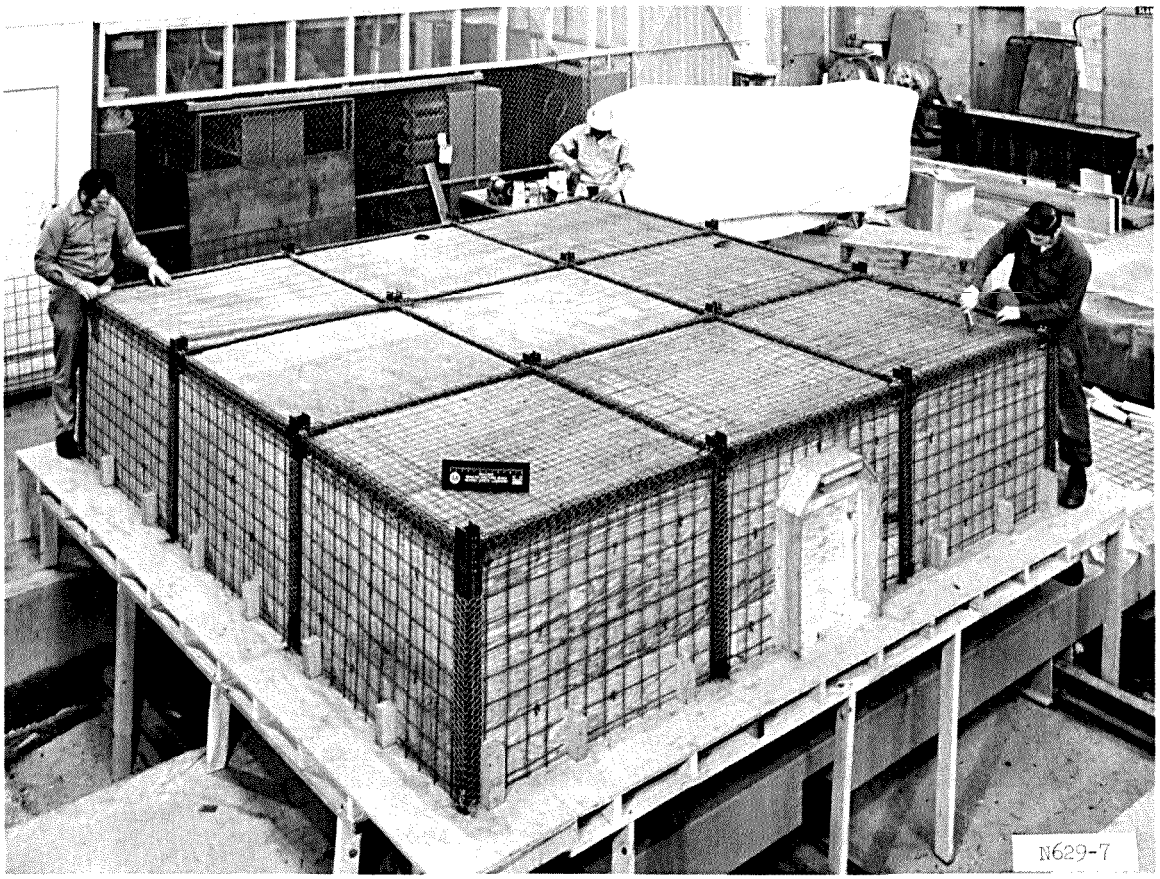

Figure 4.15 Placing floor slab reinforcing for static model.

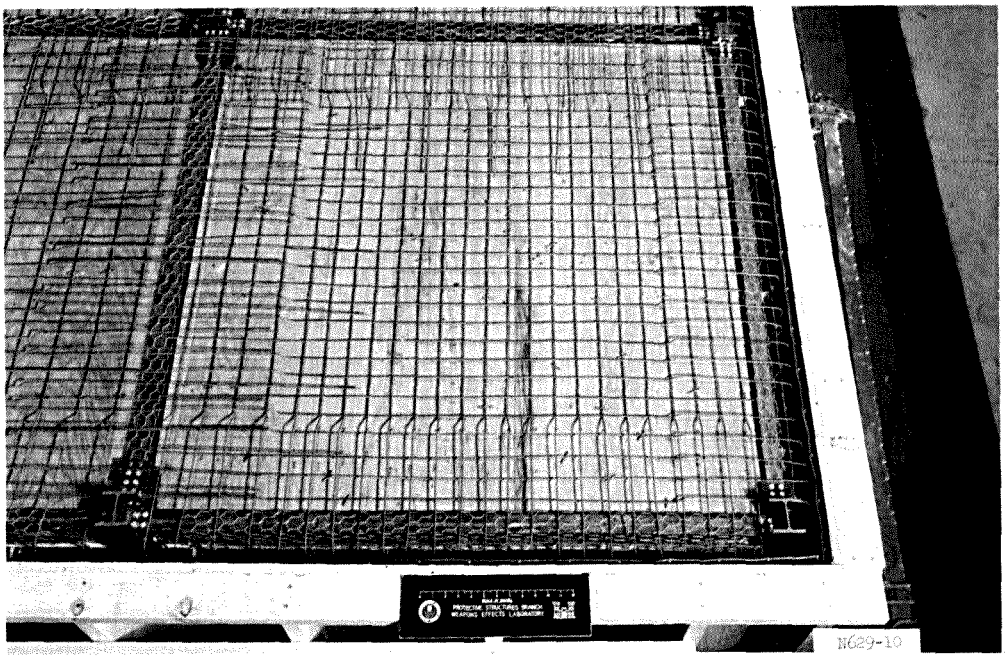

a. Detail of reinforcement of corner panel.

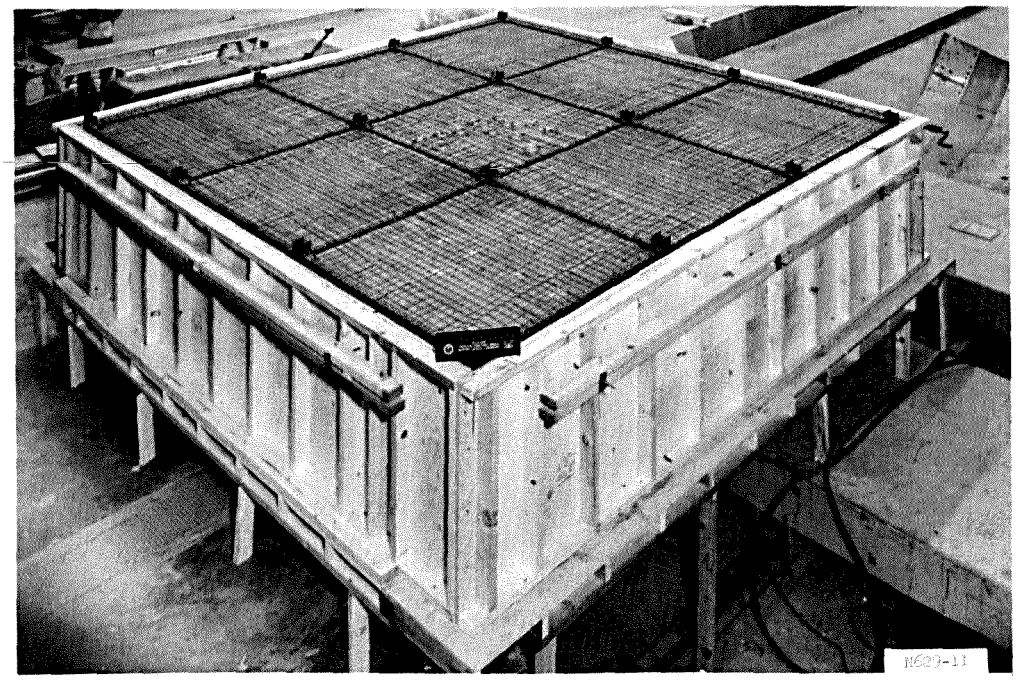

b. Slab and wall reinforcing steel in place.

Figure 4.16 Closeup and overall view of static model.

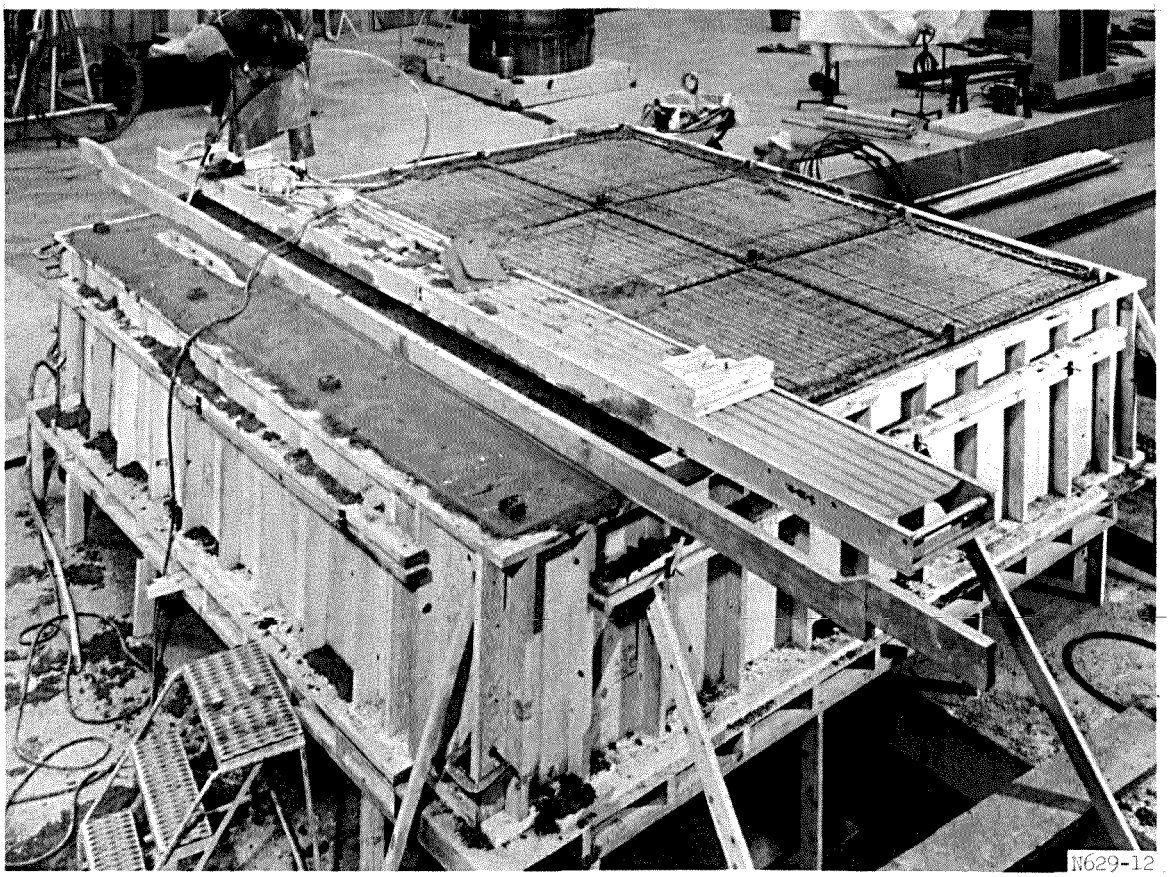

Figure 4.17 Concrete placement for static model.

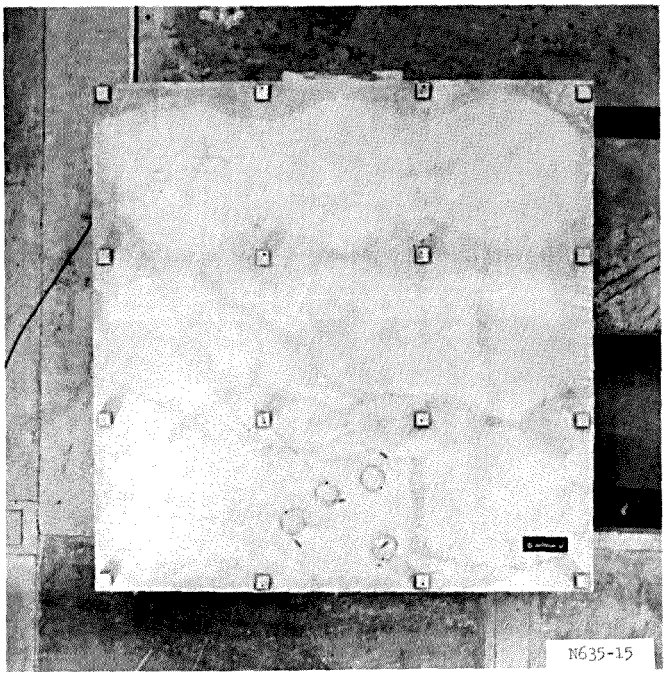

a. Pretest cracks unmarked.

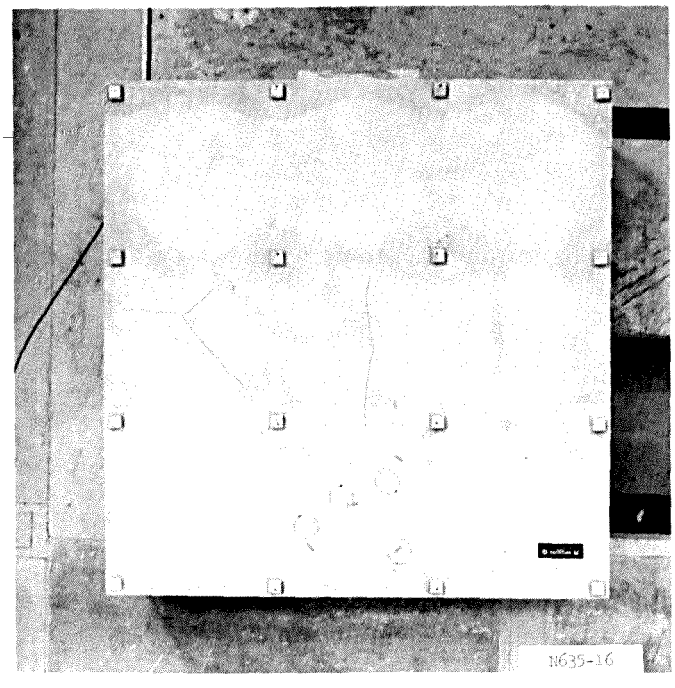

b. Pretest cracks marked.

Figure 4.18 Overhead view of static test model showing pretest cracks in floor slab.

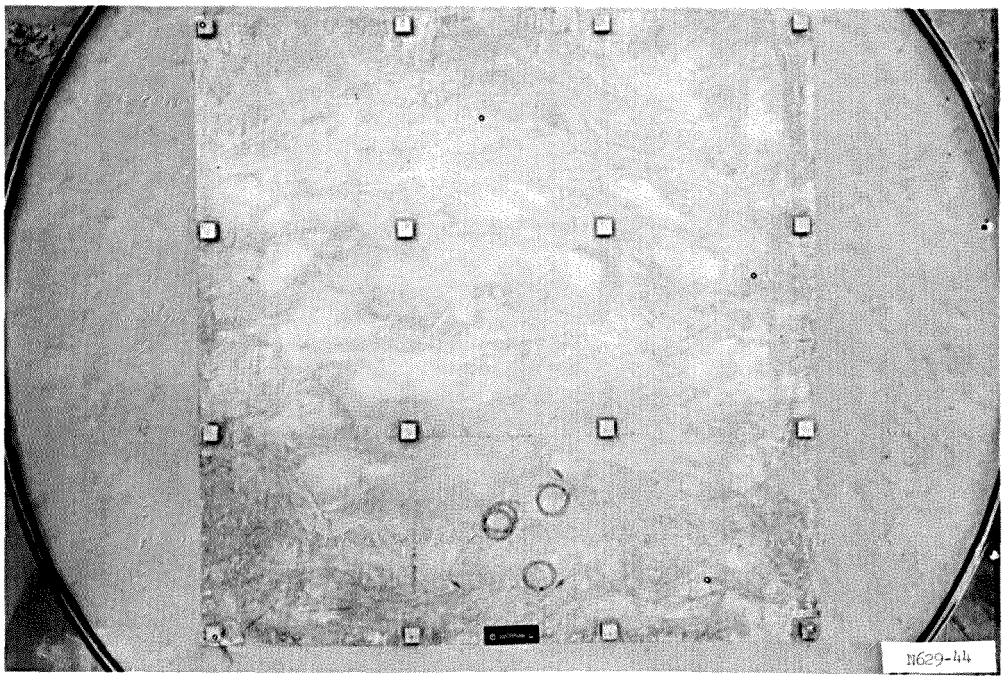

a. Pretest cracks unmarked.

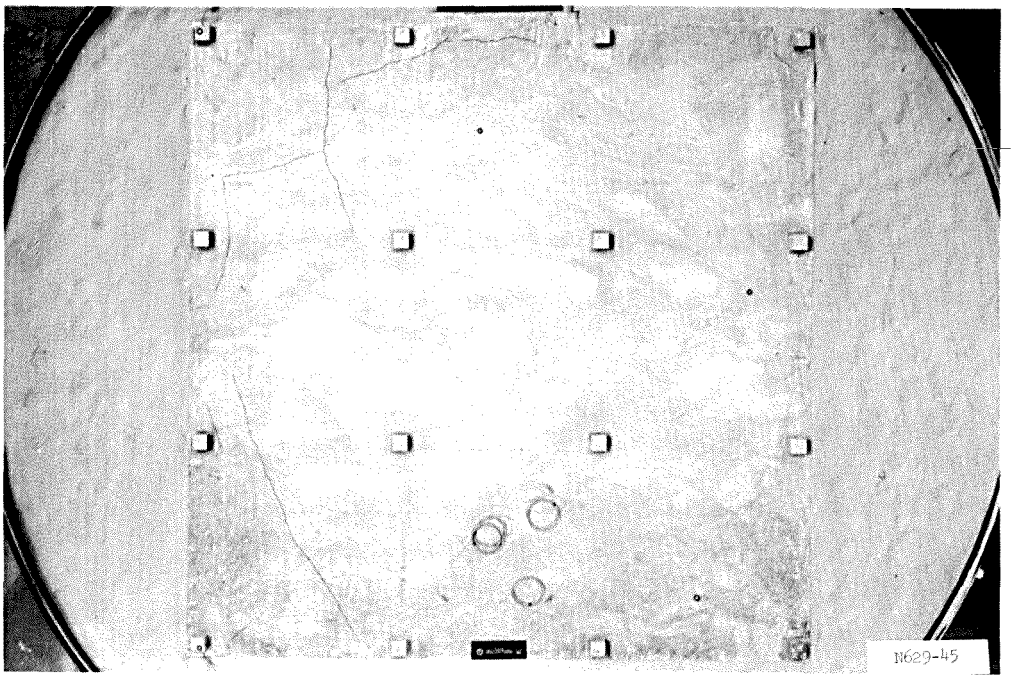

b. Pretest cracks marked.

Figure 4.19 Overhead view of dynamic test model showing pretest cracks.

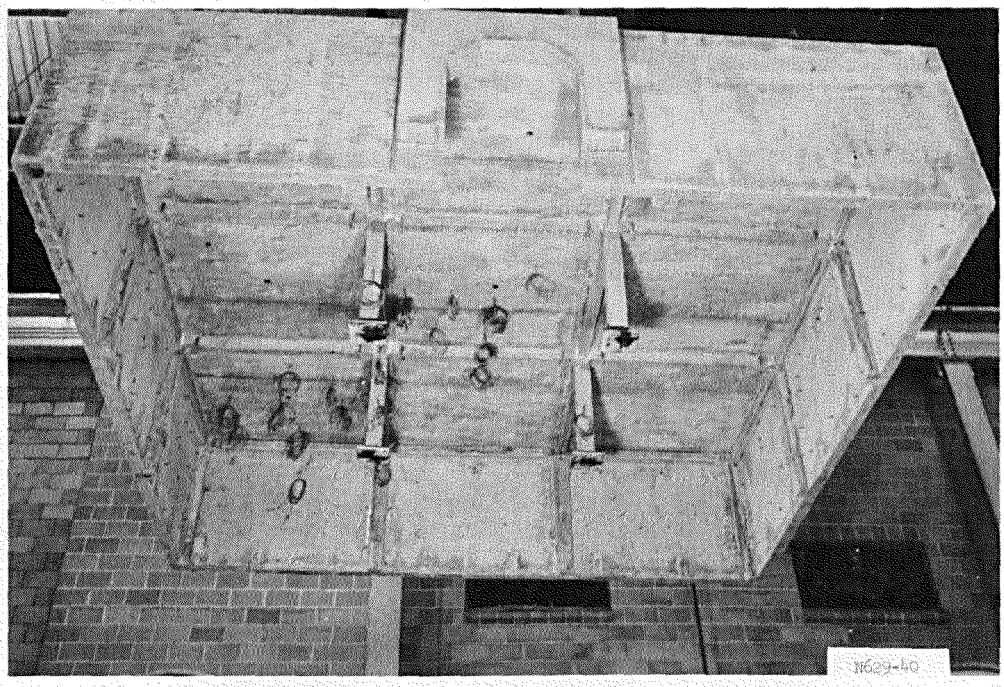

a. Interior, looking from door side of model.

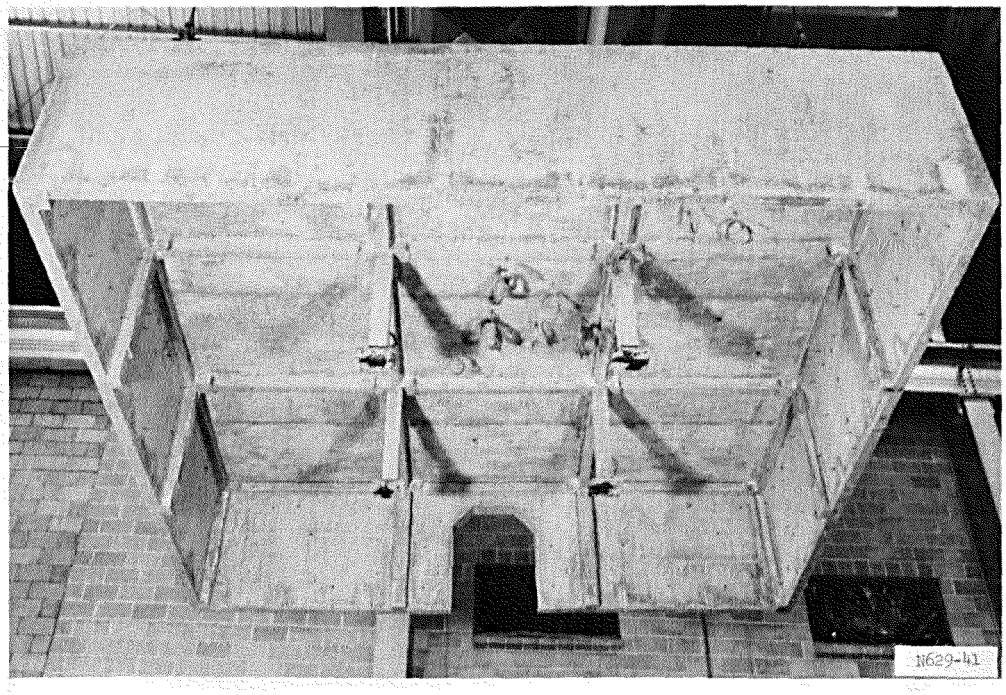

b. Interior, looking toward door side of model.

Figure 4.20 Views of the underside of the dynamic test model.

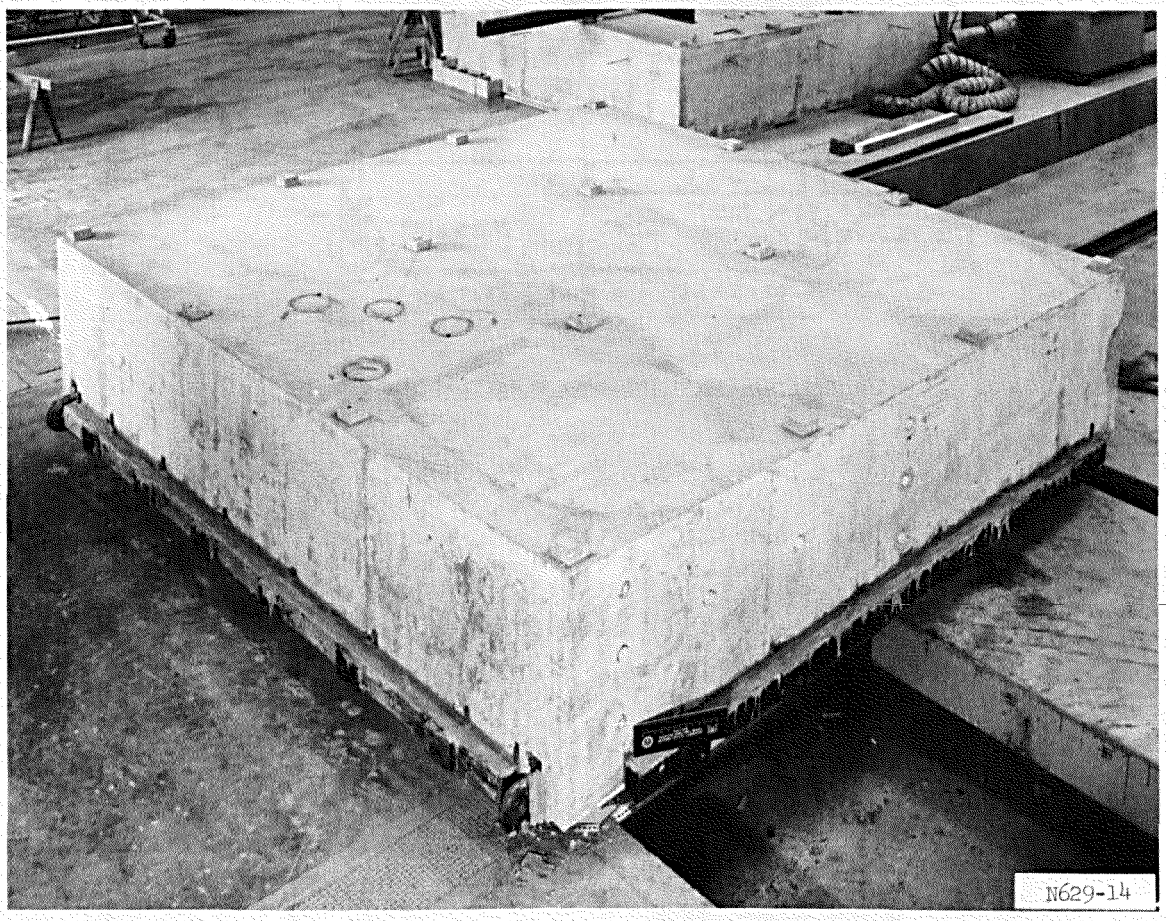

Figure 4.21 Static model grouted in place on the base slab.

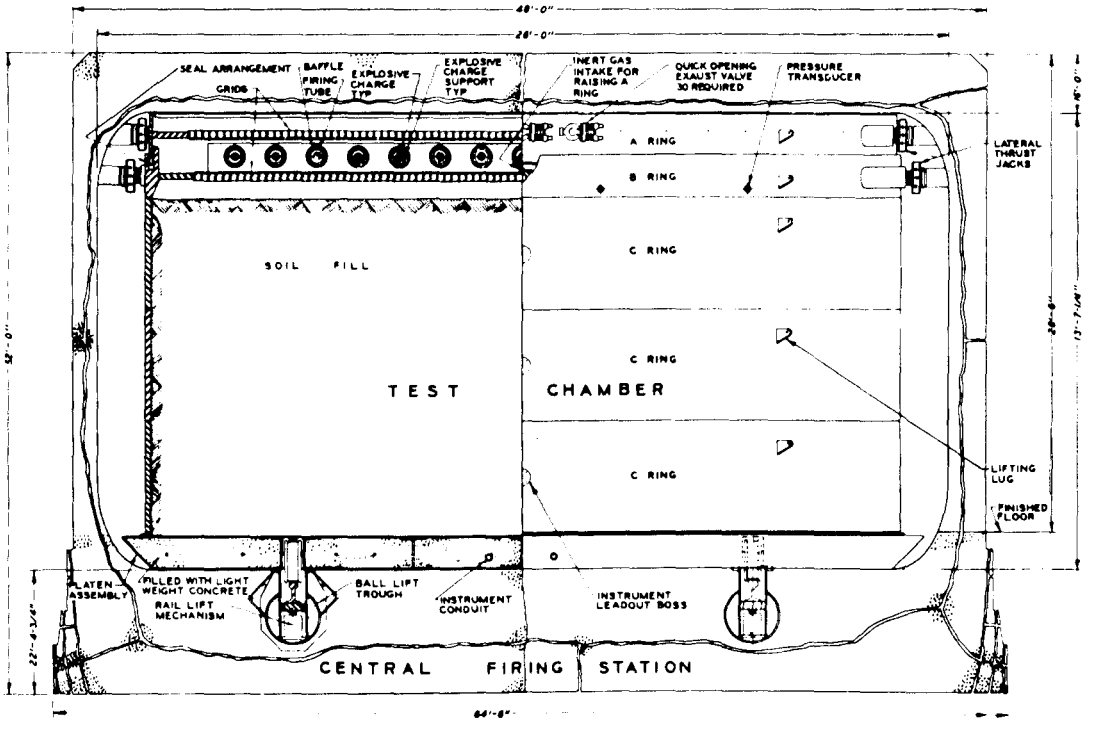

a. HALF-SECTION OF THE LARGE BLAST LOAD GENERATOR

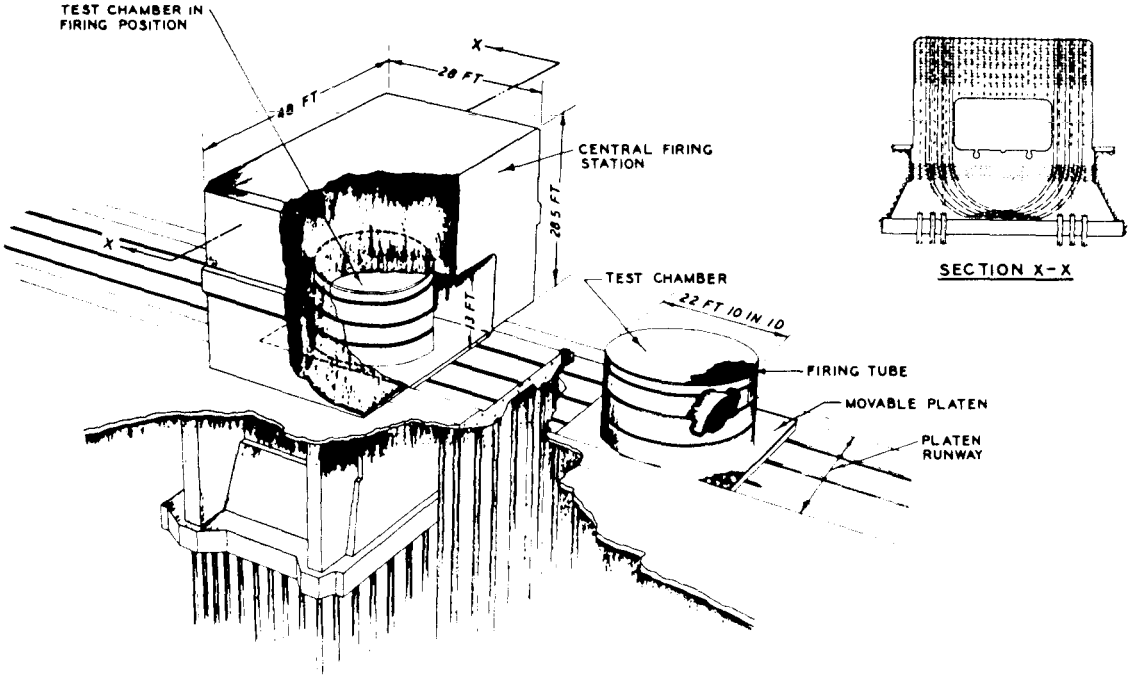

b. CUTAWAY VIEW OF THE LARGE BLAST LOAD GENERATOR

Figure 4.22 Large Blast Load Generator.

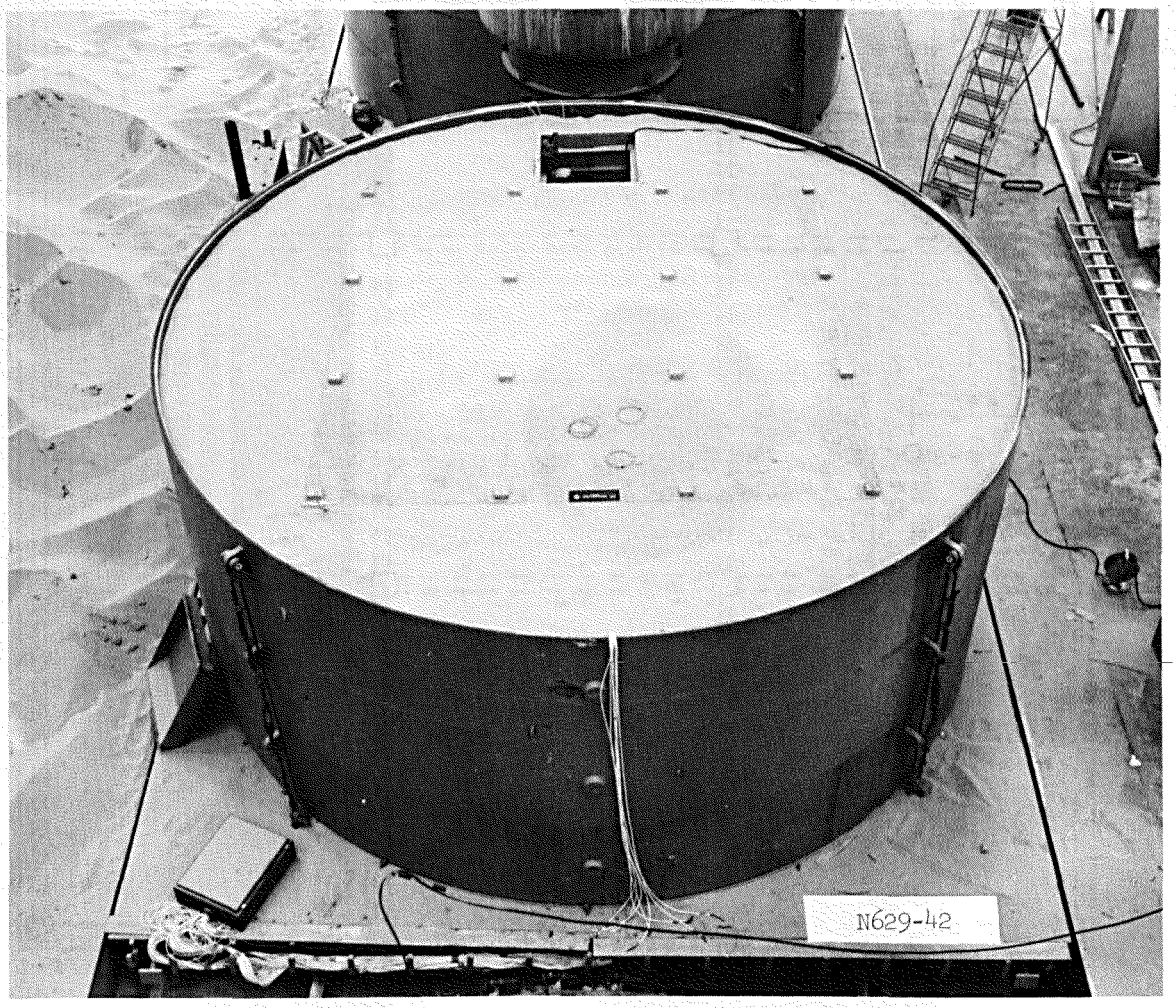

Figure 4.23 Dynamic model in test chamber.

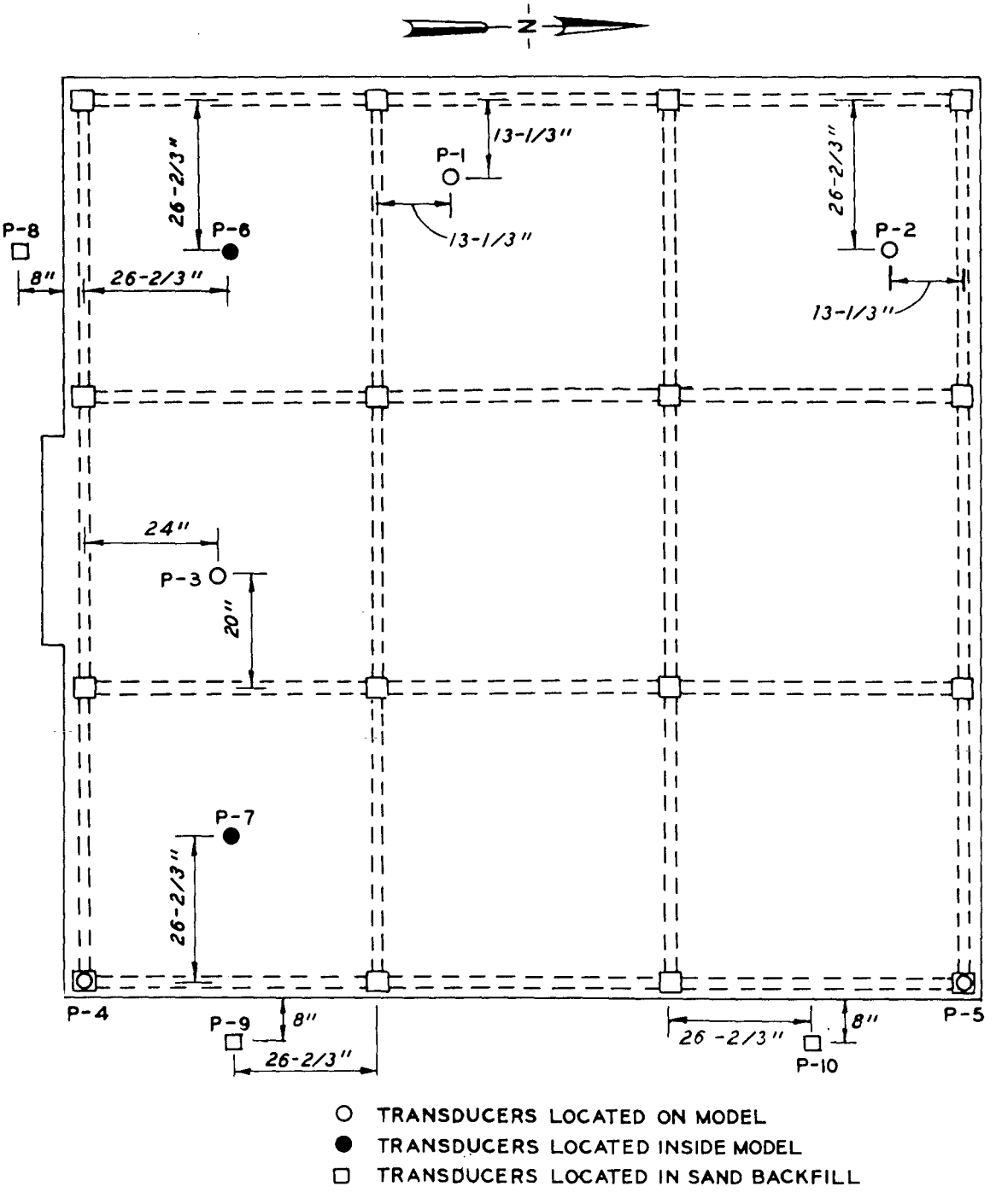

Figure 4.24 Pressure transducer locations, dynamic test.

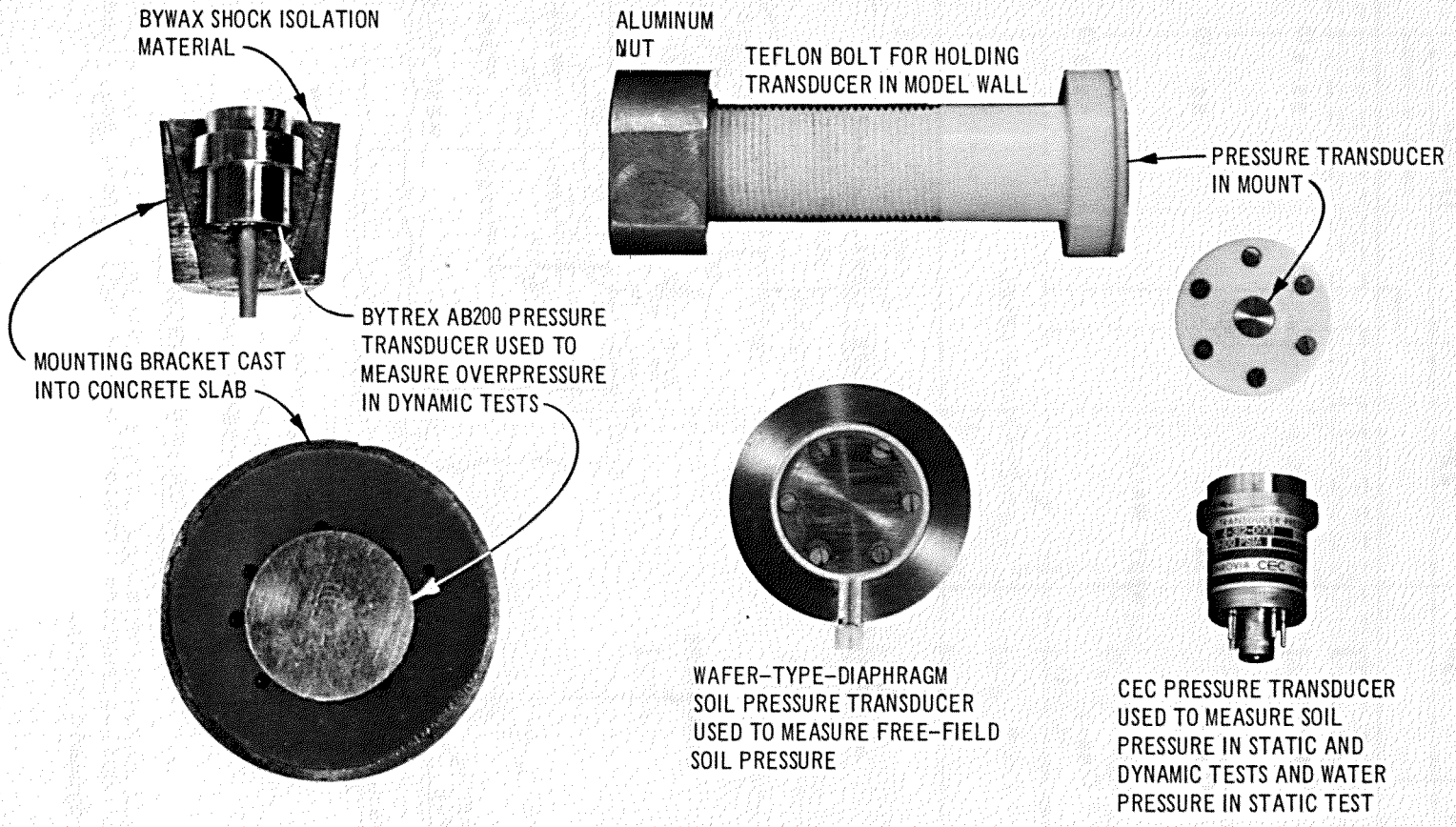

Figure 4.25 Pressure transducers

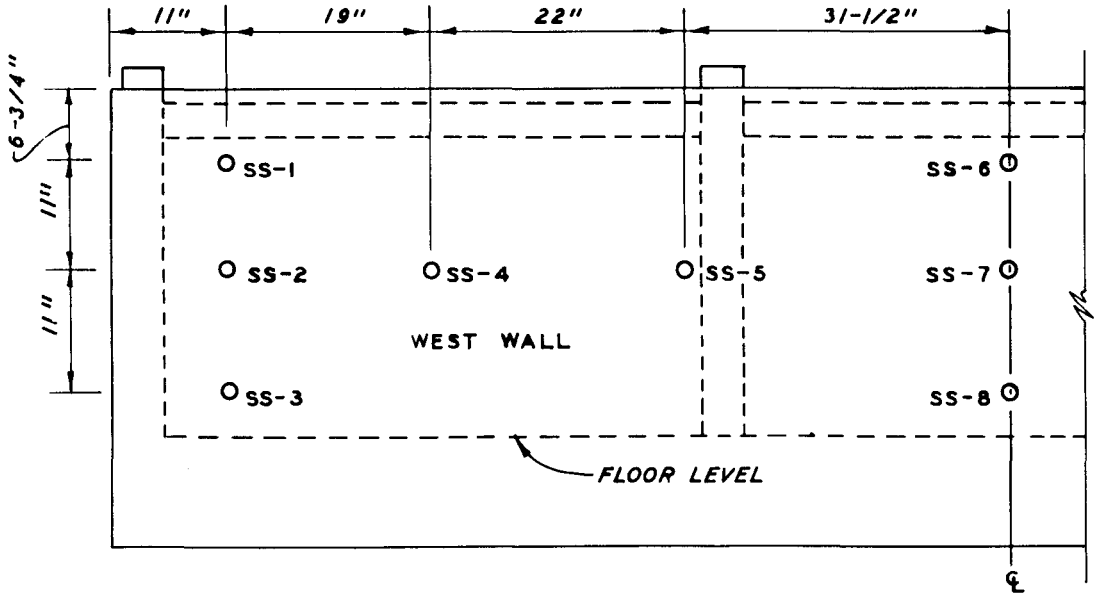

a. LOCATIONS OF SOIL-STRUCTURE INTERACTION GAGES

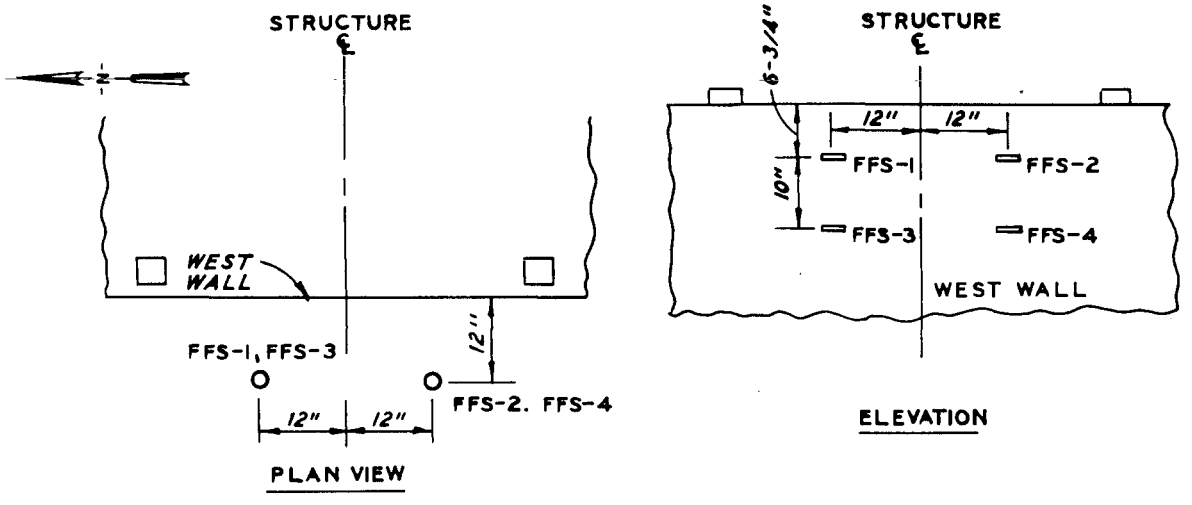

b. LOCATION OF SOIL STRESS GAGES

Figure 4.26 Soil-structure interaction and soil stress gage locations, static and dynamic tests.

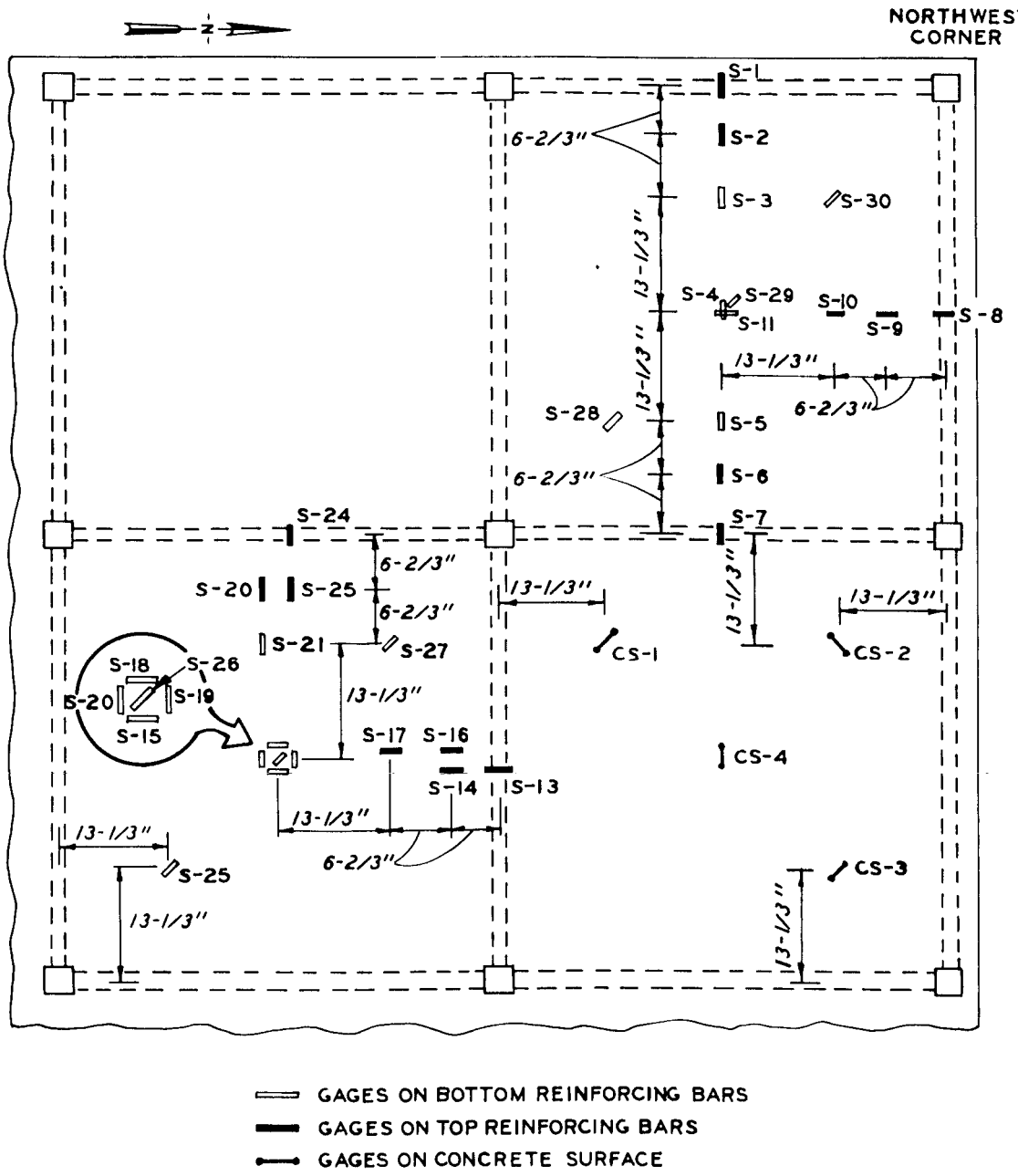

Figure 4.27 Locations of strain gages on reinforcing steel and concrete slab.

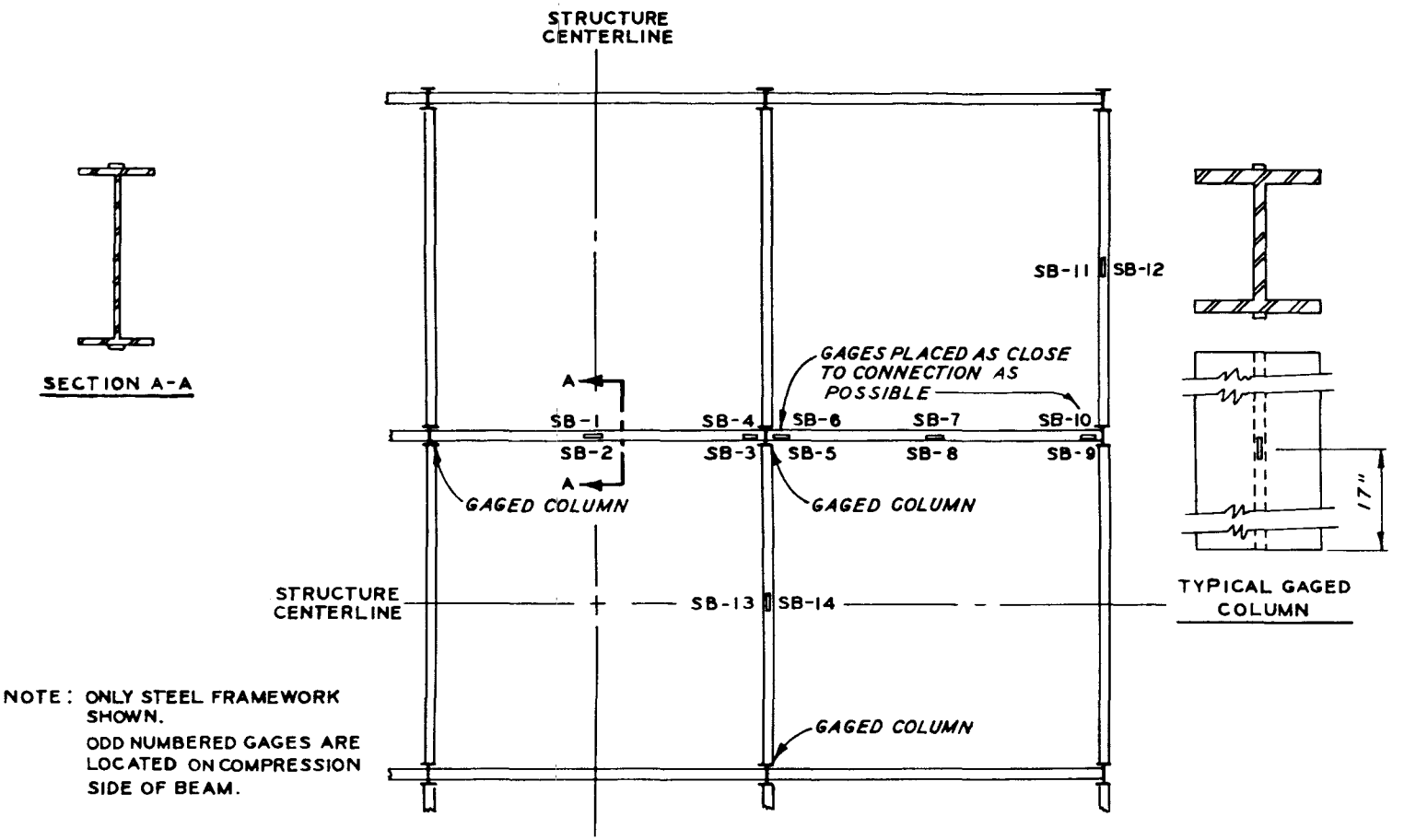

Figure 4.28 Strain gage locations on structural steel frame, static and dynamic models.

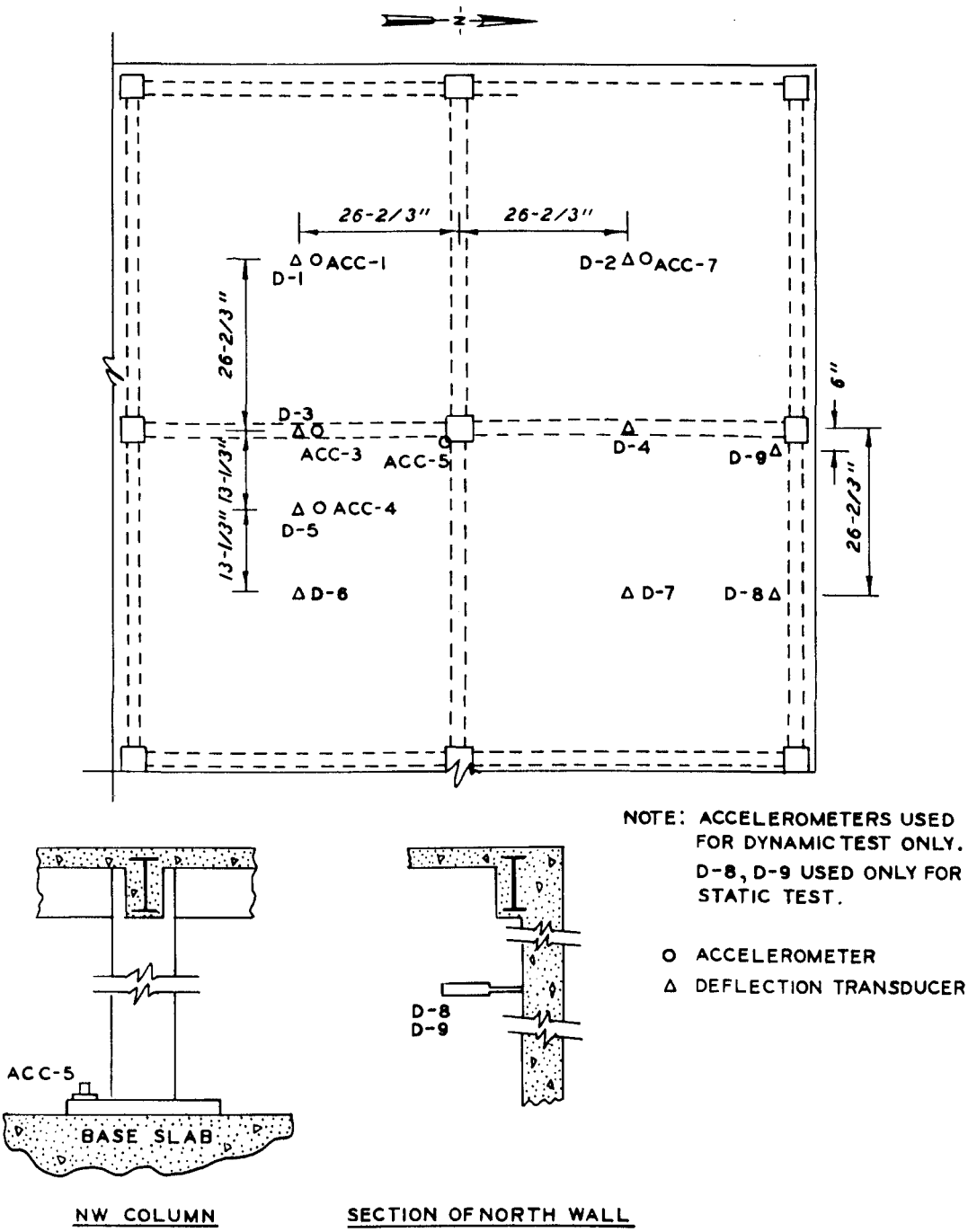

Figure 4.29 Locations of accelerometers and deflection transducers.

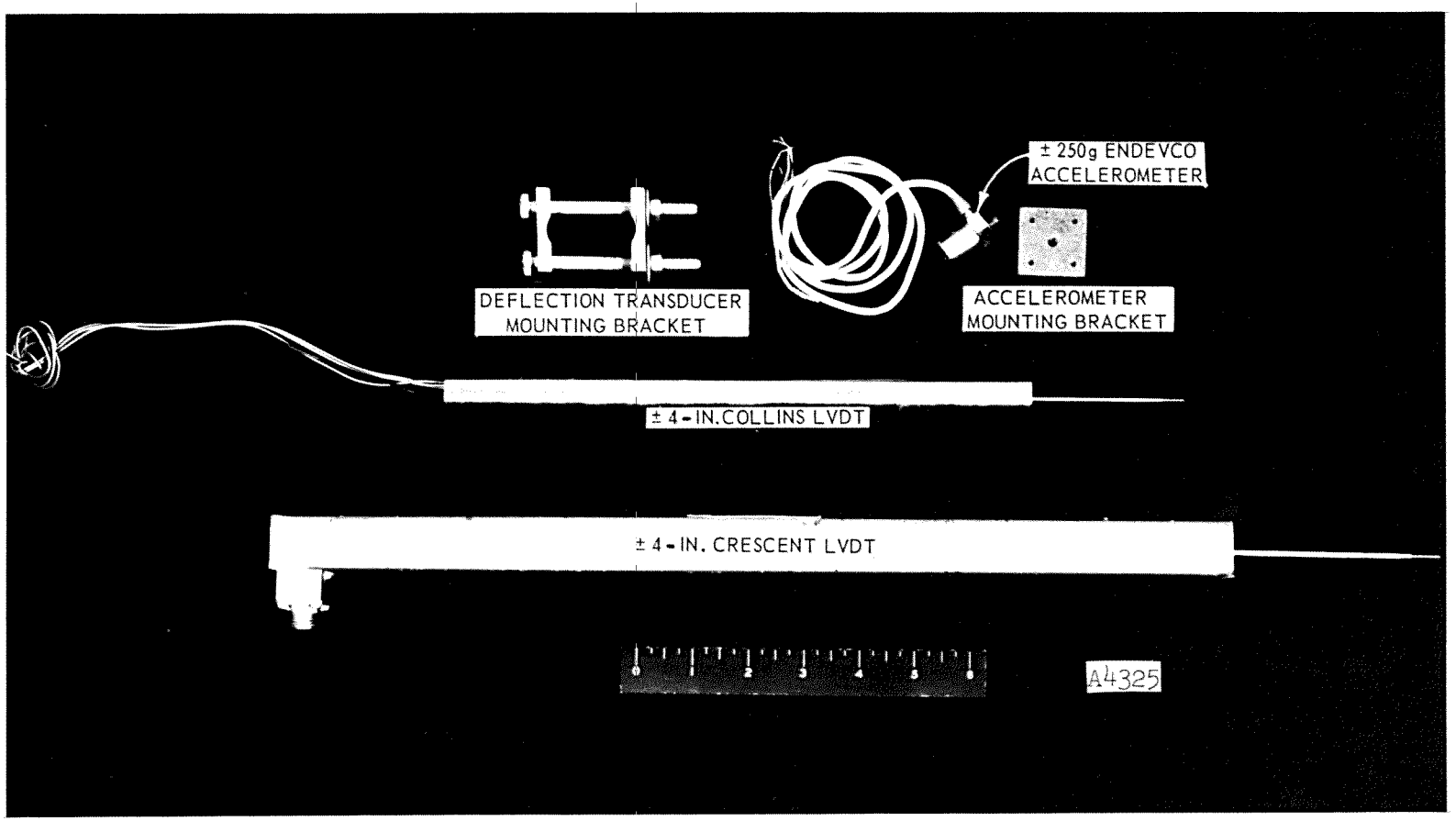

Figure 4.30 Acceleration and deflection transducers.

CHAPTER 5

EXPERIMENTAL TEST RESULTS

Plots of the test records for the static and dynamic tests are contained in Appendixes A and B, respectively. The plots were prepared by digitizing the FM magnetic tapes and utilizing a computer to plot each recorded transducer output versus time for the dynamic test and one of the pressure transducer's output versus all other recorded transducers' outputs for the static test. Presented herein is a brief discussion of the performance of the statically and dynamically tested models. An analysis of the test results is presented in Chapter 6.

5.1 STATIC MODEL

The static model failed at a pressure of 8.8 psi in a test that lasted approximately 9 minutes. Recorded data from this test are presented in Appendix A.

5.1.1. Performance of Model. Prior to the static test, it was thought that the 0.035-inch-thick polyurethane diaphragm water seal was too strong to be used over a model which was expected to fail at less than 10 psi. However, attempts to locate a thinner diaphragm proved futile, and it was necessary to use the 0.035-inch-thick diaphragm. Inspection of the diaphragm and the model after the test indicated that the diaphragm had followed the deflection of the slab. Figure 5.1 shows the static model in the test chamber prior to removal of the polyurethane diaphragm.

The model after removal of the diaphragm is shown in Figure 5.2. All nine panels of the floor slab had large permanent deflections with considerable cracking in the central portion of the panels. A yield-line crack was formed completely around the perimeter of the panels alongside the supporting beams. The conventional yield-line pattern that forms along the diagonals of the panels did not fully develop. In the photographs (Figure 5.3) of the slab panels, the beginnings of the diagonal yield lines can be seen forming.

Figure 5.4 shows the interior of the static model after the test.

As can be seen in the figure, the columns and floor support beams received very little damage.

Cracking of the underside of the slab panels can be seen in Figures 5.5 and 5.6. The crack pattern is similar to that obtained in the study described in Reference 18, in which simply supported two-way-reinforced concrete slabs were tested. The damage to the base of the walls that can be seen in Figures 5.5 and 5.6 occurred when the model was removed from the base slab and not during the test.

Deflections of the slab panels ranged from a maximum of 14 inches at the center of corner panel A-4 to a minimum of 6 inches at the center of panel C-2. Posttest profiles of the roof slab of the model are shown in Figure 5.7.

5.1.2 Recorded Data. Tracings of the paper playbacks of the magnetic-tape records display the output of each transducer versus time (Figures A.1-A.6) and the applied pressure transducer, P-1, plotted versus the remaining transducers (Figures A.7-A.21).

The tracings and the plotted data both contain a zero offset due to the water preload on the model at the start of the test. All transducers were zeroed prior to the filling of the upper portion of the test chamber with water. At the beginning of the test, the pressure transducers had approximately 24 inches of water above them and the model had approximately 32 inches of water above it. By zeroing the transducers prior to filling the chamber with water, the effects of the water preload were included in the recorded data and appeared as the zero offset at the beginning of the test.

The plotted data shown in Figures A.7 through A.21 are not shown for the entire test period. The plots were terminated either at the point at which the applied pressure suddenly dropped to approximately 25 percent of its maximum value or at the point at which the transducer failed or was overranged.

Of the 74 channels of data recorded, only two were lost. One strain gage had a wire broken inside the concrete slab; the other was a faulty strain gage. The north wall of the model did not move enough during the test for the two deflection gages monitoring its movement to

register any usable information. The outputs from these two gages appear to be recordings of the noise level in the recording system.

5.2 DYNAMIC MODEL

Physically the dynamic model was identical with the static model. Some instrumentation was changed from that used for the static test in order to better define the performance of the model under dynamic conditions. The testing procedures used for the dynamic test are discussed in Section 4.3.5.

Plots of the recorded transducer outputs versus time are presented in Appendix B.

5.2.1 Performance of Model. The dynamic model was subjected to a blast-type loading having a rise time of 14 milliseconds, a duration of several hundred milliseconds, and an average peak overpressure of 10.2 psi. The floor slab of the dynamic model failed in a manner similar to that of the static model. The static test was stopped when the reinforcing steel ruptured along the outside edges of one of the corner panels, causing a large drop in the water pressure. The reinforcing steel ruptured near the outside corner of all four corner panels in the dynamic model.

Figure 5.8 shows the dynamic model in the test chamber after it had been tested. The crack pattern over the entire floor slab and the ruptured steel in the corner panels can be seen better in Figure 5.9, a photograph taken after the smaller debris had been removed from the slab surface.

Deflections across the slab surface ranged from a maximum of 12-1/2 inches in the corner panels to a minimum of 3-3/8 inches in the center panel. Posttest profiles of the slab surface taken in both directions across the centerlines of the slab panels are shown in Figure 5.10.

Detail photographs of the slab panels are shown in Figure 5.11. All of the ruptured reinforcing steel which can be seen along the sides of Panels A-1, A-2, A-3, and A-4 in Figure 5.11 had the necked-down section characteristic of a tensile failure. It appears from Panel A-4 that failure of the reinforcing steel starts along the outside edges of

the panel and progresses toward the outside corner. The remaining slab panels have a well developed yield line along the sides of the beams and, in some of the panels, a partial development of the diagonal yield lines. The remainder of the cracking appears to follow the directions of the reinforcing steel as was the case in the static model and in the study reported in Reference 18.

The interior of the model can be seen in Figure 5.12. The four interior columns and the framing beams received very little damage. A few very small cracks were found in the center portion of some of the framing beams. Figure 5.13 shows some of these cracks which have been marked on the first framing beam inside the entranceway.

5.2.2 Recorded Data. Eighty-five data channels were recorded during the dynamic test. Plots of the various transducer outputs versus time are shown in Figures B.1 through B.20. These plots are terminated at the point at which the transducer was overranged or at 50 msec. At 50 msec the blast loading had started decaying rapidly, the strain gages had either been overranged or had reached their maximum value and leveled off, the deflection transducers had reached their maximum value, and the accelerometers had recorded their peak values and were settling back to their zero base line.

Most of the transducers recorded during the dynamic test were the same as those used for the static tests. Changes made were in the location and number of pressure transducers, the addition of accelerometers, and the deletion of two deflection transducers. The number of pressure transducers was increased to ten. Eight of these were placed randomly across the top surface of the model and in the sand backfill, and two were placed inside the model to record venting pressures as the model's roof slab failed. Four of the five accelerometers added were placed on the underside of the roof slab. The fifth was placed on the base slab to measure the downward motion of the model. The two deflection transducers used to measure horizontal movement of the model's walls were deleted since there had been little or no motion of the walls during the static test.

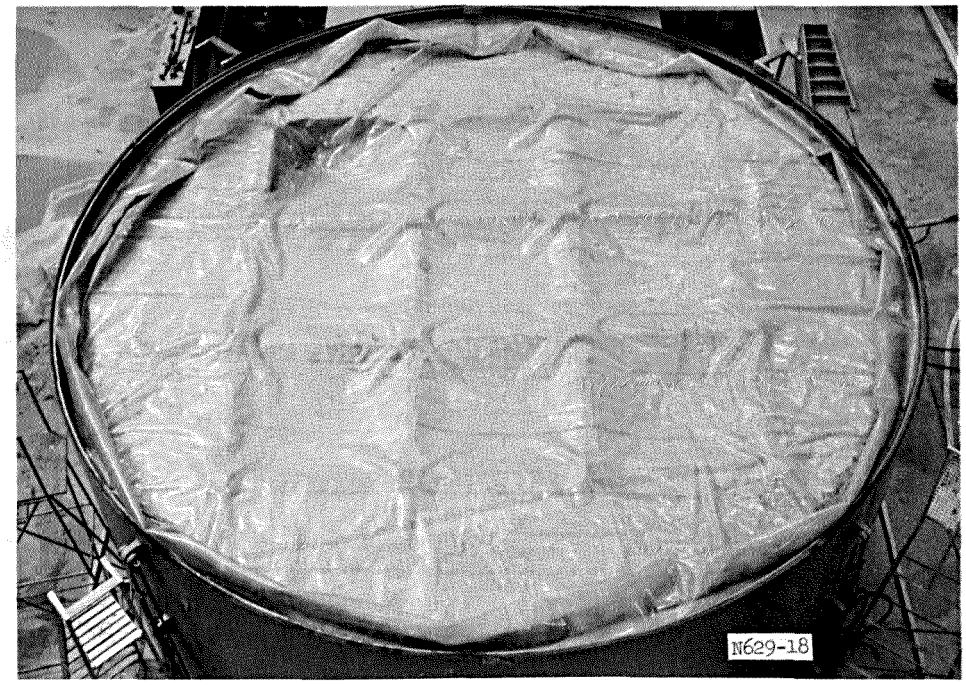

Figure 5.1 Posttest view of static model with diaphragm still in place.

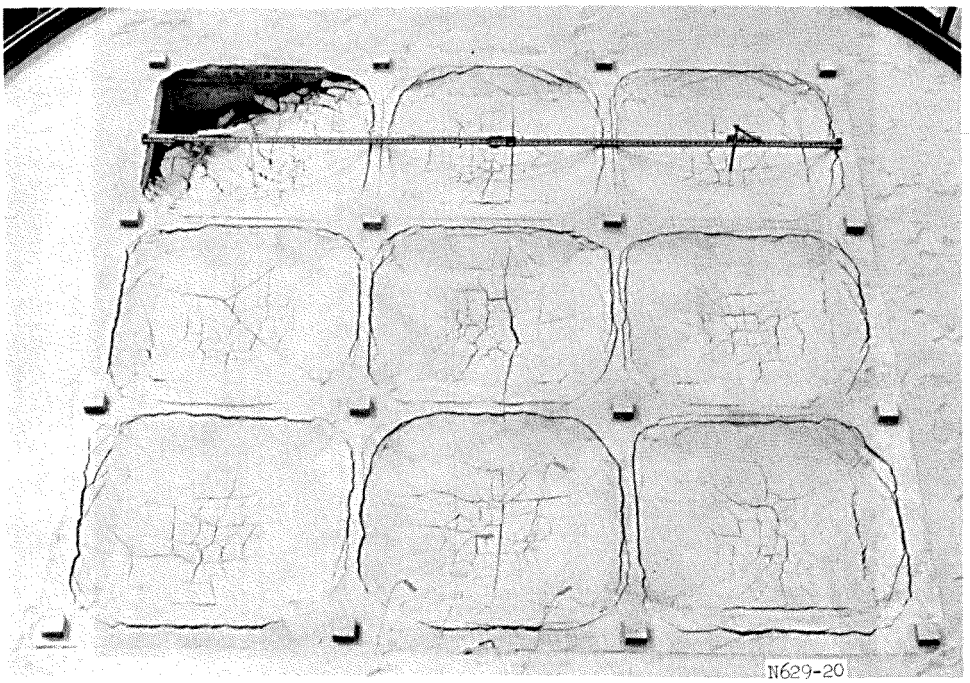

Figure 5.2 Top view of statically tested model.

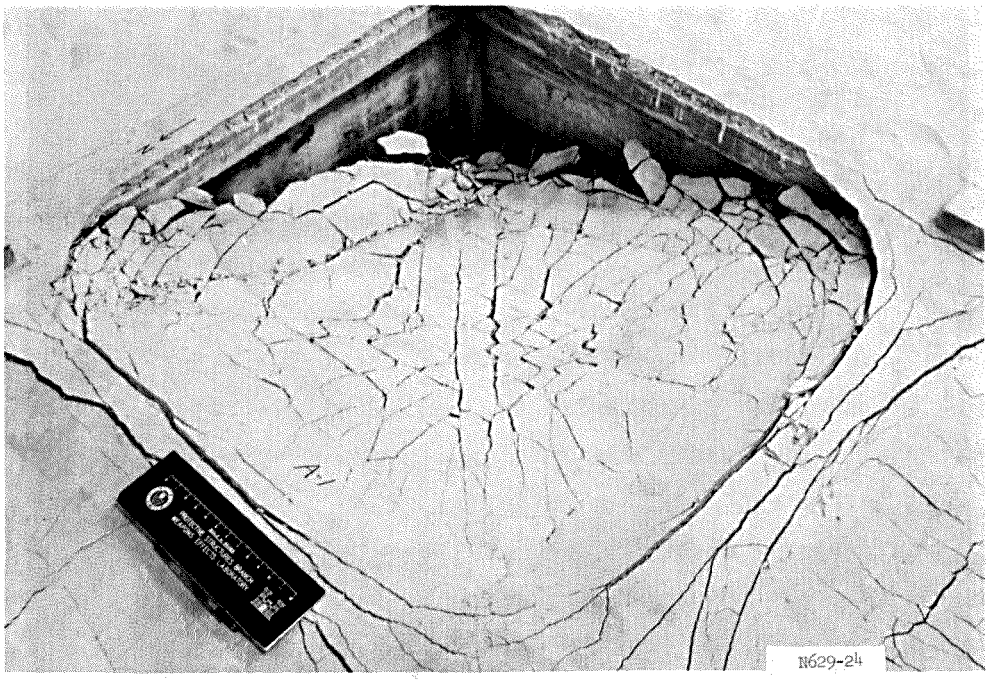

a. Panel A-1.

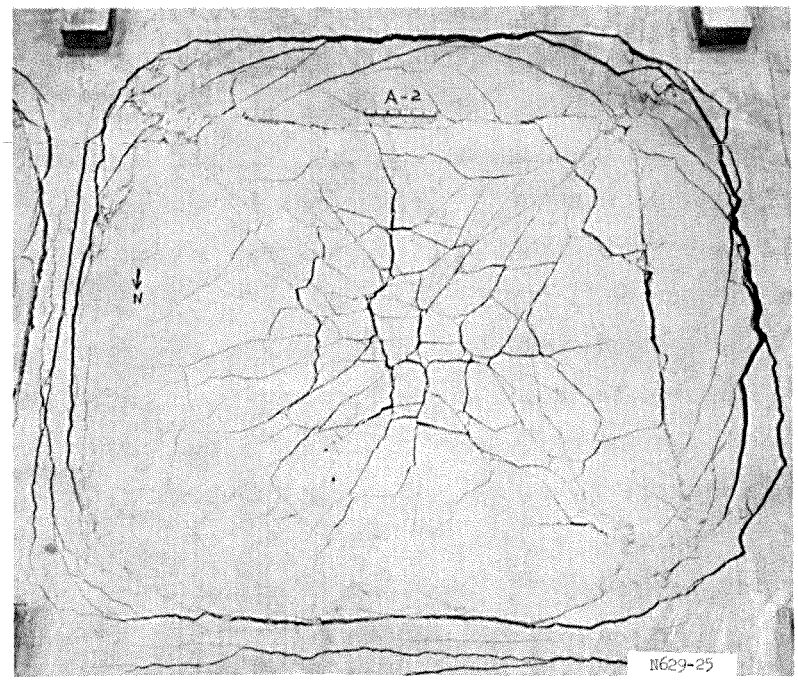

b. Panel A-2.

Figure 5.3 Details of slab panels after static test (sheet 1 of 5).

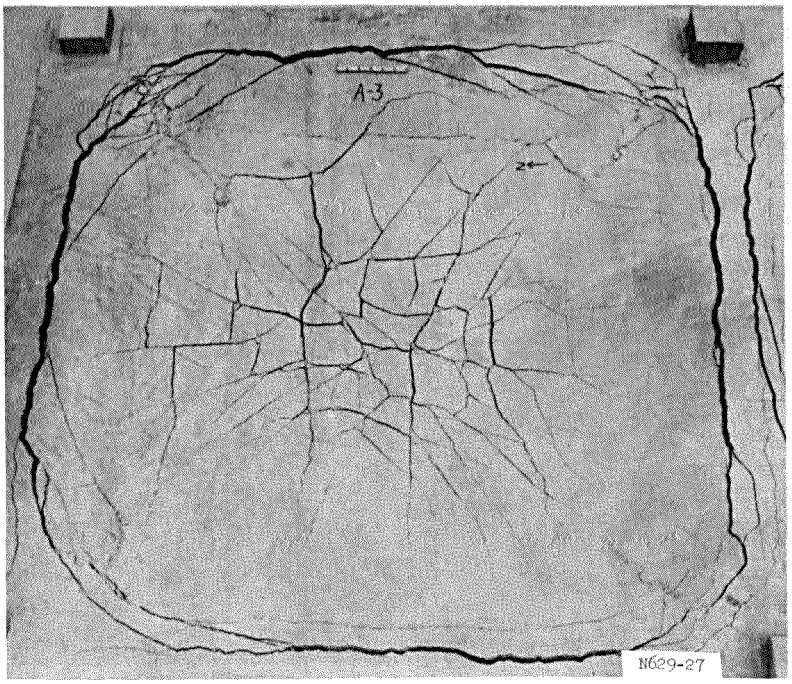

c. Panel A-3.

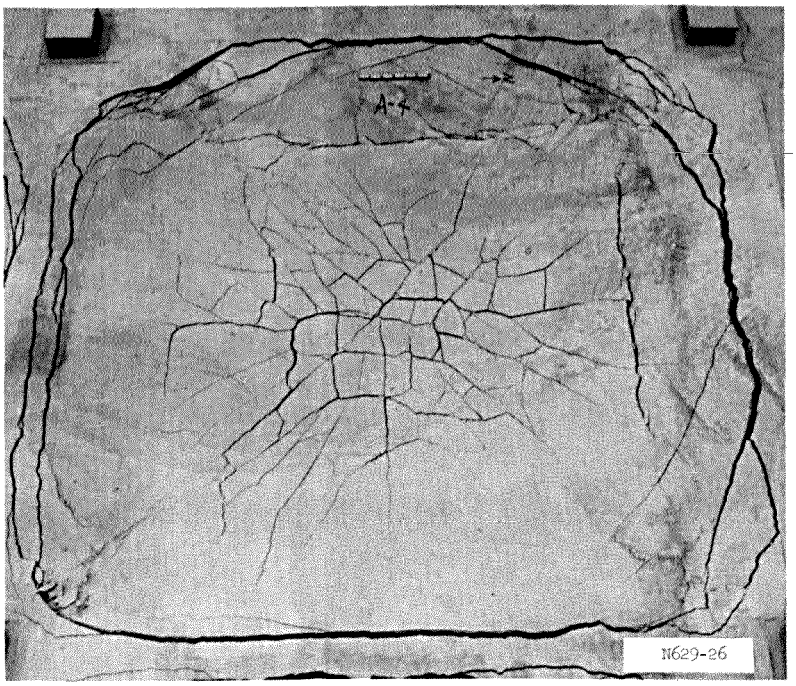

d. Panel A-4.

Figure 5.3 (sheet 2 of 5).

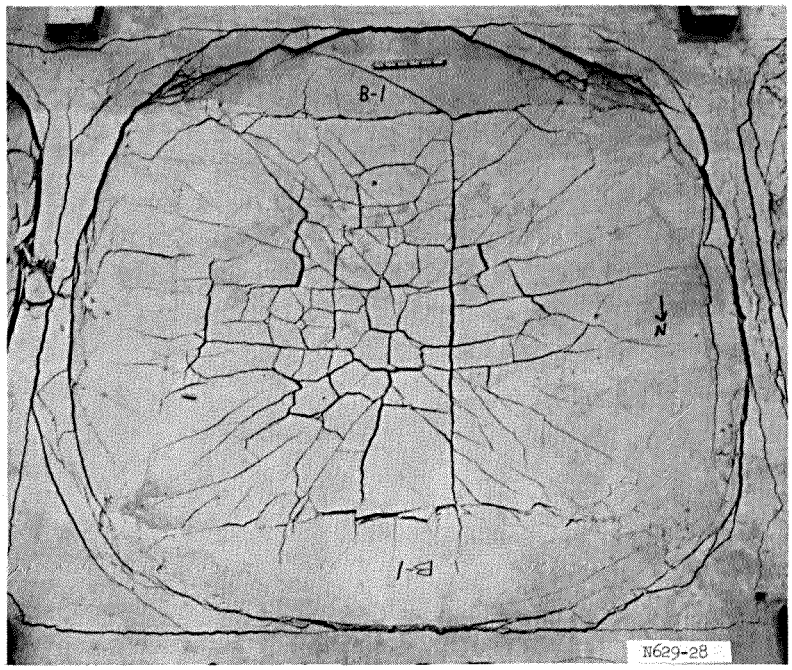

e. Panel B-1.

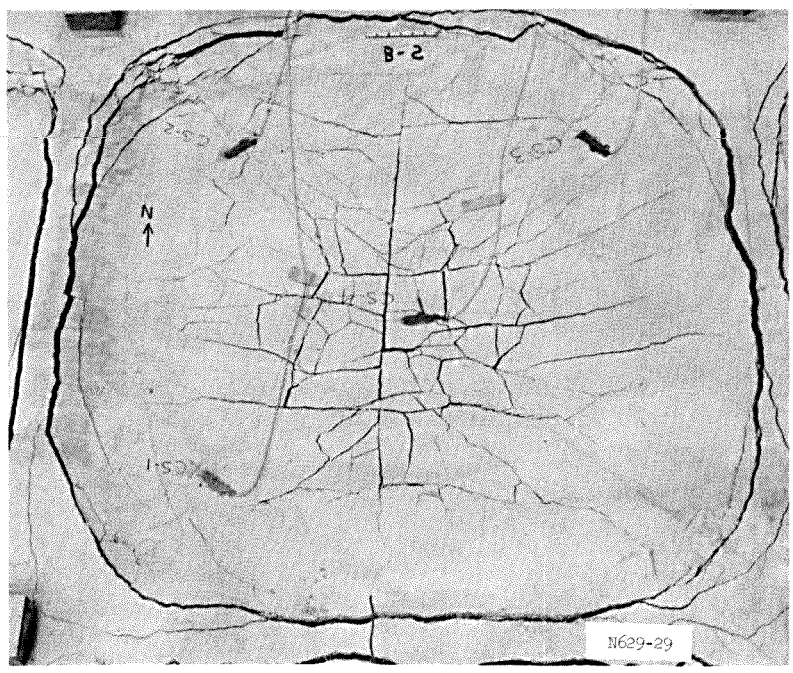

f. Panel B-2.

Figure 5.3 (sheet 3 of 5).

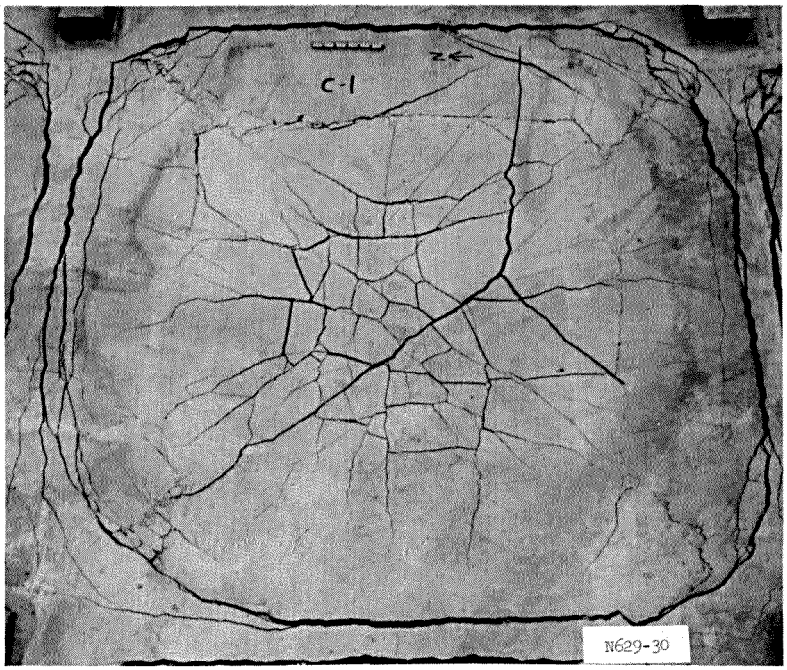

g. Panel C-1.

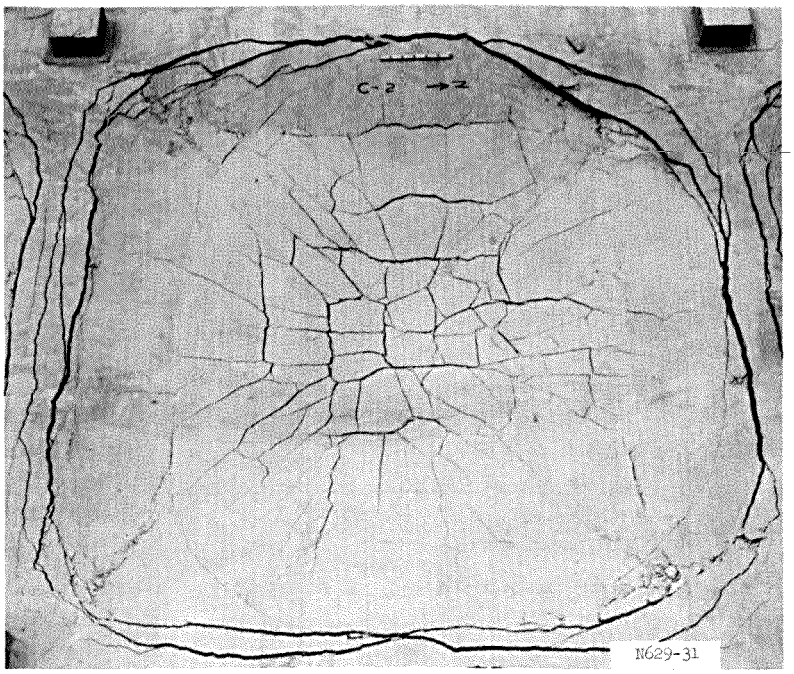

h. Panel C-2.

Figure 5.3 (sheet 4 of 5).

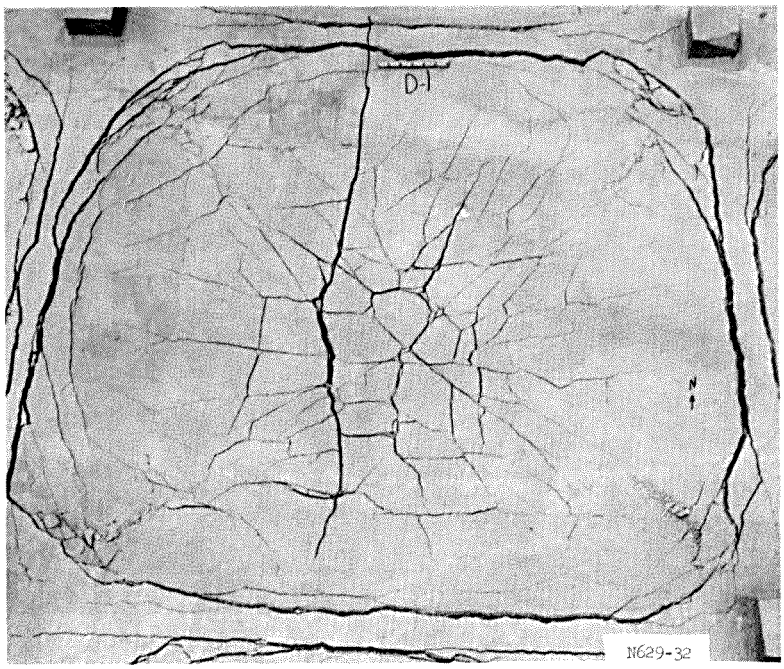

i. Panel D-1.

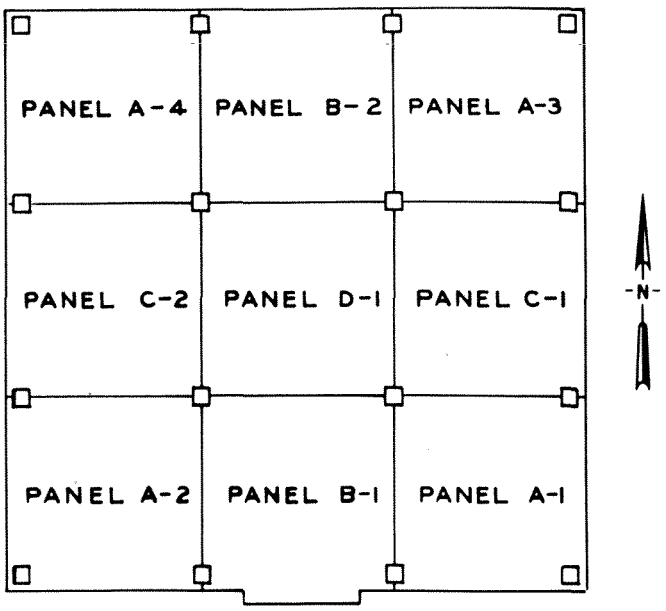

Figure 5.3 (sheet 5 of 5).

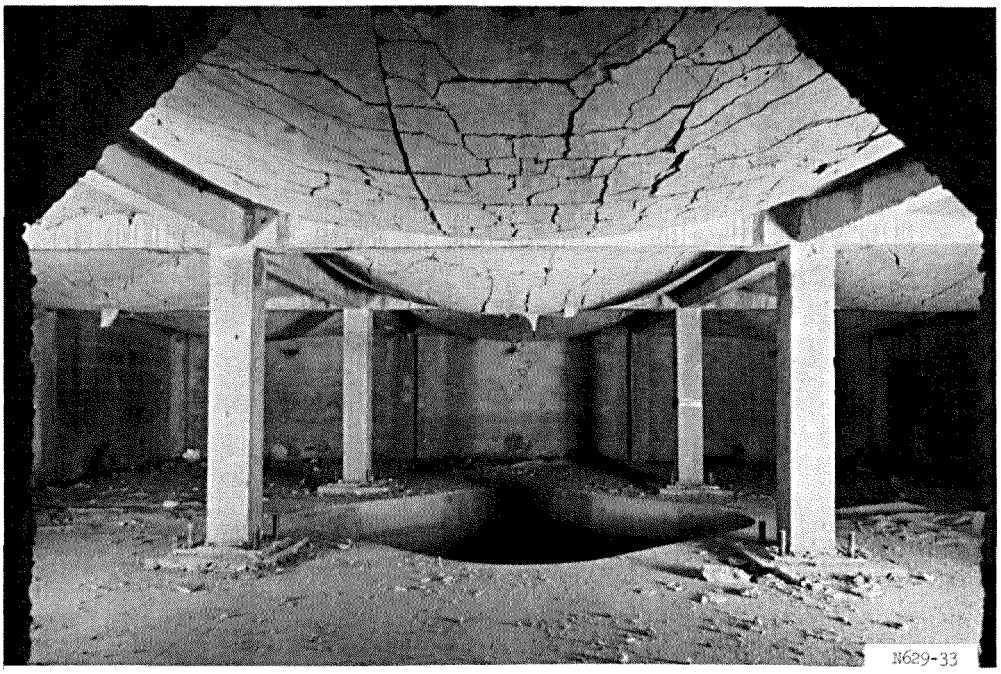

Figure 5.4 Interior view of statically tested model, looking through entranceway.

Figure 5.5 Underside of statically tested model.

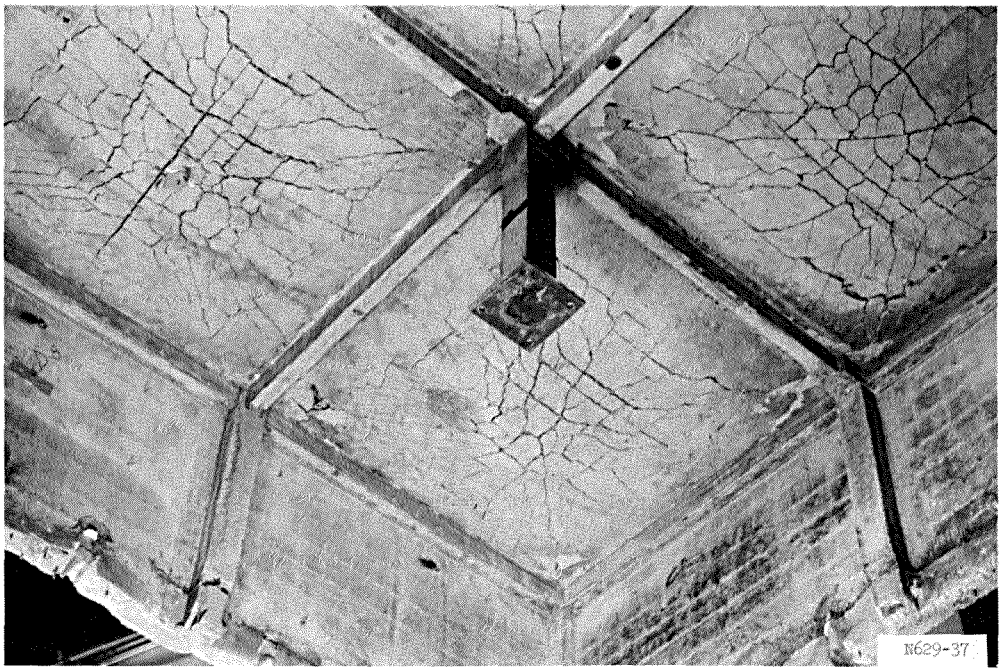

a. Northeast corner.

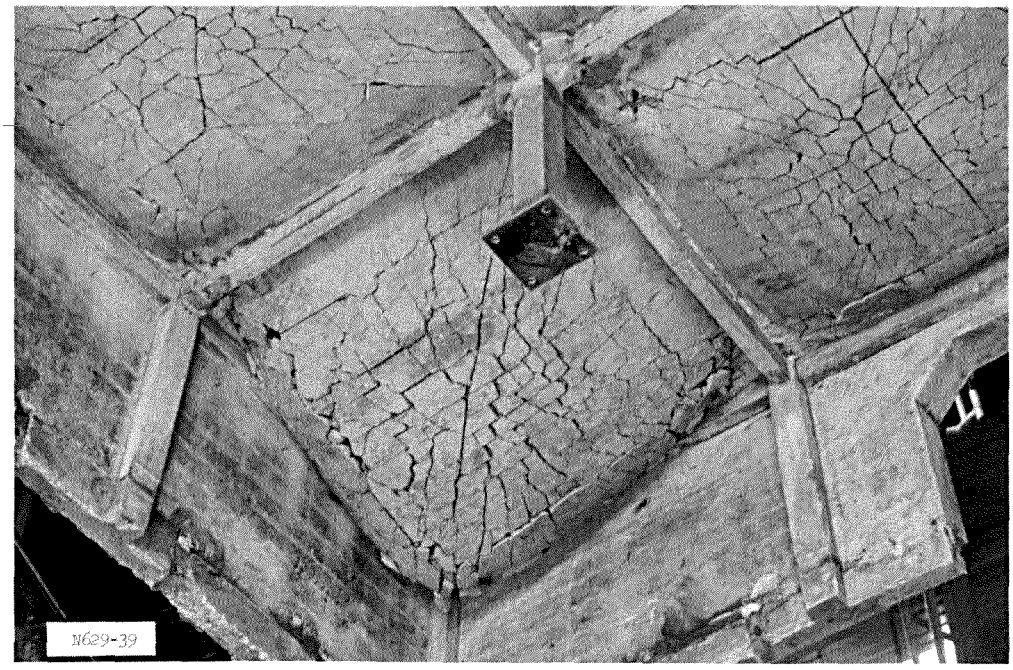

b. Southeast corner.

Figure 5.6 Details of underside of static model (sheet 1 of 2).

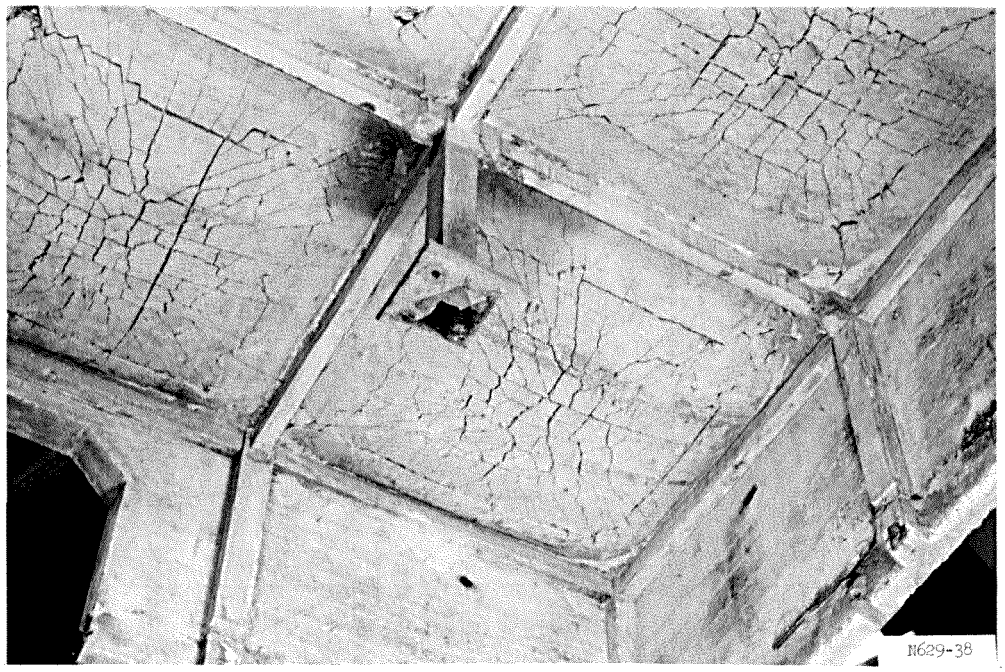

c. Southwest corner.

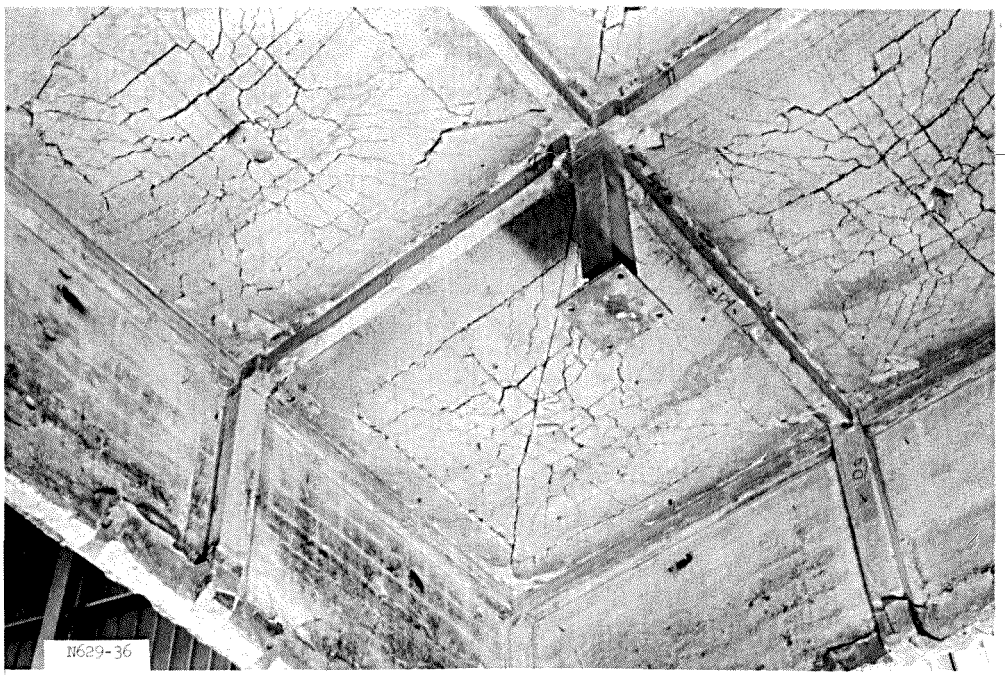

d. Northwest corner.

Figure 5.6 (sheet 2 of 2).

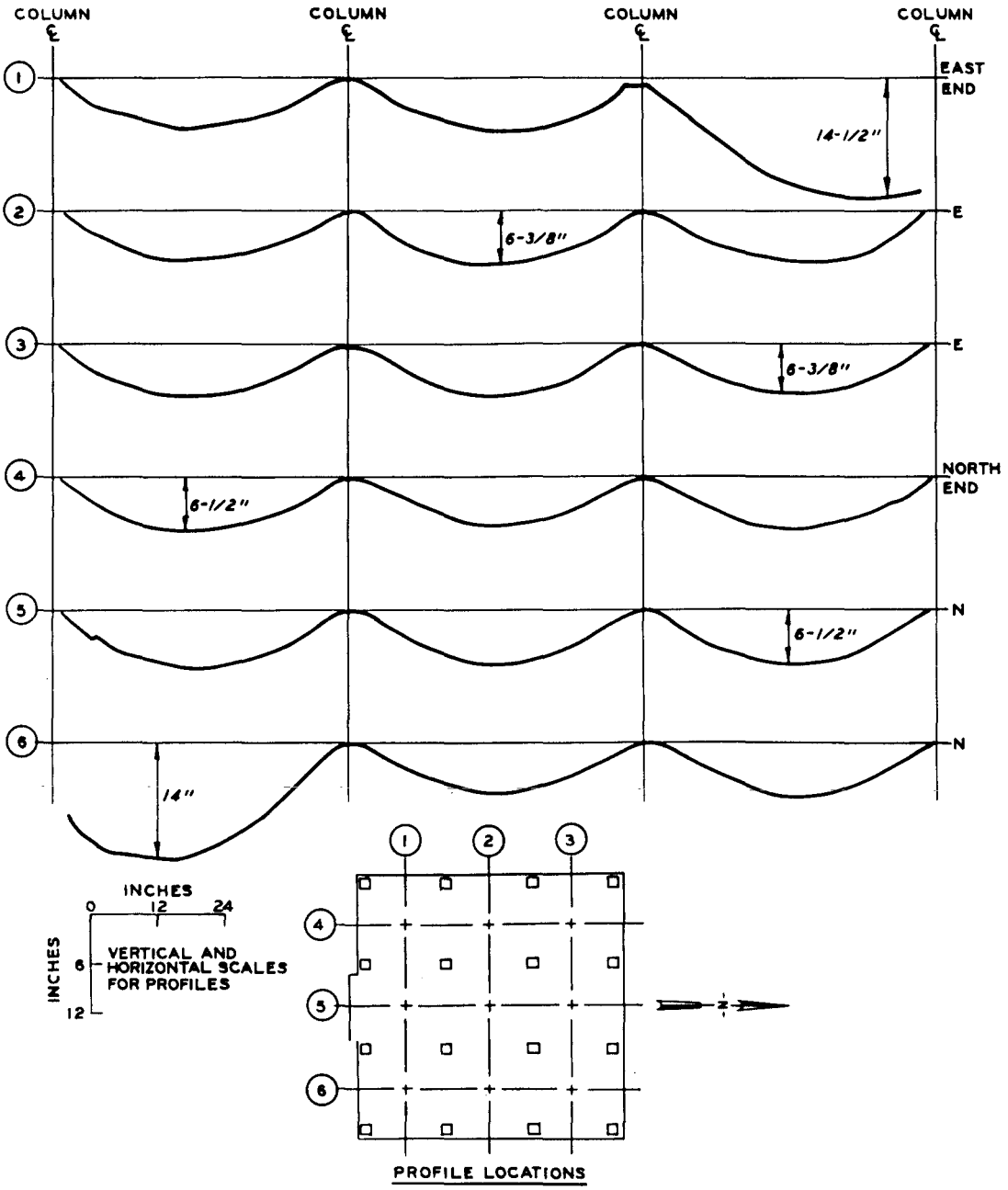

Figure 5.7 Slab profiles after static test.

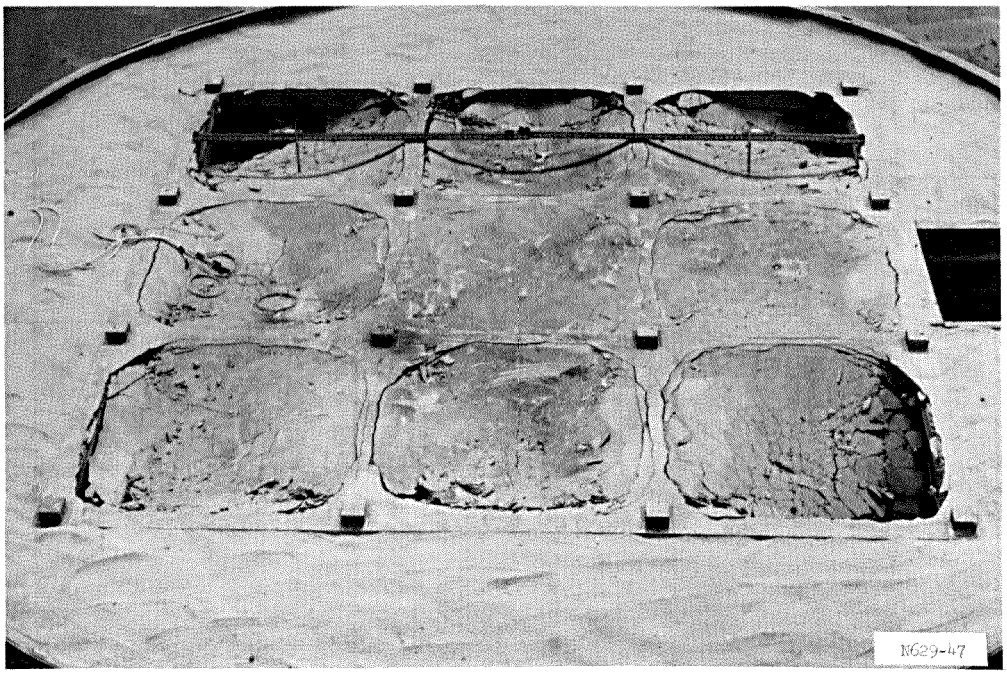

Figure 5.8 Posttest view of dynamic model prior to removal of debris.

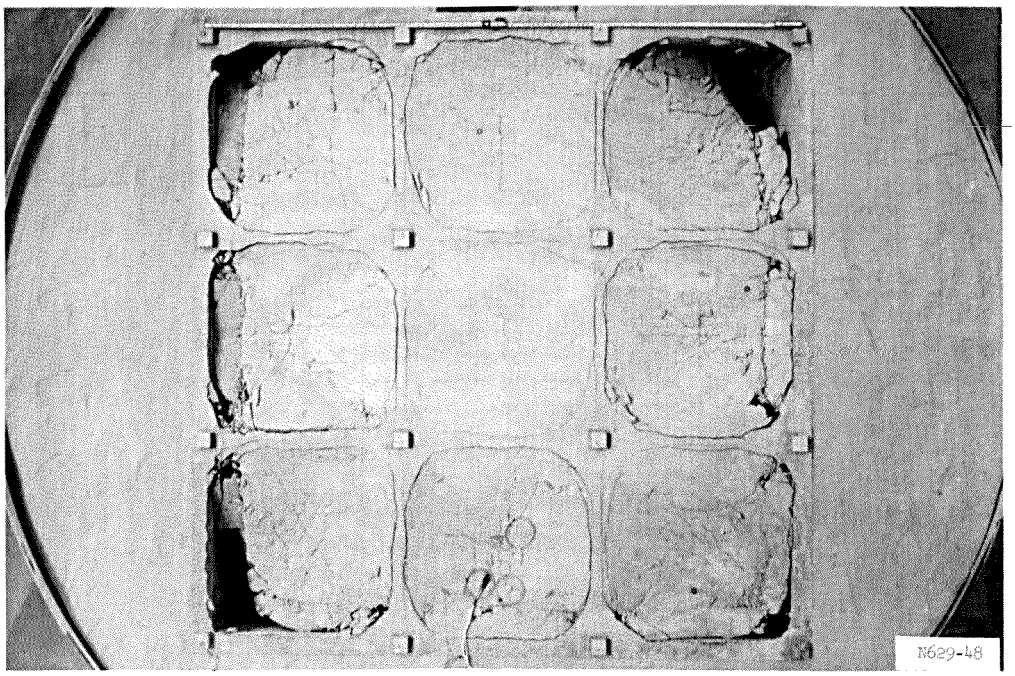

Figure 5.9 Posttest overhead view of dynamic model after removal of debris.

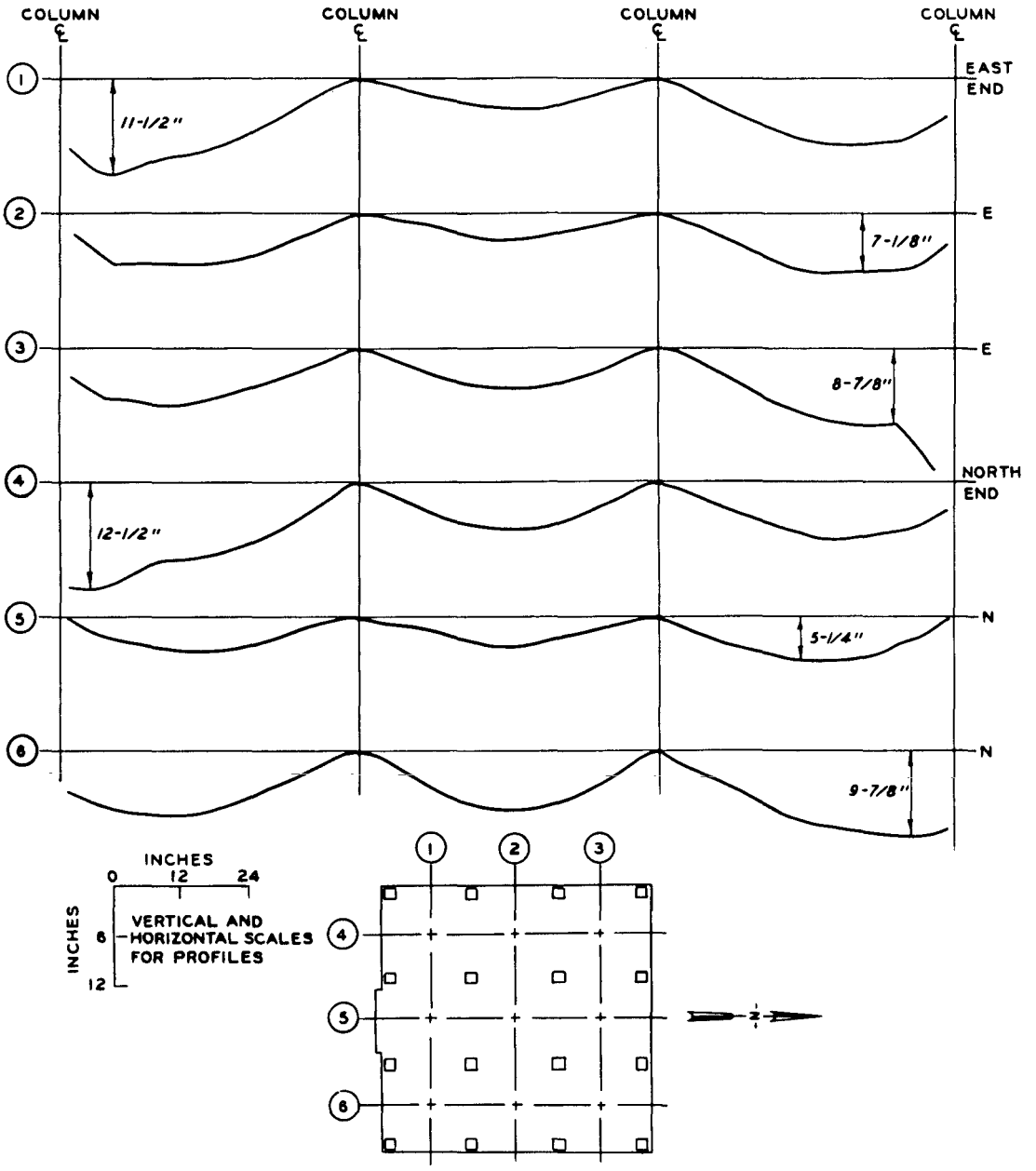

Figure 5.10 Slab profiles of dynamic model.

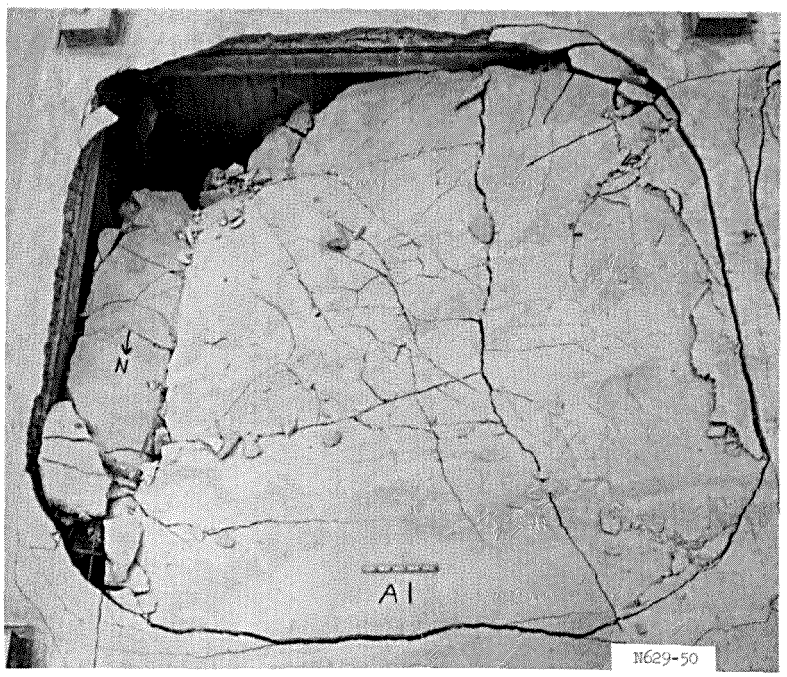

a. Panel A-1.

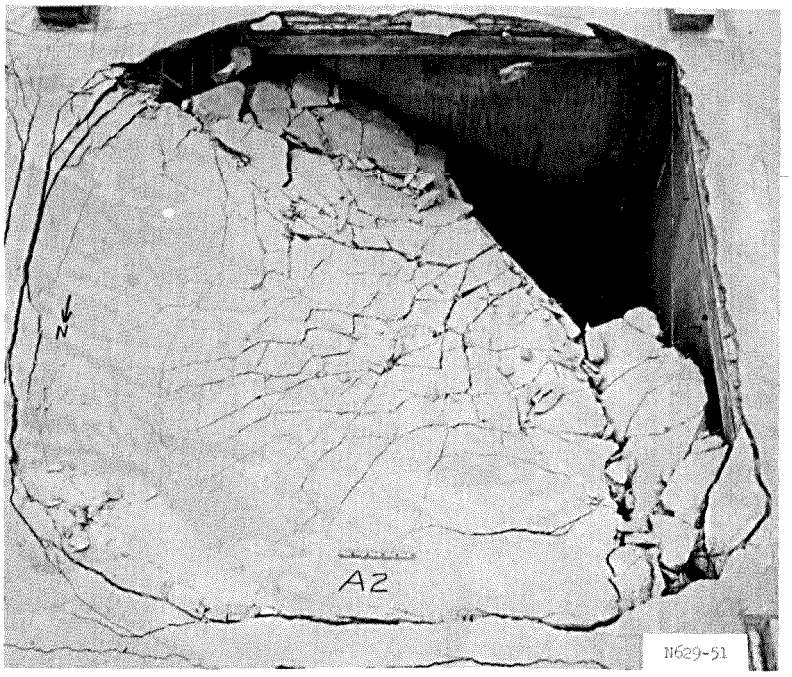

b. Panel A-2.

Figure 5.11 Details of slab panels after dynamic test (sheet 1 of 5).

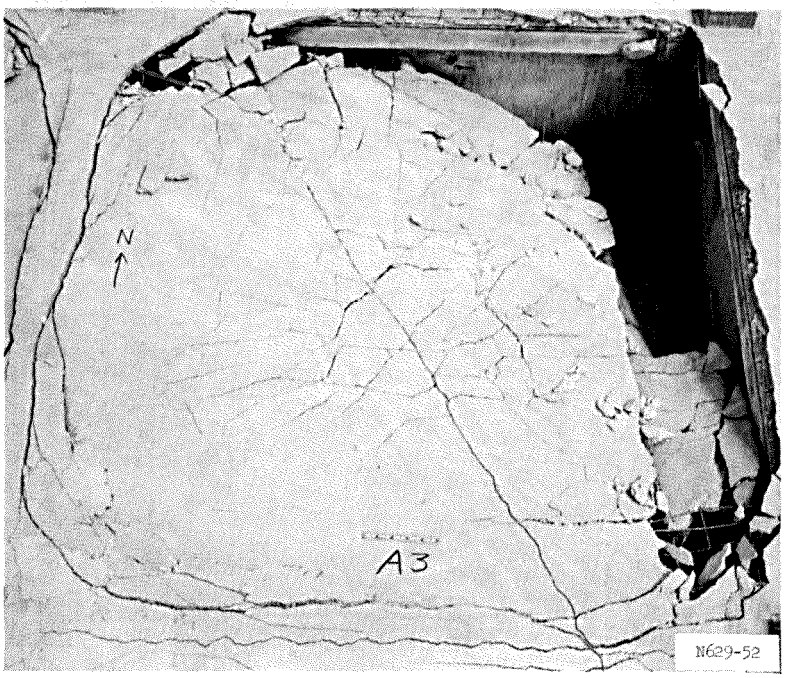

c. Panel A-3.

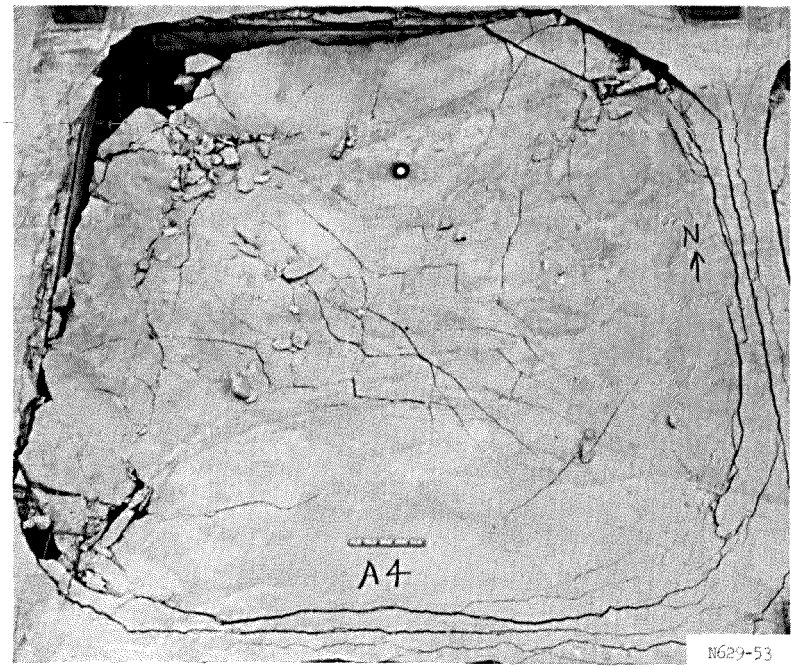

d. Panel A-4.

Figure 5.11 (sheet 2 of 5).

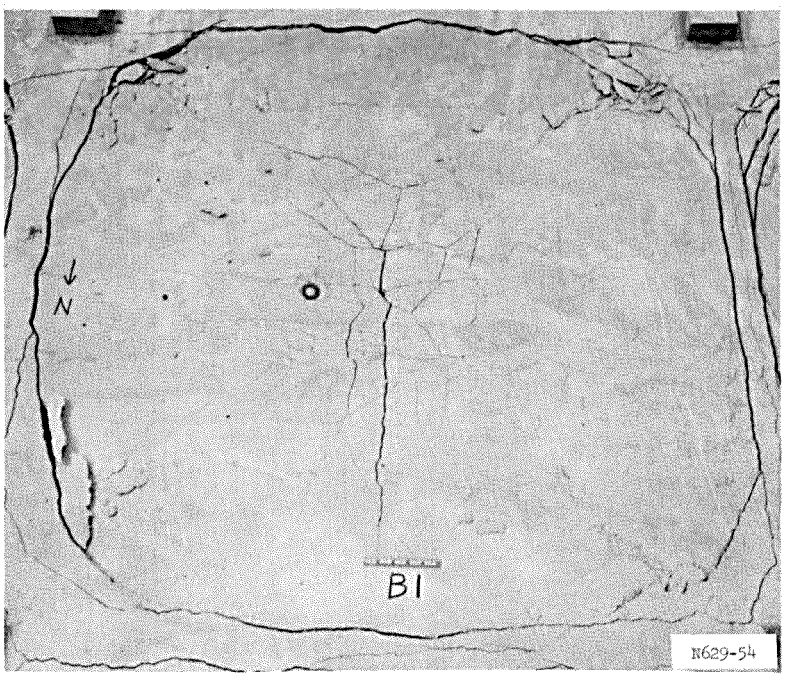

e. Panel B-1.

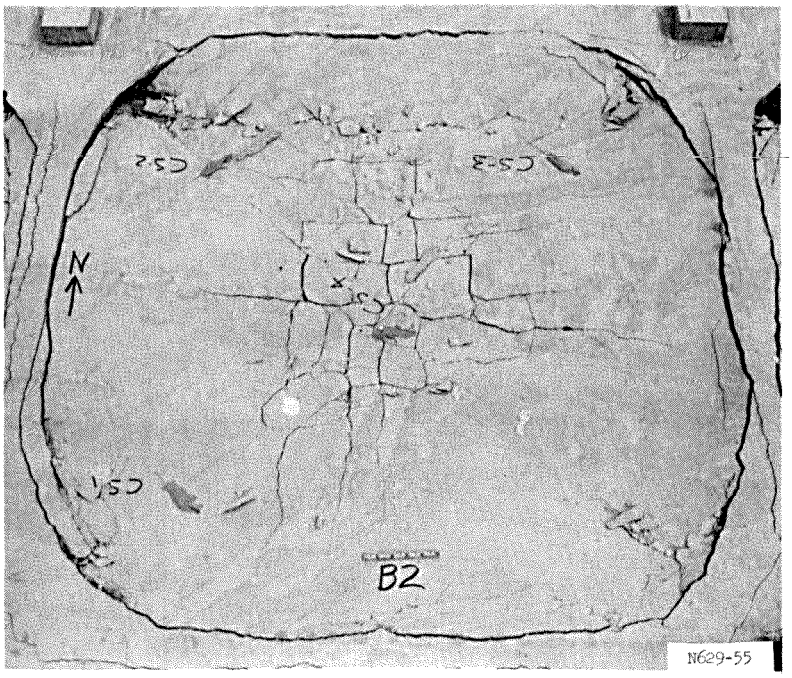

f. Panel B-2.

Figure 5.11 (sheet 3 of 5).

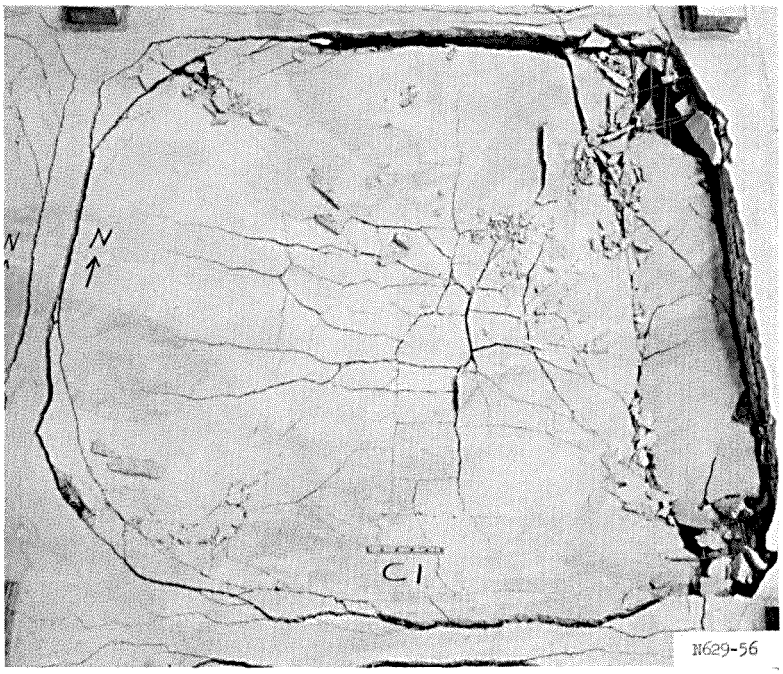

g. Panel C-1.

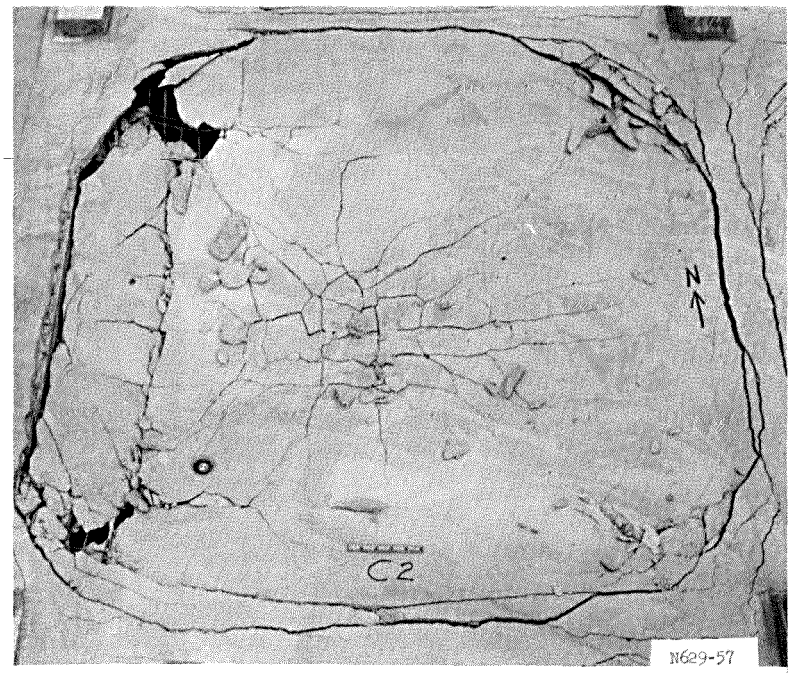

h. Panel C-2.

Figure 5.11 (sheet 4 of 5).

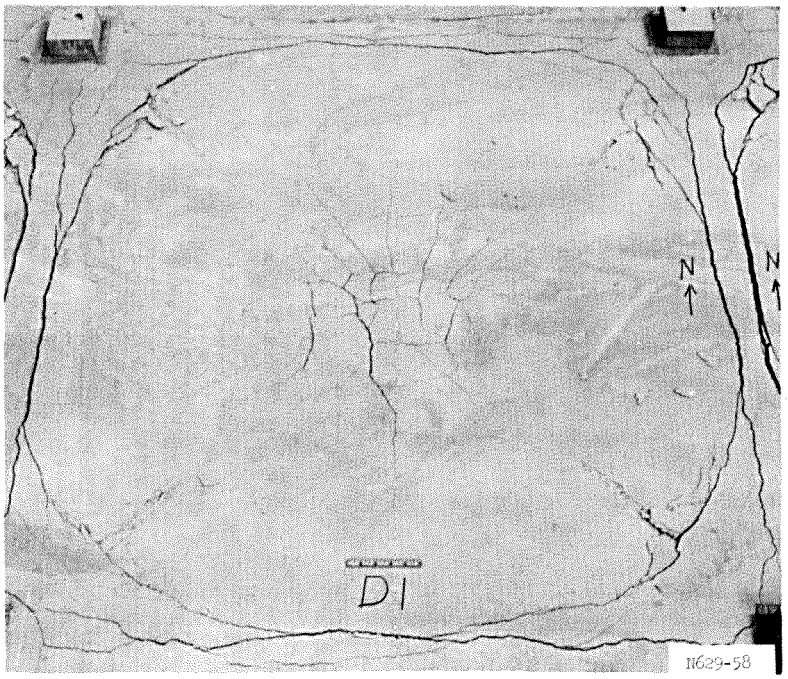

i. Panel D-1.

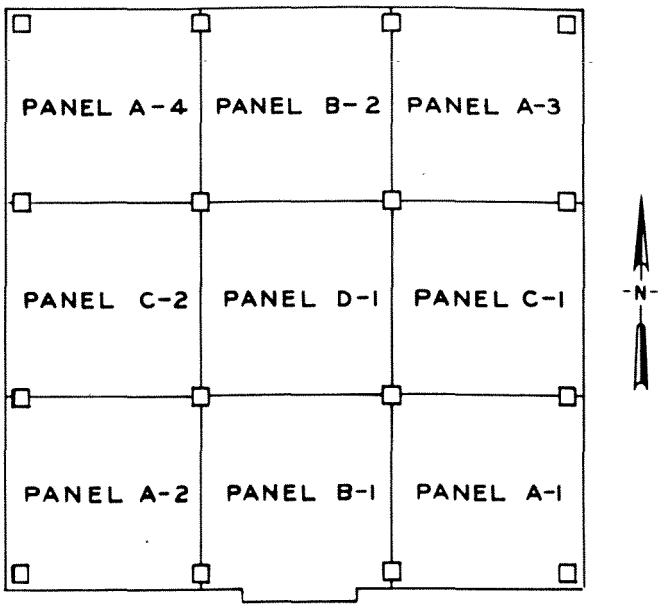

Figure 5.11 (sheet 5 of 5).

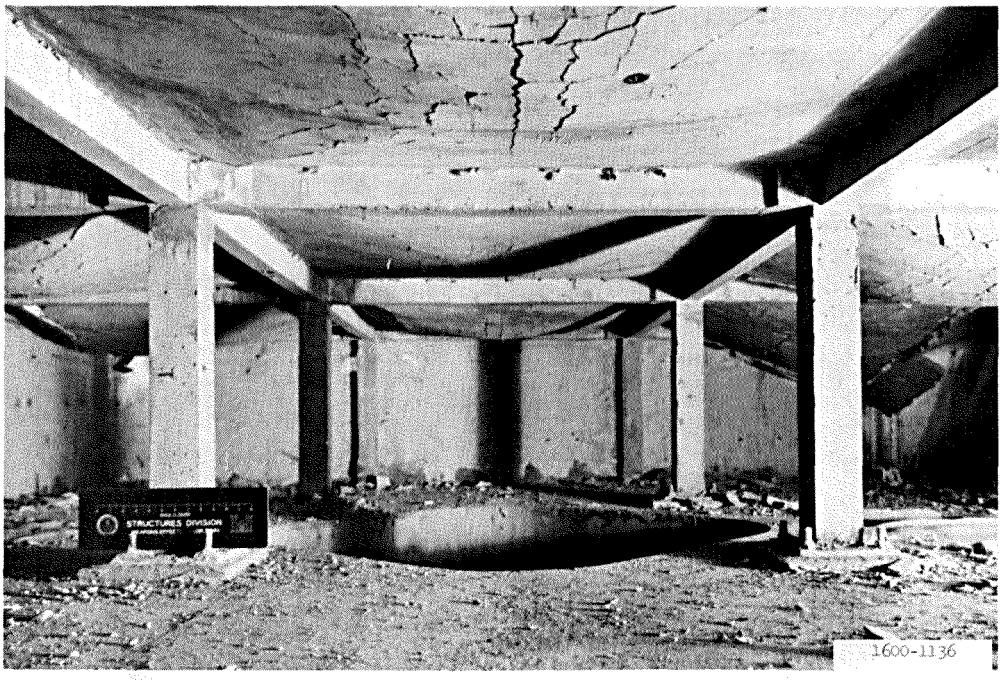

Figure 5.12 Interior view of dynamically tested model, looking through entranceway.

Figure 5.13 Posttest view of southwest column and framing beams; dynamic model.

CHAPTER 6

DISCUSSION OF TEST RESULTS

The responses of the statically and dynamically tested models were similar. The floor slab failed in both models prior to any visible damage to the steel frame support structure. In both tests the reinforcing steel ruptured along the outside edges of the corner panels. Due to the loading system being used, the static test had to be stopped when the first corner panel failed. In the dynamic test the reinforcing steel ruptured along the edge of all four corner panels.

Recorded strains along several of the interior framing beams in both models indicate that stresses in these members were at or above their yield stress. Discussion of the frame response and predictions of the response of a structure having a simple frame are contained in Section 6.2. Following also are discussions of the floor slab response, basement wall loading, and environment inside the model during the dynamic test.

6.1 FLOOR SLAB RESPONSE

6.1.1 Static Test. The static test was terminated at a maximum pressure of 8.8 psi, at which time the southeast corner panel (panel A-1) of the roof slab failed. Posttest inspection revealed that the corner panel failed in tension through the rupturing of the reinforcing bars along both outside edges of the panel. All of the ruptured reinforcing steel along the panel's edges had the necked-down region at the point of rupture normally associated with a tensile failure. The remaining eight panels of the roof slab had permanent deflections at their center averaging 6-1/2 inches.

With large deflections the reinforcing steel supports loads as a suspension net instead of as a flexural member. The slab's load-carrying capacity is then determined by the quantity of reinforcing steel which can act as a suspension net rather than by the moment-carrying capacity of the steel-concrete section for which the reinforcing was designed. Figure 6.1 shows the reinforcing steel areas per foot of width across

the edges of the three types of roof panels (corner, edge, and interior) in the models. The negative moment steel along the edges of the center panel (Panel D-1) was approximately equal on all four sides. This was not the case with the edge panel (Panel B-2) and the corner panel (Panel A-4). These two panels had only 50 to 60 percent as much reinforcing steel across the outside edges as across the other edges of the panels. Panel B-2 had the smallest quantity of steel along its outside edge; however, it still had two opposing edges with a relatively large amount of reinforcing steel which could carry an increasing share of the load as the edge steel yielded. Panel A-4 had two adjacent edges which had small quantities of reinforcing steel crossing them. When the loading was such that the reinforcing steel yielded along one of the outside edges of the corner panel, it also yielded along the other outside edge of the panel. Adding the minimum steel areas for two adjacent sides of each panel gives 0.164, 0.149, and 0.121 $in.^2/ft$ for the center, edge, and corner panels, respectively, indicating that the corner panel should be the weakest panel when acting as a suspension net.

The roof slab was designed in accordance with Method 1 in Appendix A of the 1963 ACI code. This and the other two methods given for the design of two-way slabs placed the negative moment reinforcing steel across discontinuous edges only, to account for some torsional rigidity of the supporting walls or beams. All three design methods would have given basically the same distribution of reinforcing steel across the edges of the three panels.

The roof panels of the model generally followed the static resistance curve for a uniformly loaded slab having full edge restraint. Edge restraint was provided by the surrounding panels for the center panel and by the edge beam and surrounding panels for the remainder of the panels. This response can best be followed by the load-deflection curves (plotted by an X-Y plotter during the test) for the center panel and one edge panel (Figure 6.2). The two curves are offset slightly along the vertical axis to allow the plotter pins to operate without interference. The sudden drops in pressure with no change in deflection indicate the yielding of other panels in the model. The

three zones of behavior for a fully restrained two-way slab can easily be detected on the X-Y plot for the two panels. These are the regions of ultimate flexural response denoted by A in the inset in Figure 6.2, secondary resistance denoted by B, and tensile membrane action covering the portion of the curve from point B to point C.

Since the objective of this study was to investigate the response of the entire model at or near collapse, only tensile membrane action of the slab panels will be discussed herein.

From Reference 19 a safe value for maximum centerpanel deflection during tensile membrane action is approximately $0.1\ L_s$, where L_s is the clear span of the slab in the short direction. Results of tests on small slabs reported in Reference 20 give a value of $0.15\ L_s$ for total collapse of a two-way slab acting as a tensile membrane. All of the nonfailing panels in the model had permanent midpoint deflection of approximately $0.13\ L_s$. From this and the load-deflection plots shown in Figure 6.2, it is apparent that tensile membrane action was well developed throughout the slab panels.

Figure 6.3 shows the strain distribution across the centerline of Panels A-4 and D-1 at applied pressures of 4, 6, and 8 psi. It can be seen in these plots that as the applied pressure is increased, the strain in the reinforcing steel is changing from that which would be expected for strain caused by moment, i.e., large strains at the panel edges and in the center of the panels, to that which would be found in a suspension net. Most of the gages near the inflection points (of the slab panels) (gages at 0.125 L, 0.25 L, 0.75 L, and 0.875 L) changed from almost zero strain at the 4-psi level to yield strain as the applied pressure was increased to 8 psi.

Concrete strain gages were placed across the predicted yield-line locations of edge Panel B-2. These gages recorded an increase in compressive strain up to an applied pressure of about 5-1/2 psi (see Figure A.12). At that time the compressive concrete strain increased rapidly from about 500 μin./in. to near 3000 μin./in., indicating the formation of the diagonal yield lines across the slab panel. The beginning of tensile membrane action occurred at approximately 6.8 psi, at

which time the gages recorded an abrupt change from approximately 3000-μin./in. compressive strain to tensile strains of several thousand μin./in. (Figure A.12).

In Reference 19, Park developed an expression which gives a linear relation between the center point deflection and the applied load for a uniformly loaded rectangular slab acting in a tensile membrane mode. The resulting equation was:

$$q = \frac{K_T A_{TS} f_y}{L_s^2} Y_c \tag{6.1}$$

where

q = tensile membrane resistance, psi

$$K_T = \frac{\pi^3}{4 \sum_{n=1,3,5}^{\infty} \frac{1}{n^3} (-1)^{\frac{n-1}{2}} \left[1 - \text{Sech}\left(\frac{n\pi L_L}{2L_s}\sqrt{\frac{A_{TS}}{A_{TL}}}\right)\right]}$$

A_{TS} = area (per unit width) of the reinforcing steel continuous along the short span of the slab

A_{TL} = area (per unit width) of the reinforcing steel continuous along the long span of the slab

f_y = yield strength of the reinforcing steel, psi

Y_c = center point deflection of the slab

L_s = clear span of the slab in the short direction

L_L = clear span of the slab in the long direction

Values for the K_T factor are plotted in Figure 6.4 for different values of L_L/L_s and A_{TS}/A_{TL}.

Park's equation was compared with results from experimental work in Reference 21. All of the experimental work was done with single panels which were fixed along 2 or 4 edges by casting the slabs integral with massive supports or by bolting them to massive supports. None of the previous experimental slabs depended on surrounding slab panels to provide edge restraint. The result of the comparison of Park's equation with experimental work was the multiplication of Park's equation by an

empirical constant. The modified equation is

$$q = \frac{1.5K_T A_{TS} f_y}{L_s^2} Y_c \qquad (6.2)$$

Table 6.1 contains the experimental and theoretical data for the four panels in the model on which deflection measurements were recorded during the test. The values for q were calculated using the maximum measured deflection of Y_c for each panel; the values for A_{TS} and A_{TL} are shown in the table. Since the reinforcing steel was not equal in both directions, the values for K_T were obtained by letting the larger steel area equal A_{TS} and the smaller steel area equal A_{TL} for each panel.

The theoretical pressures obtained using the recorded deflections varied from 0 percent to a maximum of 13 percent difference from the recorded overpressure. The last column in Table 6.1 gives the theoretical collapse loads for the four panels, assuming that the collapse deflection is equal to 0.15 L. The theoretical data show the center panel (D-1) to be the weakest panel in the model. The static test results and also the dynamic test results indicate that the corner panel is the weakest, the edge panels next weakest, with the center panel being the strongest.

Equation 6.2 assumes that only reinforcing steel which is continuous across the slab panel and the supports provides useful strength for tensile membrane action. The negative moment steel across an interior support is provided by reinforcing bars crossing the support from slab panels on each side of the support. For the center panel of the model, approximately 50 percent of the negative moment reinforcing steel across the supports was provided by the surrounding edge panels. This negative moment reinforcing extending into the center panel from adjacent panels apparently provided some additional tensile membrane load-carrying capacity.

Tests conducted by Denton (Reference 18) and Brown and Black (Reference 20) on two-way-reinforced concrete slabs established an upper and a lower bound for the expected response of two-way slabs which are part

of a floor system. Denton's tests were conducted on single panels which were simply supported along all four sides. The slabs tested by Brown and Black used the Denton design, but the slab panels were tested with all four edges fully restrained.

Denton's Series I slabs when tested statically supported uniform loads averaging 7.7 psi; the same slabs when tested with fixed edges by Brown and Black supported an average load of 23.2 psi. Equation 6.2 predicted the results of the Brown and Black test to within 5 percent accuracy. This equation when applied to slab panels contained in the model steel frame basement shelter test gave results having a maximum error of 15 percent. In the test by Brown and Black, all of the positive moment steel in the center of the slab was continuous into the supports. Applying Equation 6.2 and utilizing only the reinforcing steel which would be continuous across the panel and the supports, the predicted collapse overpressure would be in the range of 11 to 12 psi. This number is somewhat conservative since the negative moment reinforcing steel extending into the slab panels from the surrounding panels would carry some load during tensile membrane action.

6.1.2. Dynamic Test. The static and dynamic models received about the same degree of damage in their respective tests. The failure of the dynamic model was more symmetrical than that of the static model due to the dynamic loading being unaffected by the failure of one or more slab panels. All four corner panels failed in the dynamic model, whereas the static test was stopped when one of the corner panels failed. Seventy to 100 percent of the reinforcing steel was ruptured along the two outside edges of the corner panels and along the outside edge of edge panels C-1 and C-2 (Figures 5.11a, b, c, d, g, and h). The remaining three panels, edge panels B-1 and B-2 and center panel D-1, did not have any reinforcing bars broken nor did they deflect as much as did the same panels in the static test.

During the static test the only means of creating internal pressure in the model was by the change in volume caused by the deflecting slab panels. With the slow loading rate used for the static test, any pressure rise due to volume change would be dissipated into the sand beneath

the model. However, in the dynamic test, the blast pressure could enter the model through cracks in the roof slab and there could also be a small pressure rise due to volume changes caused by the rapidly deflecting slab panels.

Two pressure transducers were located inside the dynamic model to record the rise in internal pressure. These measurements served two purposes, to determine the effective loading on the slab system and to determine the habitability of the shelter. Figure 6.5a shows the average pressure-time curves for five of the overpressure transducers and for the two internal pressure transducers. The difference between the overpressure-time curve and the internal pressure-time curve is the effective loading on the roof slab (Figure 6.5b). The internal pressure buildup primarily affected the duration and decay of the loading. The rise time and peak pressure of the overpressure-time curve were affected very little by the internal pressure buildup.

By making several simplifying assumptions, a reasonable dynamic analysis of the slab panels can be made using the design charts contained in the Air Force Design Manual (Reference 22). If the loading function is represented by a triangular loading function having a zero rise time and the resistance of the slab panels is represented by a bilinear resistance function, Chart B-3 of Reference 22 can be used to determine the response of the slab panels.

One of the parameters necessary for the dynamic analysis was the natural period of vibration of the slab panels for elastic deformations. This quantity can be computed from the mass of the slabs and the slope of the elastic portion of the resistance curves for the slabs and is defined in Equation B-7 of Reference 22 as follows:

$$T = 2\pi\sqrt{\frac{mY_c}{q_y}}\ , \text{ seconds} \qquad (6.3)$$

where

T = natural period of slab, seconds

$m = \gamma t/g$ = mass per unit area of slab, lb-sec^2/in.^{3}

γ = weight per unit volume of concrete, lb/in.^{3}

t = slab thickness, inches

g = gravity = 386 in./sec^2

Y_c = centerpoint yield deflection of slab, inches

q_y = yield resistance of the slab, psi

Values for the previously described notation for slab panels A-4, B-2, C-2, and D-1 were obtained from the static resistance functions for these panels which are contained in Figure 6.6. Using γ = 0.00868 lb/in.^{3}, t = 1.33 inches, and Y_c and q_y as shown in Figure 6.6, the natural periods for the four slab panels were calculated and are shown in Table 6.2.

For a given value of maximum response, the energy absorbed during the displacement of the assumed elasto-plastic bilinear resistance function must equal the energy absorbed by the real resistance function. This was accomplished by making the areas marked A and B in Figure 6.6 equal.

The load function was idealized as shown in Figure 6.7a and represented the effective load-time curve of the dynamic test. In order to use the design charts contained in the Air Force Design Manual (AFDM), it was necessary to idealize the loading function as a zero rise time triangular loading (Figure 6.7b) rather than the finite rise time triangular loading. From Figure 2.9 of Reference 23, for a value of t_1/T of approximately 0.5 and ductility ratios ranging from 10 to 30, the peak pressure producing the same response of a finite rise time loading is 1.01 times that of a zero rise time loading. Therefore, the values for peak pressure obtained from Chart B-3 of the AFDM needed only to be multiplied by 1.01 to obtain peak pressures of the idealized loading function shown in Figure 6.7a.

The values of peak pressure causing the same response as obtained in the static test are labeled P_1 in Table 6.2. Also shown are the predicted times of maximum response (t_m) for the four slab panels. The calculated peak pressures are within 3/4 psi of the actual loading on the model. The predicted time of maximum panel response varied from 0.049 to 0.053 sec, which agrees closely with the time of maximum response of 0.050 sec. The deflection-time curves for the four panels are contained in Figures B.6 and B.7 of Appendix B. Since these curves are

terminated at 0.050 sec, the deflection-time curve for Panel C-2 was hand plotted to 0.100 sec (Figure 6.8).

A collapse pressure was computed for the panels using the same resistance function as before and assuming a collapse deflection of 0.15 L. These values (labeled P_c in Table 6.2) are somewhat conservative since the energy absorbed by the assumed resistance function is less than that absorbed by the real resistance function.

More accurate collapse loads can be obtained using a computer to solve the equations of motion which include the effects of tensile and possibly compressive membrane action in two-way slabs. The resistance equations for this condition are contained in References 21 and 24.

6.2 RESPONSE OF THE STRUCTURAL STEEL FRAME

The structural steel frames for both the static and dynamic models survived the test with little or no damage. From the magnitude of the strains measured at the ends and center of several of the framing beams during both tests, it appears that the structural frame was just beginning to yield when the floor slabs failed.

6.2.1 Static Test. During the static test the beam strains varied from about 1000 μin./in. to about 1900 μin./in. (Figures A.13, A.14, and A.15). Yield strain for the steel used to fabricate the beams was approximately 1500 μin./in. Although the steel strains recorded indicate that the beam stress was, in some cases, above the yield stress, there was no measurable plastic deformation of the beams. Two of the beams had deflection gages at their center points. These two beams had maximum deflections of 0.1 and 0.2 inch (Gages D-3 and D-4). The tracings of the records for the two center point beam deflections show the gages moving toward zero deflection when the record ends. Profiles of the slab surface taken after the test (Figure 5.7) did not show any permanent set of the beams which were strain gaged. However, the beam located on the west side of Panel A-1 (the panel which failed) had a permanent set of approximately 5/8-inch deflection after the test.

The steel frame for the models was designed without considering composite action between the framing beams and the fireproofing concrete

or between the framing beams and the floor slabs. There were no provisions made to insure composite action other than the bonding of the concrete to the steel beams. Composite action would increase the load-carrying capacity of the building frame. Comparing the moment of inertia of the steel beam with the moment of inertia of the beam based on the measured deflection at the time of maximum load gives an indication of the occurrence of composite action. The moment of inertia based on the measured deflection for the beam on the west side of the center panel (Panel D-1) is

$$I_{test} = \frac{WL^3}{384EY_c} = \frac{12{,}640 \text{ lb} \times (53.3 \text{ in.})^3}{384 \times 30 \times 10^6 \text{ lb/in.}^2 \times 0.1 \text{ inch}} = 1.66 \text{ in.}^4$$

where

$W = 8.9 \text{ lb/in.}^2 \times (53.3 \text{ in.})^2 \times 0.5 = 12{,}640$ pounds

L = panel width

E = modulus of elasticity (30×10^6 psi)

Y_c = center point deflection

The moment of inertia for the steel beam alone was 1.09 in.^4 and that for the composite beam, assuming that the concrete slab was cracked along the edge of the fireproofing, was 1.85 in.^4 at the center of the beam and 1.78 in.^4 at the ends of the beam. The moment of inertia based on the measured deflection is approximately 90 percent of the value calculated for the composite section and approximately 50 percent greater than the value for the steel beam alone. From this it appears that the steel beam was acting as a composite beam when the floor slabs failed.

6.2.2. Dynamic Test. Strains measured at the middle and near the ends of three interior framing beams ranged from about 900 μin./in. to 2000 μin./in. As in the static test, the beam strains were near or in the yield range. Deflection transducers (Gages D-3 and D-4) located at the center of two of the interior beams recorded maximum deflections of 0.28 inch at 25 msec after zero time. Paper playbacks of several seconds of the test showed that the deflections came back to zero. Posttest profiles of the model surface (Figure 5.10) showed no permanent set in the framing members.

6.2.3 Comparison of Rigid Frame Response with That of Simple Frame. The majority of steel frame buildings are designed as simple frames. Simple framing consists of connections which are assumed to allow the end of the girders and purlins to be substantially free to rotate under load as true simply supported beams. These connections are designed to carry shear loads only.

If the prototype structure modeled for this test program had been designed as a simple frame, the first floor framing beams would have been W16 × 45. The end connections would have consisted of two 4- by 3-1/2- by 3/8-inch angles bolted to the beam web with three 7/8-inch-diameter bolts and to the column flange with six 7/8-inch-diameter bolts.

Assuming that the connections of the two frame types act as true rigid and simple connections and that they do not fail, the relative load-carrying capacity of the framing beams of the two frame types can be obtained from

$$\sigma_y = \frac{M_S}{S} = \frac{M_R}{S}$$

where

M_S = moment at yield in simple beam

M_R = moment at yield in fixed beam

Substituting the equations for the maximum moment in a fixed and simple beam in the above equation gives

$$\frac{W_S L^2}{8S} = \frac{W_R L^2}{12S}$$

$$\frac{W_S}{8(72.4)\text{in.}^3} = \frac{W_R}{12(56.3)\text{in.}^3}$$

$$W_S = \frac{8(72.4)W_R}{12(56.3)} = 0.857W_R$$

where

W_S = uniform load on simple beam, lb/ft

W_R = uniform load on fixed beam, lb/ft

S = beam section modulus, in.^3

The framing beams of the simple frame prototype will carry 14 percent less load at yield than the beams of the rigid frame prototype. In the rigid frame model tested, recorded strain measurements indicated that the beams were just reaching yield when the floor slabs collapsed. A simple frame model having the same floor slabs as the rigid frame model tested, from the standpoint of beam stress only, would probably be on the verge of beam failure at the loads which collapsed the floor slabs in the tested models.

Knowing the collapse loads of the floor slabs in the rigid frame model, an approximation of the shear load on the connections of the simple frame prototype can be made. In the static test, the maximum load was approximately 8.8 psi. From the modeling laws used, the applied pressure in the model test is the same as the applied pressure in the prototype. Assuming that each interior beam in the prototype carries the loading on 1/2 panel, the end reaction for the interior beams of the simple framed prototype would be

$$R = (1/2)(1/2)(20\ \text{ft})(20\ \text{ft})(8.8\ \text{lb/in.}^2)(144\ \text{in.}^2/\text{ft}^2) = 126{,}720\ \text{pounds}$$

(overpressure; panel width; panel length)

Assuming that the ultimate shearing strength of the 7/8-inch-diameter bolts in the simple connection is equal to 1/2 the tensile strength of the bolts, the maximum load capacity of the connections is

$$V = 2NAf_{us} = (2)(3)(0.6013\ \text{in.}^2)(50{,}000\ \text{lb/in.}^2) = 180{,}400\ \text{pounds}$$

where

V = shear load on connection, pounds

N = number of fasteners

A = area of one fastener, in.^2

f_{us} = ultimate shearing strength of fastener, lb/in.^2

According to this equation, the simple connection would carry the static loading applied to the rigid frame model.

To obtain a general idea of the performance of the simple frame

model for a blast type loading, Reference 25 was used to obtain the dynamic end reactions for a simply supported beam. From Reference 25 an approximation of the maximum dynamic reaction for a simple beam subjected to a step loading is 1.3 times the static reaction. The rigid frame model was subjected to a peak loading of 10 psi which gives a maximum static beam reaction, calculated as before, of 144,000 pounds. Using the shear magnification factor from Reference 25, a maximum dynamic reaction of 187,000 pounds was calculated. The ultimate shearing strength of the connection will increase due to material strength increases with a dynamic load. Since the actual loading on the bolts in the connection would be a combination loading of tension and shear for the bolts through the column flange and shear due to the vertical loading and due to beam end rotation for the bolts through the beam web, the connection would most probably fail.

6.3 ENVIRONMENT WITHIN THE DYNAMIC MODEL

From the habitability aspects, the pressure-time curve for the internal pressure (Figure 6.5a) shows a constant slope from about 5 msec and 0 internal pressure to about 29 msec and 0.8-psi internal pressure. The measured deflection at the center of the corner panel (Panel A-4) and two edge panels (Panels C-2 and B-2) was 3-1/2 inches at 29 msec; the deflection of the center panel (Panel D-1) was 2.6 inches at this time. Assuming that the remainder of the corner and edge panels deflected in the same manner as the measured panels, the internal pressure rise caused by the decrease in volume due to the deflected slab panels would be approximately 0.65 psi. This indicates that, from 5 to about 29 msec into the test, the internal pressure rise was due mainly to the change in volume that was taking place.

The pressure-time curve for the internal pressure has a change in slope at approximately 29 msec into the test. At that point, the blast pressure is starting to enter the model though cracks in the concrete and along the outside edges of the corner panels where the slab was failing. The internal and external pressures equalized at about 70 msec into the test. The model shelter filled during a period of about

40 msec. During this fill period there were probably high-velocity air jets in the corners of the model where the slab was failing. These air jets were directed toward the wall and floor of the model. Since there were no measurements made of the air flow in the model, one can only guess about what happened inside the model. The pressure transducers inside the model were taped to the floor approximately 3 feet from the corner of the model toward its center. After the test, the tape on one of the transducers had pulled loose from the floor on one side. It seems feasible that the air stream entering the model at its corners was deflected by the walls and the floor slab and directed toward the center of the model, most probably at a much reduced velocity.

The internal pressure buildup changed the loading on the model roof from a long-duration load, as was recorded on the overpressure transducers, to a short-duration load as shown in Figure 6.5b.

6.4 BASEMENT WALLS

The horizontal soil pressure distribution on the model walls is shown for two pressure levels for the statically tested model and for one time during the dynamic test in Figure 6.9. As can be seen from these plots, the horizontal soil pressure varied down the wall face, being highest near the top of the wall and lowest near the wall base. The horizontal soil pressure near the top of the wall at the static overpressure level of 6.5 psi was approximately 1.8 and 1.45 times the overpressure. In the plot shown for the dynamic test, the horizontal soil pressure near the top of the wall is 1.45 and 2.1 times the overpressure. From the pressure plot for the static test at 9-psi overpressure, it appears that the wall has started bending slightly, causing the horizontal soil pressure to decrease drastically at the top of the wall and to increase slightly in the middle of the wall. The deflection gages located at midheight of the wall measuring horizontal movement indicated a movement in the range of 0.01 inch. The same pressure distribution across the face of the wall was also reported in Reference 12.

The magnitude of the forces on a basement wall is influenced by the properties of the backfill material, compaction, and water table.

Slight wall movements during the loading produce large changes in the magnitude and distribution of the forces on the wall. On a real basement wall, these forces could vary significantly from those measured in this test.

Shock tunnel tests on concrete block walls described in References 13 and 26 indicate that the failure pressure is less than 2 psi for an 8-inch-thick concrete block wall. When preloaded, the walls failed at 4 psi; and when the supports were such that arching could occur, the walls failed at 9 psi. These results do not apply directly to concrete block basement walls, which are normally 12 inches thick and loaded in a different manner. However, the results do indicate that concrete block walls fail at pressure levels which are in the range of those measured in this test. The data from this test are not sufficient to determine if the soil pressure would fail a concrete block basement wall. However, the data do indicate a need for additional investigation of the interaction of basement walls and the soil forces.

TABLE 6.1 THEORETICAL VALUES OF TENSILE MEMBRANE RESISTANCE q FOR SLAB PANELS A-4, B-2, C-2, AND D-1

Panel	Measured Deflection in.	A_{TS}	A_{TL}	Theoretical Pressure, psi	Theory Test[a]	Theoretical Collapse Loading[b], psi
A-4	6.8	0.0497	0.0461	8.6	1.0	9.7
B-2	7.0	0.0567	0.0479	9.7	1.13	10.6
C-2	6.2	0.0639	0.0373	8.3	0.97	10.2
D-1	7.0	0.0426	0.0426	7.8	0.91	8.5

[a]Applied pressure = 8.6 psi.

[b]Assumes collapse deflection of 0.15L = 7.64 in.

TABLE 6.2 PREDICTED DYNAMIC RESPONSE OF SLAB PANELS A-4, B-2, C-2, AND D-1

Panel	T sec	μ	P_1 psi[a]	t_m sec	P_c psi[b]
A-4	0.027	17	9.7	0.051	9.9
B-2	0.022	28	9.5	0.053	9.7
C-2	0.027	15	9.5	0.049	9.9
D-1	0.032	12	9.6	0.050	9.7

[a]Dynamic pressure required to cause same damage level as static test.

[b]Collapse pressure assuming collapse deflection of 0.15L = 7.64 in.

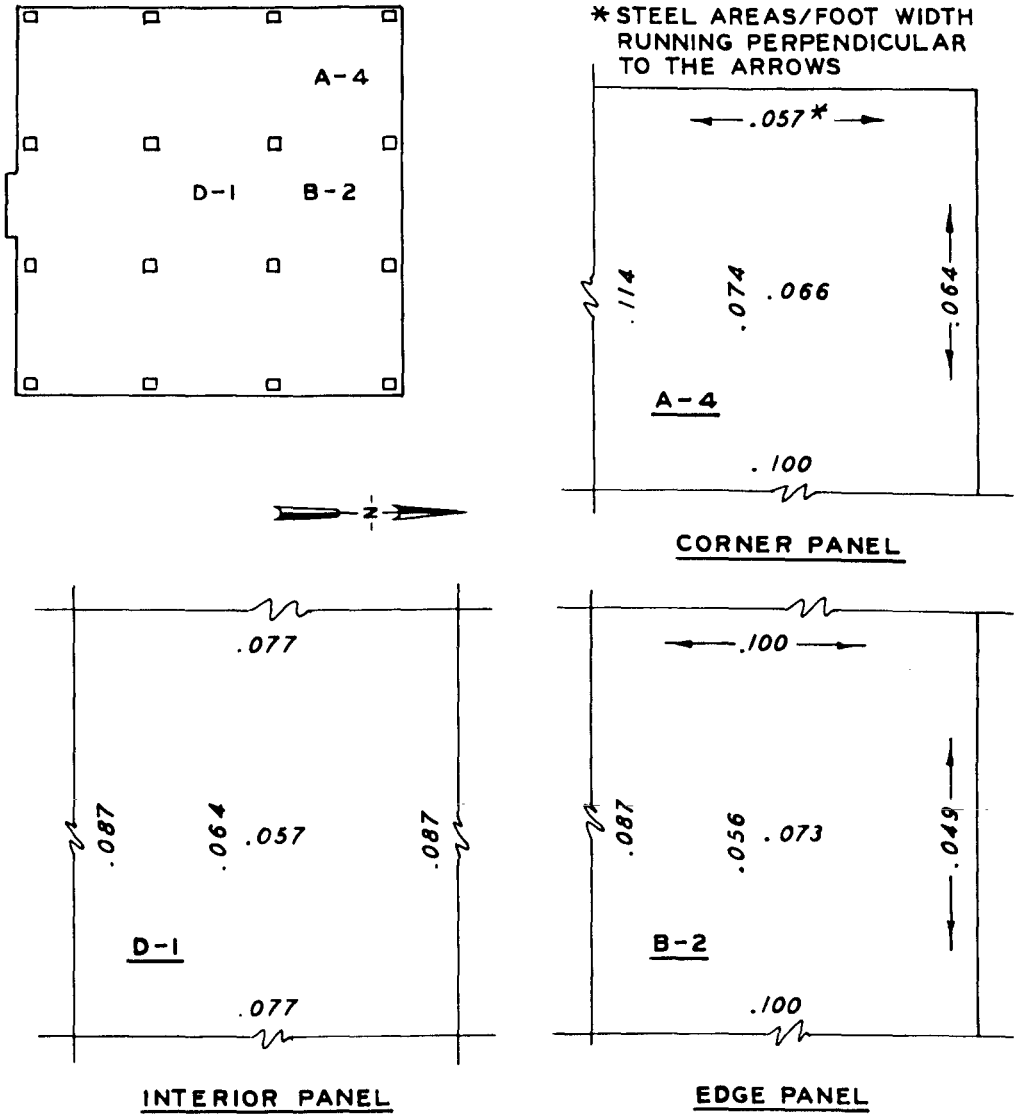

Figure 6.1 Reinforcing steel areas for corner, edge, and interior panels.

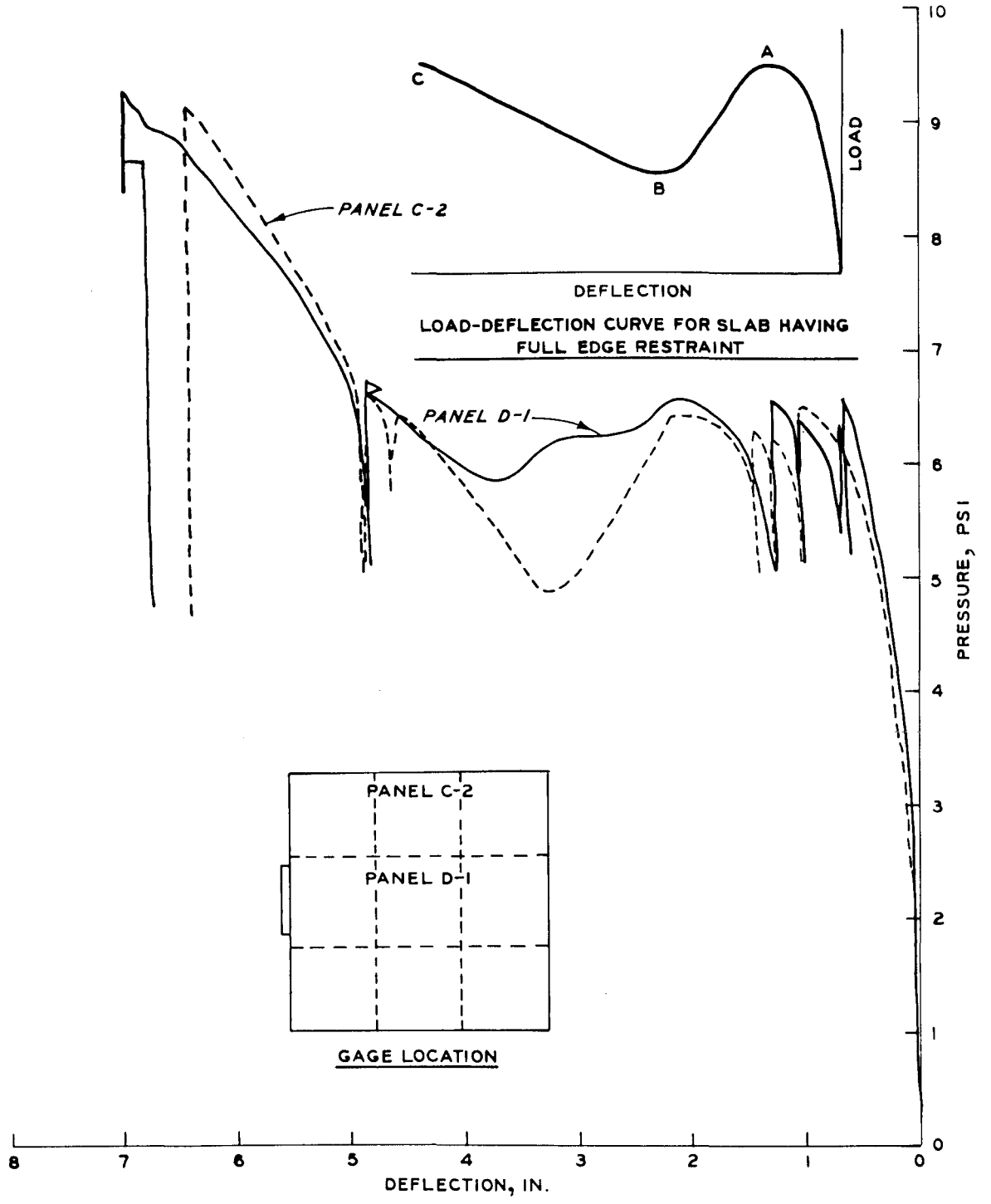

Figure 6.2 Load-deflection curve for Panels C-2 and D-1.

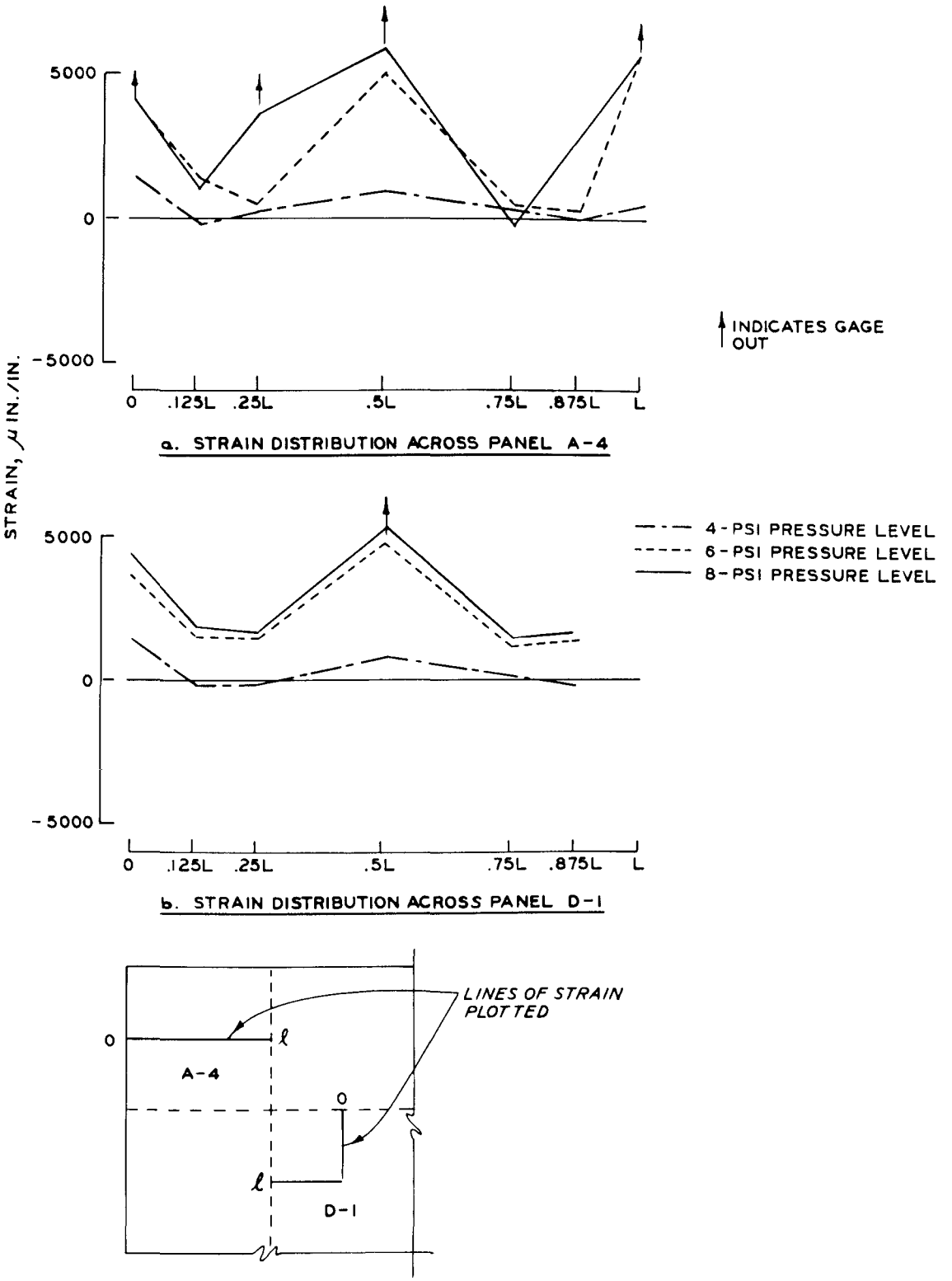

Figure 6.3 Strain distribution across Panels A-4 and D-1, static test.

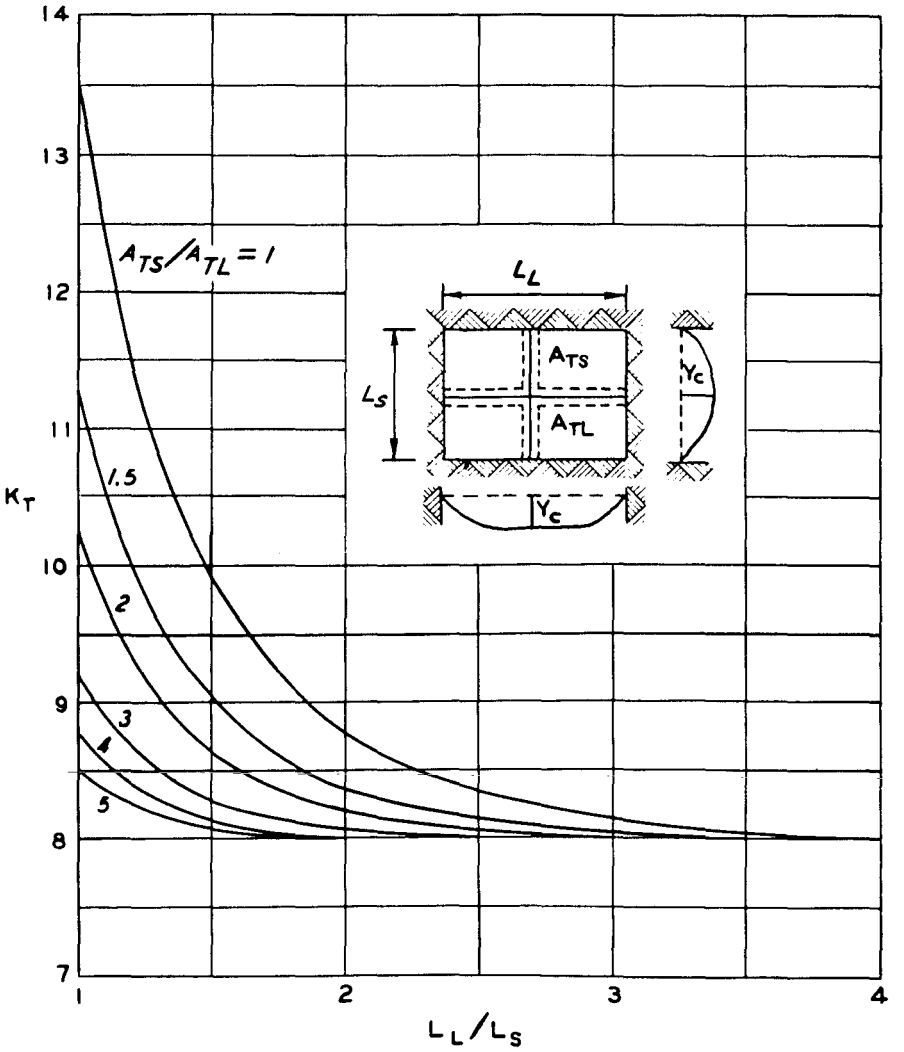

Figure 6.4 Coefficients for tensile membrane resistance.

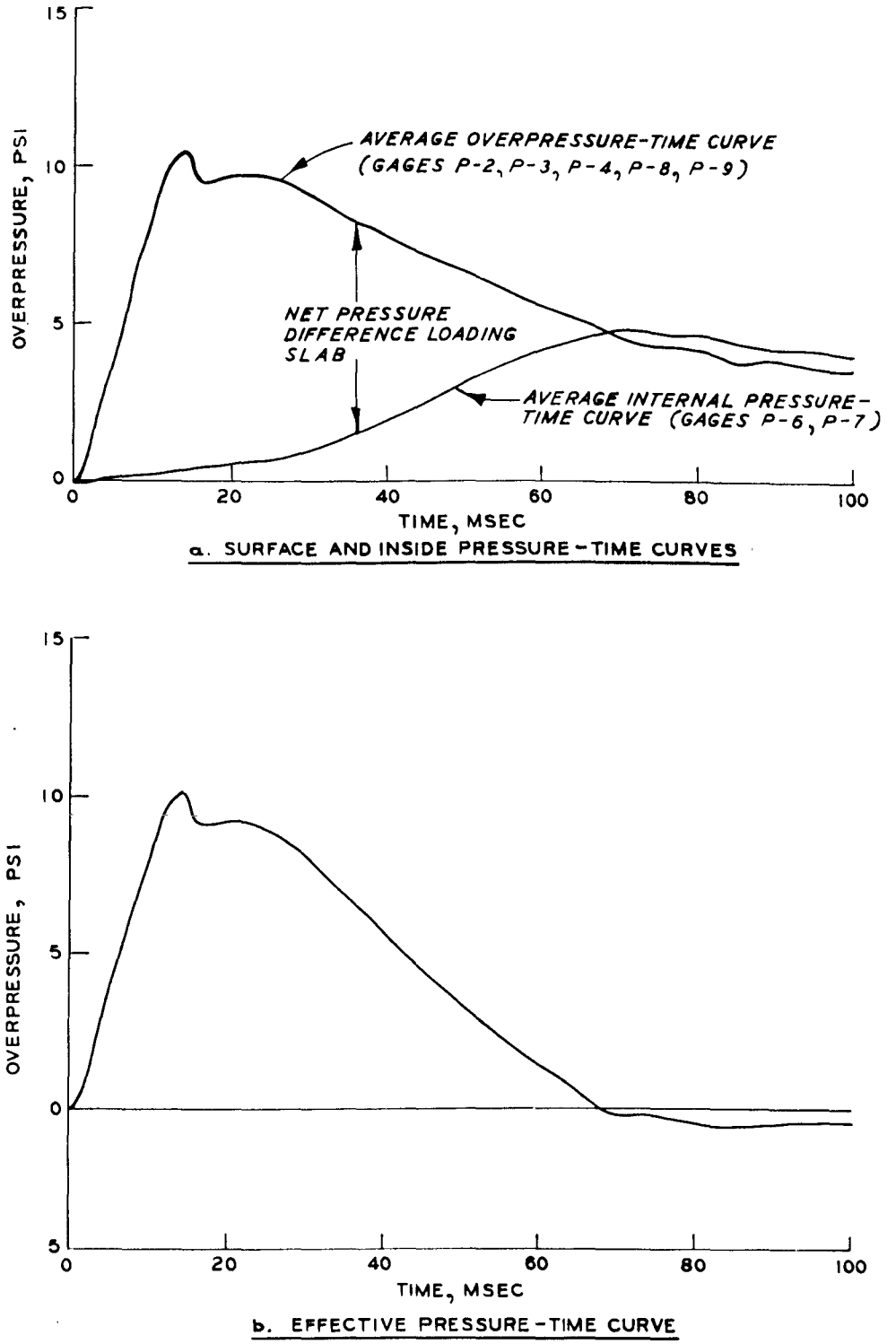

Figure 6.5 Net overpressure loading slab.

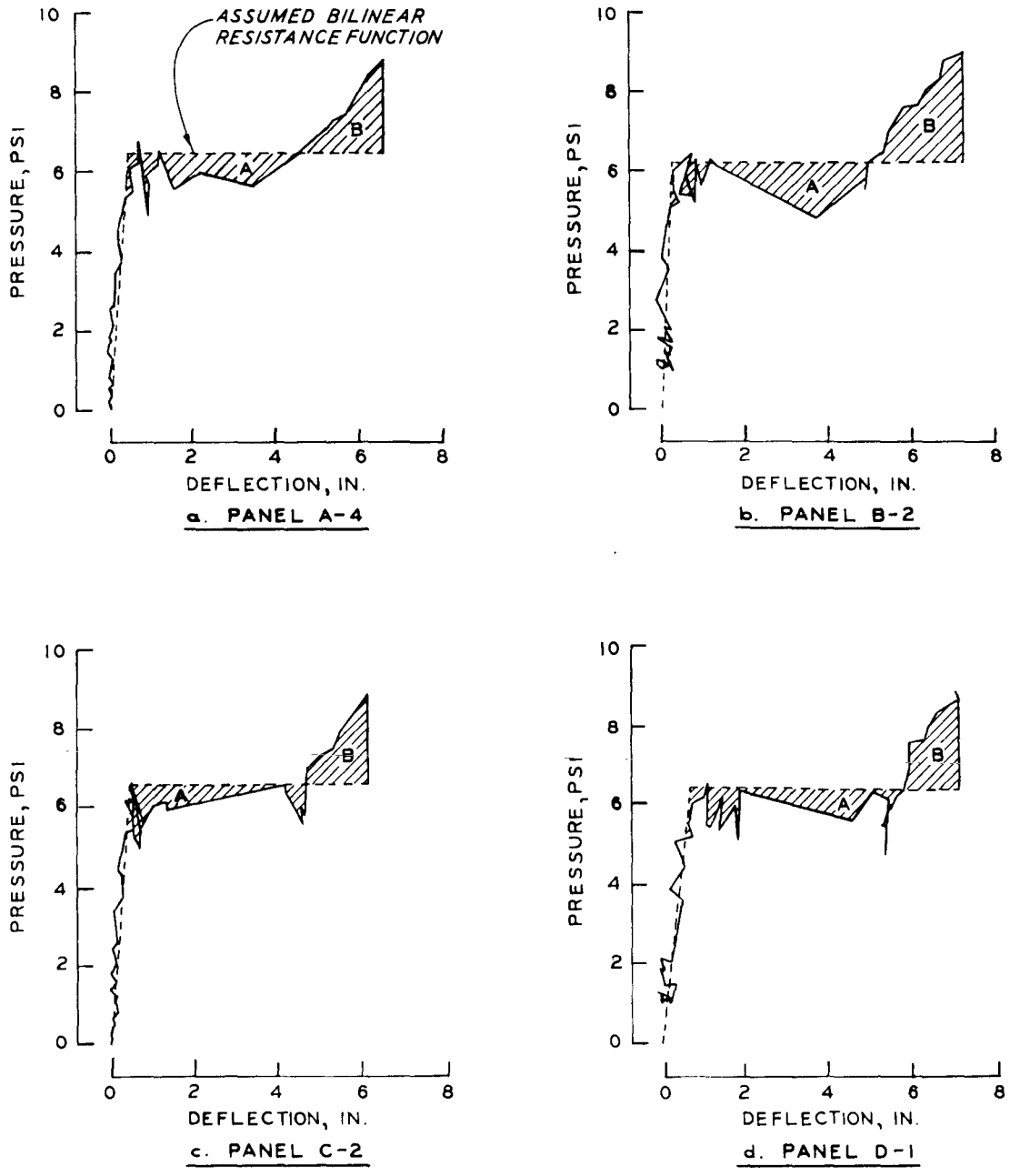

Figure 6.6 Resistance-displacement relations for assumed dynamic condition.

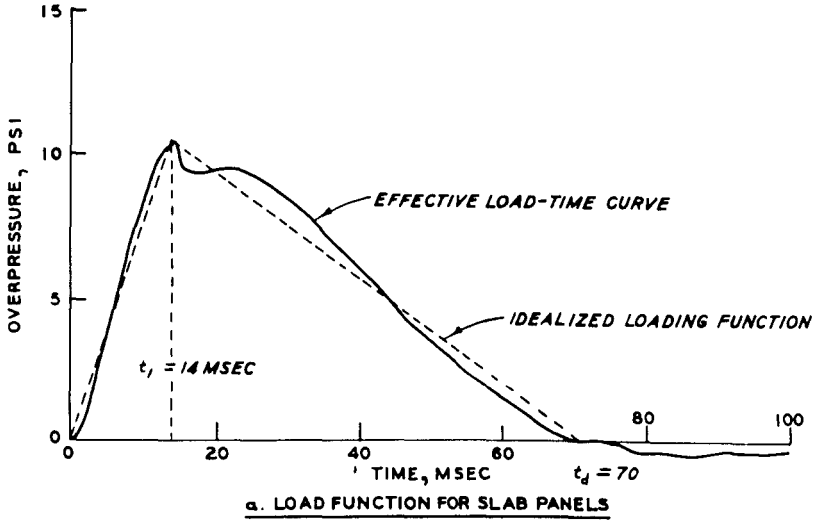

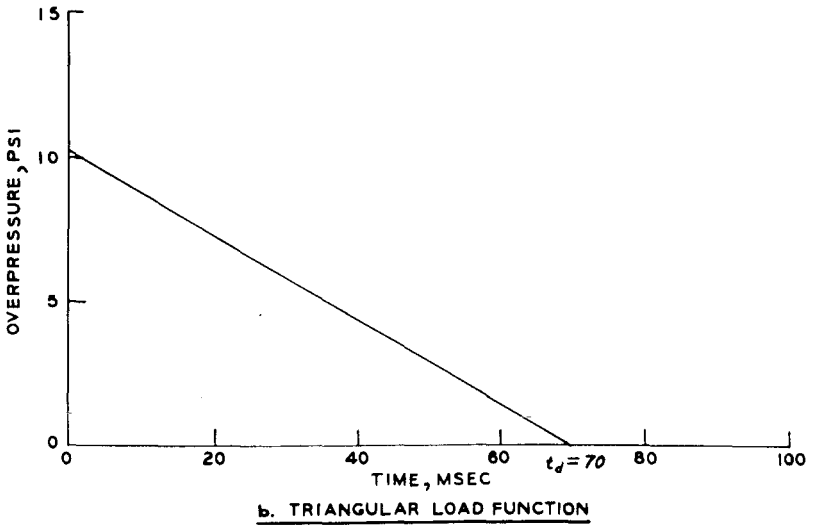

Figure 6.7 Idealized load-time functions.

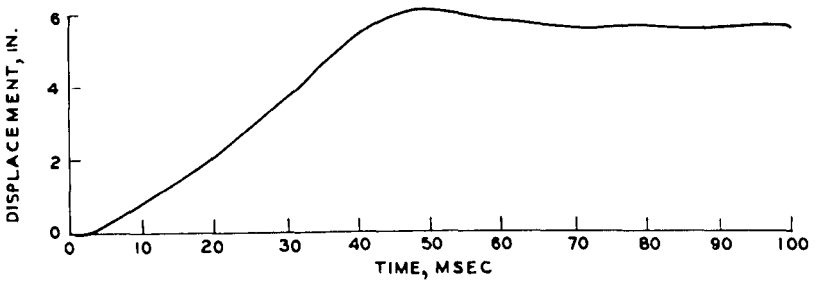

Figure 6.8 Displacement-time curve, center of Panel C-2.

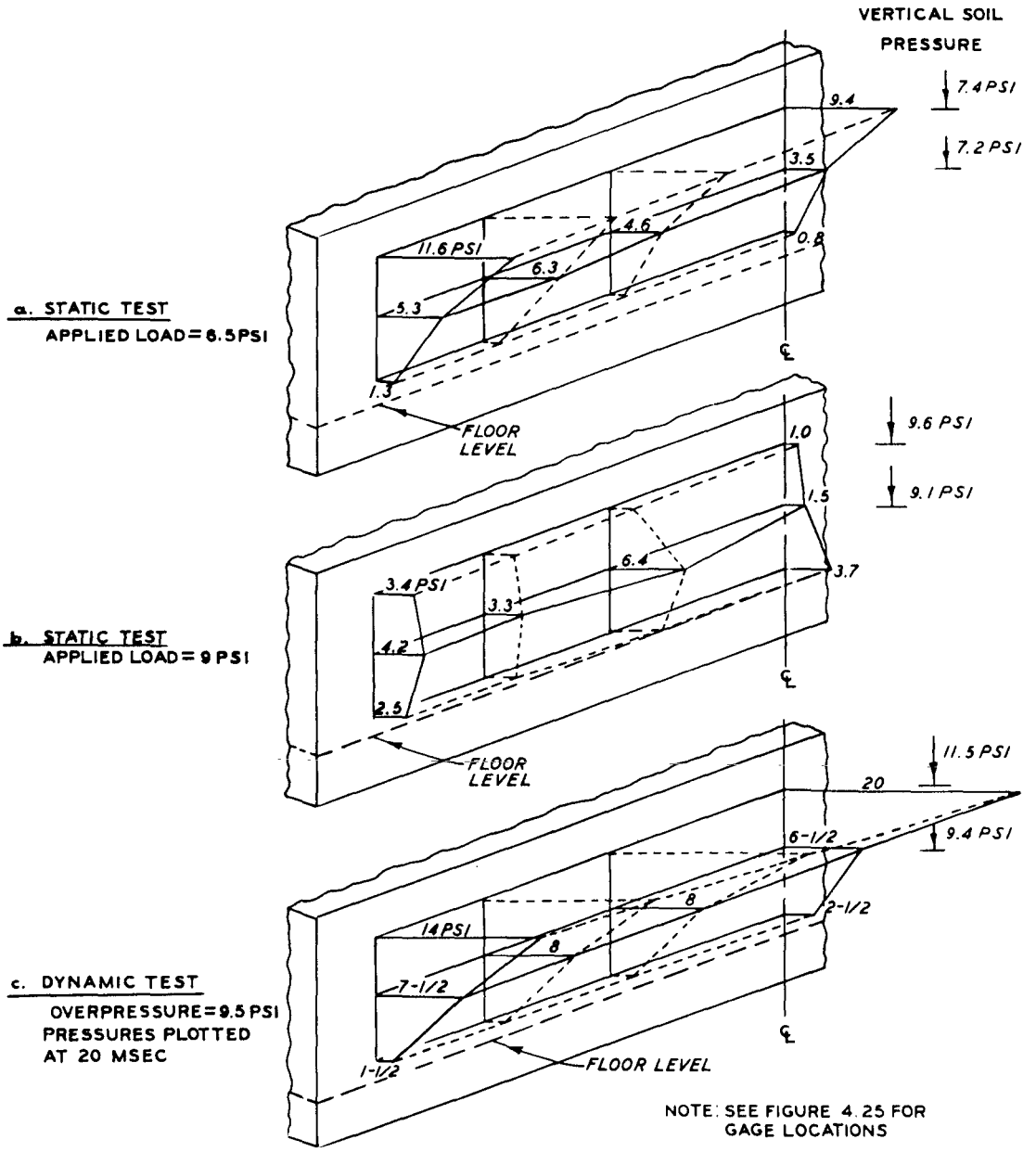

Figure 6.9 Soil pressure distribution across half of the west wall for the static and dynamic models.

CHAPTER 7

CONCLUSIONS AND RECOMMENDATIONS

7.1 RESULTS AND CONCLUSIONS

Two 1/4.5-scale models of a basement shelter from a steel frame multistory building were subjected to static and dynamic loads to determine the collapse loading for the shelter and the mode of failure. In both tests the corner panels of the shelter roof slab failed prior to any structural damage to the steel frame support structure.

In the static test, the reinforcing steel across the two outside edge supports of one of the corner panels ruptured at an applied pressure of 8.8 psi. The dynamic model was subjected to a peak pressure loading of 10.2 psi with a rise time of 14 msec and an effective duration of 70 msec. All four corner panels of the dynamic model had 70 to 100 percent of the reinforcing steel crossing the outside edges of the panels to rupture. The roof slab of both models was carrying the loading as a tensile membrane when the reinforcing steel ruptured.

Park's modified tensile membrane equation (Equation 6.2) gave good correlation with the experimental data obtained in the static test. The predicted applied pressure levels using Equation 6.2 were within 15 percent of the measured overpressure.

In extending Equation 6.2 to predict collapse pressures of the different slab panels of the model, the center panel was found to be the weakest. However, the corner panels collapsed first in both the static and the dynamic test and two of the edge panels in the dynamic test were also very near collapse. Equation 6.2 is based on the quantity of continuous reinforcing steel in a panel and does not consider any load-carrying capacity for negative moment steel extending into a slab from the surrounding panels. The results of the tests conducted in this program indicate that the reinforcing steel extending into a panel from the surrounding panels contributes to the tensile membrane load-carrying capacity of the slab panel. However, data obtained from these tests are insufficient to determine the full benefit of this reinforcing steel.

The steel frame and connections survived both tests with little, if

any, structural damage. The loading in both tests was sufficient for the measured strains along several of the framing beams to attain or slightly exceed yield strain. A comparison of the response of a simple frame subjected to the same loadings as the rigid frame models revealed that the simple frame would probably collapse prior to the collapse of the roof slab. In the hypothetical simple frame model, both the connections and the framing beams were carrying collapse or near-collapse loads at the collapse load level for the roof slabs.

The horizontal soil loading on the basement walls of the two models varied from 1.45 to 2 times the applied overpressure near the top of the walls to a few pounds per square inch near the base of the wall. Similar results were reported in Reference 12. The soil backfill in the test consisted of a fine, dry sand which did not represent a real soil backfill.

7.2 RECOMMENDATIONS

Experimental work conducted thus far on basement shelters has neglected the interaction of the aboveground structure with the structural frame in the basement area. This was done in order to obtain data on the total response of the shelter's roof slab to the blast loading only. In reality, the blast loading on the aboveground wall and frame of the building will affect the structural frame in the basement, thus also affecting the roof slab over the basement shelter.

In Reference 21, 50 percent of the analyzed aboveground walls were predicted to collapse at incident overpressures greater than 6 psi. One building in which the steel frame was also analyzed had an incident collapse pressure of 3 to 4 psi for the frame. The basement roof slabs tested in this program failed at near 10 psi.

A model of a multistory structure complete with frame, floors, exterior walls, and basement shelter included in an HE test would provide valuable information on the response of the entire building system along with useful data on debris quantity and distribution for fire research.

In order to accurately predict the maximum load-carrying capacity of two-way slabs which are part of a floor system, additional information is required on the effect of negative moment reinforcing steel at the supports which is not continuous across the slab panel. This information could be obtained from small slab tests similar to those described in Reference 20.

Consideration should be given to the placement of shelter occupants inside a shelter on the basis of the type of roof slab over the shelter. From the results of the tests described herein, the worst place to be in a shelter having a two-way-reinforced concrete roof slab is near the outside corners. The tests on flat slabs described in Reference 12 indicated that near the interior columns was the worst place to be.

Horizontal soil forces on basement walls due to the blast overpressure need to be defined for the various types of commonly used backfill material. These data could possibly be obtained by the compilation of previous field and laboratory test data with laboratory tests as necessary to fill gaps in the data.

REFERENCES

1. E. L. Hill and others; "Structural Characteristics of NFSS Buildings"; Vols I-V and Summary, Subcontract B-8183 (4949A-54), June 1967; Research Triangle Institute, Research Triangle Park, N. C.

2. G. F. Jensen; "Existing Structures Evaluation, Part III: Structural Steel Connections"; (AD-701 088) December 1969; Stanford Research Institute, Menlo Park, Calif.

3. United States Steel Corporation; "Building Design Data"; 1965; Pittsburgh, Pa.

4. American Institute of Steel Construction; "Manual of Steel Construction"; Sixth Edition, 1963; New York, N. Y.

5. J. C. McCormac; "Structural Steel Design"; Second Edition, 1971; Intext Educational Publishers, Scranton, Pa.

6. International Conference of Building Officials; "Uniform Building Code"; 1970 Edition, 1970; Whittier, Calif.

7. J. E. Lothers; "Advanced Design in Structural Steel"; 1960; Prentice-Hall, Inc., Englewood Cliffs, N. J.

8. E. L. Wilson; "SAP, A General Structural Analysis Program"; Report No. SESM 70-20, September 1970; Division of Structural Engineering and Structural Mechanics, University of California, Berkeley, Calif.

9. L. S. Beedle and L. Tall; "Structural Steel Design"; 1964; The Ronald Press Company, New York, N. Y.

10. ACI Committee 318; "Building Code Requirements for Reinforced Concrete"; ACI Standard 318-63, June 1963; American Concrete Institute, Detroit, Mich.

11. P. M. Ferguson; "Reinforced Concrete Fundamentals"; 1962; John Wiley and Sons, Inc., New York, N. Y.

12. M. E. Criswell; "Design and Testing of a Blast-Resistant Reinforced Concrete Slab System"; Technical Report N-72-10, November 1972; U. S. Army Engineer Waterways Experiment Station, CE, Vicksburg, Miss.

13. C. Wilton and B. L. Gabrielsen; "Shock Tunnel Tests of Preloaded and Arched Wall Panels"; Report No. URS 7030-10, June 1973; URS Research Company, San Mateo, Calif.

14. G. E. Albritton; "Description, Proof Test, and Evaluation of Large Blast Load Generator Facility"; Technical Report No. 1-707, December 1965; U. S. Army Engineer Waterways Experiment Station, CE, Vicksburg, Miss.

15. W. L. Huff; "Test Devices, Blast Load Generator Facility"; Miscellaneous Paper N-69-1, April 1969; U. S. Army Engineer Waterways Experiment Station, CE, Vicksburg, Miss.

16. T. E. Kennedy, G. E. Albritton, and R. E. Walker; "Initial Evaluation of the Free-Field Response of the Large Blast Load Generator"; Technical Report No. 1-723, June 1966; U. S. Army Engineer Waterways Experiment Station, CE, Vicksburg, Miss.

17. J. P. Balsara; "Similitude Study of Flexible Buried Arches Subjected to Blast Loads"; Technical Report No. 1-807, January 1968; U. S. Army Engineer Waterways Experiment Station, CE, Vicksburg, Miss.

18. D. R. Denton; "A Dynamic Ultimate Strength Study of Simply Supported Two-Way-Reinforced Concrete Slabs"; Technical Report No. 1-789, July 1967; U. S. Army Engineer Waterways Experiment Station, CE, Vicksburg, Miss.

19. R. Park; "Tensile Membrane Behavior of Uniformly Loaded Rectangular Reinforced Concrete Slabs with Fully Restrained Edges"; Magazine of Concrete Research, March 1964, Vol. 16, No. 46, Pages 39-44; Cement and Concrete Association, London, England.

20. W. M. Brown and M. S. Black; "Dynamic Strength Study of Small, Fixed-Edge, Longitudinally Restrained, Two-Way-Reinforced Concrete Slabs"; Technical Report N-73-8, December 1973; U. S. Army Engineer Waterways Experiment Station, CE, Vicksburg, Miss.

21. C. K. Wiehle; "Blast Analysis of Building Elements"; April 1974; Stanford Research Institute, Menlo Park, Calif.

22. N. M. Newmark and J. D. Haltiwanger; "Air Force Design Manual; Principles and Practices for Design of Hardened Structures"; Technical Documentary Report No. AFSWC-TDR-62-138, December 1962; Air Force Special Weapons Center, Kirtland Air Force Base, N. Mex.

23. J. W. Melin and S. Sutcliffe; "Development of Procedures for Rapid Computation of Dynamic Structural Response"; Structural Research Series No. 171, January 1958; University of Illinois, Urbana, Ill.

24. C. K. Wiehle and J. L. Bockholt; "Dynamic Analysis of Reinforced Concrete Floor Systems"; (AD-768 206) May 1973; Stanford Research Institute, Menlo Park, Calif.

25. J. R. Allgood and G. R. Swihart; "Design of Flexural Members for Static and Blast Loadings"; ACI Monograph No. 5, 1970; American Concrete Institute, Detroit, Mich.

26. C. Wilton and B. Gabrielsen; "Shock Tunnel Tests of Wall Panels"; Report No. URS 7030-7, January 1972; URS Research Company, San Mateo, Calif.

APPENDIX A

STATIC TEST

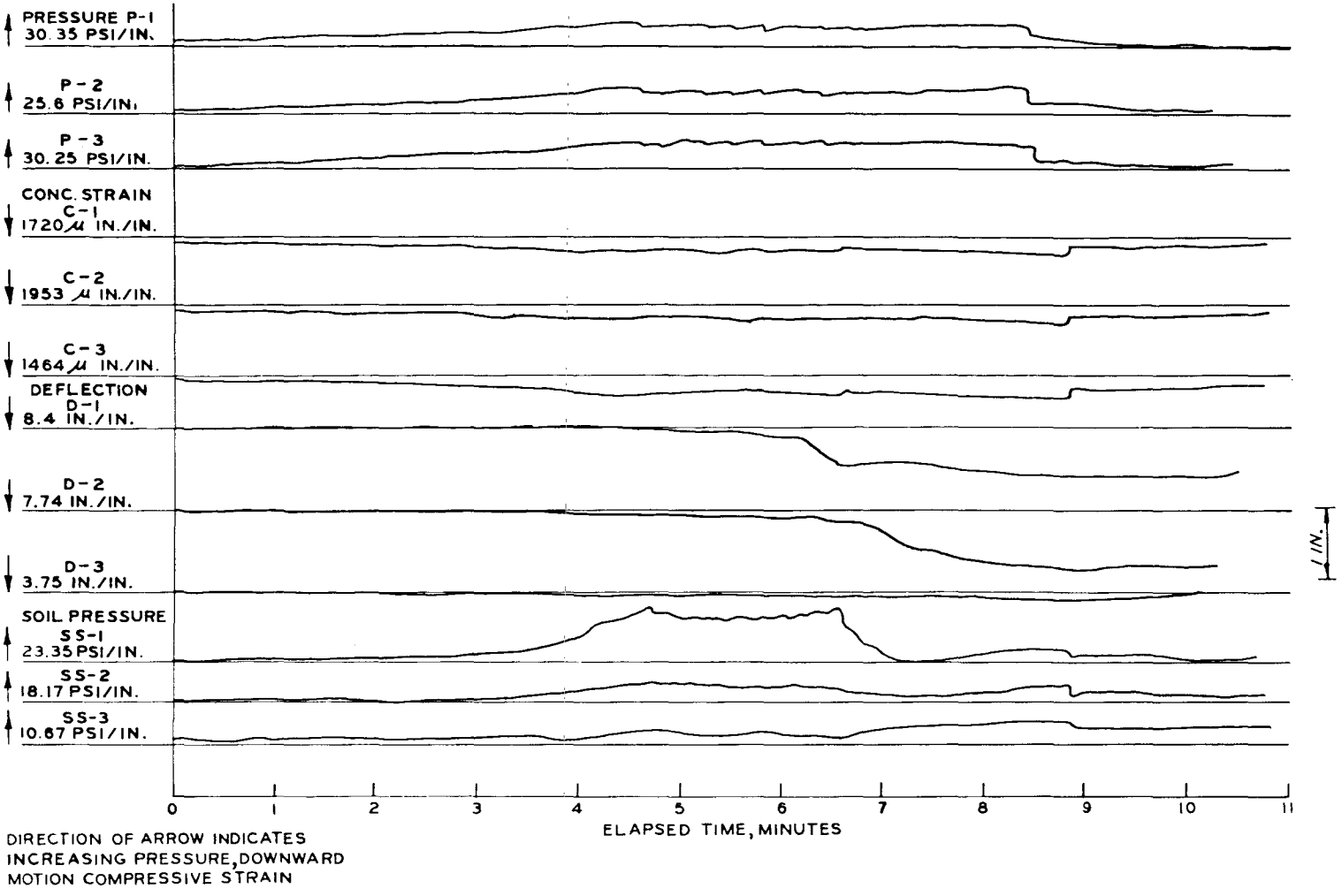

Figure A.1 Tracings from Recorder 1, static test.

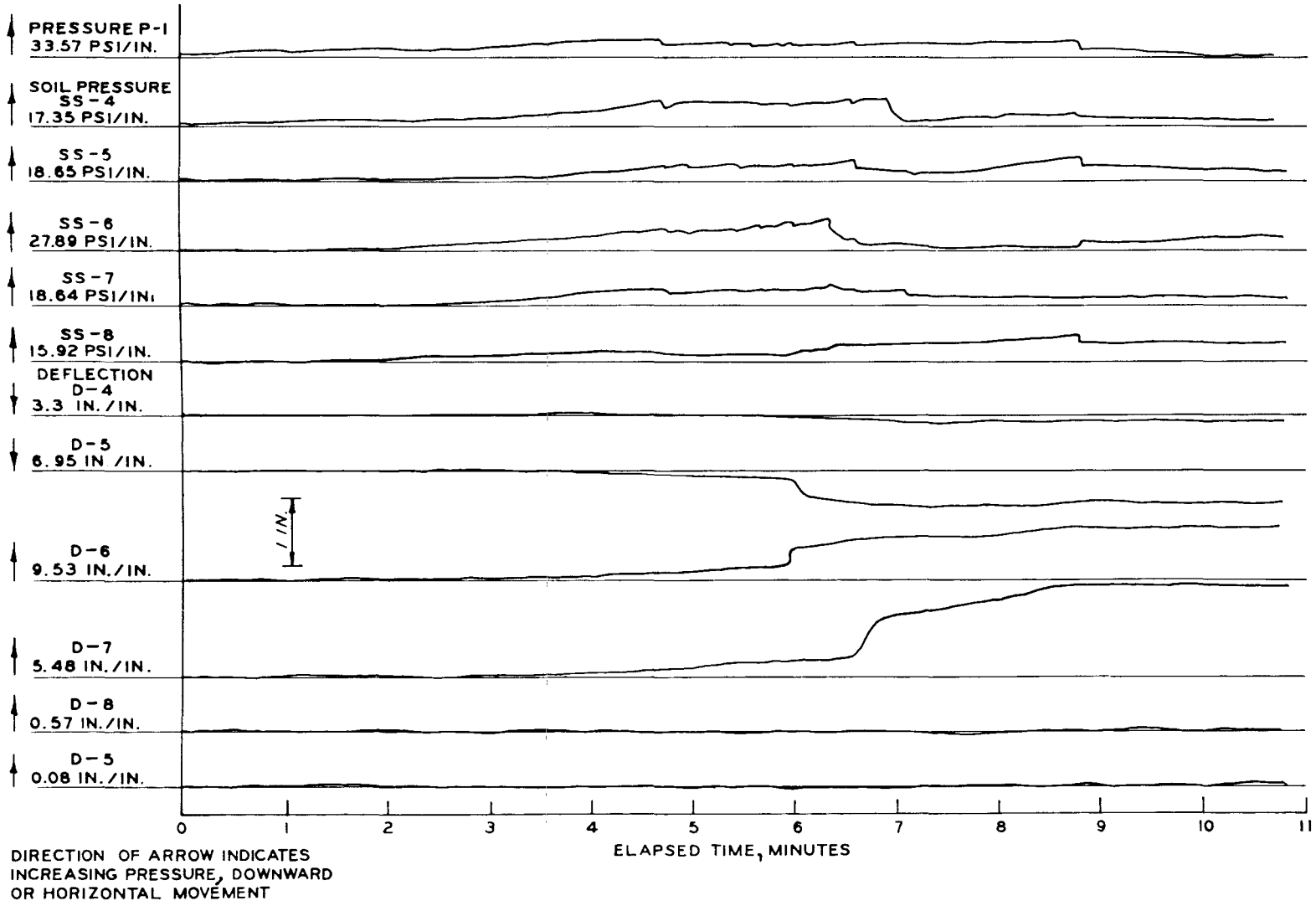

Figure A.2 Tracings from Recorder 2, static test.

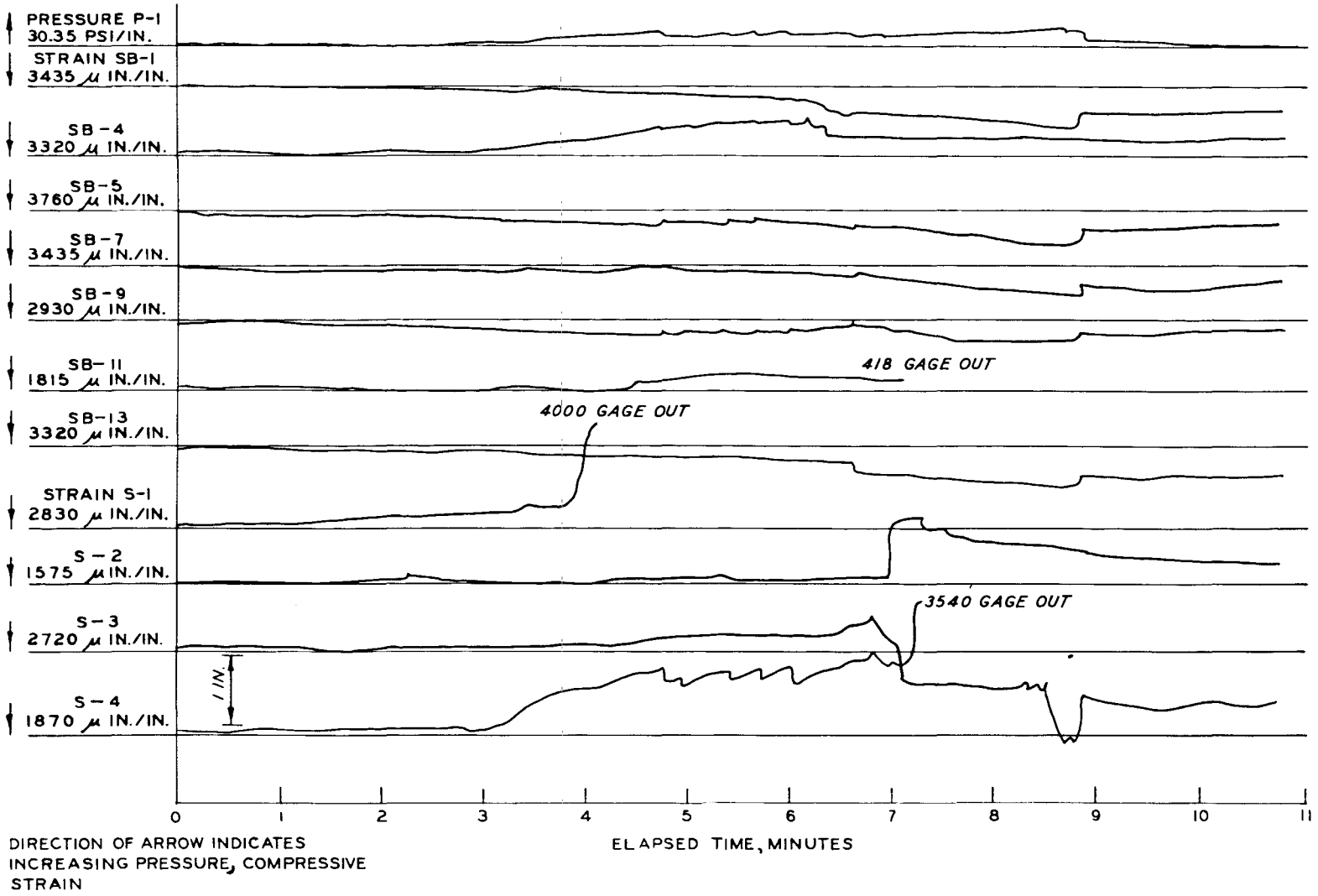

Figure A.3 Tracings from Recorder 3, static test.

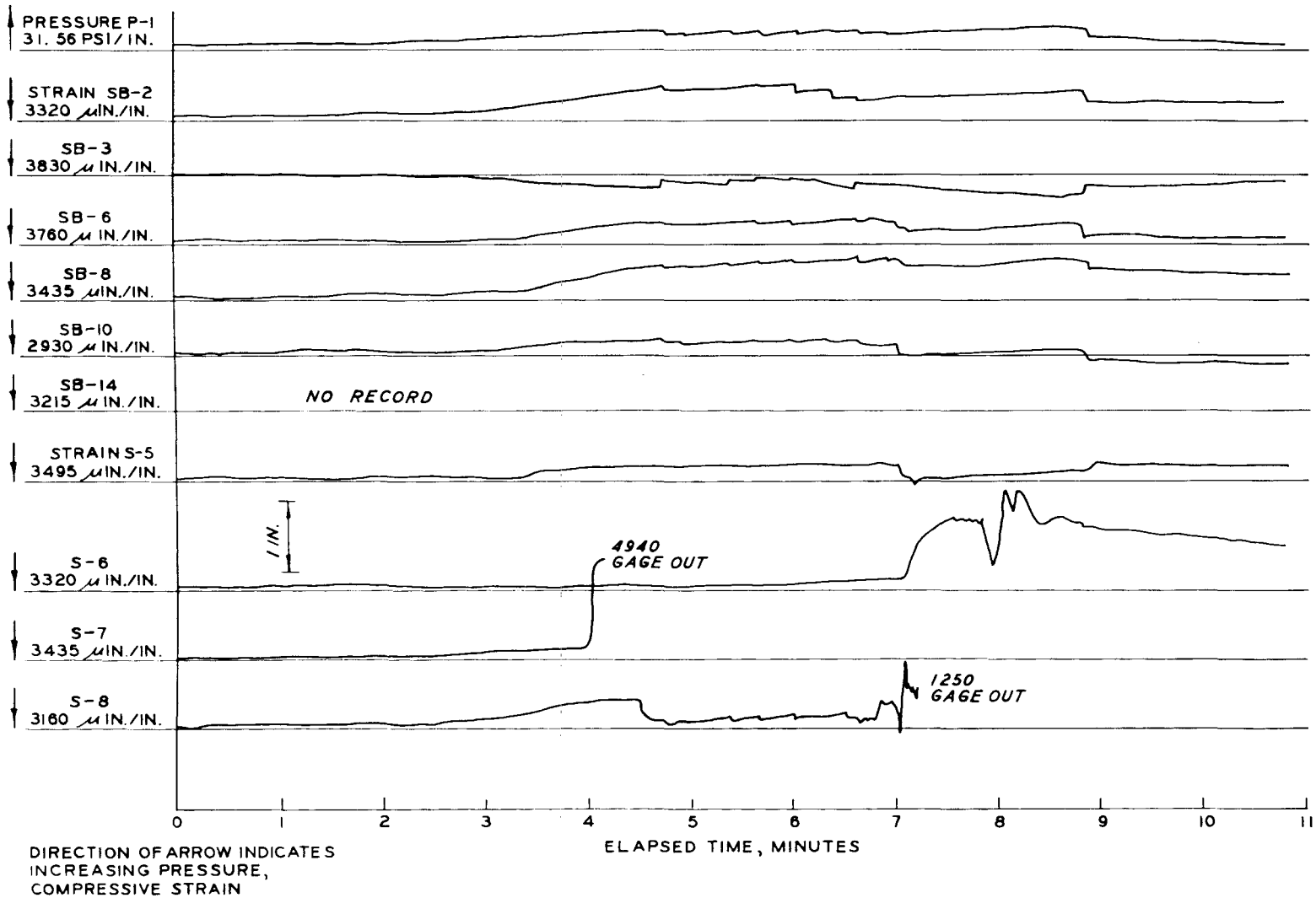

Figure A.4 Tracings from Recorder 4, static test.

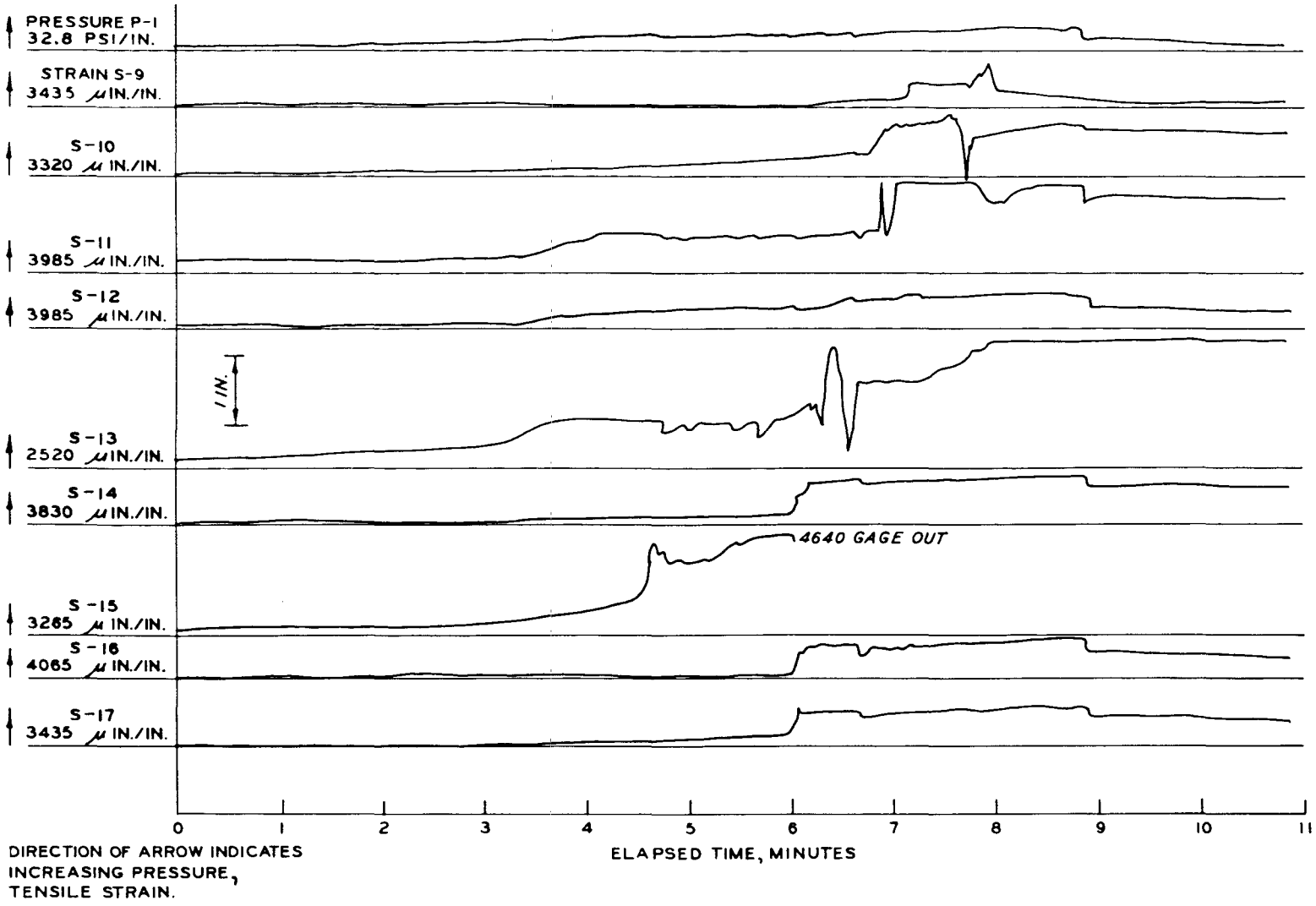

Figure A.5 Tracings from Recorder 5, static test (sheet 1 of 2).

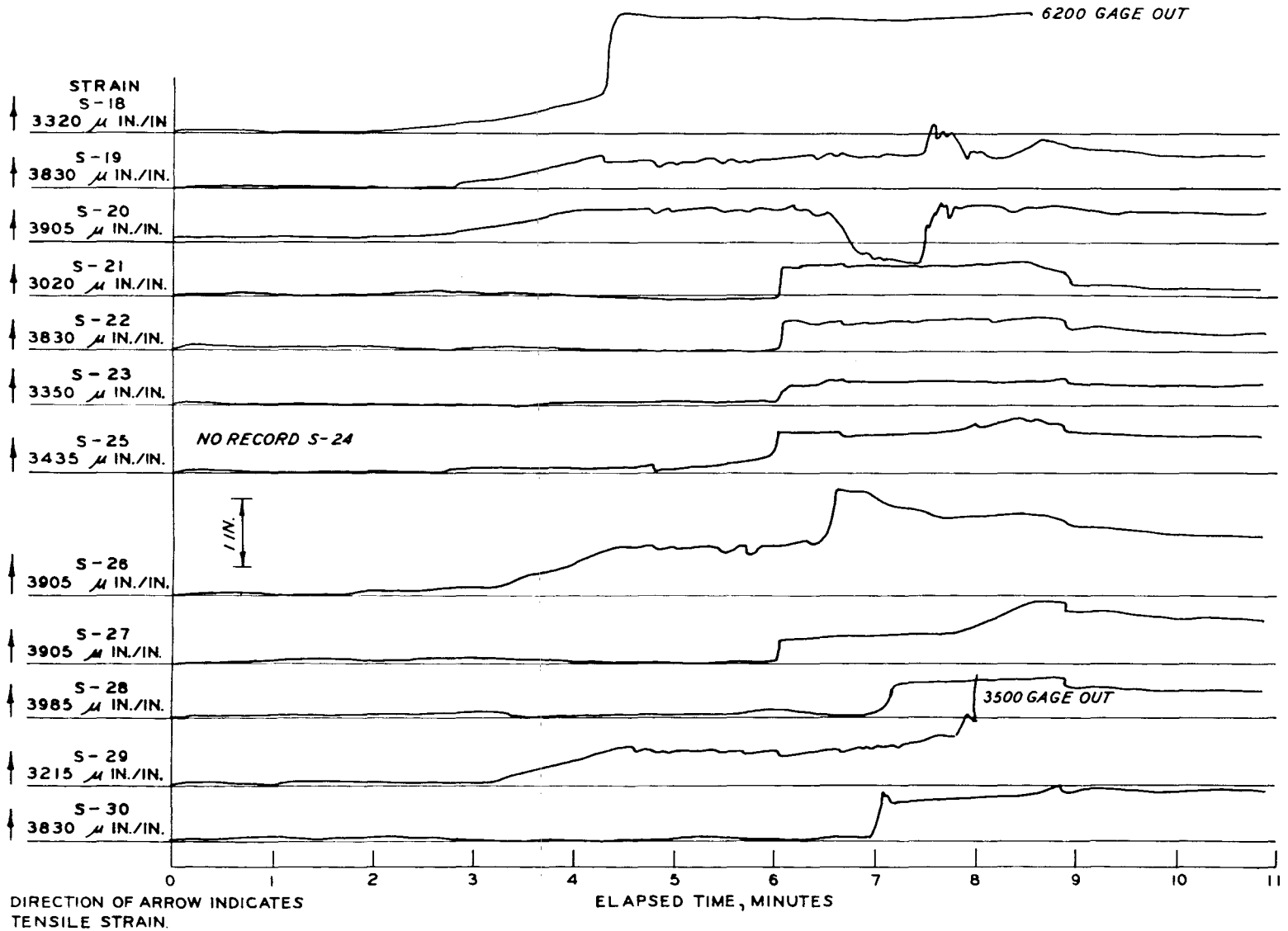

Figure A.5 (sheet 2 of 2).

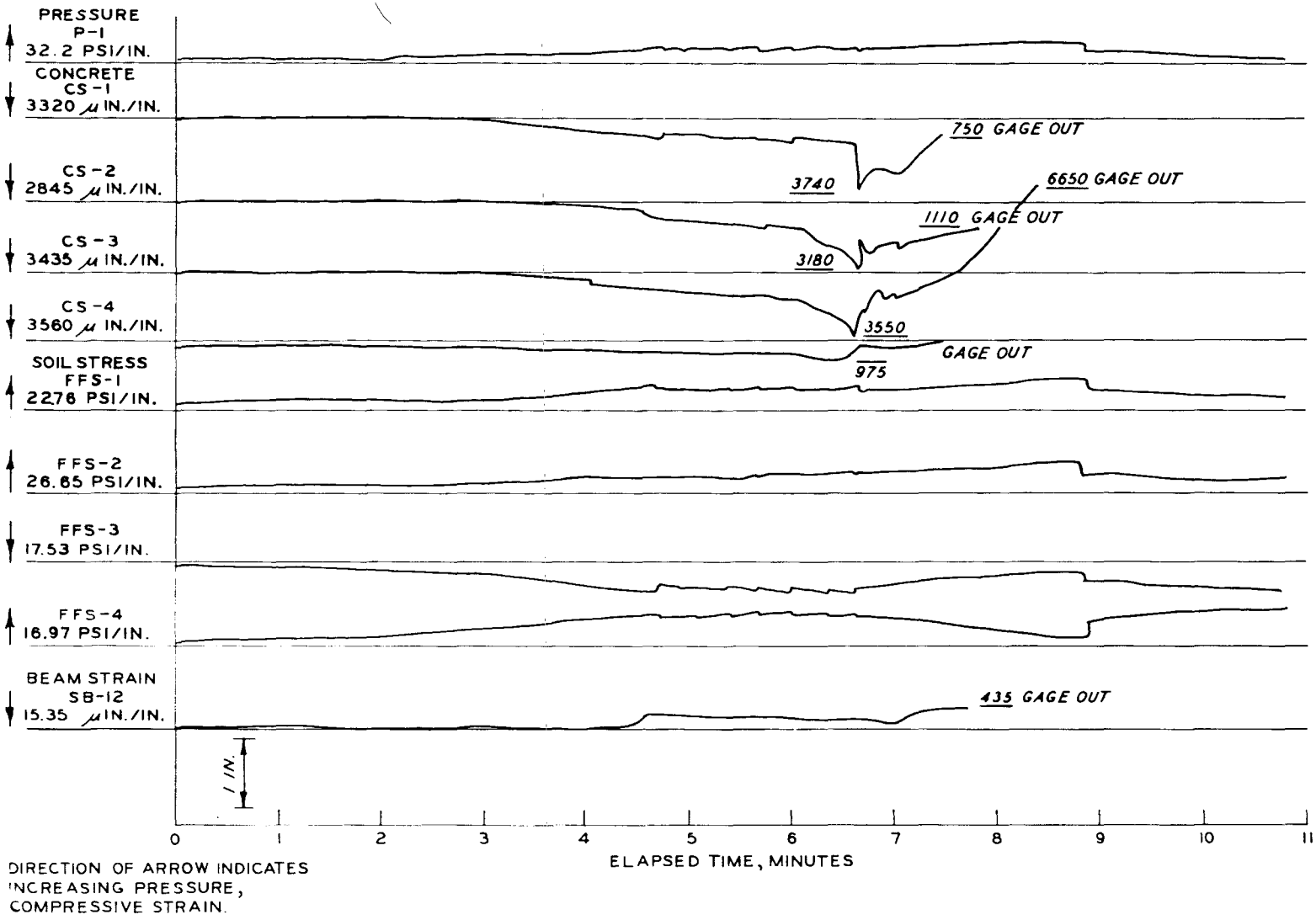

Figure A.6 Tracings from Recorder 6, static test.

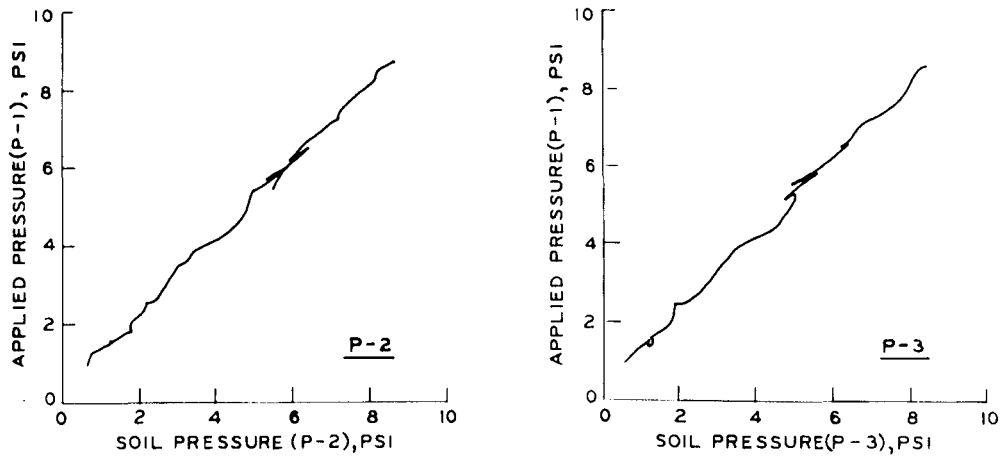

a. APPLIED PRESSURE RECORDS

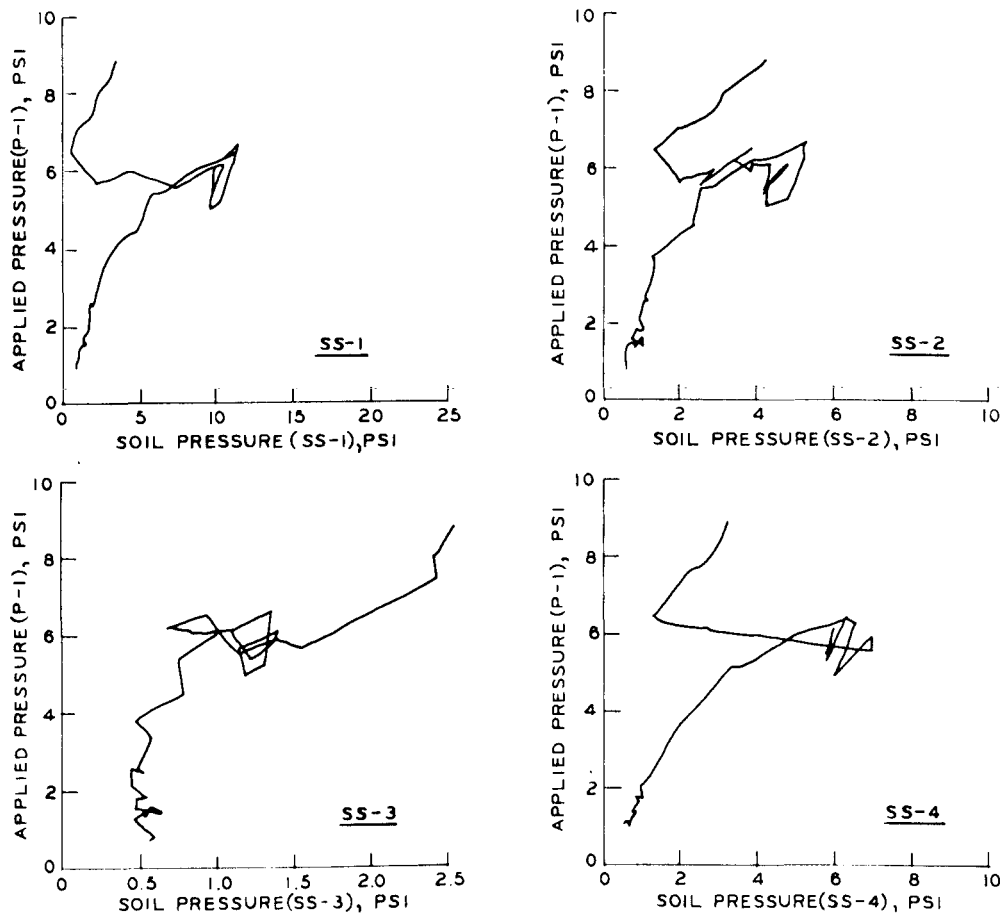

b. SOIL-STRUCTURE INTERFACE PRESSURE

Figure A.7 Applied pressure and soil-structure interface pressure, Gages SS-1 through SS-4, static test.

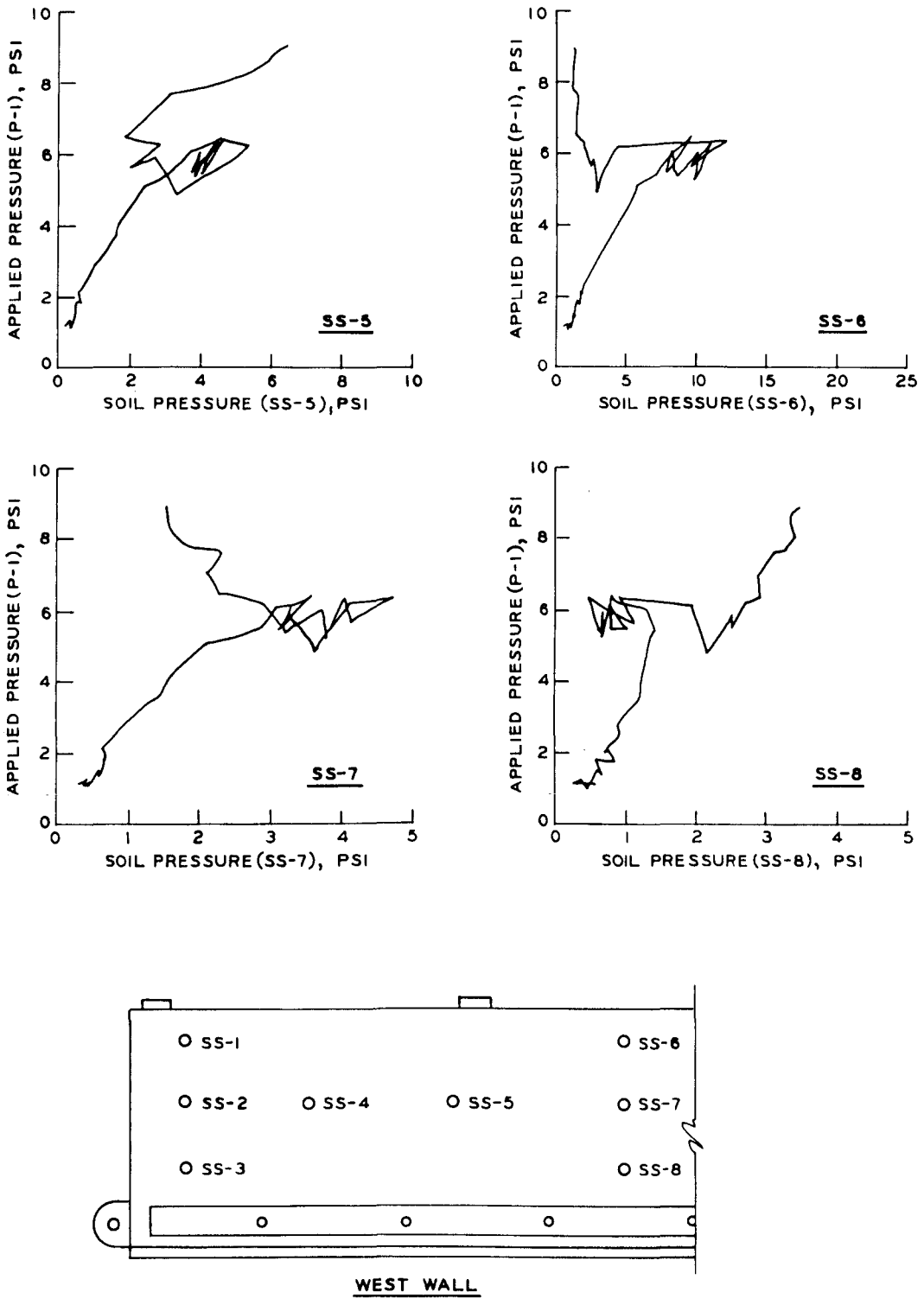

Figure A.8 Soil-structure interface pressure, Gages SS-5 through SS-8, static test.

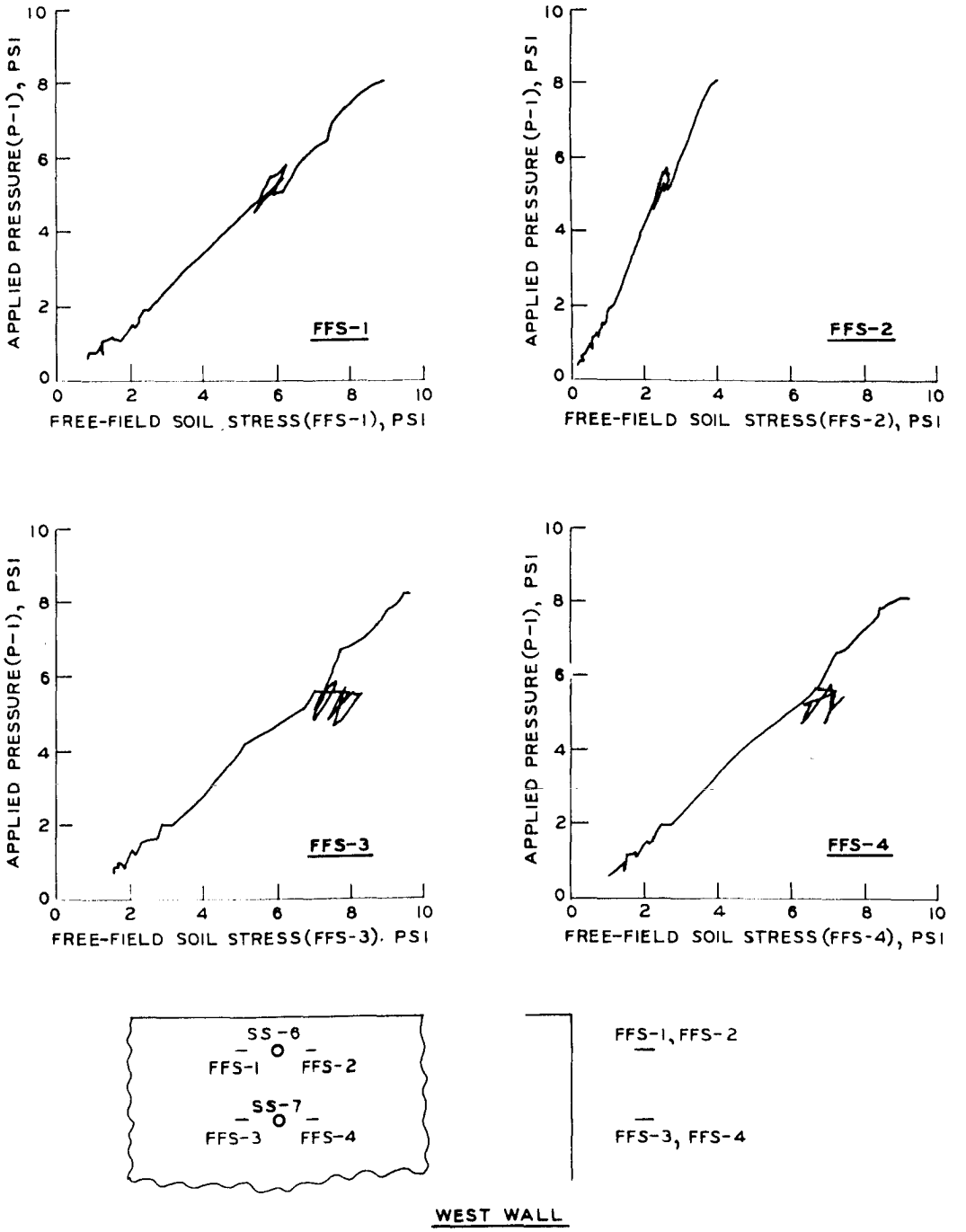

Figure A.9 Free-field soil stress, static test.

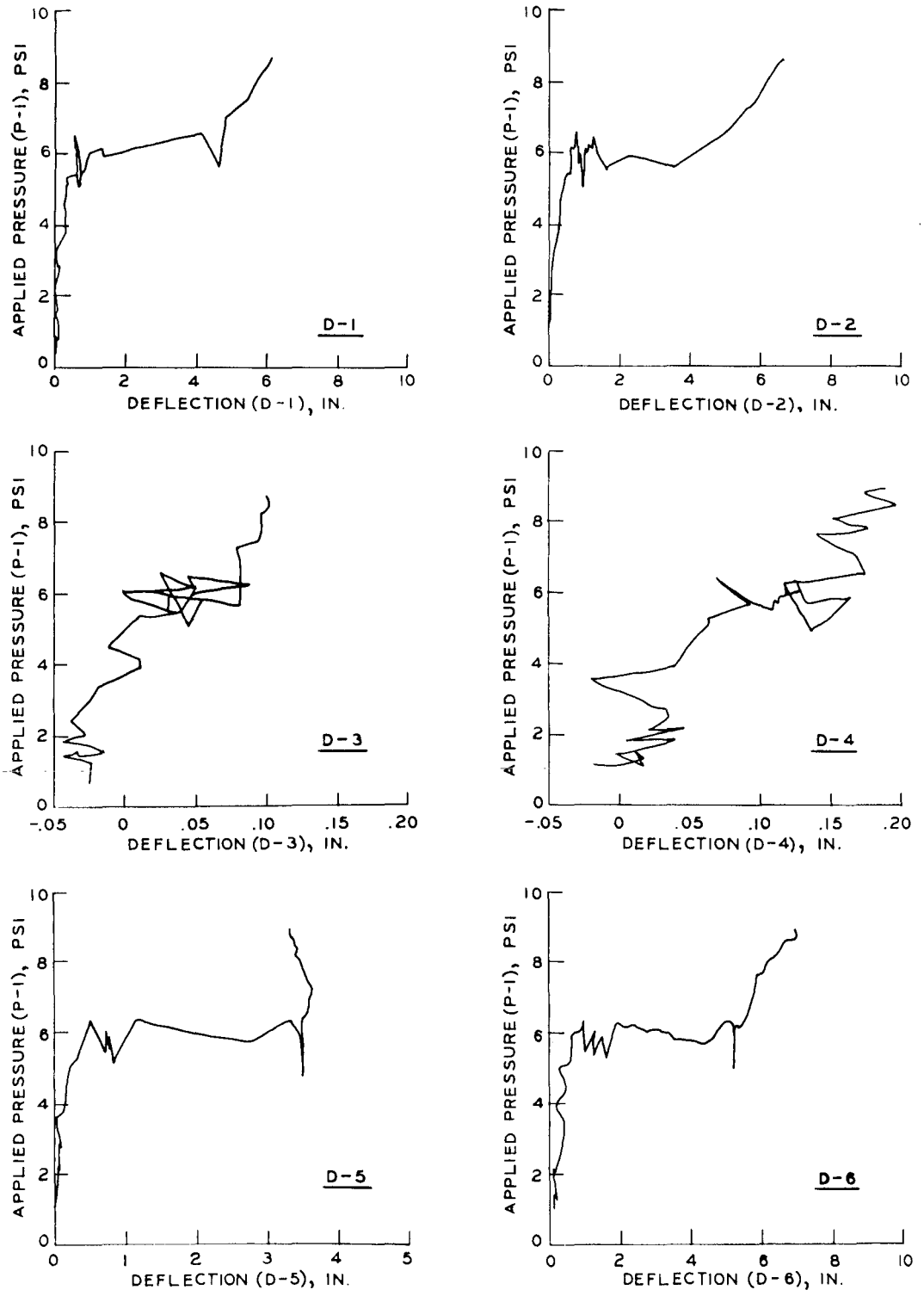

Figure A.10 Slab deflection, Gages D-1 through D-6, static test.

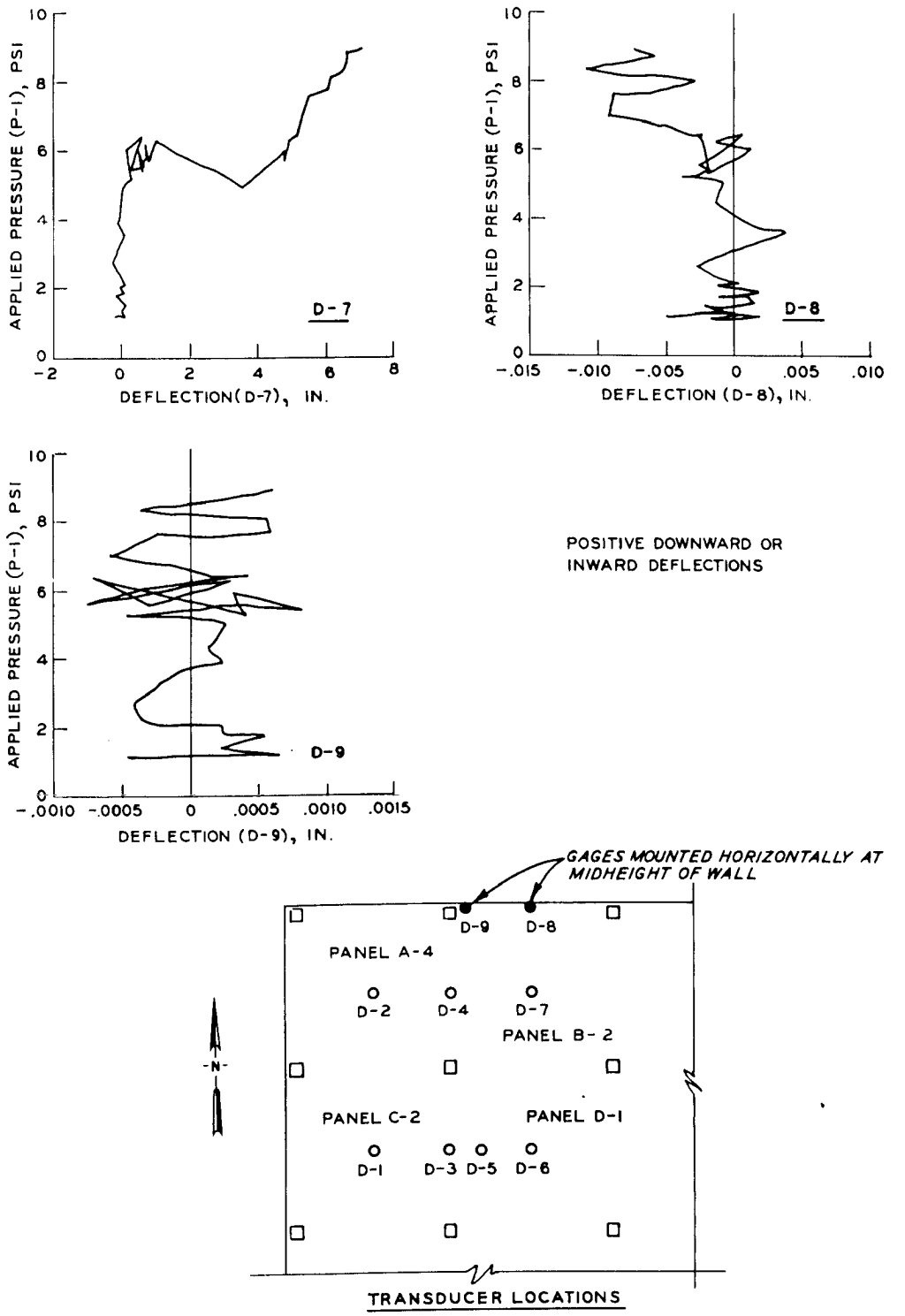

Figure A.11 Slab deflection, Gages D-7 through D-9, static test.

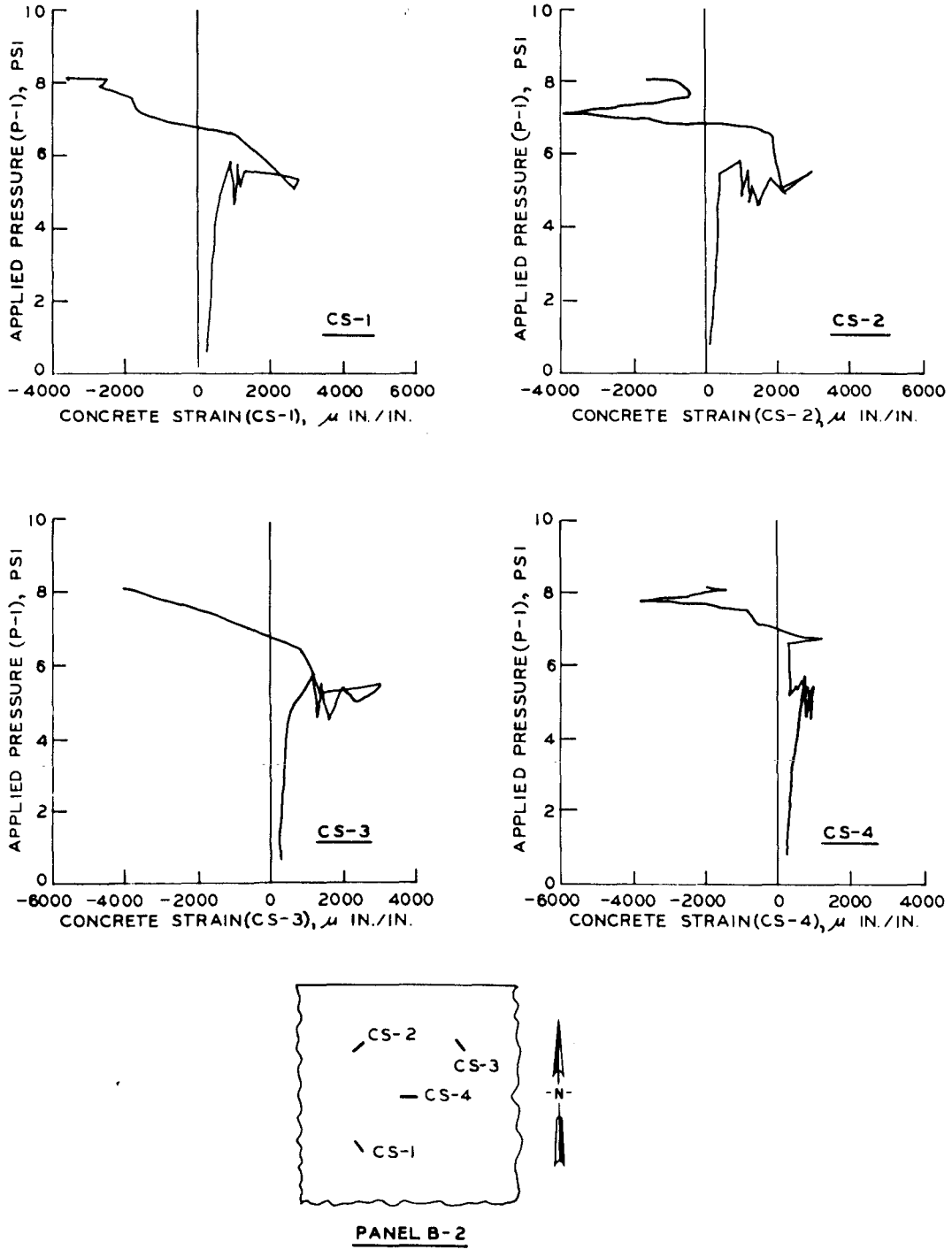

Figure A.12 Concrete strains, static test.

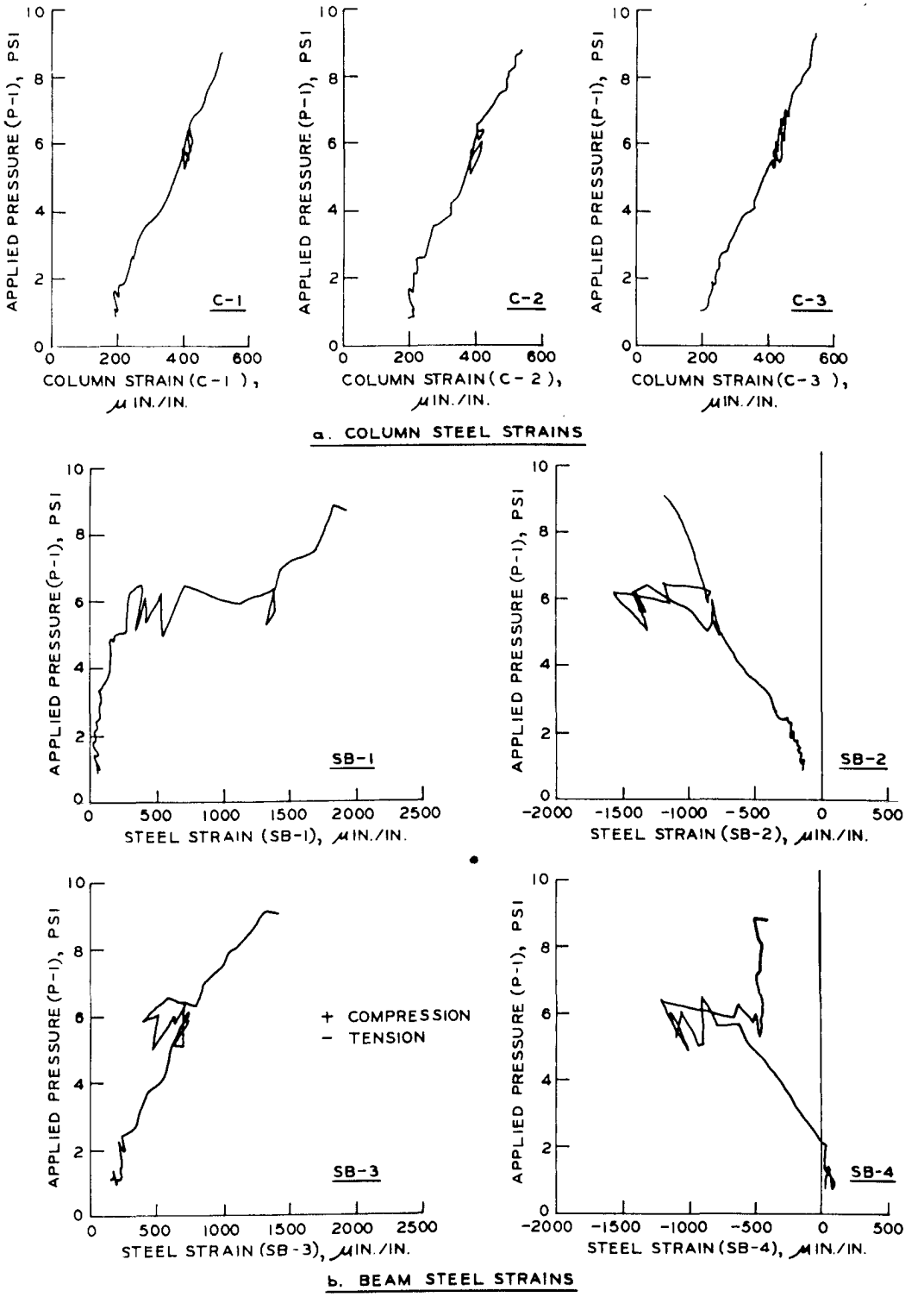

Figure A.13 Column and beam steel strains, Gages SB-1 through SB-4, static test.

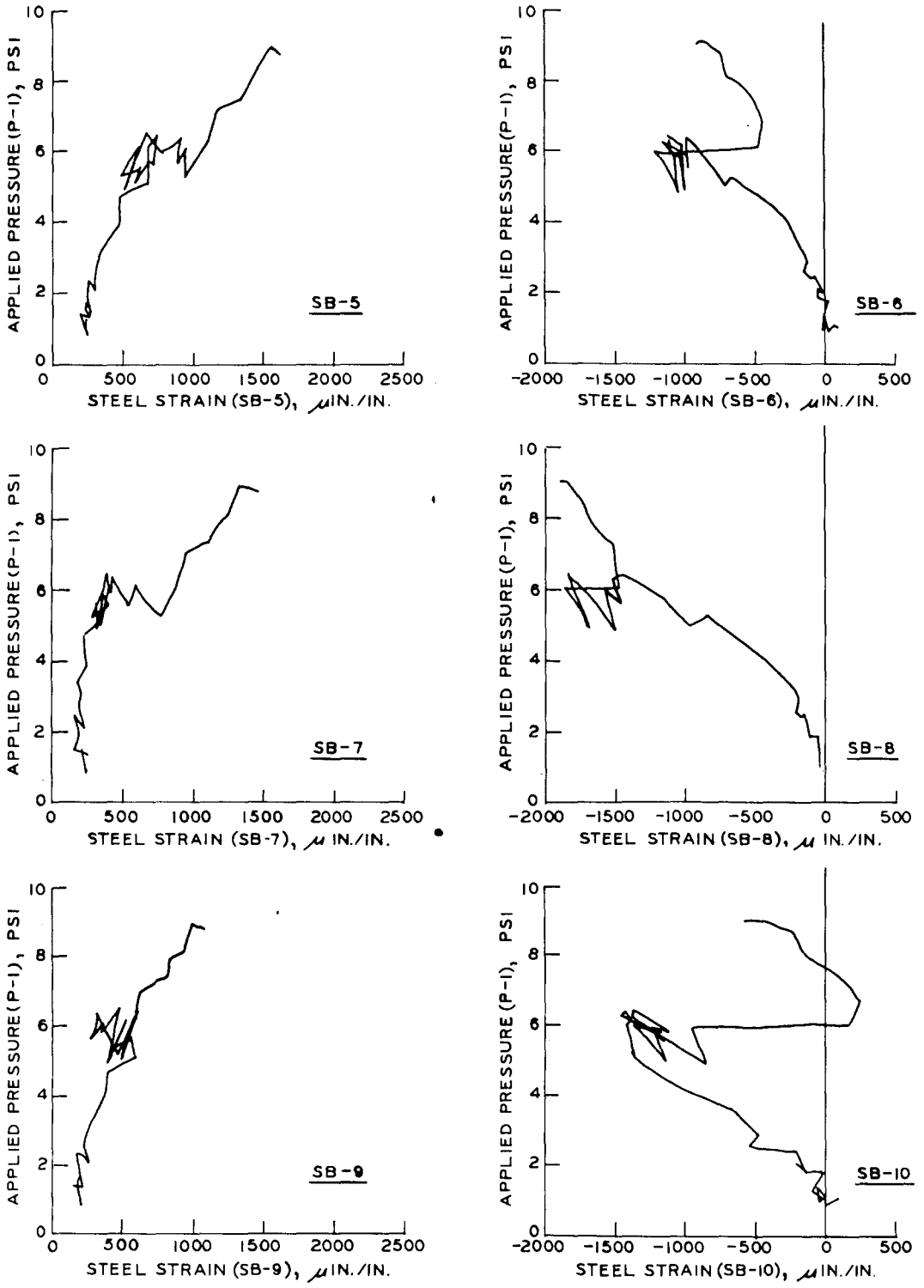

Figure A.14 Beam steel strain, Gages SB-5 through SB-10, static test.

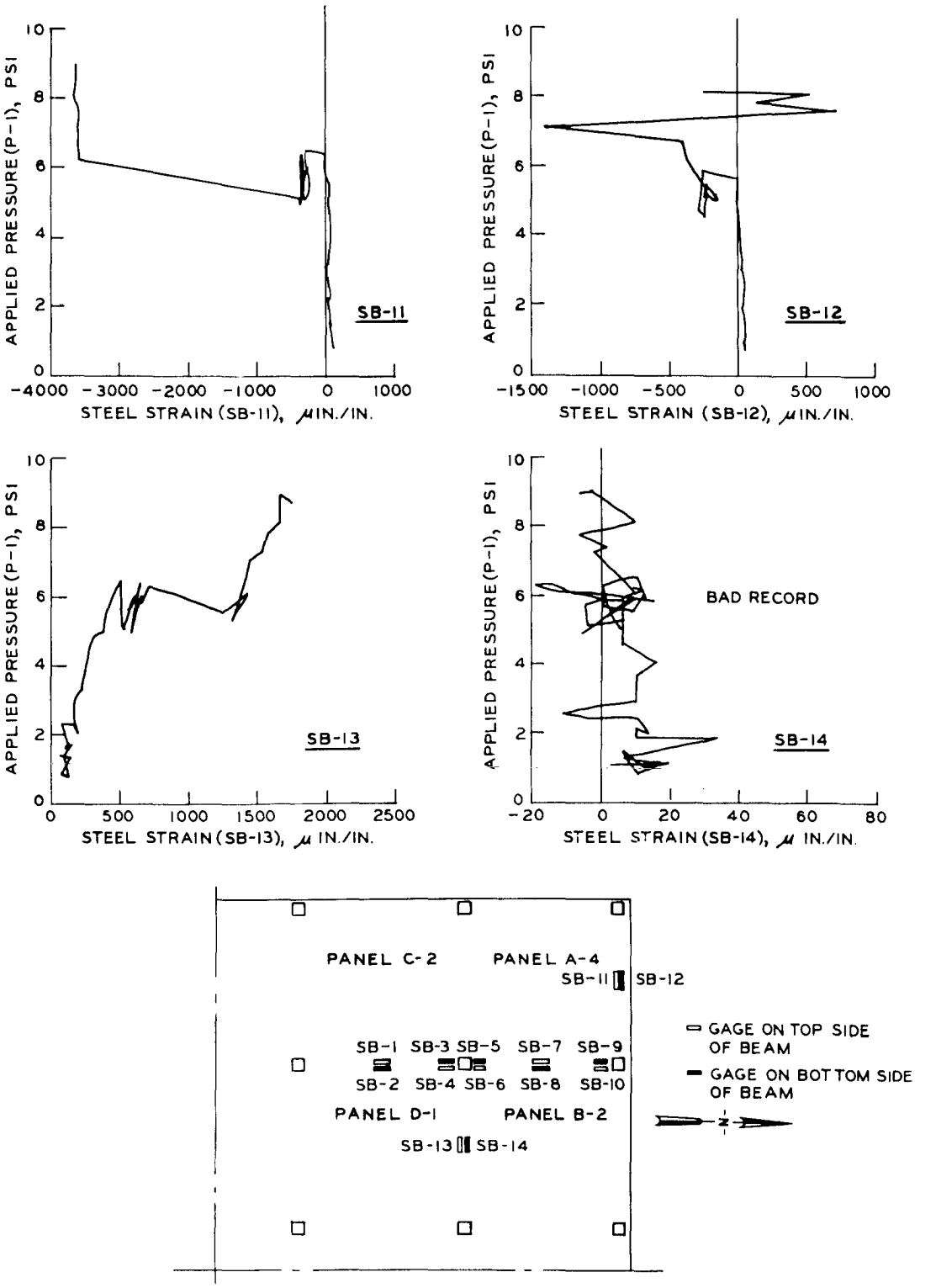

Figure A.15 Beam steel strain, Gages SB-11 through SB-14, static test.

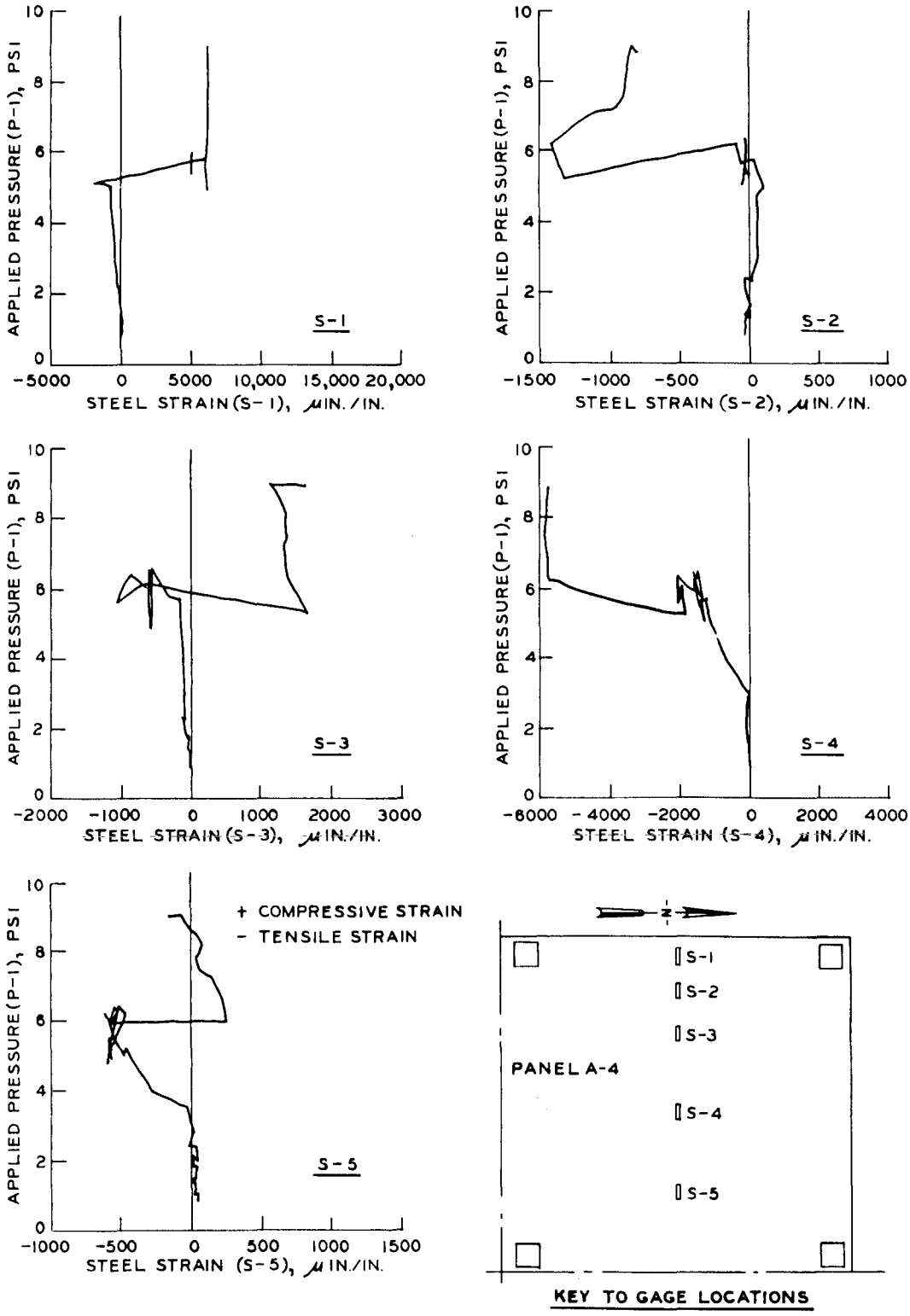

Figure A.16 Reinforcing steel strain, Gages S-1 through S-5, static test.

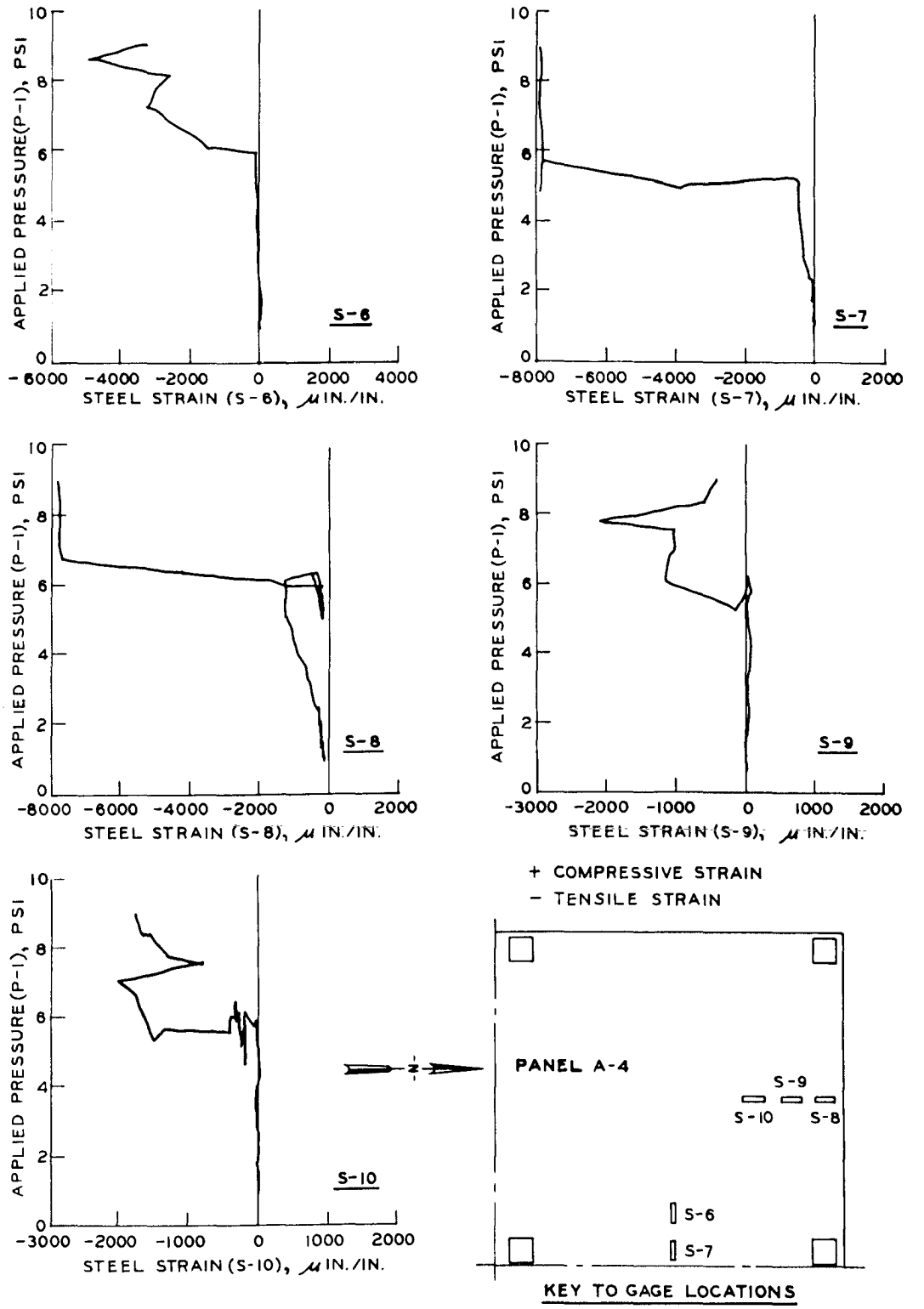

Figure A.17 Reinforcing steel strain, Gages S-6 through S-10, static test.

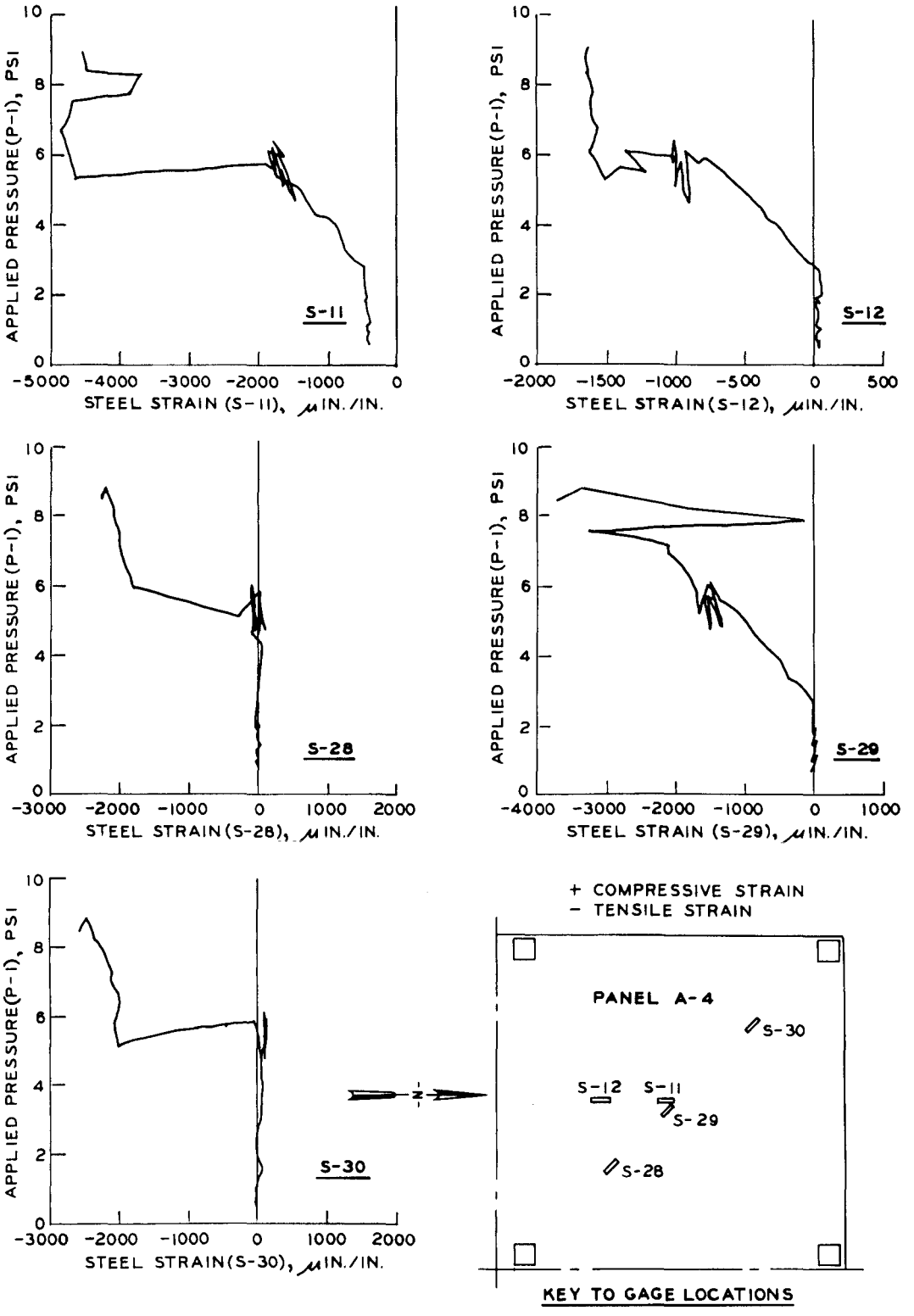

Figure A.18 Reinforcing steel strain, Gages S-11, S-12, and S-28 through S-30, static test.

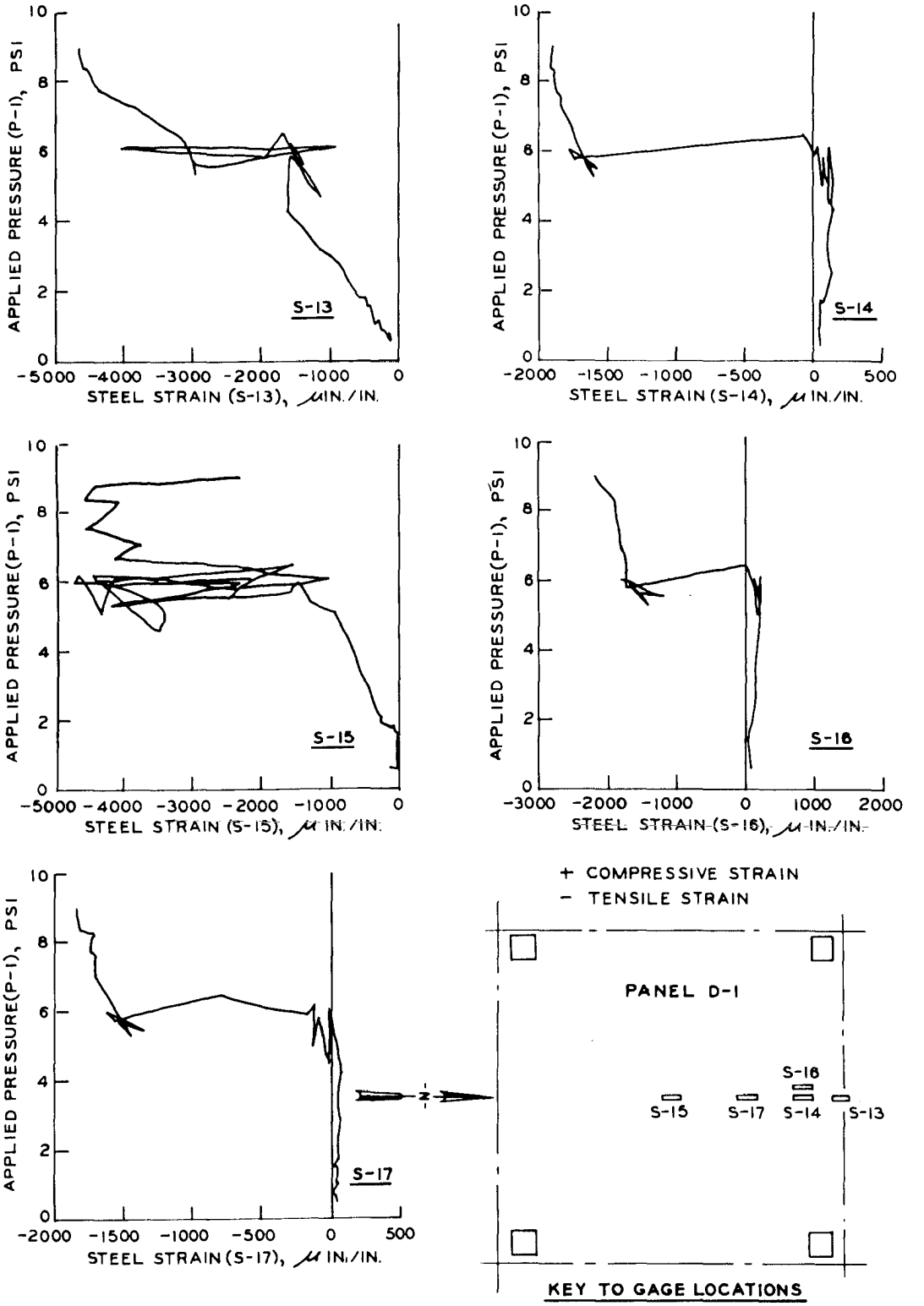

Figure A.19 Reinforcing steel strain, Gages S-13 through S-17, static test.

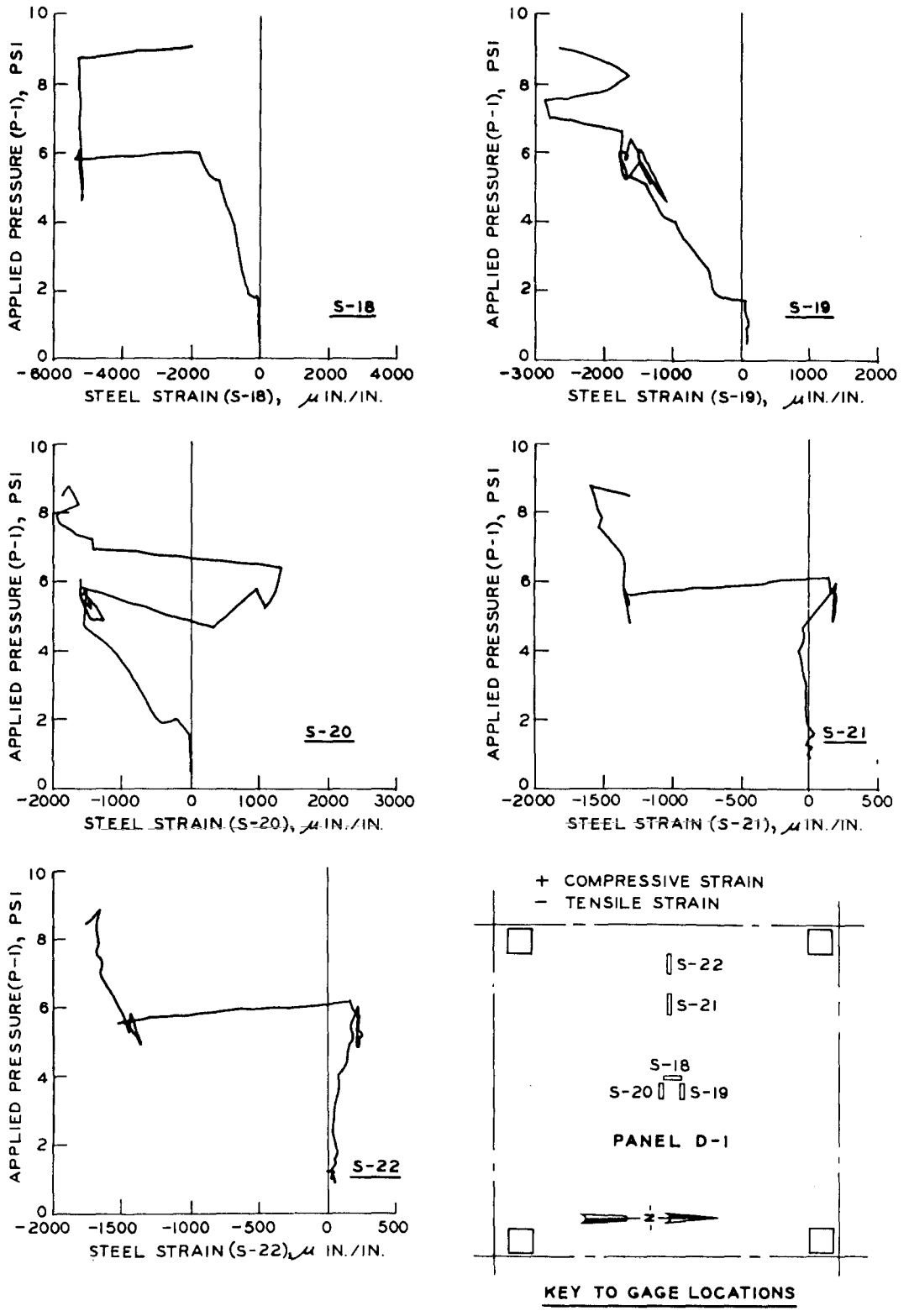

Figure A.20 Reinforcing steel strain, Gages S-18 through S-22, static test.

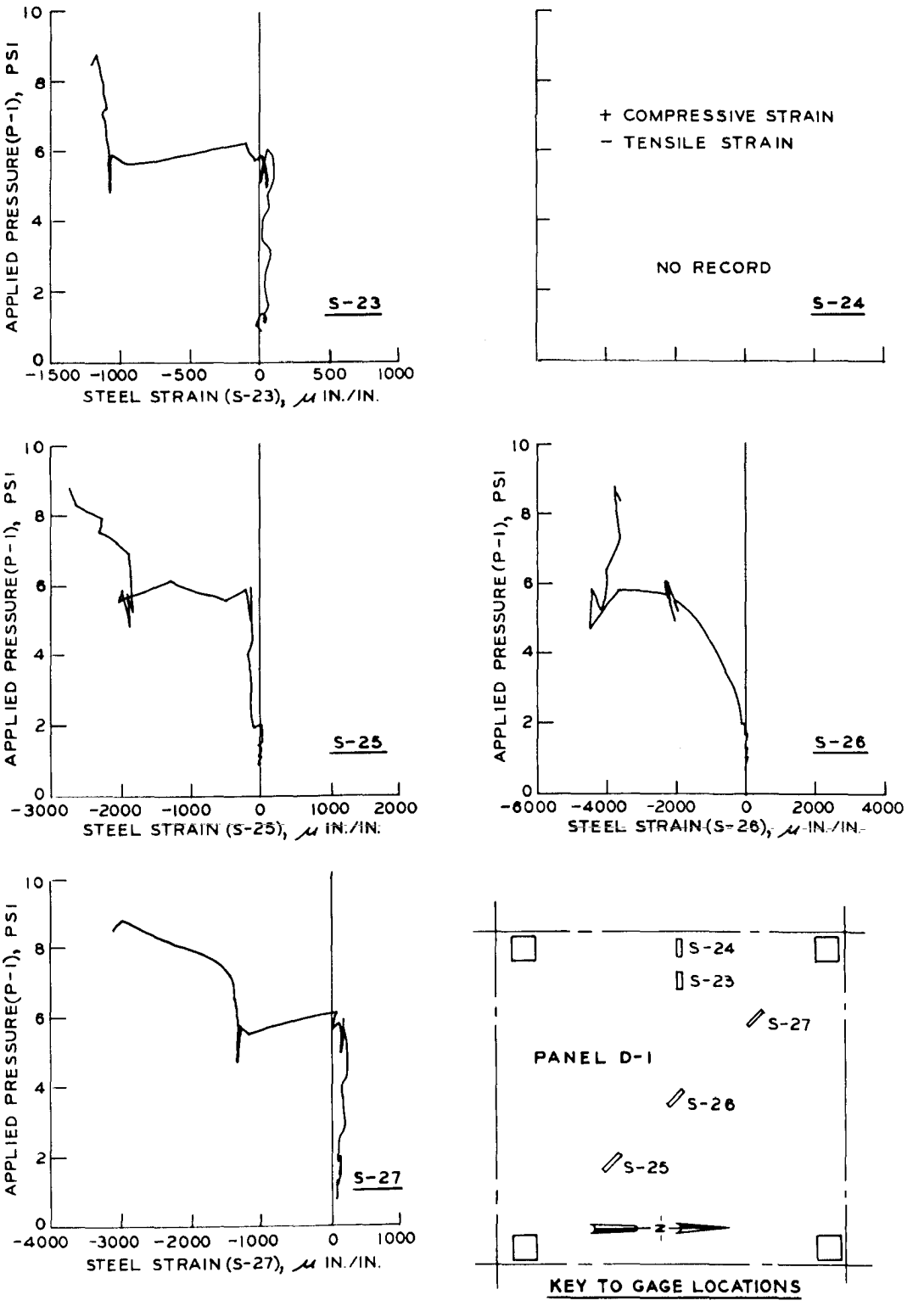

Figure A.21 Reinforcing steel strain, Gages S-23 through S-27, static test.

APPENDIX B

DYNAMIC TEST

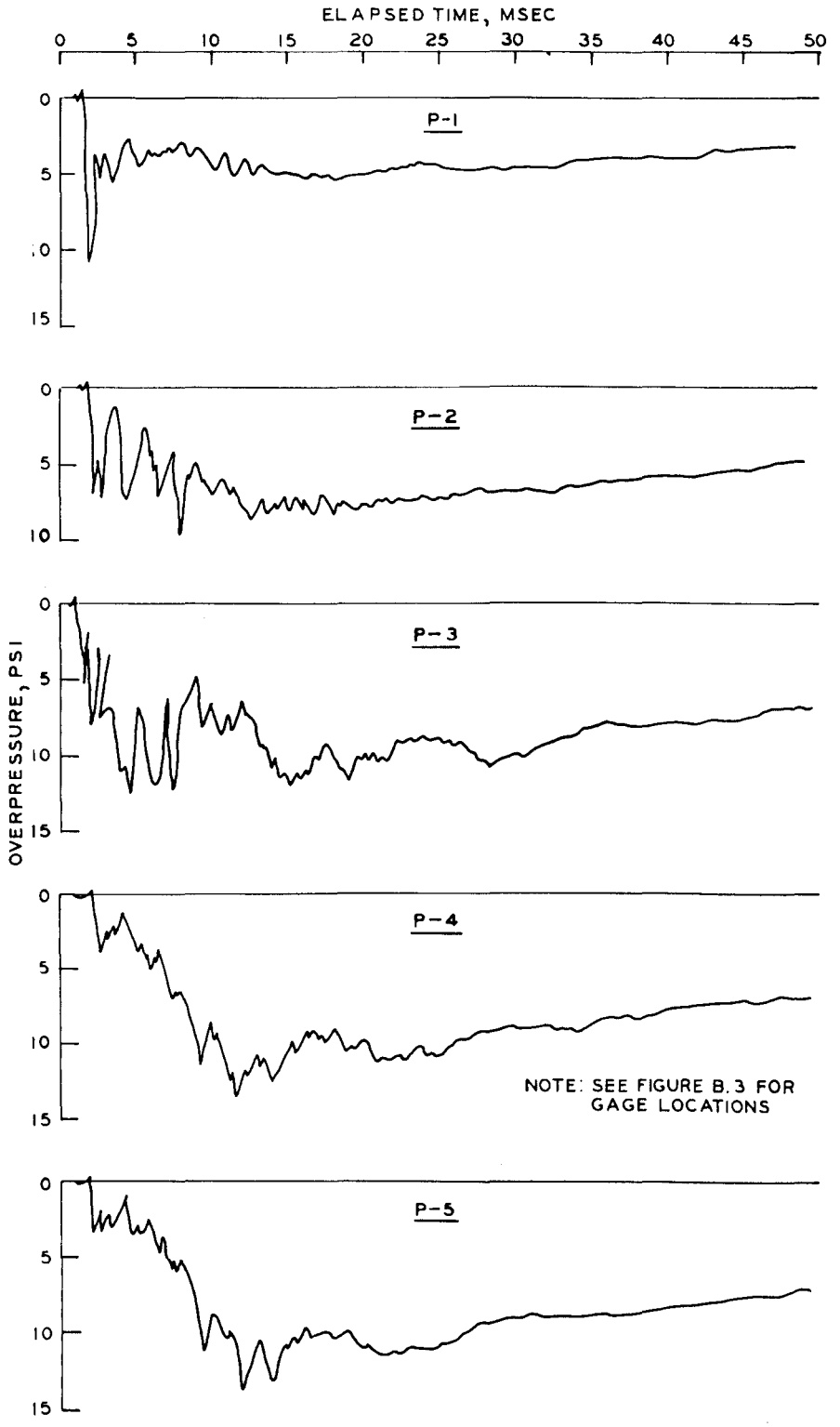

Figure B.1 Overpressure, Gages P-1 through P-5, dynamic test.

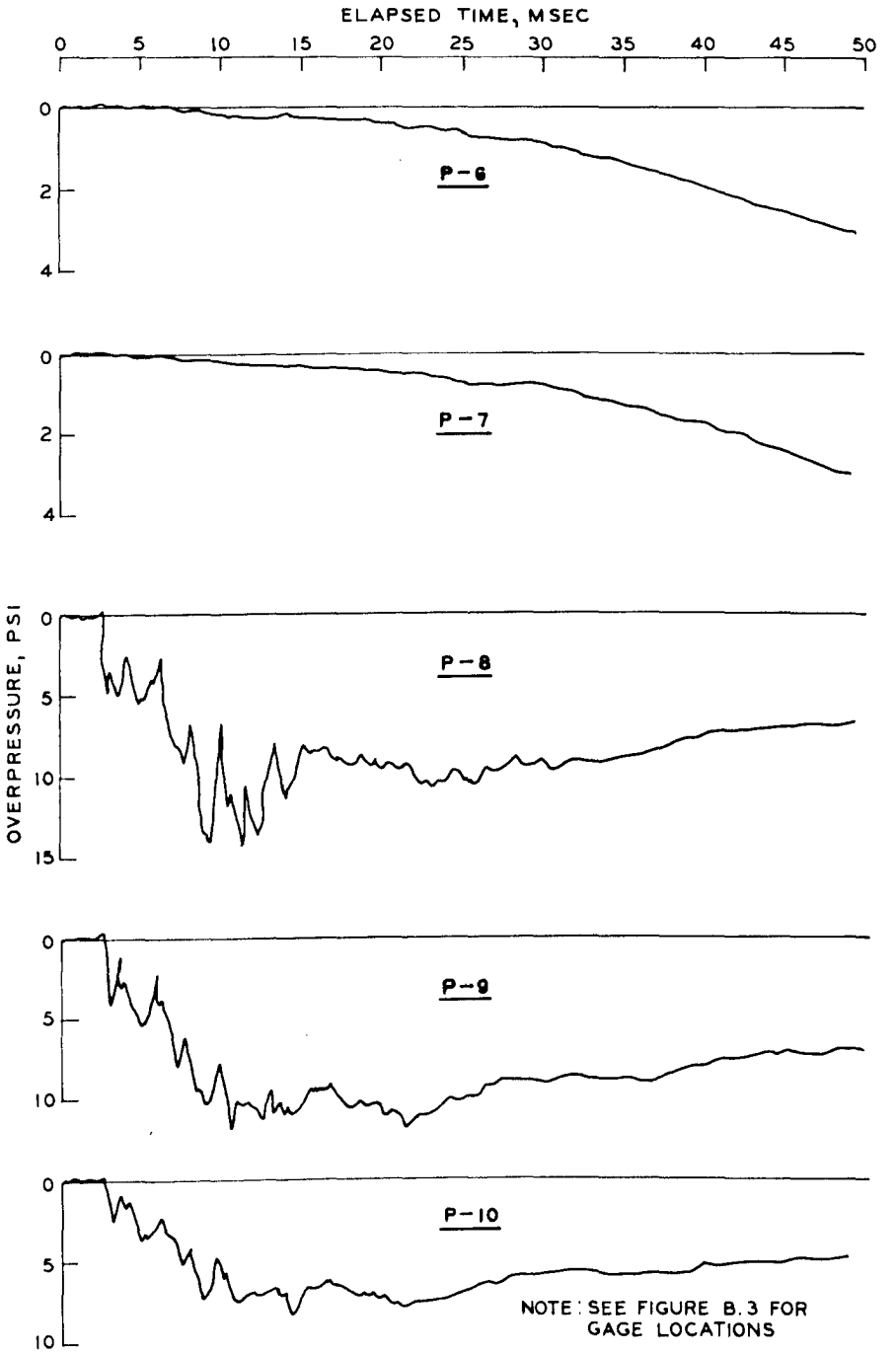

Figure B.2 Overpressure, Gages P-6 through P-10, dynamic test.

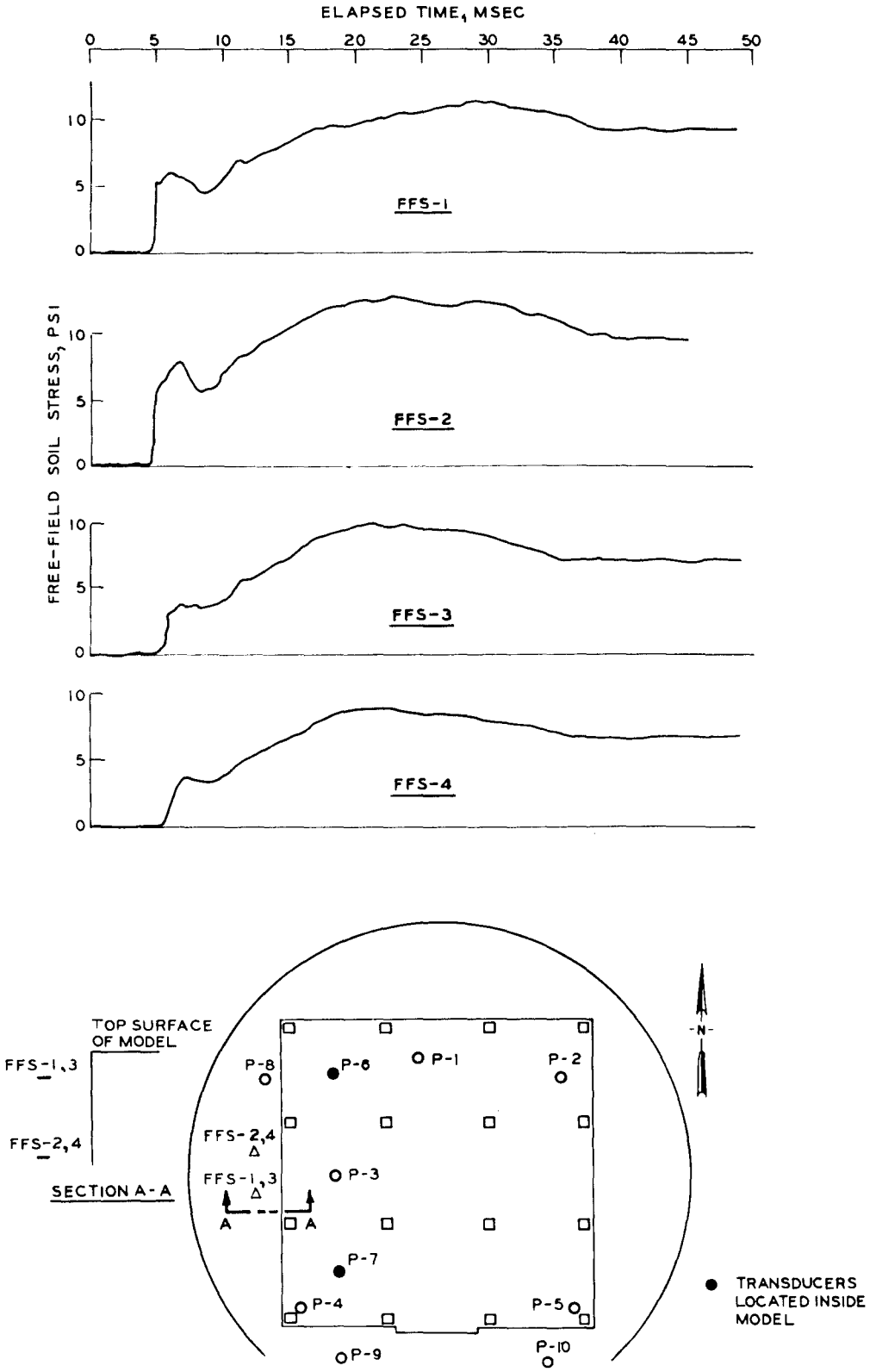

Figure B.3 Free-field soil stress, dynamic test.

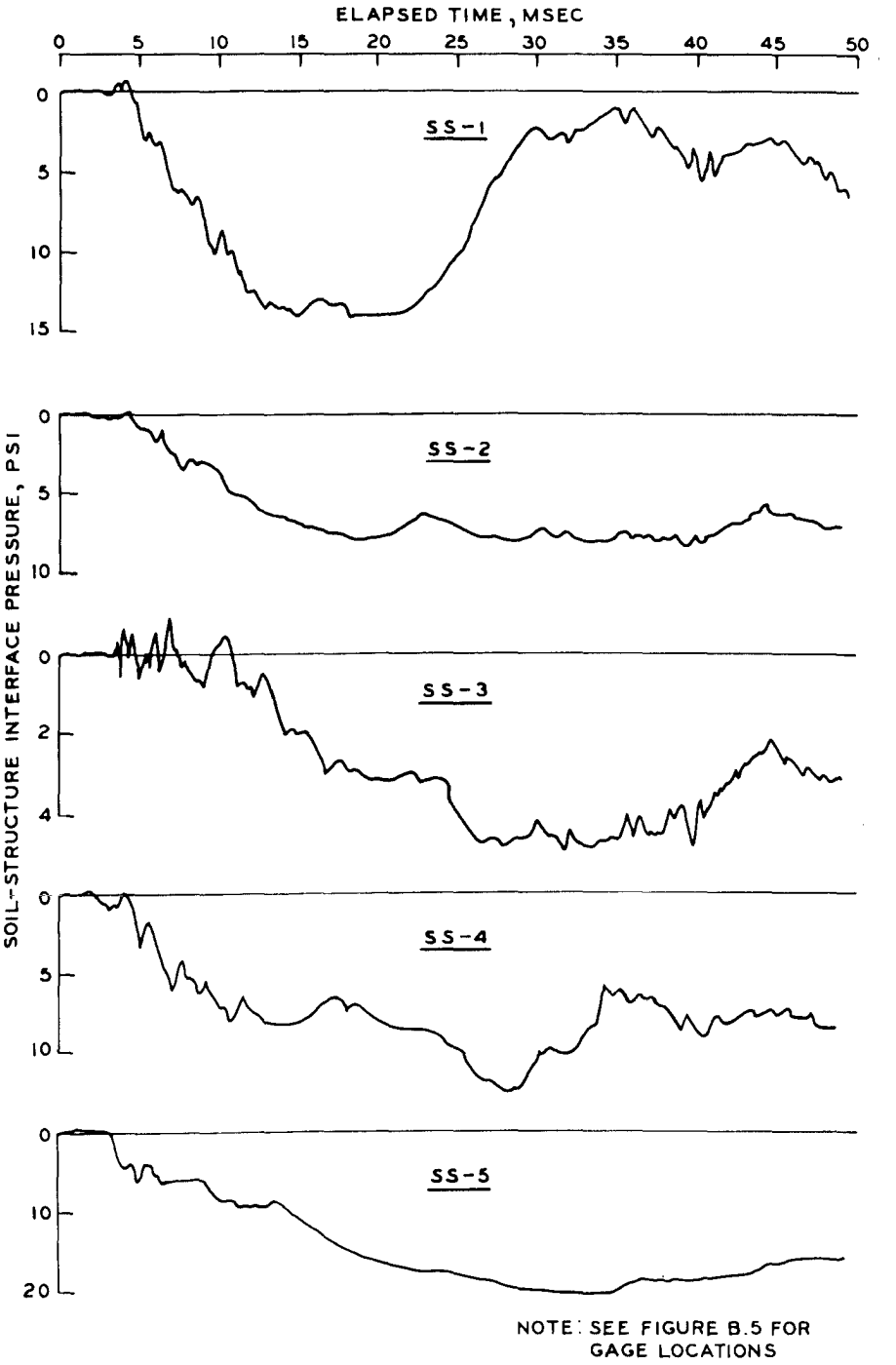

Figure B.4 Soil-structure interface pressure, Gages SS-1 through SS-5, dynamic test.

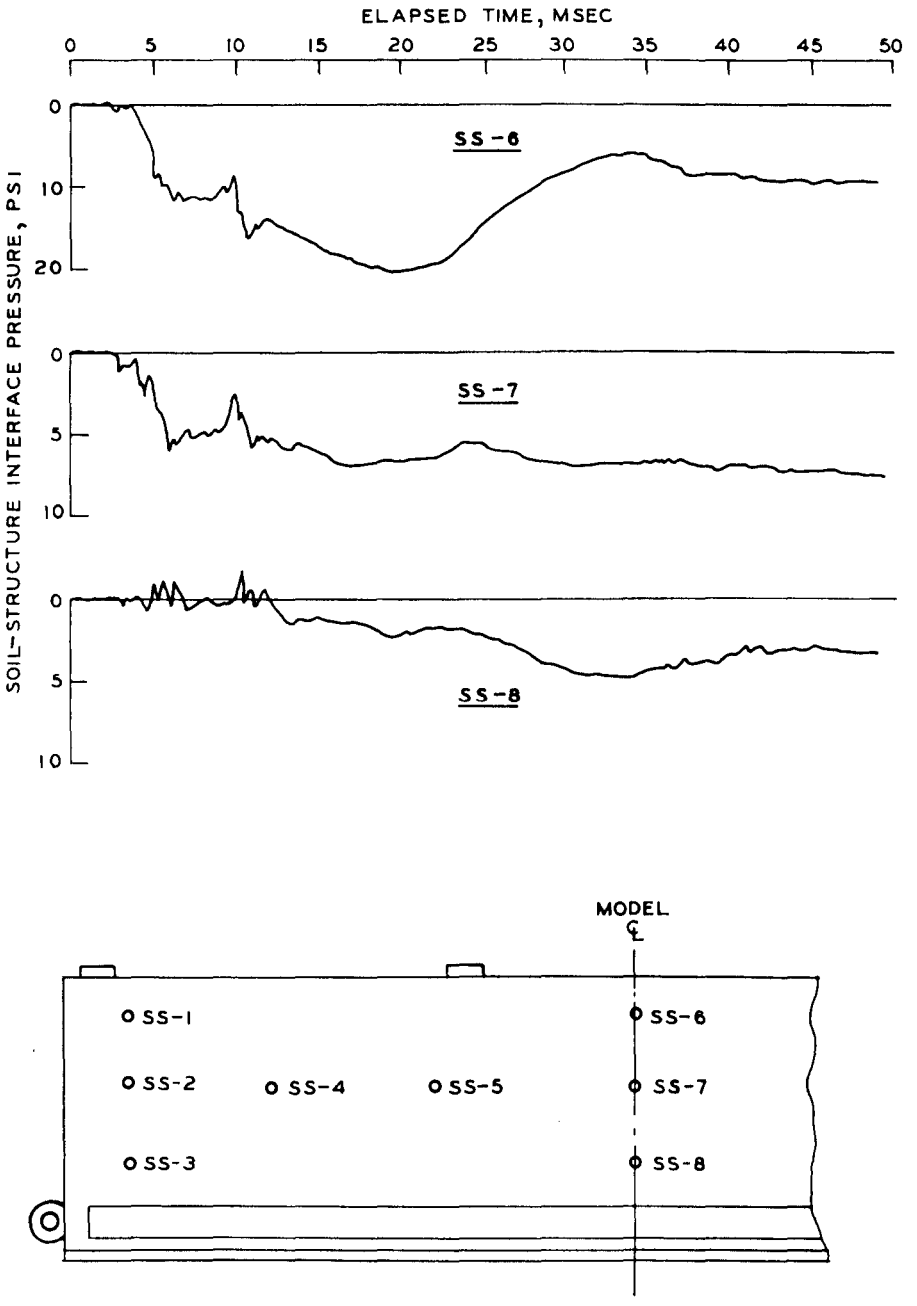

Figure B.5 Soil-structure interface pressure, Gages SS-6 through SS-8, dynamic test.

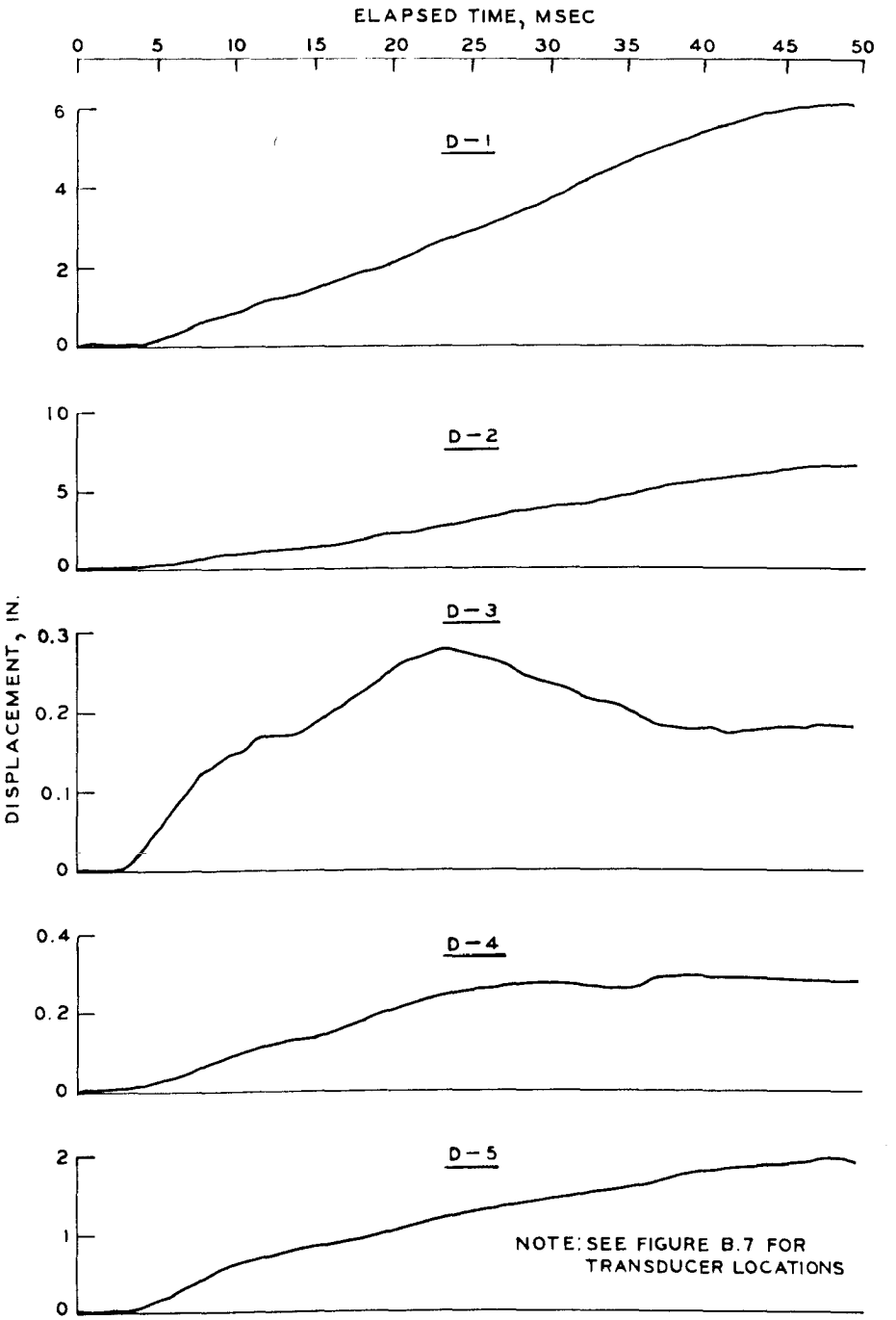

Figure B.6 Displacement, transducers D-1 through D-5, dynamic test.

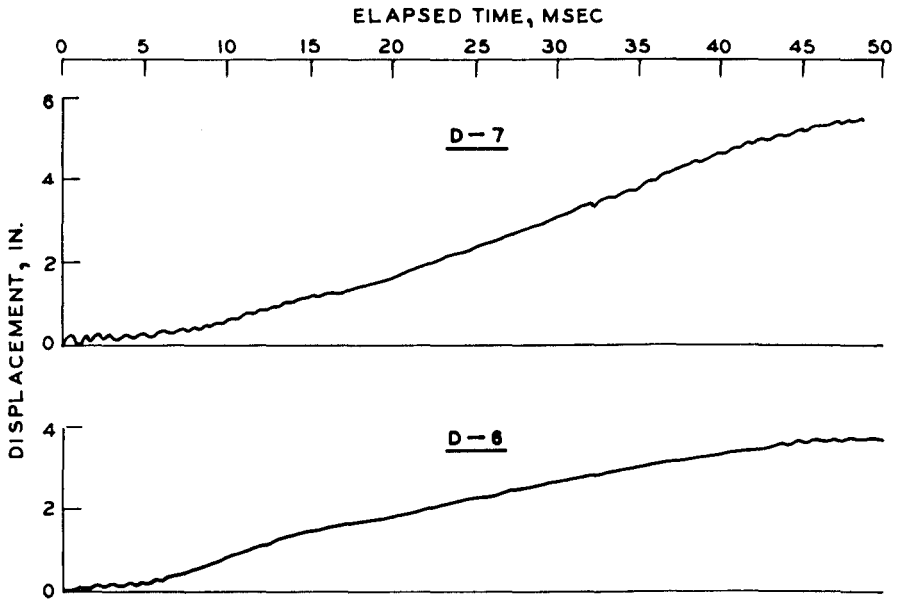

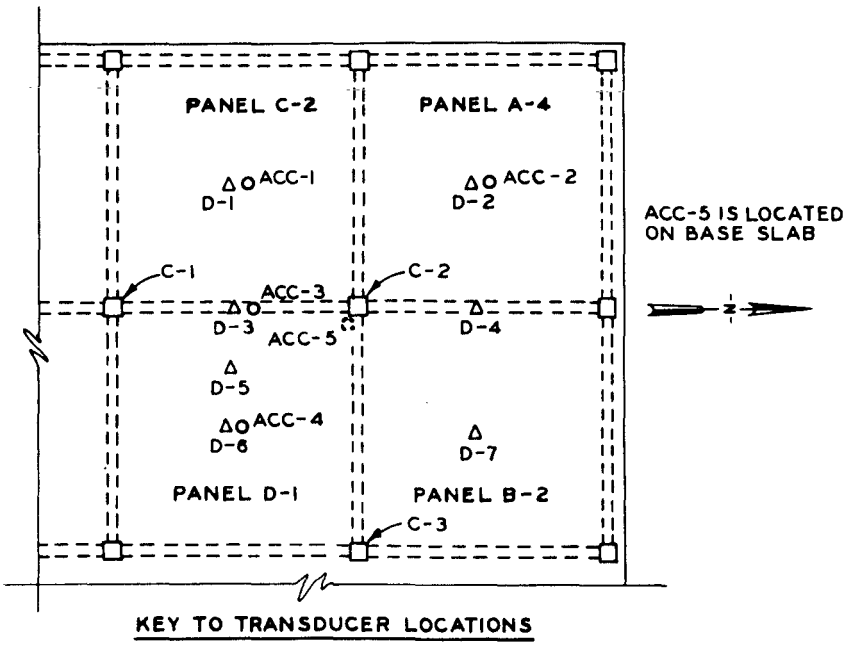

Figure B.7 Displacement, transducers D-6 and D-7, dynamic test.

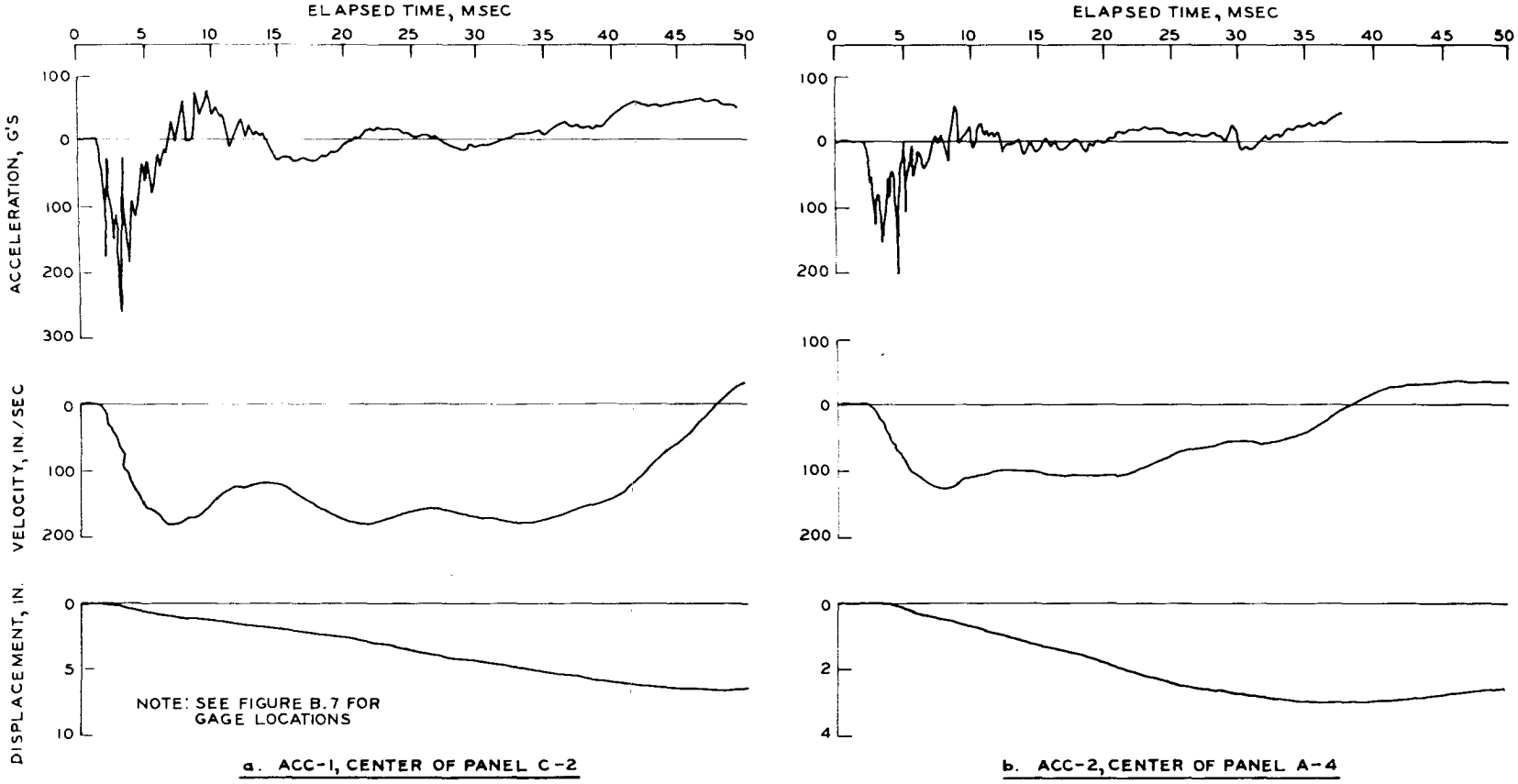

Figure B.8 Acceleration-, velocity-, and displacement-time curves, Gages ACC-1 and ACC-2, dynamic test.

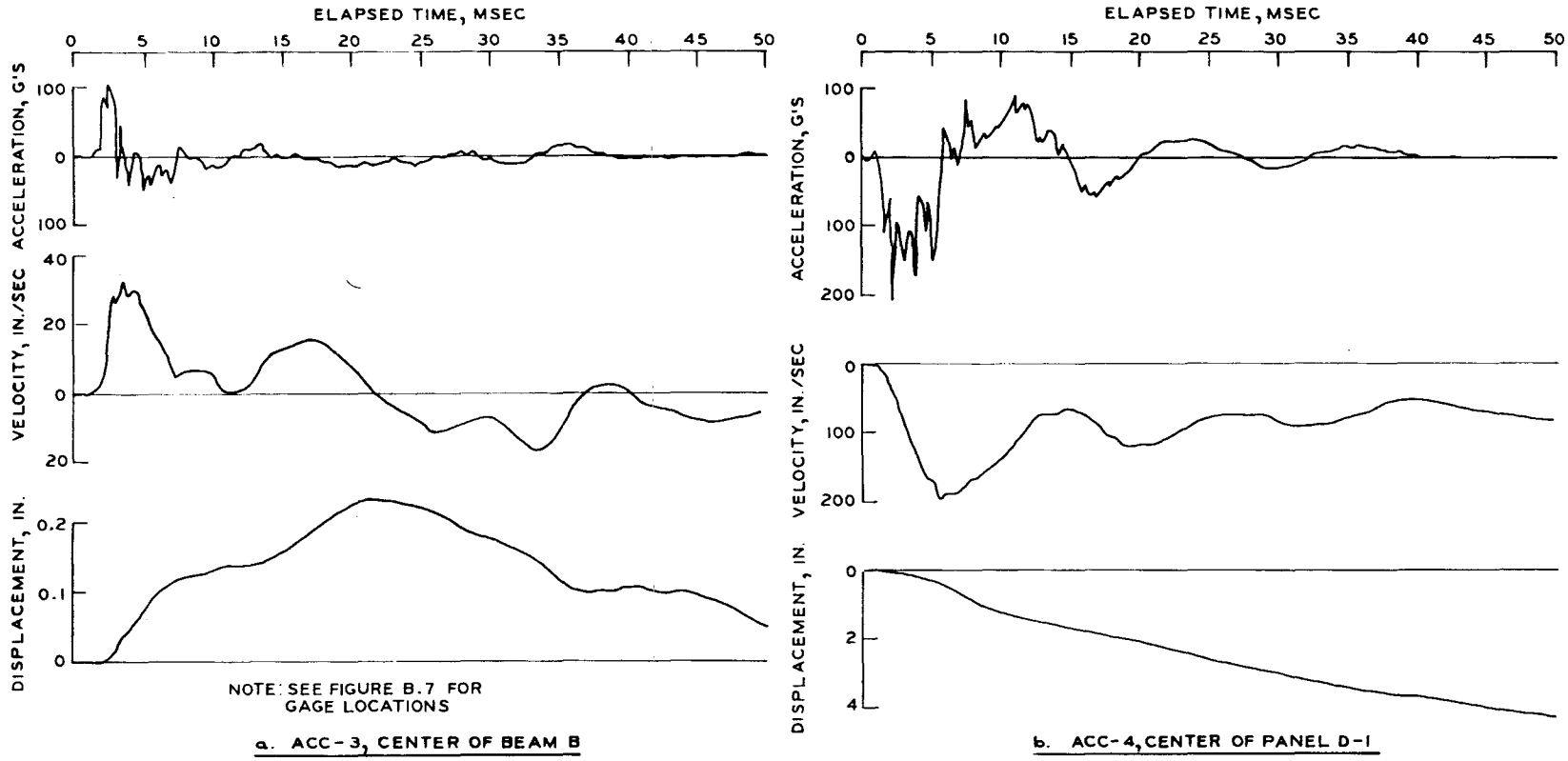

Figure B.9 Acceleration-, velocity-, and displacement-time curves, Gages ACC-3 and ACC-4, dynamic test.

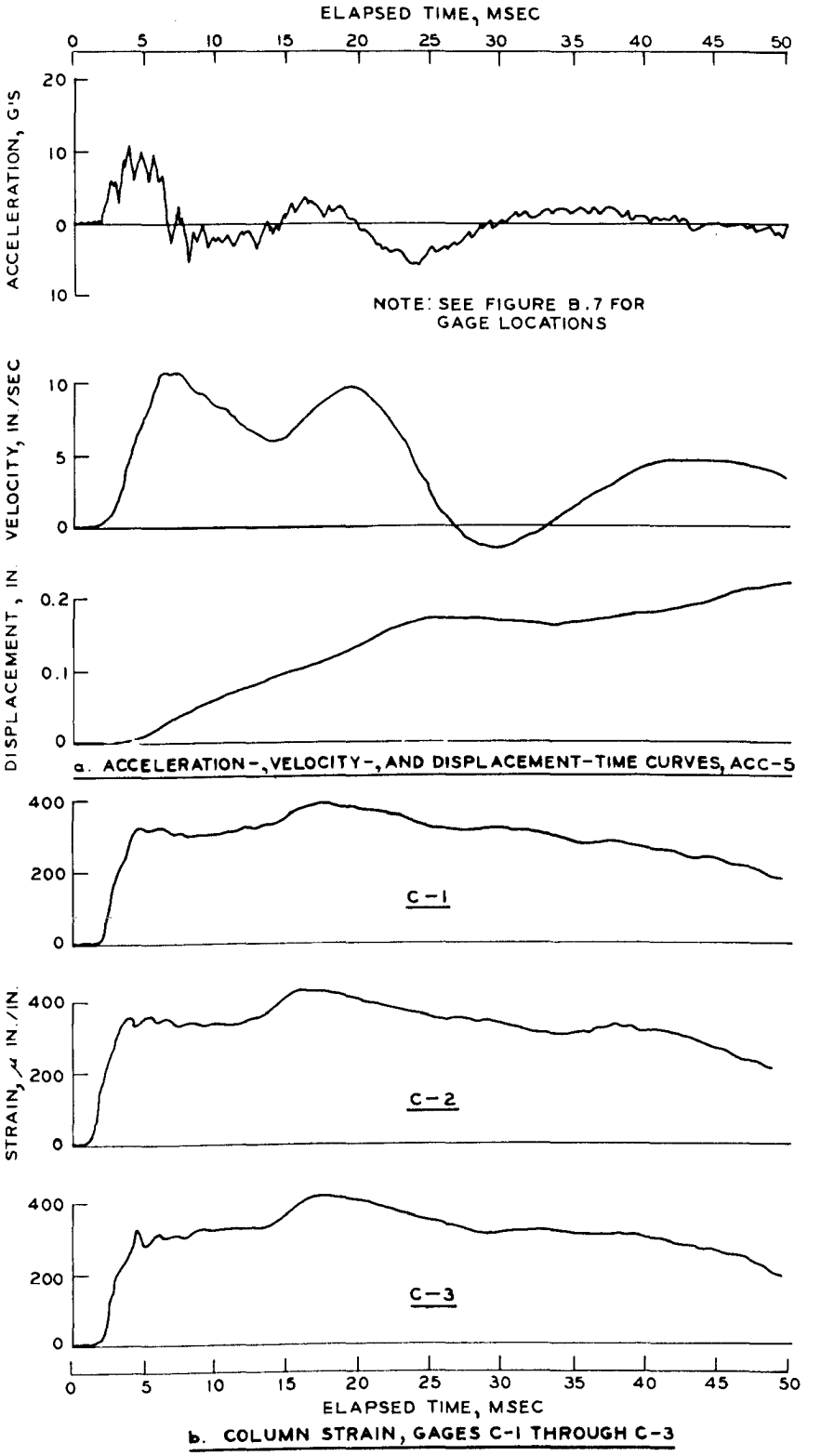

Figure B.10 Column strain and acceleration-, velocity-, and displacement-time curves for location ACC-5, dynamic test.

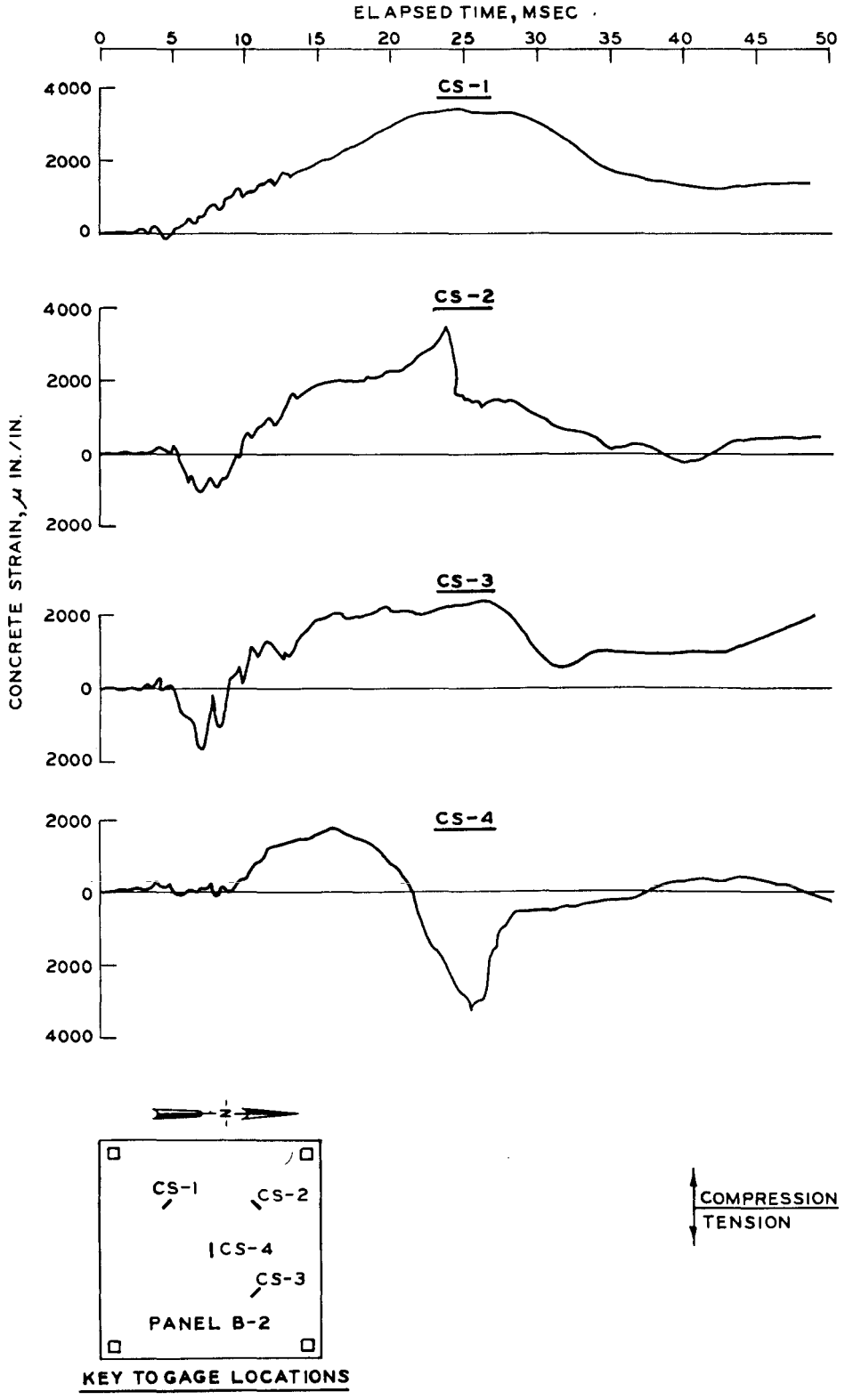

Figure B.11 Concrete strain, Gages CS-1 through CS-4, dynamic test.

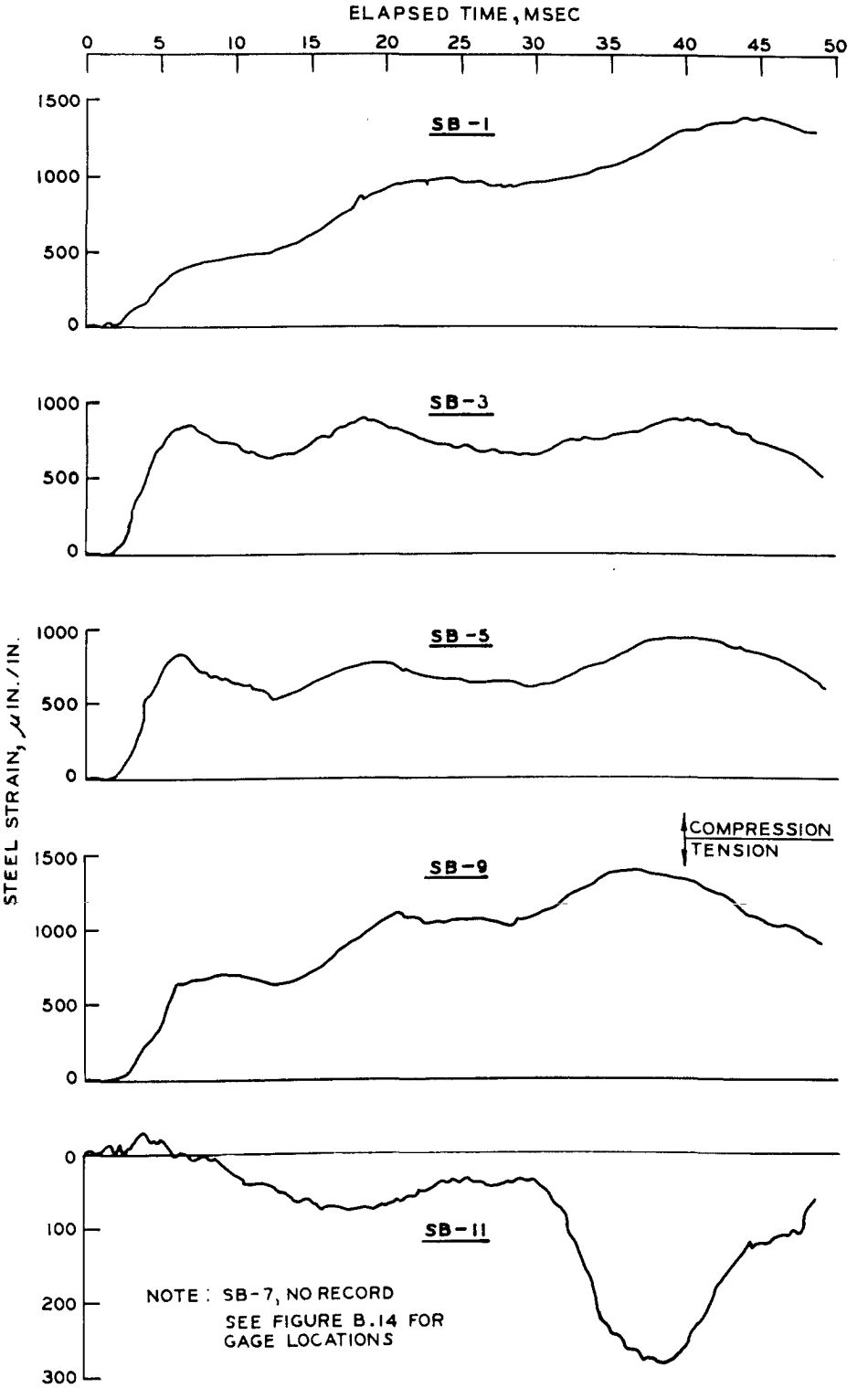

Figure B.12 Steel strain, odd-numbered Gages SB-1 through SB-11, dynamic test.

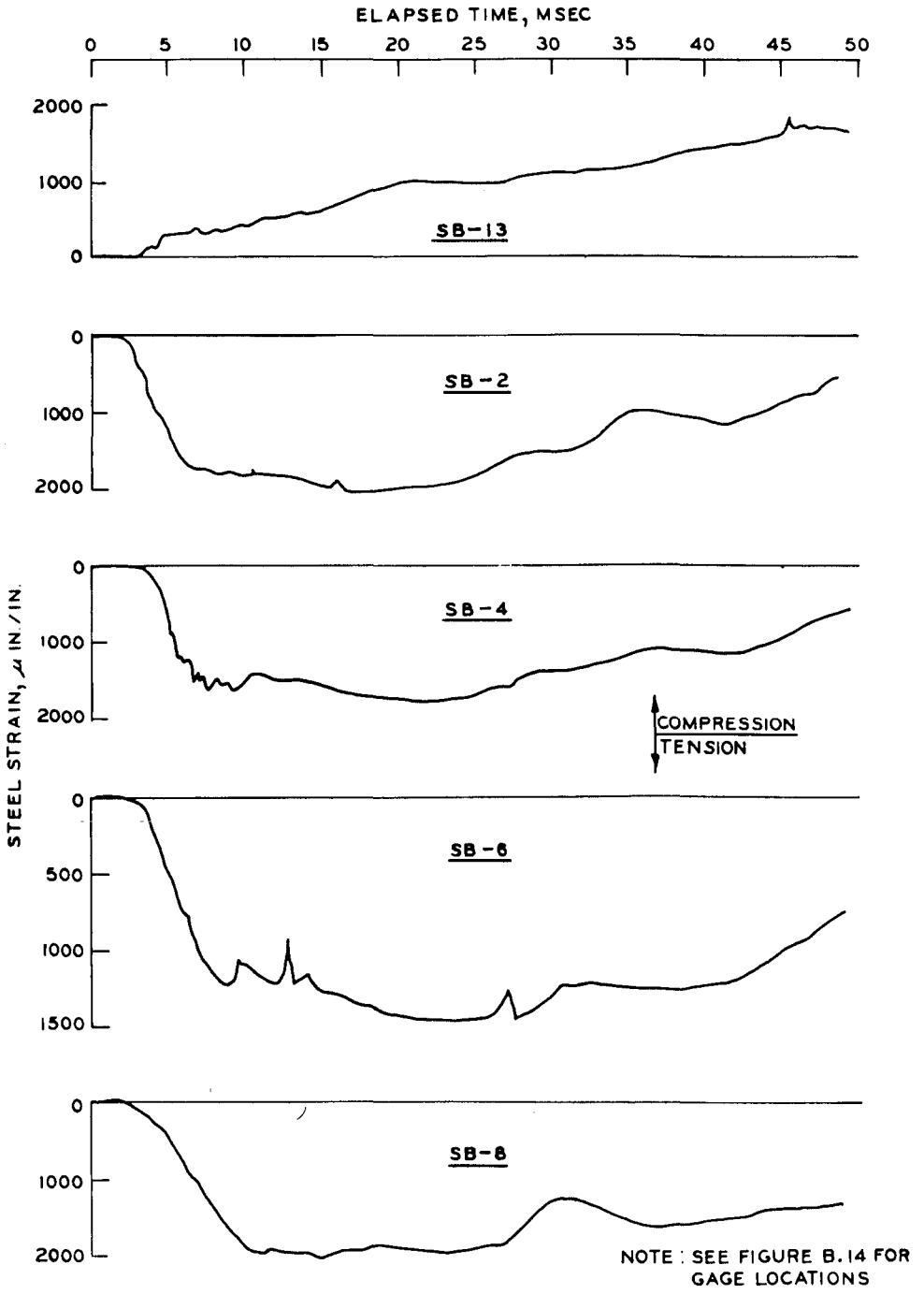

Figure B.13 Beam steel strain, Gage SB-13 and even-numbered Gages SB-2 through SB-8, dynamic test.

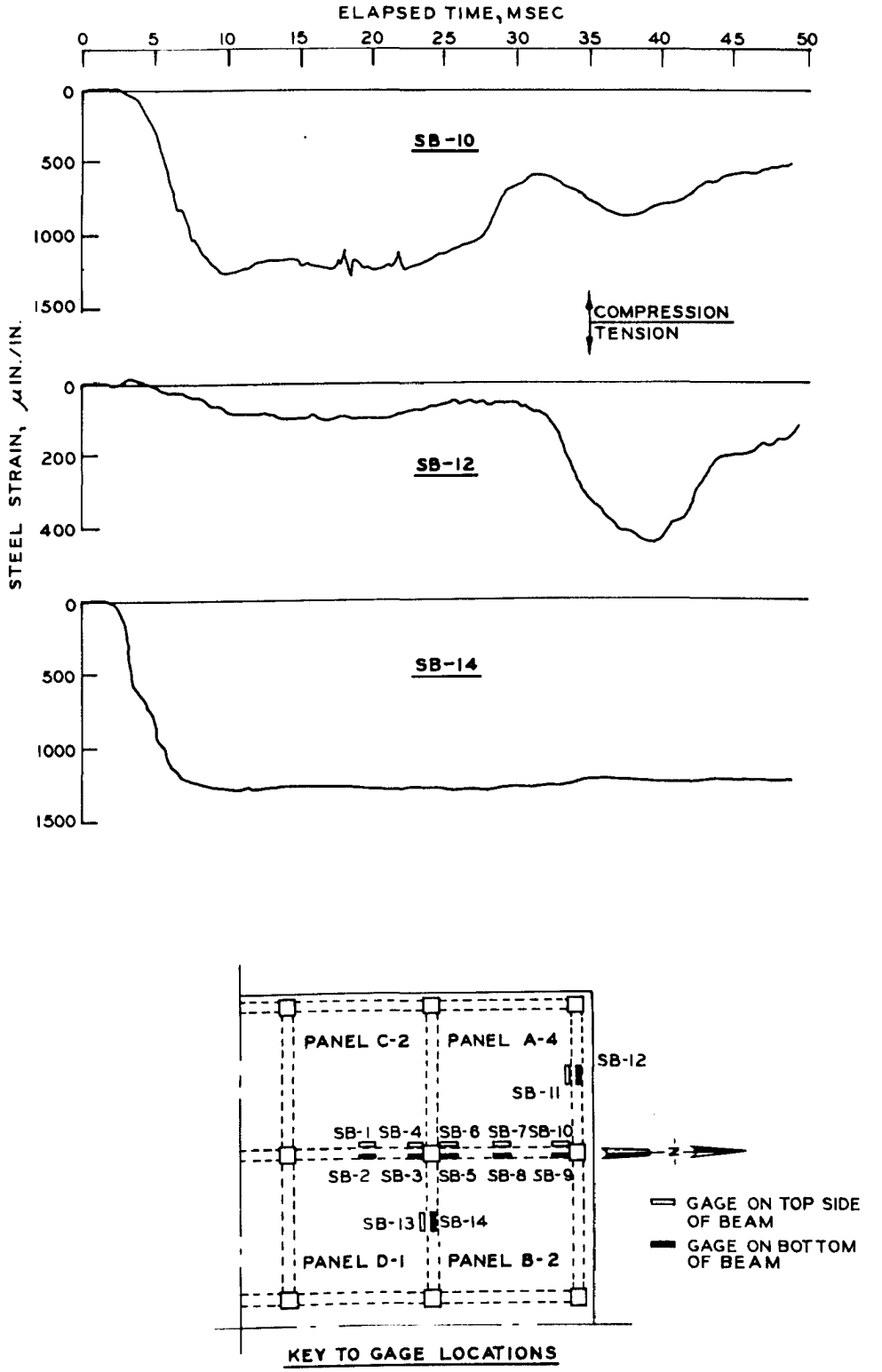

Figure B.14 Beam steel strain, Gages SB-10, SB-12, and SB-14, dynamic test.

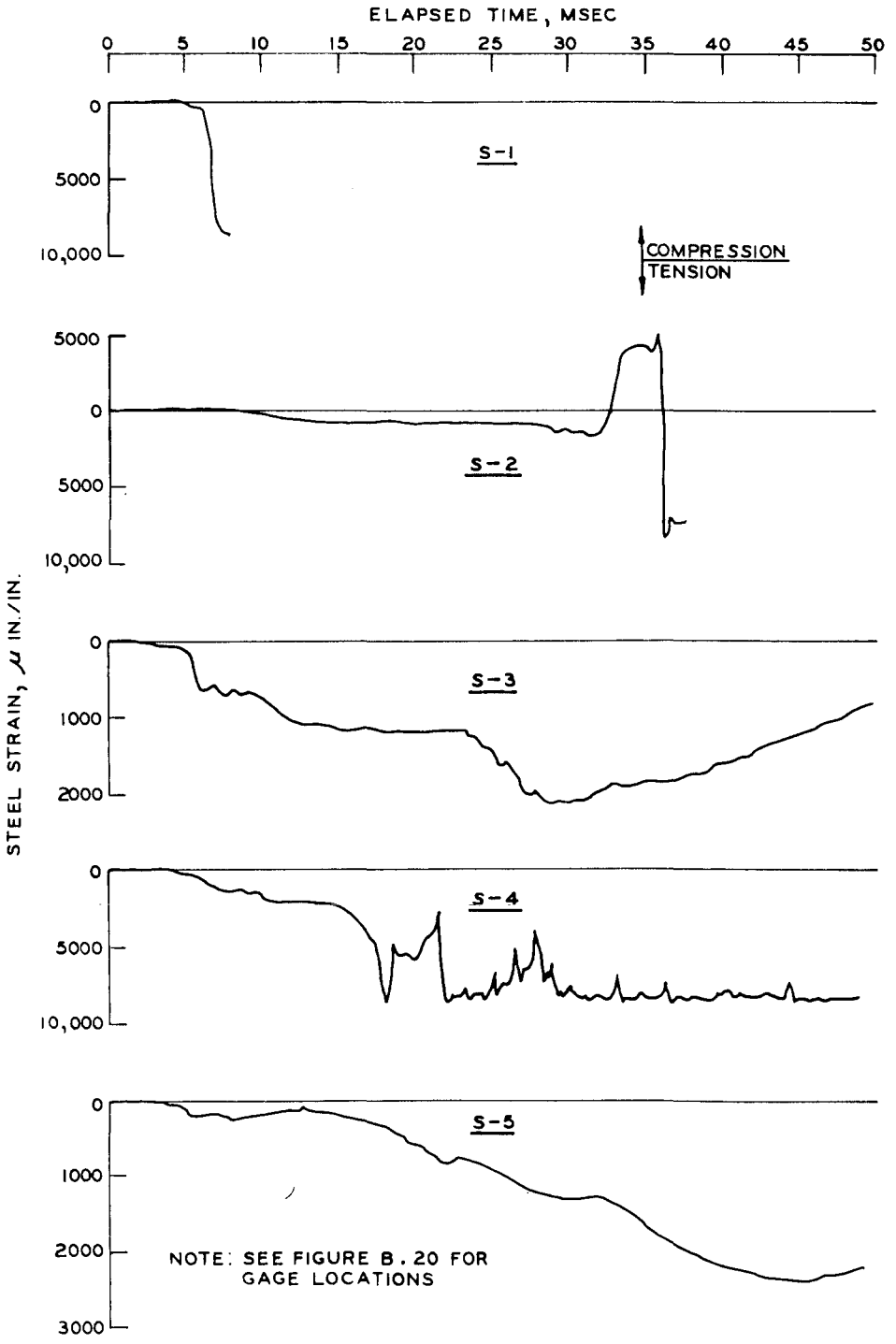

Figure B.15 Reinforcing steel strain, Gages S-1 through S-5, dynamic test.

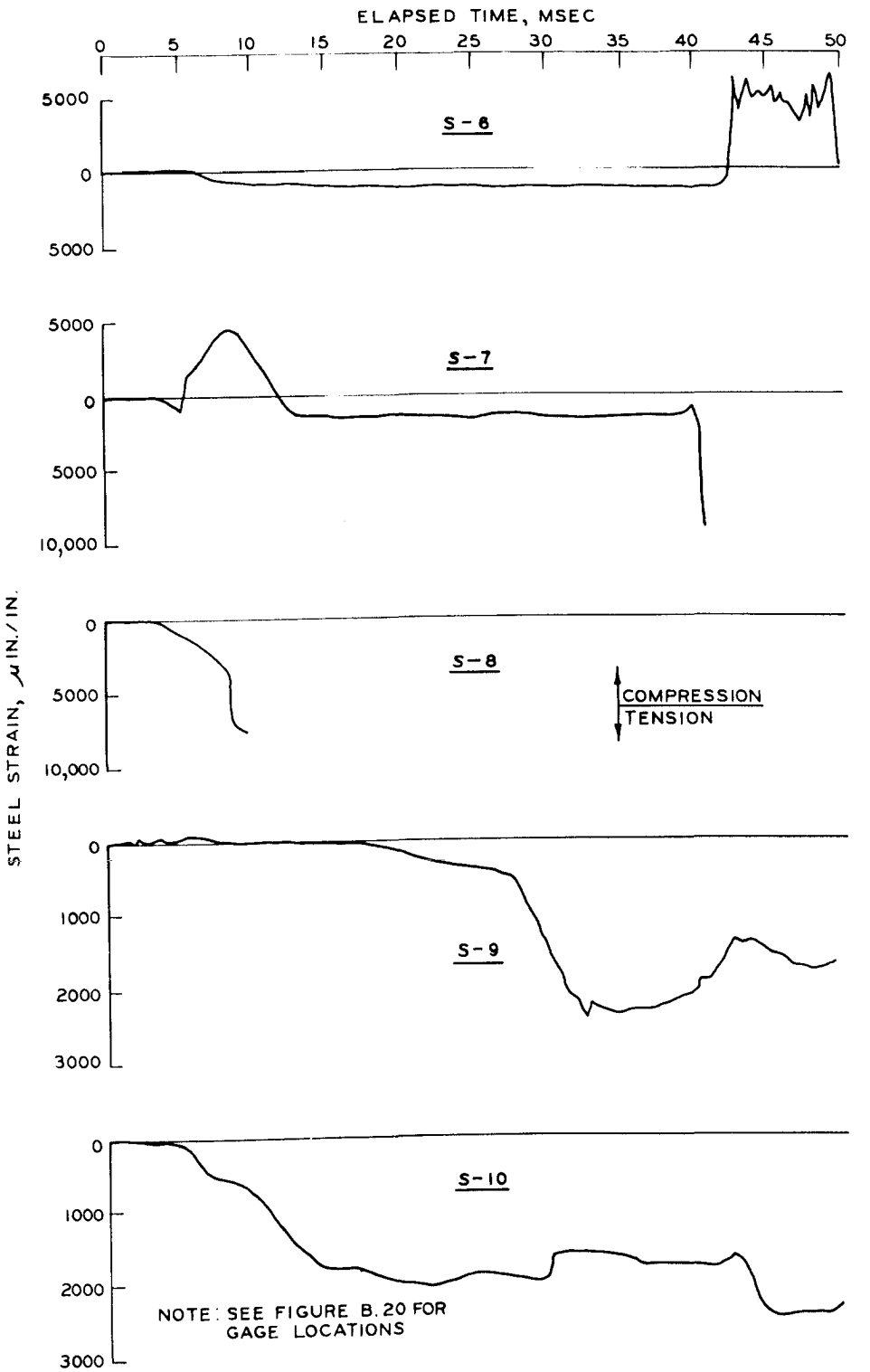

Figure B.16 Reinforcing steel strain, Gages S-6 through S-10, dynamic test.

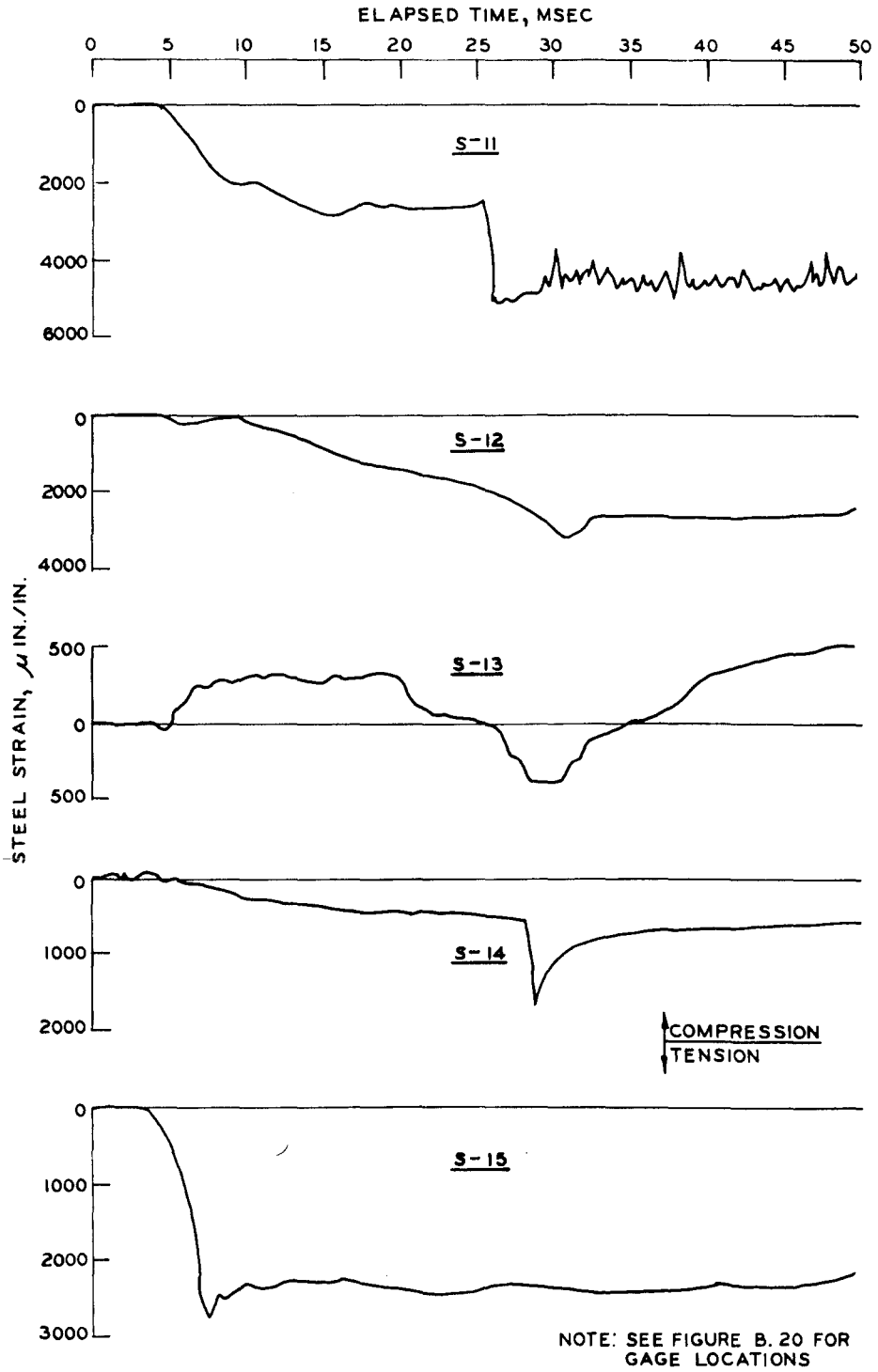

Figure B.17 Reinforcing steel strain, Gages S-11 through S-15, dynamic test.

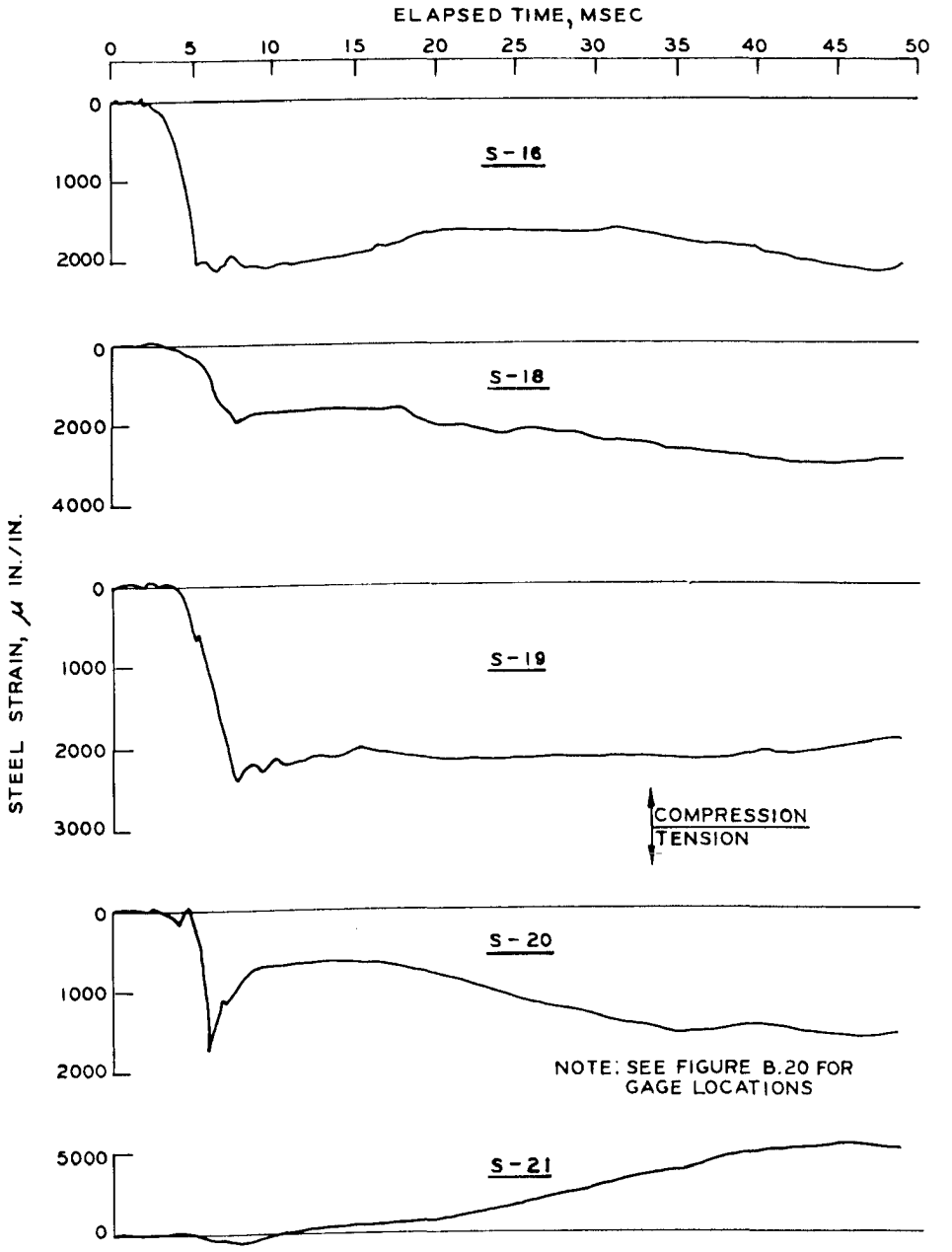

Figure B.18 Reinforcing steel strain, Gages S-16 and S-18 through S-21, dynamic test.

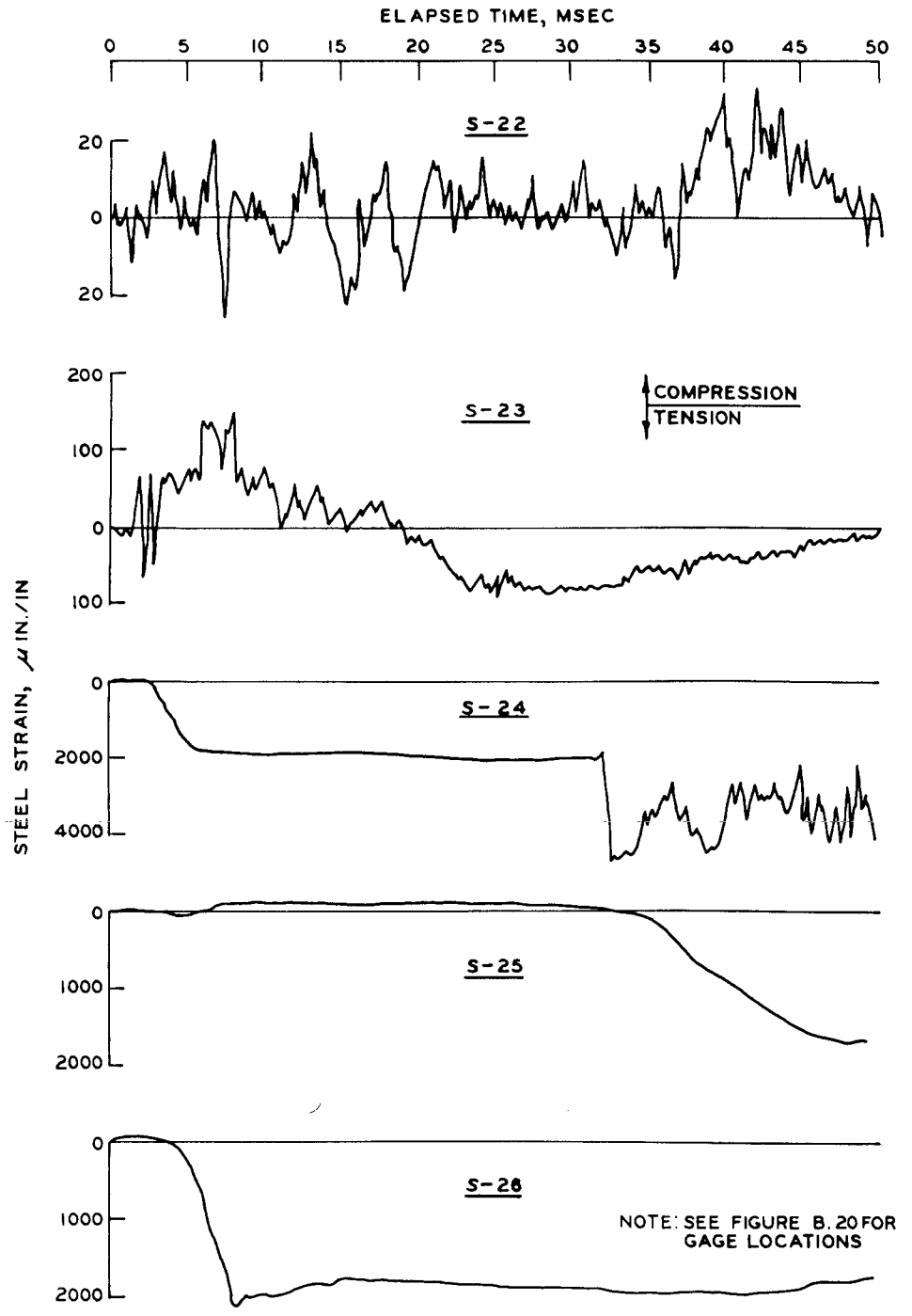

Figure B.19 Reinforcing steel strain, Gages S-22 through S-26, dynamic test.

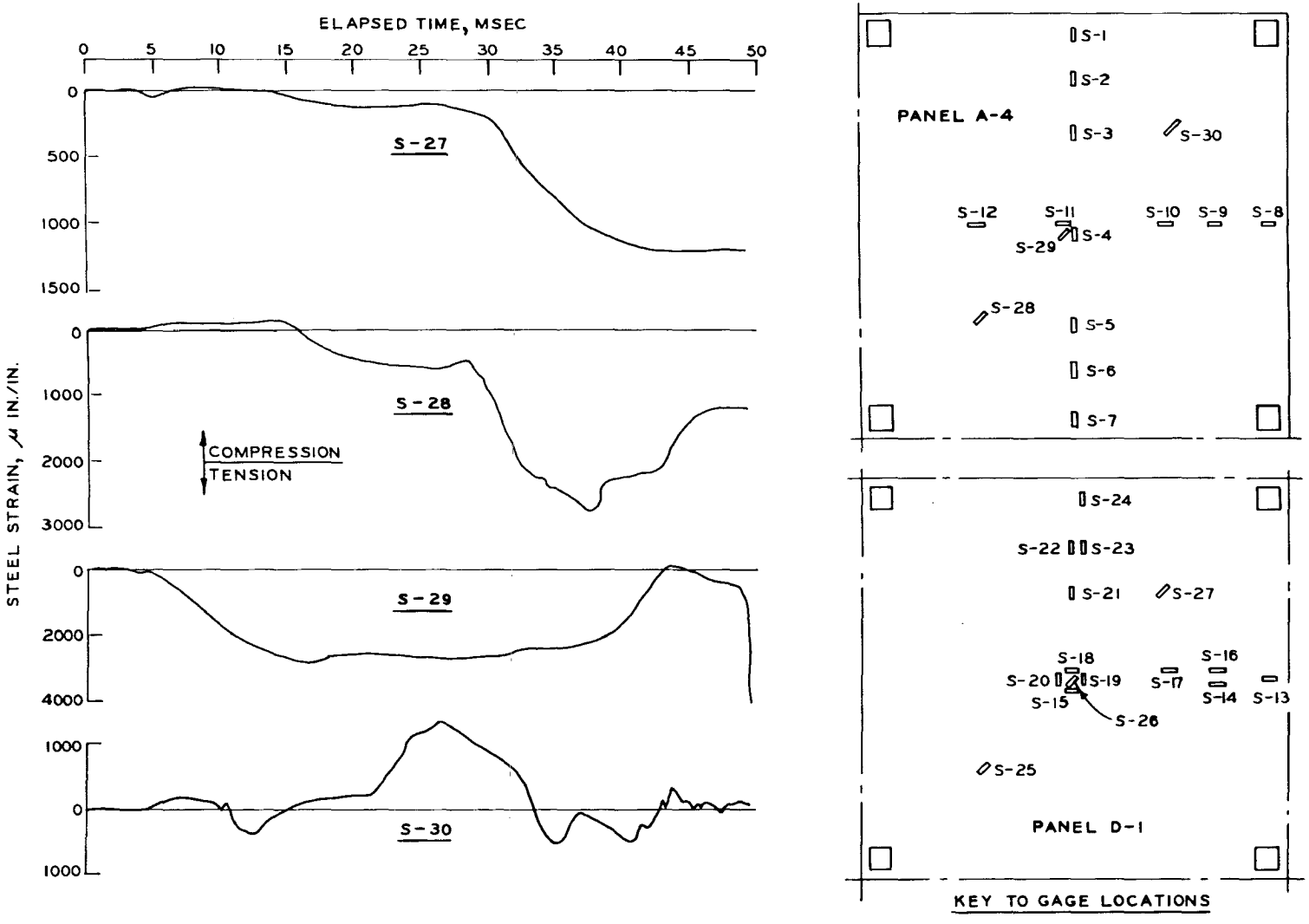

Figure B.20 Reinforcing steel strain, Gages S-27 through S-30, dynamic test.

APPENDIX C

NOTATION

A	Area of one fastener
A_{TL}	Area (per unit width) of the reinforcing steel continuous along the long span of a slab panel
A_{TS}	Area (per unit width) of the reinforcing steel continuous along the short span of a slab panel
d	Effective depth of a reinforced concrete section
E	Modulus of elasticity
f'_c	Compressive strength of concrete
f_y	Yield strength of the reinforcing steel
f_{us}	Ultimate shear strength of fasteners
g	Acceleration of gravity, 386 in./sec^2
K_T	Constant
L	Clear span of slab, inches
L_L, L_S	Clear span of the slab in the long and short directions, respectively
m	Mass per unit area of slab panel, lb-sec^2/in.^{2}
M_R, M_S	Moment at yield in a fixed-end and simply supported beam, respectively
N	Number of fasteners in a connection
p	Tensile reinforcement ratio of a flexural member
P_c	Collapse overpressure
P_1	Dynamic pressure required to produce same damage as obtained in static test
q	Tensile membrane resistance, psi
q_y	Resistance at yield, psi
R	End reaction of a simply supported beam
S	Section modulus
t	Slab thickness
t_d	Load duration
t_m	Time to maximum response of slab panels
t_r	Rise time of dynamic load
T	Natural period of vibration
V	Shear load
W_R, W_S	Total uniform loading on a fixed-end and simply supported beam, respectively

Y_c Center point deflection of slab

γ Weight per unit volume of concrete, lb/in.^{3}

μ Ductility ratio

DISTRIBUTION LIST

Address	No. of Copies
Director, Defense Civil Preparedness Agency Research and Engineering Washington, D. C. 20301 ATTN: Administrative Officer	50
Assistant Secretary of the Army (R&D) Washington, D. C. 20310 ATTN: Assistant for Research	1
Chief of Naval Research Washington, D. C. 20360	1
Commander, Naval Supply Systems Command (Code 0652) Department of the Navy Washington, D. C. 20390	1
Commander, Naval Facilities Engineering Command Research and Development (Code 0322C) Department of the Navy Washington, D. C. 20390	1
Advisory Committee on Civil Defense National Academy of Sciences 2101 Constitution Ave., N.W. Washington, D. C. 20418 ATTN: Mr. Richard Park	1
Defense Documentation Center Cameron Station Alexandria, Virginia 22314	12
Civil Defense Research Project Oak Ridge National Laboratory P. O. Box X Oak Ridge, Tennessee 37830 ATTN: Librarian	1
Office, Chief of Engineers, Department of the Army Washington, D. C. 20314 ATTN: DAEN-RDZ-A/Mr. W. B. Taylor	1
Director, Defense Nuclear Agency Washington, D. C. 20305 ATTN: Mr. Jack R. Kelso	1
STTL, Technical Library	1

Address	No. of Copies
Defense Civil Preparedness Agency Research and Engineering Directorate Washington, D. C. 20301	
ATTN: Mr. George N. Sisson	1
Mr. James E. Roembke	1
Mr. Samuel Kramer Chief, Office of Federal Building Technology Center for Building Technology National Bureau of Standards Washington, D. C. 20234	1
Mr. Anatole Longinow IIT Research Institute 10 West 35th St. Chicago, Illinois 60616	1
Director, Lovelace Foundation 5200 Gibson Boulevard, S.E. Albuquerque, New Mexico 87108	1
Sandia Laboratories Box 5800, Albuquerque, New Mexico 87115	
ATTN: Dr. Clarence R. Mehl, Department 5230	1
Mr. Luke J. Vortman, Division 5412	1
Professor Robert Bailey Nuclear Engineering Department Duncan Annex, Purdue University Lafayette,Indiana 47907	1
Dr. Stanley B. Martin Stanford Research Institute 333 Ravenswood Ave. Menlo Park, California 94025	1
Mr. Lyndon Welch Eberle Smith Associates, Inc. 950 West Fort St. Detroit, Michigan 48226	1
Dr. Lewis V. Spencer Radiation Theory Section 4.3 National Bureau of Standards Washington, D. C. 20234	1

Address	No. of Copies
Mr. William H. Van Horn URS Research Company 155 Bovet Road San Mateo, California 94402	1
Mr. Bert Greenglass Director, Office of Administration Program Planning and Control Dept. of Housing & Urban Development Washington, D. C. 20410	1
Dr. Rudolf J. Engelmann Division of Biomedical and Environmental Research (DBER) U. S. Energy Research and Development Administration Washington, D. C. 20545	1
Office, Chief of Research, Development, and Acquisition Department of the Army Washington, D. C. 20310 ATTN: Mr. Paul F. Carlton (DAMA-CSS-D)	1
Officer in Charge, Naval Construction Battalion Center Civil Engineering Laboratory Port Hueneme, California 93041 ATTN: Technical Library	1
Dr. William Hall 111 Talbot Laboratory University of Illinois Urbana, Illinois 61801	1
Commander, AFWL/Civil Engineering Division Kirtland Air Force Base, New Mexico 87117 ATTN: SUL, Technical Library	1
Civil Engineering Center/AF/PRECET Wright-Patterson Air Force Base Dayton, Ohio 45433 ATTN: Technical Library	1
Director, U. S. Army Engineer Waterways Experiment Station P. O. Box 631, Vicksburg, Mississippi 39180 ATTN: Weapons Effects Laboratory Library	25 3
Director, U. S. Army Ballistic Research Laboratories Aberdeen Proving Ground, Maryland 21005 ATTN: Mr. William J. Taylor (AMXRD-BTL) Technical Library	1 1

Address	No. of Copies
Research Triangle Institute P. O. Box 12194, Research Triangle Park, North Carolina 27709	
ATTN: Mr. Edward L. Hill	1
Mr. Milton D. Wright	1
Stanford Research Institute 333 Ravenswood Ave. Menlo Park, California 94025	
ATTN: Mr. Carl K. Wiehle	1
Mr. H. L. Murphy	1
Dikewood Industries, Inc. 1009 Bradbury Drive, S.E. University Research Park Albuquerque, New Mexico 87106	1
Mr. Thomas E. Waterman IIT Research Institute 10 West 35th St. Chicago, Illinois 60616	1
Bell Telephone Laboratories Whippany Road Whippany, New Jersey 07981	
ATTN: Mr. R. W. Mayo	1
Mr. Eugene F. Witt	1
Mr. John W. Foss Supervisor, Building Studies Group Bell Telephone Laboratories Whippany Road Whippany, New Jersey 07981	1
General American Transportation Corporation General American Research Division 7449 North Natchez Ave. Niles, Illinois 60648	1
Mr. Paul Zigman Environmental Science Associates 770 Airport Boulevard Burlingame, California 94010	1
Dr. Merit P. White School of Engineering University of Massachusetts Amherst, Massachusetts 01002	1

Address	No. of Copies
Dr. Abner Sachs Institute for Defense Analyses 400 Army-Navy Drive Arlington, Virginia 22202	1
The RAND Corporation 1700 Main St. Santa Monica, California 90406 ATTN: Document Library	1
Mr. Henry S. Wakabayashi Research and Engineering Directorate Defense Civil Preparedness Agency Washington, D. C. 20301	1
Office, Chief of Engineers, Department of the Army Washington, D. C. 20314 ATTN: Mr. Roy T. Spurlock	1
Mr. Curtis Lang Agbabian Associates 250 North Nash St. El Segundo, California 90245	1
Mr. Charles Wilton Scientific Service, Inc. 830 Charter St. Redwood City, California 94063	1

In accordance with ER 70-2-3, paragraph 6c(1)(b), dated 15 February 1973, a facsimile catalog card in Library of Congress format is reproduced below.

Huff, William L

Collapse strength of a two-way-reinforced concrete slab contained within a steel frame structure, by William L. Huff. Vicksburg, U. S. Army Engineer Waterways Experiment Station, 1975.

204 p. illus. 27 cm. (U. S. Waterways Experiment Station. Technical report N-75-2)

Prepared for Defense Civil Preparedness Agency, Washington, D. C., under Contract DAHC 20-68-W-0192, Work Unit 1127E.

References: p. 148-150.

1. Basements. 2. Collapse. 3. Concrete slabs. 4. Dynamic tests. 5. Fallout shelters. 6. Reinforced concrete. 7. Shelters. 8. Static tests. 9. Steel frame structures. 10. Subsurface structures. I. Defense Civil Preparedness Agency. (Series: U. S. Waterways Experiment Station, Vicksburg, Miss. Technical report N-75-2)

TA7.W34 no.N-75-2

U. S. Army Engineer Waterways Experiment Station, CE, Vicksburg, Miss. COLLAPSE STRENGTH OF A TWO-WAY-REINFORCED CONCRETE SLAB CONTAINED WITHIN A STEEL FRAME STRUCTURE, by W. L. Huff. June 1975, 204 pp. (Technical Report N-75-2)

Contract DAHC 20-68-W-0192 Unclassified Report
Work Unit 1127E

This investigation concerned the determination of the response, up to collapse, of a typical floor and framing system located over a basement fallout shelter in a multiple-story steel frame building. Specific objectives were to determine strength variations between the building components (floor slabs, connections, and beams) and to determine strength variations between the different types of floor panels that make up the floor system (i.e. corner, edge, and interior). Static and dynamic tests were conducted on two 1:4.5-scale models of the basement shelter area from a multiple-story steel frame building. The five-story prototype structure designed for this study had a basement shelter area that was 60 by 60 feet. In plan, the prototype structure contained three 20-foot bays in each direction, which produced the three possible types of floor panels (corner, edge, and interior). Design of the prototype structure followed the requirements of the American Institute of Steel Construction (AISC) Specifications for the steel frame and the requirements of the 1963 American Concrete Institute (ACI) Building Code for the floor slabs and basement walls. The two models were tested in the 22-foot-10-inch-diameter Large Blast Load Generator located at the U. S. Army Engineer Waterways Experiment Station. Water pressure was used to statically load one of the models. The other model was dynamically loaded with a blast type loading. During both tests, approximately 80 channels of data consisting of strain, deflection, and pressure measurements were recorded. Acceleration measurements were recorded during the dynamic test only. In the static test, one of the corner panels of the model collapsed at an applied pressure of 8.8 psi. The remaining floor panels of the model

UNCLASSIFIED

1. Basements
2. Collapse
3. Concrete slabs
4. Dynamic tests
5. Fallout shelters
6. Reinforced concrete
7. Shelters
8. Static tests
9. Steel frame structures
10. Subsurface structures

I. Huff, W. L.
II. Waterways Experiment Station, Technical Report N-75-2

U. S. Army Engineer Waterways Experiment Station, CE, Vicksburg, Miss. COLLAPSE STRENGTH OF A TWO-WAY-REINFORCED CONCRETE SLAB CONTAINED WITHIN A STEEL FRAME STRUCTURE, by W. L. Huff. June 1975, 204 pp. (Technical Report N-75-2)

Contract DAHC 20-68-W-0192 Unclassified Report
Work Unit 1127E

This investigation concerned the determination of the response, up to collapse, of a typical floor and framing system located over a basement fallout shelter in a multiple-story steel frame building. Specific objectives were to determine strength variations between the building components (floor slabs, connections, and beams) and to determine strength variations between the different types of floor panels that make up the floor system (i.e. corner, edge, and interior). Static and dynamic tests were conducted on two 1:4.5-scale models of the basement shelter area from a multiple-story steel frame building. The five-story prototype structure designed for this study had a basement shelter area that was 60 by 60 feet. In plan, the prototype structure contained three 20-foot bays in each direction, which produced the three possible types of floor panels (corner, edge, and interior). Design of the prototype structure followed the requirements of the American Institute of Steel Construction (AISC) Specifications for the steel frame and the requirements of the 1963 American Concrete Institute (ACI) Building Code for the floor slabs and basement walls. The two models were tested in the 22-foot-10-inch-diameter Large Blast Load Generator located at the U. S. Army Engineer Waterways Experiment Station. Water pressure was used to statically load one of the models. The other model was dynamically loaded with a blast type loading. During both tests, approximately 80 channels of data consisting of strain, deflection, and pressure measurements were recorded. Acceleration measurements were recorded during the dynamic test only. In the static test, one of the corner panels of the model collapsed at an applied pressure of 8.8 psi. The remaining floor panels of the model

UNCLASSIFIED

1. Basements
2. Collapse
3. Concrete slabs
4. Dynamic tests
5. Fallout shelters
6. Reinforced concrete
7. Shelters
8. Static tests
9. Steel frame structures
10. Subsurface structures

I. Huff, W. L.
II. Waterways Experiment Station, Technical Report N-75-2

U. S. Army Engineer Waterways Experiment Station, CE, Vicksburg, Miss. COLLAPSE STRENGTH OF A TWO-WAY-REINFORCED CONCRETE SLAB CONTAINED WITHIN A STEEL FRAME STRUCTURE, by W. L. Huff. June 1975, 204 pp. (Technical Report N-75-2)

Contract DAHC 20-68-W-0192 Unclassified Report
Work Unit 1127E

This investigation concerned the determination of the response, up to collapse, of a typical floor and framing system located over a basement fallout shelter in a multiple-story steel frame building. Specific objectives were to determine strength variations between the building components (floor slabs, connections, and beams) and to determine strength variations between the different types of floor panels that make up the floor system (i.e. corner, edge, and interior). Static and dynamic tests were conducted on two 1:4.5-scale models of the basement shelter area from a multiple-story steel frame building. The five-story prototype structure designed for this study had a basement shelter area that was 60 by 60 feet. In plan, the prototype structure contained three 20-foot bays in each direction, which produced the three possible types of floor panels (corner, edge, and interior). Design of the prototype structure followed the requirements of the American Institute of Steel Construction (AISC) Specifications for the steel frame and the requirements of the 1963 American Concrete Institute (ACI) Building Code for the floor slabs and basement walls. The two models were tested in the 22-foot-10-inch-diameter Large Blast Load Generator located at the U. S. Army Engineer Waterways Experiment Station. Water pressure was used to statically load one of the models. The other model was dynamically loaded with a blast type loading. During both tests, approximately 80 channels of data consisting of strain, deflection, and pressure measurements were recorded. Acceleration measurements were recorded during the dynamic test only. In the static test, one of the corner panels of the model collapsed at an applied pressure of 8.8 psi. The remaining floor panels of the model

UNCLASSIFIED

1. Basements
2. Collapse
3. Concrete slabs
4. Dynamic tests
5. Fallout shelters
6. Reinforced concrete
7. Shelters
8. Static tests
9. Steel frame structures
10. Subsurface structures

I. Huff, W. L.
II. Waterways Experiment Station, Technical Report N-75-2

U. S. Army Engineer Waterways Experiment Station, CE, Vicksburg, Miss. COLLAPSE STRENGTH OF A TWO-WAY-REINFORCED CONCRETE SLAB CONTAINED WITHIN A STEEL FRAME STRUCTURE, by W. L. Huff. June 1975, 204 pp. (Technical Report N-75-2)

Contract DAHC 20-68-W-0192 Unclassified Report
Work Unit 1127E

This investigation concerned the determination of the response, up to collapse, of a typical floor and framing system located over a basement fallout shelter in a multiple-story steel frame building. Specific objectives were to determine strength variations between the building components (floor slabs, connections, and beams) and to determine strength variations between the different types of floor panels that make up the floor system (i.e. corner, edge, and interior). Static and dynamic tests were conducted on two 1:4.5-scale models of the basement shelter area from a multiple-story steel frame building. The five-story prototype structure designed for this study had a basement shelter area that was 60 by 60 feet. In plan, the prototype structure contained three 20-foot bays in each direction, which produced the three possible types of floor panels (corner, edge, and interior). Design of the prototype structure followed the requirements of the American Institute of Steel Construction (AISC) Specifications for the steel frame and the requirements of the 1963 American Concrete Institute (ACI) Building Code for the floor slabs and basement walls. The two models were tested in the 22-foot-10-inch-diameter Large Blast Load Generator located at the U. S. Army Engineer Waterways Experiment Station. Water pressure was used to statically load one of the models. The other model was dynamically loaded with a blast type loading. During both tests, approximately 80 channels of data consisting of strain, deflection, and pressure measurements were recorded. Acceleration measurements were recorded during the dynamic test only. In the static test, one of the corner panels of the model collapsed at an applied pressure of 8.8 psi. The remaining floor panels of the model

UNCLASSIFIED

1. Basements
2. Collapse
3. Concrete slabs
4. Dynamic tests
5. Fallout shelters
6. Reinforced concrete
7. Shelters
8. Static tests
9. Steel frame structures
10. Subsurface structures

I. Huff, W. L.
II. Waterways Experiment Station, Technical Report N-75-2

had permanent deflections of approximately 0.12 times the clear span of the slab panels. All panels, as evidenced by their deflection and recorded strain, were acting as tensile membranes when the test was terminated due to the collapse of the corner panel. The steel frame showed no signs of failure at the end of the test. However, the recorded strains along the framing beams were near yield strain. The dynamic model was subjected to a peak blast pressure of 10.2 psi. The negative moment reinforcing steel ruptured along 70 to 100 percent of the outside edges of all four corner panels of the floor slab. The negative moment reinforcing steel ruptured along the outside edge of two edge panels. The strain gages along the steel framing beams again recorded near-yield strains. Tensile membrane theory developed for two-way slabs having fixed edges was used to predict the response of the three panel types in the model. Good correlation was obtained using this theory, even though the edges of the slab panels in the models were restrained only by the adjacent slab panels. Tensile membrane theory predicted the interior panel to be the weakest panel of the floor system, whereas the test results proved the corner panel to be the weakest. The tensile membrane theory used did not consider any load-carrying capacity for negative moment reinforcing steel extending into a panel from adjacent panels. Insufficient data were available from these tests to define the full benefit of this reinforcing steel. Predictions were made for the response of a simple frame prototype structure designed to carry the same service loads as the rigid frame prototype modeled in this test program. The framing beams and connections of the simple frame prototype structure were found to have collapse loads essentially equal to those of the reinforced concrete floor slabs.

had permanent deflections of approximately 0.12 times the clear span of the slab panels. All panels, as evidenced by their deflection and recorded strain, were acting as tensile membranes when the test was terminated due to the collapse of the corner panel. The steel frame showed no signs of failure at the end of the test. However, the recorded strains along the framing beams were near yield strain. The dynamic model was subjected to a peak blast pressure of 10.2 psi. The negative moment reinforcing steel ruptured along 70 to 100 percent of the outside edges of all four corner panels of the floor slab. The negative moment reinforcing steel ruptured along the outside edge of two edge panels. The strain gages along the steel framing beams again recorded near-yield strains. Tensile membrane theory developed for two-way slabs having fixed edges was used to predict the response of the three panel types in the model. Good correlation was obtained using this theory, even though the edges of the slab panels in the models were restrained only by the adjacent slab panels. Tensile membrane theory predicted the interior panel to be the weakest panel of the floor system, whereas the test results proved the corner panel to be the weakest. The tensile membrane theory used did not consider any load-carrying capacity for negative moment reinforcing steel extending into a panel from adjacent panels. Insufficient data were available from these tests to define the full benefit of this reinforcing steel. Predictions were made for the response of a simple frame prototype structure designed to carry the same service loads as the rigid frame prototype modeled in this test program. The framing beams and connections of the simple frame prototype structure were found to have collapse loads essentially equal to those of the reinforced concrete floor slabs.

had permanent deflections of approximately 0.12 times the clear span of the slab panels. All panels, as evidenced by their deflection and recorded strain, were acting as tensile membranes when the test was terminated due to the collapse of the corner panel. The steel frame showed no signs of failure at the end of the test. However, the recorded strains along the framing beams were near yield strain. The dynamic model was subjected to a peak blast pressure of 10.2 psi. The negative moment reinforcing steel ruptured along 70 to 100 percent of the outside edges of all four corner panels of the floor slab. The negative moment reinforcing steel ruptured along the outside edge of two edge panels. The strain gages along the steel framing beams again recorded near-yield strains. Tensile membrane theory developed for two-way slabs having fixed edges was used to predict the response of the three panel types in the model. Good correlation was obtained using this theory, even though the edges of the slab panels in the models were restrained only by the adjacent slab panels. Tensile membrane theory predicted the interior panel to be the weakest panel of the floor system, whereas the test results proved the corner panel to be the weakest. The tensile membrane theory used did not consider any load-carrying capacity for negative moment reinforcing steel extending into a panel from adjacent panels. Insufficient data were available from these tests to define the full benefit of this reinforcing steel. Predictions were made for the response of a simple frame prototype structure designed to carry the same service loads as the rigid frame prototype modeled in this test program. The framing beams and connections of the simple frame prototype structure were found to have collapse loads essentially equal to those of the reinforced concrete floor slabs.

had permanent deflections of approximately 0.12 times the clear span of the slab panels. All panels, as evidenced by their deflection and recorded strain, were acting as tensile membranes when the test was terminated due to the collapse of the corner panel. The steel frame showed no signs of failure at the end of the test. However, the recorded strains along the framing beams were near yield strain. The dynamic model was subjected to a peak blast pressure of 10.2 psi. The negative moment reinforcing steel ruptured along 70 to 100 percent of the outside edges of all four corner panels of the floor slab. The negative moment reinforcing steel ruptured along the outside edge of two edge panels. The strain gages along the steel framing beams again recorded near-yield strains. Tensile membrane theory developed for two-way slabs having fixed edges was used to predict the response of the three panel types in the model. Good correlation was obtained using this theory, even though the edges of the slab panels in the models were restrained only by the adjacent slab panels. Tensile membrane theory predicted the interior panel to be the weakest panel of the floor system, whereas the test results proved the corner panel to be the weakest. The tensile membrane theory used did not consider any load-carrying capacity for negative moment reinforcing steel extending into a panel from adjacent panels. Insufficient data were available from these tests to define the full benefit of this reinforcing steel. Predictions were made for the response of a simple frame prototype structure designed to carry the same service loads as the rigid frame prototype modeled in this test program. The framing beams and connections of the simple frame prototype structure were found to have collapse loads essentially equal to those of the reinforced concrete floor slabs.